The role of fast ATP-Gated P2X receptors in inflammation

Moore, Samantha

Award date:
2008

Awarding institution:
University of Bath

The Role of Fast ATP-Gated P2X Receptors in Inflammation

Volume 1 of 1

Samantha Frances Moore

A Thesis Submitted for the Degree of Doctor of Philosophy

University of Bath
Department of Pharmacy & Pharmacology
December 2008

ABSTRACT

Over the years purinergic receptors have emerged as important players in the onset of inflammation and modulation of immune responses. One of these receptors; the $P2X_7R$ is an attractive drug target due to its involvement in triggering the processing and secretion of the proinflammatory cytokine IL-1β. The $P2X_7R$ may play a potential role in conditions such as rheumatoid arthritis, atherosclerosis, Alzheimer's disease and neuropathic pain.

In this study I initially established that activation of this receptor is highly dependent on the species, agonist and extracellular milieu. This demonstrated not only that caution should be exercised in designing assays to study the $P2X_7R$ but more importantly that changes to the extracellular environment during inflammation could easily modulate activation of the receptor.

It was also observed that activation of the receptor could induce a range of morphological changes in the absence of cell death. These processes could potentially play a role not only in signal transduction and dissemination of pro-inflammatory responses but also in propagating and amplifying procoagulant signals.

Finally I determined that extracellular ATP could evoke significant changes in the redox status of the cell; not only activating generators of reactive oxygen species but modulating the activity of cellular reductants. Furthermore these redox pathways were observed to play a highly significant role in the activation of caspase-1, processing and secretion of IL-1β and ultimately cell death.

Here I have demonstrated that extracellular ATP and the $P2X_7R$ play an important role in immunomodulation, inflammation and coagulation. Therefore I conclude that purinergic receptors make an exciting target for new drug therapies.

ACKNOWLEDGMENTS

I would first like to express my gratitude to my supervisor Dr Amanda Mackenzie for her continued support. Her expertise, understanding and enthusiasm, has made my PhD an interesting and rewarding experience.

I would also like to thank all the members of the Mackenzie team for their help and support and for providing a fun and friendly environment to work in. Special thanks go to Dr James Hewinson for providing the ground work for some of the assays used during the course of this study and for answering my hundreds perhaps thousands of questions. Special thanks also go to Catherine Hobbs for all the proof-reading I have roped her in too and for putting up with my constant gossiping, cheekiness and rants both in and outside of the lab.

Thanks also go to the Ward group whose advice; support and friendship have been invaluable. Furthermore I would like to thank them for their willingness to share knowledge, to give constructive criticism and to provide cakes at Friday morning lab meetings. Special thanks go to Dr Richard Parry and Stephanie Harris for maxipreping plasmids and Ian Willox for FACS.

I also wish to acknowledge Dr Alison Cave and Professor Ajay Shah (Kings College London) for providing $p47^{-/-}$ and $gp91^{-/-}$ macrophages, Dr Kim Dora and Professor Chris Garland for use of their confocal microscopes, Professor Annemarie Surprenant (The University of Manchester) for $P2X_7R$ plasmids and Mrs Ursula Potter for help with the scanning electron microscopy. Without their generosity parts of this study would not have been possible. I also thank anyone in the Department of Pharmacy & Pharmacology who has ever provided me with their time and help or who I have ever "borrowed" reagents from.

I must also express my gratitude to my mother who has always trusted my decisions, taught me to strive towards my goals and given me her full support and love. Lastly I would like to thank Richard, for his love and encouragement and for not complaining too much when accompanying me to the lab to tend to my cells even at midnight.

PUBLICATIONS

Moore S.F., Mackenzie A.B (2008) Species and Agonist Dependent Zinc Modulation of Endogenous and Recombinant ATP-gated $P2X_7$ Receptors. *Biochemical Pharmacology* **76**(12): 1740-1747

Hewinson, J., Moore, S.F., Glover, C., Watts, A.G., Mackenzie, A.B (2008) A Key Role for Redox Signaling in Rapid $P2X_7$ Receptor-Induced Interleukin-1β Processing in Human Monocytes. *Journal of Immunology* **180**(12)**:** 8410-8420.

Moore, S.F., Mackenzie, A.B (2007) Murine Macrophage $P2X_7$ Receptors Support Rapid Prothrombotic Responses. *Cellular Signaling* **19**(4): 855-866.

Oral Communication Abstracts

Moore, S.F., Mackenzie, A.B (2008) ATP Elicited Intracellular Reactive Oxygen Species Generation via NADPH Oxidase in Murine Macrophages can Induce Cell Death. Purines 2008, Copenhagen, Denmark: *Purinergic Signaling* **4**(S1): S145 – S146.

Moore, S.F., Mackenzie, A.B. (2006) Divalent Cation Regulation of Murine $P2X_7$ Receptors Expressed by RAW 264.7 Macrophages. BPS Winter 2006 Meeting, Oxford, UK: *Proceedings of the British Pharmacological Society*.

Poster Abstracts

Moore, S.F., Murray, K.S., Mackenzie, A.B. (2007) The Macrophage $P2X_7$ Receptor Elicits Tissue Factor De-Encryption. LifeSciences 2007, Glasgow, UK: *Proceedings of the Physiology Society*.

Moore, S.F., Mackenzie, A.B. (2006) Extracellular ATP acting on Murine RAW264.7 Macrophages Enhances Thrombin Generation in the Absence of Cell Death. 8^{th} International Symposium on Adenine and Adenosine Nucleotides, Ferrara, Italy: *Purinergic Signaling* **2**(1): 208-209.

TABLE OF CONTENTS

LIST OF FIGURES

LIST OF TABLES

LIST OF ABBREVIATIONS

Maxima	α
β,γ-methylene adenosine 5' triphosphate	βγmeATP
α,βmethylene adenosine 5'-triphosphate	α,βmeATP
2-(Methylthio)adenosine 5'-triphosphate	2meSATP
Adenylyl cyclase	AC
Adenosine 5'diphosphate	ADP
Adenosine 5'-monophosphate	AMP
Analyses of variance	ANOVA
Annexin-V	An-V
Activator protein 1	AP-1
Apoptotic-associated speck-like protein	ASC
Apoptosis signal-regulating kinase	ASK-1
Activating transcription factor 2	ATF-2
Adenosine 5'-triphosphate	ATP
Brilliant blue G	BBG
Bone marrow derived macrophages	BMDMϕ
Albumin from Bovine Serum	BSA
2',3'-O-(4-benzoyl-benzoyl)	BzATP
Calcium	Ca^{2+}
Caspase-activated DNase	CAD
Cyclic adenosine monophosphate	cAMP
Caspase recruitment domain	CARD
Cadmium	Cd^{2+}
Chronic infantile neurological cutaneous and articular syndrome	CINCA
C-type lectin domain	CTLD
4',6-diamidino-2-phenylindole	DAPI
Deoxyribonucleic acid	DNA
2,4-dinitrochlorobenzene	DNCB
Diphenyleneiodonium	DPI
Ethylenediaminetetraacetic acid	EDTA
Ethylene Glycol Tetraacetic Acid	EGTA
Extracellular signal regulated kinase	ERK1/2
Ethidium bromide	EtBr
Coagulation factor	F
Fas-Associated protein with Death Domain	FADD
Foetal bovine serum	FBS
Familial cold urticaria	FCU
5,10,15,20-Tetrakis(4-sulfonatophenyl)porphyrinato Iron (III), Chloride	FeTPPS
Granulocyte-macrophage colony-stimulating factor	GM-CSF
G-protein coupled metabotrophic receptors	GPCR
Glycosylphosphatidylinositol	GPI
Glutaredoxin	Grx
Glutathione	GSH
Hydrogen	H^+
2,7 gichlorodihydrofluorescein diacetate	H_2DCF-DA / DCF
Hydrogen Peroxide	H_2O_2
Human embryonic kidney cell	HEK293
4-(2-hydroxyethyl)-1- piperazineethanesulfonic acid	HEPES
Mercury	Hg^{2+}
Hypochlorous acid	HOCl
Interferon	IFN
Interferon-beta	IFNβ
Immunoglobulin G	IgG
Interleukin	IL
Inducible nitric oxide synthase	iNOS
Interferon-gamma-induced protein (10kD)	IP-10/CXCL10
Jun-N-terminal kinase	JNK
Potassium	K^+

N-[1-[N-methyl-p-(5 isoquinolinesulfonyl)benzyl]-2-(4 phenylpiperazine)ethyl]-5-isoquinolinesulfonamide	KN-04
1-[N, O-Bis(5-isoquinolinesulfonyl)-N-methyl-L-tyrosyl]-4-phenylpiperazine	KN-62
Lipopolysaccharide	LPS
Leucine-rich repeat	LRR
Mitogen activated protein kinase	MAPK
Monocyte chemotactic protein-1	MCP-1
Macrophage colony stimulating factor	MCSF
Macrophage Inflammatory Protein -2	MIP2/CXCL2
Myeloperoxidase	MPO
Muckle-Wells syndrome	MWS
Sodium	Na^+
Nucleotide-binding site	NBS
N-ethylmaleimide	NEM
Nuclear factor-kappa B	$NF_\kappa B$
Hill slope	n_H
NOD-like receptors	NLR
Nitric oxide	NO
Phagocytic NADPH Oxidase	Nox2
Superoxide	O_2^-
Peroxynitrite	$ONOO^-$
Purinergic 1/Adenosine Receptors	P1/AR
Purinergic 2X Receptors	P2X
Purinergic 2Y Receptors	P2YR
Pathogen-associated molecular pattern	PAMP
Phenylarsine oxide	PAO
Protease activated receptor	PAR
Phosphate Buffered Saline	PBS
Phosphatidylethanolamine	PE
Protease Inhibitor Cocktail	PIC
Phospholipase A_2	PLA_2
Phospholipase-C	PLC
Pyridoxal-phosphate-6-azophenyl-2', 4'-disulfonate	PPADS
Pattern recognition receptors	PRR
Phosphatidylserine	PS
Pyrin domain	PYD
Rheumatoid arthritis	RA
Regulated on activation normal T cell expressed and secreted	RANTES/CCL5
Receptor-interaction protein 2	Rip2
Ribonucleic acid	RNA
Reactive Nitrogen Species	RNS
Reactive Oxygen Species	ROS
Room temperature	RT
Standard deviation of the mean	s.e.m
Sodium Dodecyl Sulfate	SDS
3-morpholinosydnonimine, HCl	SIN-1
S-nitrosylated	*S*-NO
Superoxide dismutase	SOD
Tetramethylethylenediamine	TEMED
Tissue factor	TF
Toll-/IL-1 receptor	TIR
Toll-IL-1R domain-containing adaptor protein	TIRAP
Toll-like receptors	TLR
Tumour necrosis factor	TNF
2′,3′-O-(2,4,6-Trinitrophenyl) adenosine 5′-triphosphate	TNP-ATP
Toll-IL-1R domain-containing adaptor inducing IFNβ related adaptor molecule	TRAM
Toll-IL-1R domain-containing adaptor inducing IFNβ	TRIF
Tris(hydroxymethyl)aminomethane hydrochloride	Tris-HCl
Thioredoxin	Trx
Thioredoxin reductase	TrxR

Thromboxane A_2	TxA_2
Uridine-disphosphate	UDP
Uridine-triphosphate	UTP
Zinc	Zn^{2+}

AMINO ACID CODE

Alanine	A	Ala
Arginine	R	Arg
Asparagine	N	Asn
Aspartic Acid	D	Asp
Cysteine	C	Cys
Glutamic Acid	E	Glu
Glutamine	Q	Gln
Glycine	G	Gly
Histidine	H	His
Isoleucine	I	Ile
Leucine	L	Leu
Lysine	K	Lys
Methionine	M	Met
Phenylalanine	F	Phe
Proline	P	Pro
Serine	S	Ser
Threonine	T	Thr
Tryptophan	W	Trp
Tyrosine	Y	Tyr
Valine	V	Val

CHAPTER 1

INTRODUCTION

In recent years the role of ATP and the receptors it acts at have been increasingly linked to the regulation of inflammatory processes. These processes range from the killing of intracellular pathogens (Fairbairn et *al.,* 2001), cell migration (Ohsawa *et al.,* 2007) and the processing and release of cytokines (Pelegrin *et al.,* 2008). In particular the $P2X_7$ receptor which is primarily expressed on cells of haemopoetic origin, is thought to play a key role in inflammatory processes due to its ability to activate the interlukin-1β (IL-1β) converting enzyme caspase-1 (Solle *et al.,* 2001) and induce cell death (Surprenant *et al.,* 1996). ATP is usually retained within the cell cytoplasm therefore its release in to the extracellular mileu could potentially act as a danger signal activating the innate immune system. In this study I hypothesise that purinergic receptors are involved in modulating the innate immune response and are therefore involved in propagating pro-inflammatory and pro-coagulant processes.

1.1 PURINERGIC SIGNALING

The naturally occurring nucleotide adenosine 5'-triphosphate (ATP) is present in every living cell. It is an important multifunctional molecule; it is a cell's molecular currency involved in transporting chemical energy, it is an intracellular signaling molecule which is critical for signal transduction processes and also an extracellular signaling molecule involved in inducing a number of physiological and pathophysiological events.

ATP consists of adenosine (adenine ring and a ribose sugar) and three phosphate groups (triphosphate) and through hydrolysis can form adenosine 5'-diphosphate (ADP), adenosine 5'-monophosphate (AMP) and adenosine (Figure 1-1). ATP was originally discovered by chemist Karl Lohmann in 1929 (Langen *et al.*, 2008) and determined to be the universal carrier of chemical energy in the cell by Lipmann during his work in 1939-41(Lipmann, 1941). ATP is able to function as a carrier of energy in all living organisms due to the release of energy achieved when one phosphate group is removed forming ADP (Figure 1-2). ATP itself is synthesised from ADP in a process determined in the 1960s to be catalysed by ATP synthase (F_0F_1 ATPase / Complex V). Work by Mitchell determined that cellular respiration led to a difference in hydrogen ion concentration inside and outside

the mitochondrial membrane and that the movement of hydrogen ions would drive the formation of ATP (Figure 1-3) (Mitchell *et al.*, 1968).

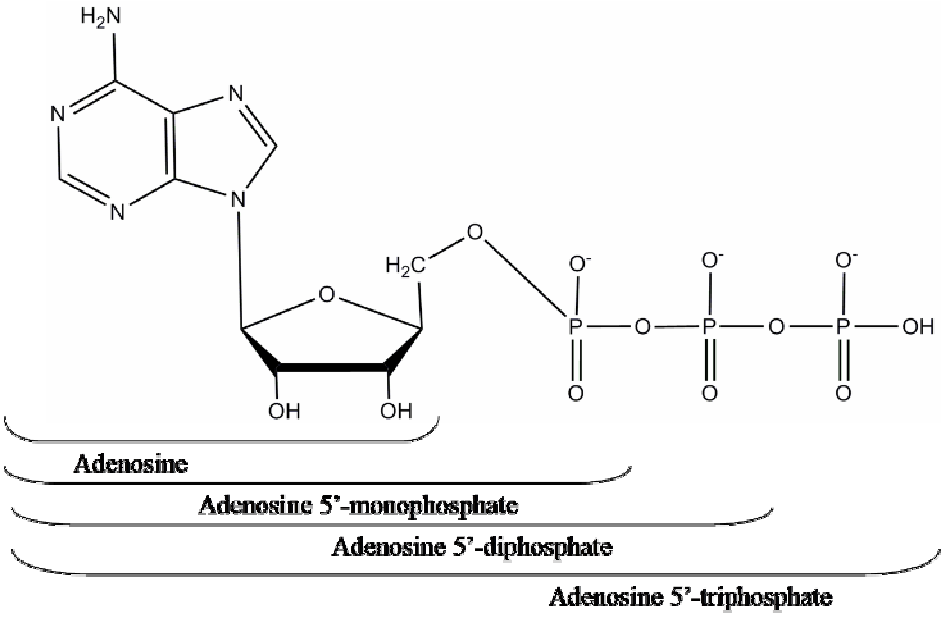

Figure 1-1. ATP can be rapidly hydrolysed forming ADP, AMP & Adenosine.

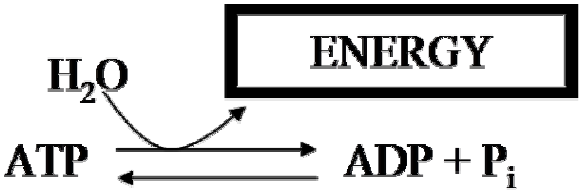

Figure 1-2. Hydrolysis of ATP leads to the formation of ADP & the Release of Energy from High-Energy Bonds.

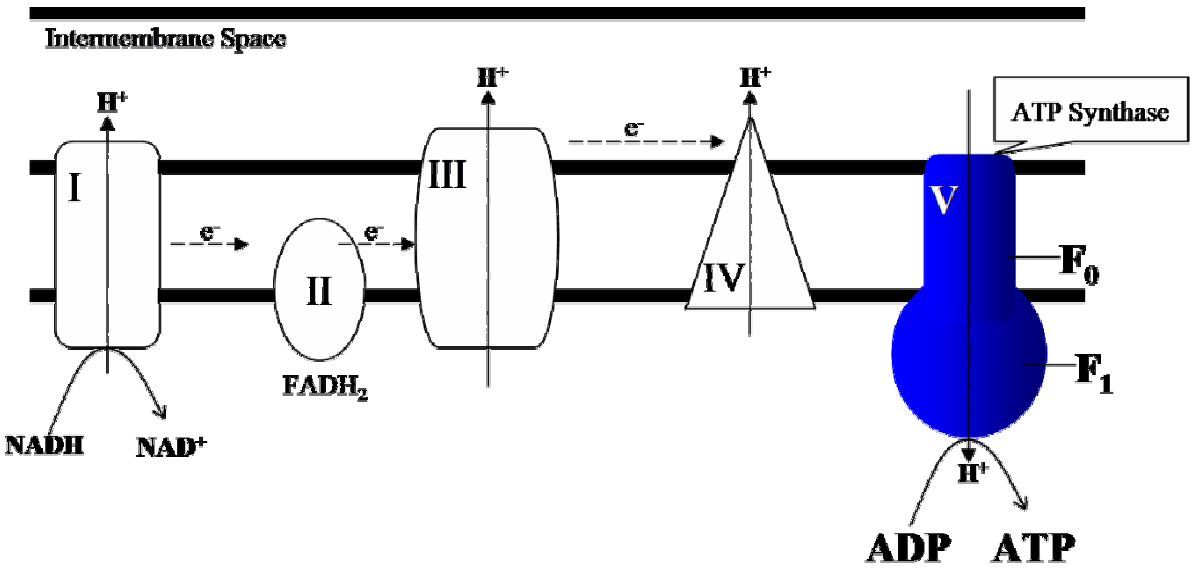

Figure 1-3. Schematic of the generation of an electrochemical gradient across the inner membrane of the mitochondria by complex's I, II, III and IV in order for the generation of ATP to occur via complex V.

In the same year as the discovery of ATP, Drury and Szent-Györgi described the potent actions of purine nucleotides and nucleosides (specifically adenosine and AMP) on the heart and blood vessels (Drury *et al.*, 1929). In the 1970's seminal work by Geoffrey Burnstock summarized the evidence that had accumulated over the years since this initial observation and proposed the purinergic neurotransmission hypothesis. This hypothesis proposed that ATP was a neurotransmitter in nonadrenergic, noncholinergic (NANC) nerves (Burnstock, 1972). Implicit to this concept was the existence of purinergic receptors which Burnstock defined in 1976 and later in 1978 suggested the potential presence of two purinergic receptor families, the P1-receptors where adenosine is the principle ligand and P2-receptors which recognise both ATP and ADP (Burnstock, 1978; Burnstock, 1976). However due to the establishment of ATP being an intracellular energy source this concept was met with considerable resistance, as it was thought that such a ubiquitous molecule was unlikely to be involved in selective extracellular signaling. However the identification, cloning and studies of transduction mechanisms of specific purinergic receptors in the 1980's and 1990's has led to the concept of ATP and other purine and pyrimidine molecules being extracellular signaling molecules to become widely accepted.

As stated the P1/Adenosine receptors (P1/AR) are preferentially activated by adenosine whereas the P2 receptors are preferentially activated by ATP and/or ADP (Figure 1-4). To

date four subtypes of P1/AR have been cloned –A_1, A_2A, A_2B and A_3 which are all seven transmembrane G-protein coupled receptors. The P2 receptors family is split into two major subfamilies termed P2Y and P2X. The P2Y receptors (P2YR) are G-protein coupled metabotrophic receptors (GPCR) while the P2X are ligand-gated ionotrophic receptors (P2XR).

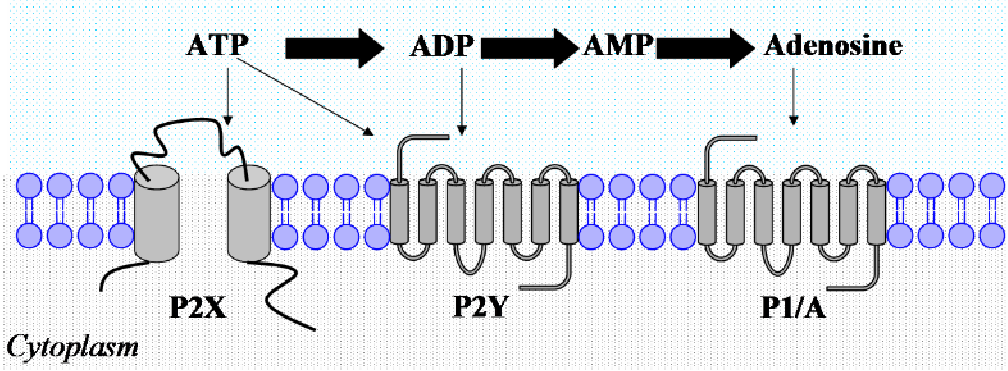

Figure 1-4. Schematic of P1/A, P2Y & P2X Receptors & their Activation by Adenosine, ADP & AMP. P1/A and P2Y receptors are GPCRs which are typified as having seven transmembrane spanning domains, extracellular N-terminus and intracellular C-terminus. The P2X receptors are ligand gated ionotrophic receptors; each subunit consists of two transmembrane spanning domains, intracellular N and C-termini and a large extracellular domain.

1.1.1 P2Y Receptors

Originally P2YRs were classified based on native purinergic responses with the observation that they showed greater responses to 2-(Methylthio) ATP (2meSATP) than to ATP (Burnstock *et al.*, 1985). The cloning of the first P2YR occurred in 1993 (Webb *et al.*, 1993) and there have so far been eight mammalian P2Y subunits cloned -$P2Y_1$, $P2Y_2$, $P2Y_4$, $P2Y_6$, $P2Y_{11}$, $P2Y_{12}$, $P2Y_{13}$ and $P2Y_{14}$.

The $P2Y_1$, $P2Y_{12}$ and $P2Y_{13}$ receptors are all primarily activated by ADP (Figure 1-5). The $P2Y_2R$ can be activated by both ATP and uridine-triphosphate (UTP). The $P2Y_4R$ is activated by UTP and the $P2Y_6R$ by uridine-disphosphate (UDP). $P2Y_{11}$ is activated most potently by ATP and the $P2Y_{14}R$ by UTP-glucose. $P2Y_1$, $P2Y_2$, $P2Y_4$, $P2Y_6$, $P2Y_{11}$ all couple to the G-protein $G\alpha_q$ which can activate phospholipase-C (PLC) causing the mobilization of intracellular calcium (Figure 1-6). $P2Y_{11}$ is also able to couple in to $G\alpha_s$ causing an activation of adenylyl cyclase (AC) and therefore an increase in the cellular

cyclic adenosine monophosphate (cAMP) levels. Whereas $P2Y_{12}$, $P2Y_{13}$ and $P2Y_{14}$ can couple to $G\alpha_i$ inhibiting AC and therefore decreasing cellular levels of cAMP.

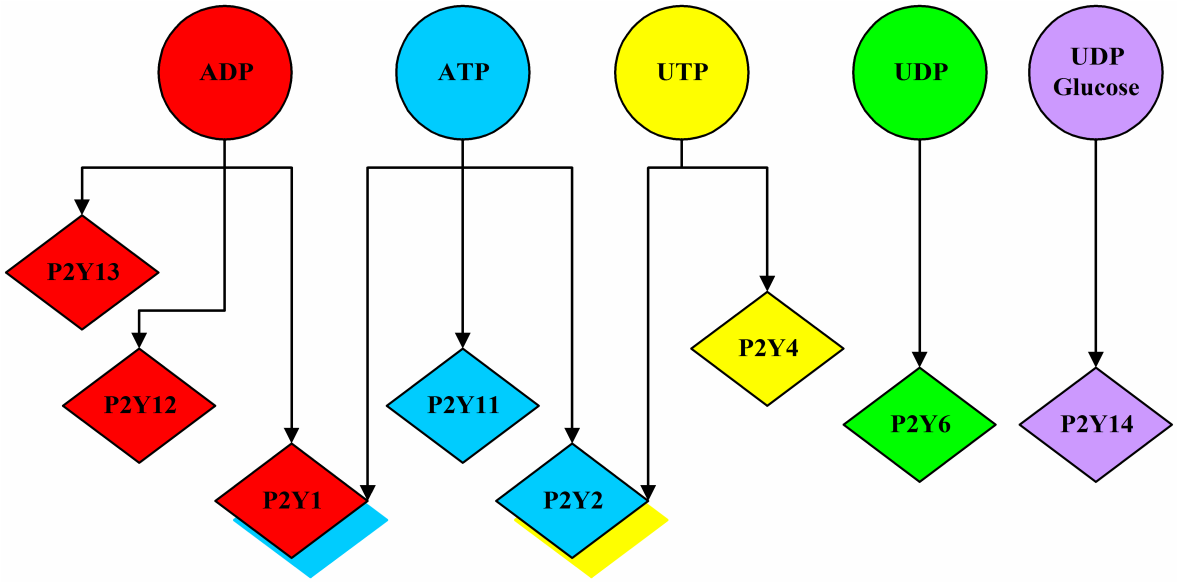

Figure 1-5. Schematic of the Activators of P2YRs. ADP is able to activate $P2Y_{1,\ 12\ \&\ 13}$. ATP is able to activate $P2Y_{1,\ 2\ \&\ 11}$. UTP is able to activate $P2Y_{2\ \&\ 4}$. UDP is able to activate $P2Y_6$ and UDP-glucose $P2Y_{14}$.

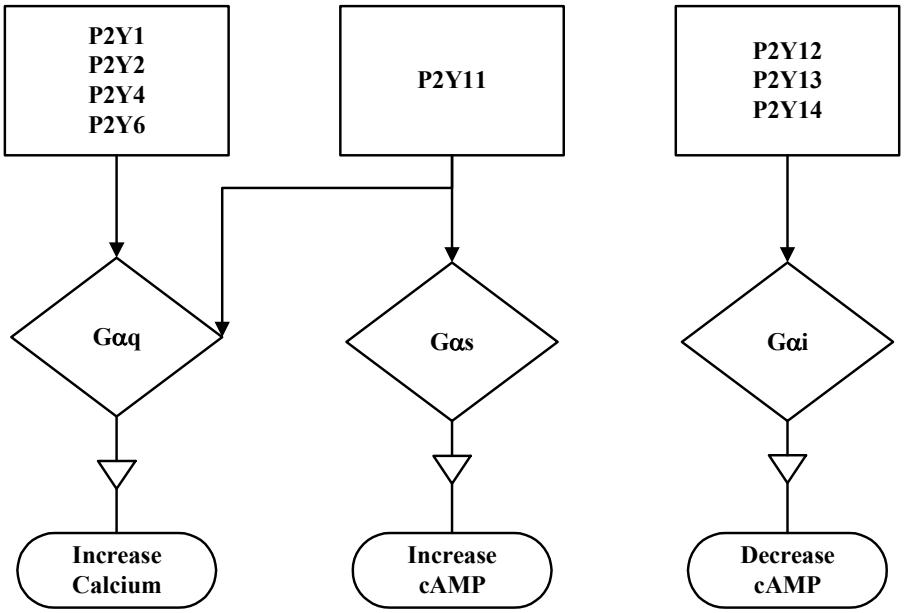

Figure 1-6. Coupling of P2YRs to G-Proteins. $P2Y_{1,\ 2,\ 4,\ 6\ \&\ 11}$ couple to $G\alpha_q$ which is able to activate PLC leading to the mobilization of calcium ions from intracellular stores. $P2Y_{11}$ is also able to couple to $G\alpha_s$ which activates AC leading to the synthesis of cAMP. $P2Y_{12,\ 13\ \&\ 14}$ couple to Gαi which inhibits AC therefore leading to a decrease in cellular cAMP levels.

1.1.2 P2X Receptors

P2XRs were originally classified based on native purinergic responses which determined that they showed greater responses to α,βmethylene ATP (α,βmeATP) and β,γ-methylene ATP (βγmeATP) than ATP (Burnstock *et al.*, 1985). Cloning of the $P2X_1$ (Valera *et al.*, 1994) and the $P2X_2$ receptor subunits (Brake *et al.*, 1994) took place simultaneously in 1994 and to date seven P2X subunits have been identified ($P2X_{1-7}$). Each subunit has been suggested to consist of an intracellular amino and carboxy terminus and two hydrophobic, putative membrane spanning domains separated by a large ectodomain (Figure 1-4). Each P2X channel is thought to be composed of a trimer of subunits with supportive evidence from Nicke *et al.,* (Nicke *et al.*, 1998) who observed that $P2X_1$ and $P2X_3$ receptors migrate as trimers on BN-PAGE and Barrera *et al.,* (Barrera *et al.*, 2005) who determined using atomic force microscopy on purified $P2X_2$ subunits that the average angle between subunits was approximately 120^o constituent with these subunits forming a functional trimer. These subunits can either all be the same (e.g. homomeric $P2X_7R$ channel) or a mixture of two types (e.g. $P2X_{2/3}R$ channel). All of the P2XRs are non-selective cation channels, where upon activation of the receptor there is an influx of calcium (Ca^{2+}) and sodium (Na^+) ions and an efflux of potassium (K^+) ions.

The physiological agonist of all the P2XRs is ATP; however ATP derivatives can be used to distinguish some of the receptors from each other (Table 1-1A). For example homomeric $P2X_1R$ is activated by submicromolar concentrations of ATP, α,βmeATP and 2',3'-O-(4-benzoyl-benzoyl) ATP (BzATP). In contrast the homomeric $P2X_7R$ requires ATP within the high micromolar to low milllimolar range for activation.

The receptors can also be differentiated pharmacologically from each other by the use of antagonists (Table 1-1B). Suramin is widely used as a generic P2XR antagonist although its IC_{50} values at each receptor varies widely; it blocks $P2X_1$, $P2X_2$, $P2X_3$ and $P2X_5$ in the low micromolar range whereas the $P2X_4R$ is relatively insensitive to blockade both by suramin and its analogue NF279. Furthermore as yet no selective antagonists for the $P2X_4R$ have yet to been identified. Over the past few years several specific human $P2X_7R$ antagonists have been identified; primarily due to the drug industry's interest in $P2X_7R$ blockers being used as a therapies in chronic inflammation and pain. The isoquinolines 1-[N, O-Bis(5-isoquinolinesulfonyl)-N-methyl-L-tyrosyl]-4-phenylpiperazine (KN-62) and

N-[1-[N-methyl-p-(5 isoquinolinesulfonyl)benzyl]-2-(4 phenylpiperazine)ethyl]-5-isoquinolinesulfonamide (KN-04) were identified in 1998 (Humphreys *et al.*, 1998) to be highly selective human $P2X_7R$ antagonists. Since then AstraZeneca (Stokes *et al.*, 2006), GlaxoSmithKline (Broom *et al.*, 2008) and Abbott Laboratories (McGaraughty *et al.*, 2007) have all developed selective $P2X_7R$ antagonists. Of note AstraZeneca currently have AZD9056 in phase II clinical trials for the treatment of rheumatoid arthritis (RA).

The P2XRs are also differentially modulated by a range of species; for example the broad spectrum antiparasitic medication ivermectin potentiates $P2X_4$ mediated currents with an EC_{50} of 250 nM (Priel *et al.*, 2004). Other modulators include divalent cations such as Ca^{2+} and zinc (Zn^{2+}), hydrogen ions (H^+) and heavy metals such as mercury (Hg^{2+}) and cadmium (Cd^{2+}) (Coddou *et al.,* 2005, Coddou *et al.,* 2003, Virginio *et al.,* 1997).

A

EC_{50} (μM)	P2X1	P2X2	P2X3	P2X4	P2X5	P2X6	P2X7
ATP	0.07	1.2	0.5	10	10	12	100
2meSATP	0.07	1.2	0.3	10	10	9	100
α,βmeATP	0.3	> 300	0.8	> 300	> 300	> 100	> 300
BzATP	0.003	0.75	0.08	7	> 500	-	20

B

IC_{50} (μM)	P2X1	P2X2	P2X3	P2X4	P2X5	P2X6	P2X7
Suramin	1	10	3	>500	4	>100	500
PPADS	1	1	1	>500	3	>100	50
TNP-ATP	0.006	1	0.001	15	-	-	>30
KN-04 KN-62	-	-	-	-	-	-	0.3
A-438079	>100	>100	>100	>100	-	>100	0.06
NF279	9	30	50	>100	-	-	20
GSK314181A	>10	>10	>10	>10	-	-	0.10
AZ11645373	>10	>10	>10	>10	>10	-	0.10

Table 1-1. Agonist EC_{50} and Antagonist IC_{50} Values at Recombinant Human P2XRs. Tables adapted from (Jarvis *et al.,* 2009) with original data from (Bianchi *et al.*, 1999; Donnelly-Roberts *et al.*, 2007b; Gever *et al.*, 2006; Honore *et al.*, 2006; Jacobson *et al.*, 2002; Jarvis *et al.*, 2002; McGaraughty *et al.*, 2007; Nelson *et al.*, 2006; Romagnoli *et al.*, 2008).[1]

1.1.3 The Role of Purinergic Signaling in Immunity & Inflammation

As already stated extracellular ATP is involved in a number of physiological and pathophysiological events. These events include local control of vessel tone (through modulation of sympathetic transmission), detection and communication of taste, pain sensing and many others. However the focus of my work has been on the role of purinergic signaling in the initiation and modulation of immunity and inflammation; with a particular focus on the effect of extracellular ATP on the macrophage.

[1] EC_{50} and IC_{50} values at P2X receptors in different species can vary widely. IC_{50} values are only indicators of antagonist potency as different concentrations of agonist and agonist species will affect the value.

Macrophages are part of the mononuclear phagocyte family. Mononuclear phagocytes are innate immune cells that originate in the bone marrow from a colony-forming unit granulocyte-macrophage precursor with the least mature cell of the mononuclear phagocyte system being the monoblast (Figure 1-7). Once a monocyte is generated it will enter the peripheral blood. From there monocytes can migrate into extravascular tissues and become resident macrophages, which are able to acquire morphological and functional properties that are characteristic of the tissue in which they reside (Figure 1-7) (Ross *et al.*, 2002). Monocytes are also capable of migrating into various tissues in response to damage or infection transforming into macrophages. These macrophages are a major source of secretary proteins that are able to modulate immune and inflammatory responses (Table 1-2).

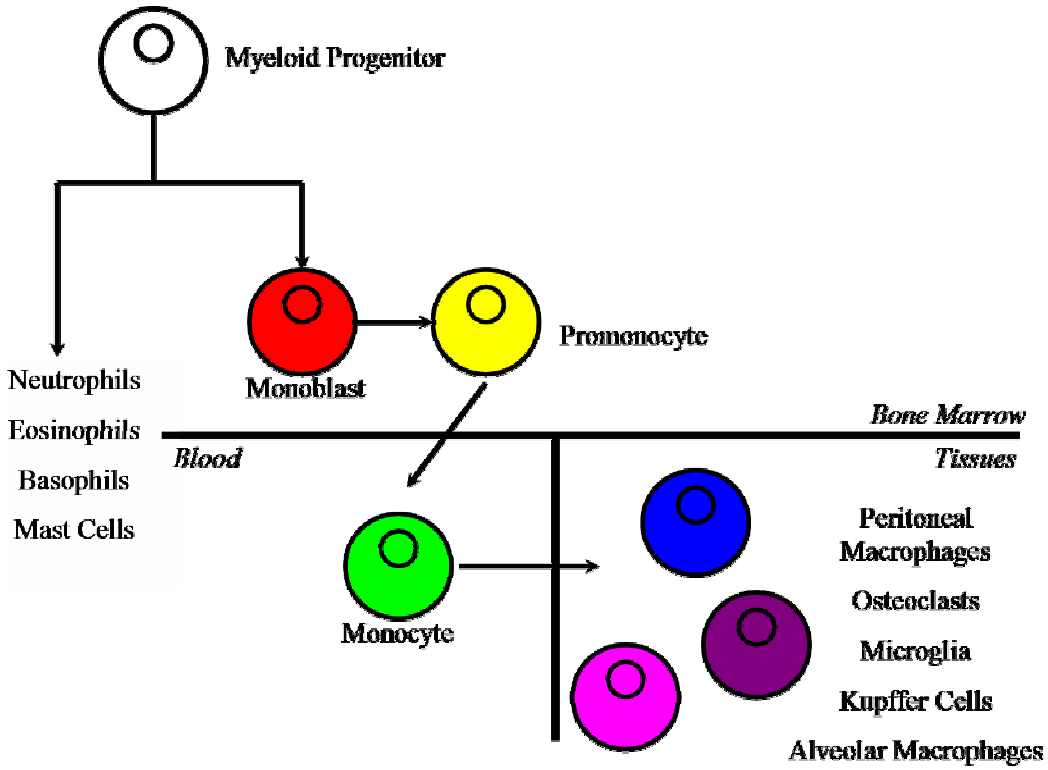

Figure1-7. Mononuclear Phagocyte System.

Enzymes	*Reactive Oxygen Intermediates*
Lysozyme	Superoxide
Lysosomal Acid Hydrolases	Hydrogen Peroxide
Neutral Proteases	Hydroxyl Radical
Complement Components	Nitric Oxide
C1, C4, C2, C3, C5, C3a, C3b, C5a, Bb	Peroxynitrite
Factor B, Factor D, Properdin	*Cytokines*
Coagulation Factors	IL-1, IL-6, IL-10, IL-12, IL-15
Tissue Factor	TNF-α, CXC chemokines
Prothrombin activator	*Enzyme/Cytokine Inhibitors*
FII, FVII, FIX, FX, FXII	IL-1 inhibitors, Protease Inhibitors

Table 1-2. Selection of the 100 + Substances that have been Reported to be Secreted from Macrophages. (Ross *et al.*, 2002)

At sites of infection/inflammation it has been observed that ATP is released leading to activation of P2Rs on macrophages that play a pivotal role in inflammation and immunomodulation. This includes the processing and release of cytokines, killing of intracellular pathogens by inducing apoptosis of host cells, chemoattraction and cell adhesion. Monocytes/macrophages express multiple P2R subtypes, i.e., monocytes express $P2Y_{1, 2, 4, 6, 11, 12, 13}$ and $P2X_{1, 4, 5, 7}$, and macrophages the same receptor subtypes except for $P2Y_{13}$ (Bours *et al.*, 2006).

ATP at the $P2X_7R$ as already stated has a much lower potency than compared to other purinergic receptors. This might suggest that this receptor is unlikely to be activated under resting/physiological conditions. Pro-inflammatory conditions where cell activation, stress, damage and lysis and changes to the extracellular milieu occur could create a situation where the $P2X_7R$ could be activated. The $P2X_7R$ has already been attributed to be involved in inflammatory conditions/diseases with knockout mice studies demonstrating that loss of the $P2X_7R$ leads to:

- Loss of ATP evoked IL-1β processing and secretion (Solle *et al.*, 2001)
- Attenuation of collagen induced arthritis (Labasi *et al.*, 2002)
- The loss of hypersensitivity in inflammatory (adjuvant-induced) and neuropathic (partial nerve ligation) pain models (Chessell *et al.*, 2005). Work which has been

further confirmed by the observation that administration of the $P2X_7R$ antagonist A-740003 to rats produced antinociception in a spinal nerve ligation model and attenuated tactile allodynia in both chronic constriction injury of the sciatic nerve and vincristin-induced neuropathy (Honore *et al.*, 2006).

- Changes in animal models of depression and anxiety (Basso *et al.*, 2008).

1.2 INNATE IMMUNE SYSTEM

As previously stated the focus of my research is based on the role of purinergic signaling in the initiation and modulation of immunity and inflammation with respect to macrophage responses. These phagocytic cells form part of the innate immune system which is the first line of defence against infectious disease. The innate immune system's primary role is to defend the host from infection by allowing immune cells to recognize and respond to pathogens in a non-specific manner. It however does not confer long-lasting protection/immunity to the host.

Upon activation of an immune cell following detection of a pathogen, several responses will occur including:

- Production of cytokines that will trigger a range of inflammatory responses.
- Initiation of coagulation.
- Pathogen phagocytosis and digestion.
- Apoptosis and clearance of infected/damage host cells.

1.2.1 Detection of Pathogens

In order for the immune system to work the host cells needs to be able to discriminate between self and pathogenic cells. The innate immune system does this by using a limited number of germline-encoded pattern recognition receptors (PRRs). These PRR's are able to recognize microbial components termed pathogen-associated molecular patterns (PAMPs) which are essential for microbial survival and therefore difficult for the pathogen to alter (Akira *et al.*, 2006). There is deemed to be four important families of pathogen sensor these are the Toll-like receptors (TLR), NOD-like receptors (NLR), Rig-I-like receptors and C-type lectin receptors. All of these receptors upon sensing a pathogen can induce and up-regulate a range of immune and inflammatory genes. These receptors are also found to be structurally conserved involving seven distinct domains: the LRR

(leucine-rich repeat) domain, the TIR (Toll-IL-1 receptor) domain, the NBS (nucleotide-binding site), the CARD (caspase recruitment domain), the PYD (pyrin domain), the helicase domain and the CTLD (C-type lectin domain)(Pålsson-McDermott *et al.*, 2007).

The most commonly known set of pattern recognition receptors are the TLRs which are able to recognize pathogens either at the cell surface or lysosome/endosome membranes (Kawai *et al.*, 2006). There have so far been 10 human TLRs identified (13 in mouse) and between them they are able to recognize a range of ligands such as bacterial lipopolysaccharide (LPS) by TLR4; viral and bacterial nucleic acids by TLR3, 7, 8 and 9; and glycosylphosphatidylinositol (GPI)-anchored proteins in parasites. The TLR signaling pathway loosely consists of a MyD88-dependent pathway common to all TLRs, and a MyD88-independent pathway that is selective to TLR3 and TLR4 (Figure 1-8) (Chen *et al.*, 2007). The MyD88-dependent pathway will result in the activation of the transcription factors $NF_{\kappa}B$ and AP-1 and therefore an increase in the expression of inflammatory cytokines such as IL-1β, TNFα and IL-6 (Medzhitov *et al.*, 1998). The MyD88-independent pathway or Trif-dependent pathway will result in the induction of type I IFN genes such as IFNβ, RANTES and IP-10 and activation of $NF_{\kappa}B$ and AP-1 (Yamamoto *et al.*, 2002).

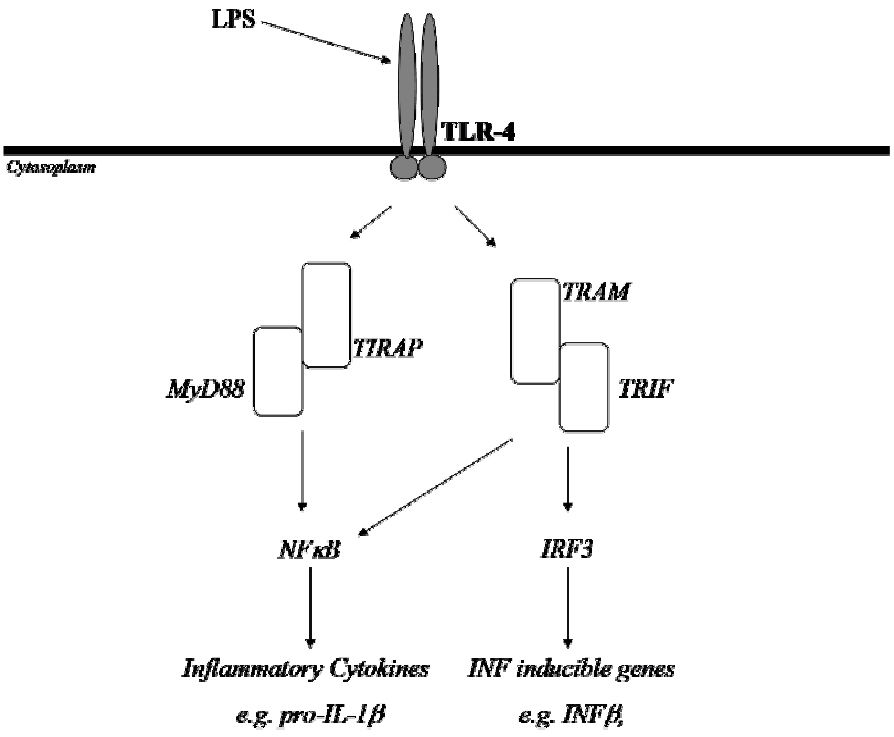

Figure 1-8. Schematic of TLR4 signaling through MyD88 Dependent & Independent Pathways.

The second major family of pattern recognition receptor is the NLRs which unlike the TLRs are cytoplasmic proteins that can clear the invading pathogen by up-regulating expression of chemokines such as MIP-2 and IL-8 (Vavricka *et al.*, 2004; Viala *et al.*, 2004) and cytokines such as IL-1β, IL-18 and IL-6 (Kufer *et al.*, 2005; Martinon *et al.*, 2002). Upon activation of an NLR, two major signaling pathways have found to be initiated (Wilmanski *et al.*, 2008). The first occurs when the NLR proteins Nod1 or Nod2 are activated by active moieties in bacterial peptidolycan. These proteins signal through receptor-interaction protein 2 (Rip2) which activates NF-κB and mitogen-activated protein kinases (MAPKs). The second occurs when NLRs such as NALP3, NALP1, IPAF or NAIP are activated leading to an association with apoptotic-associated speck-like protein (ASC) that will ultimately lead to the activation of caspase-1 (Figure 1-9). Caspase-1 has dual roles in that it is involved in the maturation/processing of IL-1β and the induction of programmed cell death of host cells (Brough *et al.*, 2007; Fink *et al.*, 2007).

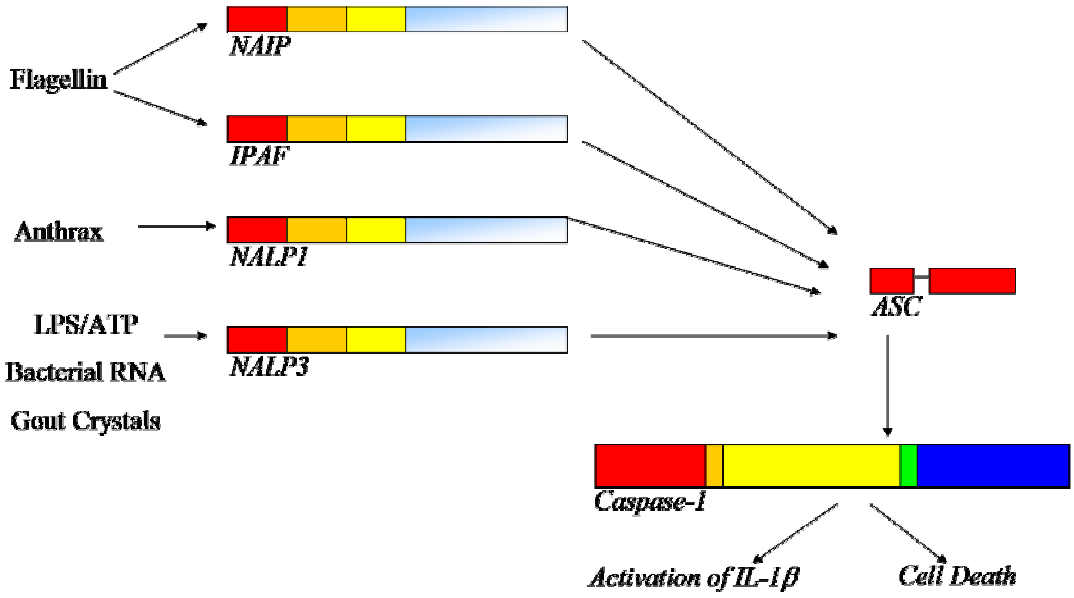

Figure 1-9. Schematic of NLR Signaling via the ASC-Dependent Pathway Resulting in Caspase-1 Activation.

1.2.2 Production, Secretion and Effect of Members of the Interleukin-1 Superfamily

IL-1 is produced in response to many stimuli including LPS, other microbial products, cytokines (TNFα, IFNγ, GM-CSF, and IL-2), T-cell/antigen presenting cell interaction and immune complexes (Dinarello, 1996). Both IL-1α and IL-1β are translated as 31kD

leaderless secretory pro-peptides. IL-1α is active in this pro form; however IL-1β needs to undergo a proteolytic step to become active. This cleavage is mediated by active caspase-1 within the cytosol of the cell leading to the generation of a 17kD mature form of IL-1β (Cerretti *et al.*, 1992). Furthermore IL-18 which is synthesized as a 24kD pro-peptide is cleaved by caspase-1 to form a mature 18kD form (Ghayur *et al.*, 1997; Gu *et al.*, 1997) and IL-33 an IL-1β-like cytokine acting at the ST2 receptor has been observed to be processed by caspase-1 (Schmitz *et al.*, 2005).

Once IL-1 cytokines have been synthesized they then require to be released, however they do not follow the classical endoplasmic reticulum/Golgi secretory pathway as they lack a signal peptide (Dinarello, 1996). In the case of LPS induced synthesis of IL-1 propeptides, a second stimulus is required to evoke both the production of mature/active cytokines and the release of both the pro and mature peptides. The physiological second stimulus has been reported to be activation of the $P2X_7R$ by ATP (Ferrari *et al.*, 2006; Pelegrin *et al.*, 2008).

Upon release of IL-1α and IL-1β they are able to bind and activate the IL-1RI receptor. This receptor belongs to the same super family as the TLRs (IL-1 receptor/TLR receptor superfamily) and the IL-18 receptor (IL-18R); all of which have striking sequence similarity in their cytosolic regions (Dunne *et al.*, 2003; Rock *et al.*, 1998). Activation of this receptor can induce the expression of many genes via activation of protein kinase cascades leading to the modulation of transcription factors such as NF-κB, AP-1, ATF-2 and NF-IL6 and therefore inducing the expression of immune and inflammatory genes (Akira *et al.*, 1990; Chedid *et al.*, 1991; Krasnow *et al.*, 1991; Welsh, 1996). The original responses evoked by IL-1 were reported to be the elicitation of inflammatory responses, induction of fever and increased production of acute phase proteins (Dinarello *et al.*, 1983). The inflammatory responses evoked by IL-1 include (i) promotion of leukocyte extravasation by inducing adhesion receptors on vascular endothelium and stimulating chemokine production, (ii) production of other cytokines, (iii) accumulation of arachidonic acid metabolites and (iv) the up-regulation of inducible nitric oxide synthase (iNOS).

1.2.3 Activation of Coagulation & Cross-Talk with Inflammation

Damage to blood vessels and capillaries will induce three mechanisms that promote haemostasis these are (i) vasoconstriction, (ii) platelet activation and adhesion with release of serotonin, ADP and thromboxane A_2 (TxA_2) and (iii) coagulation. The coagulation cascade has two pathways (Figure 1-10) termed the contact activation pathway (intrinsic) and the tissue factor (TF) pathway (extrinsic); the primary pathway for maintenance of normal haemostasis. Both pathways are a series of reactions in which inactive enzyme precursors (zymogens) of a serine protease and a glycoprotein co-factor are activated to become active components which catalyze the next reaction in the cascade. The pathways will ultimately lead to the activation of the final common pathway whereby the activation of factor X (FX), thrombin and fibrin occurs finally leading to the formation of a fibrin clot.

The coagulation cascade and innate immunity are intimately linked, to the point that it is now believed that the two systems co-evolved from a common ancestral substrate early in eukaryotic development (Opal *et al.*, 2003). Inflammatory signals that induce immune activation will also evoke procoagulant responses; something that is evident in systemic inflammatory states where activation of the extrinsic coagulation cascade appears to be an essential component in the development of multi-organ failure.

Both pathways of the coagulation cascade can be activated via inflammatory/immune responses. The contact factors of the intrinsic coagulation cascade are able to recognise damaged host cell membranes, foreign substances (including LPS) and endothelial abnormalities; (Levi *et al.*, 1999; Opal *et al.*, 2003; Pixley *et al.*, 1993). The extrinsic/TF dependent pathway is usually activated when vascular damage occurs leading to contact of blood cells with extravascular TF expressing cells. TF expression however can be induced on monocytes/macrophages systemically during microbial invasion by endotoxins, cytokines (e.g. IL-1α and IL-1β) and C-reactive protein (Levi, 2003; Levi *et al.*, 2003; Osnes *et al.*, 1996). It has been hypothesized that localized TF expression and subsequent induction of coagulation might occur in order to aid the containment of infection/inflammation.

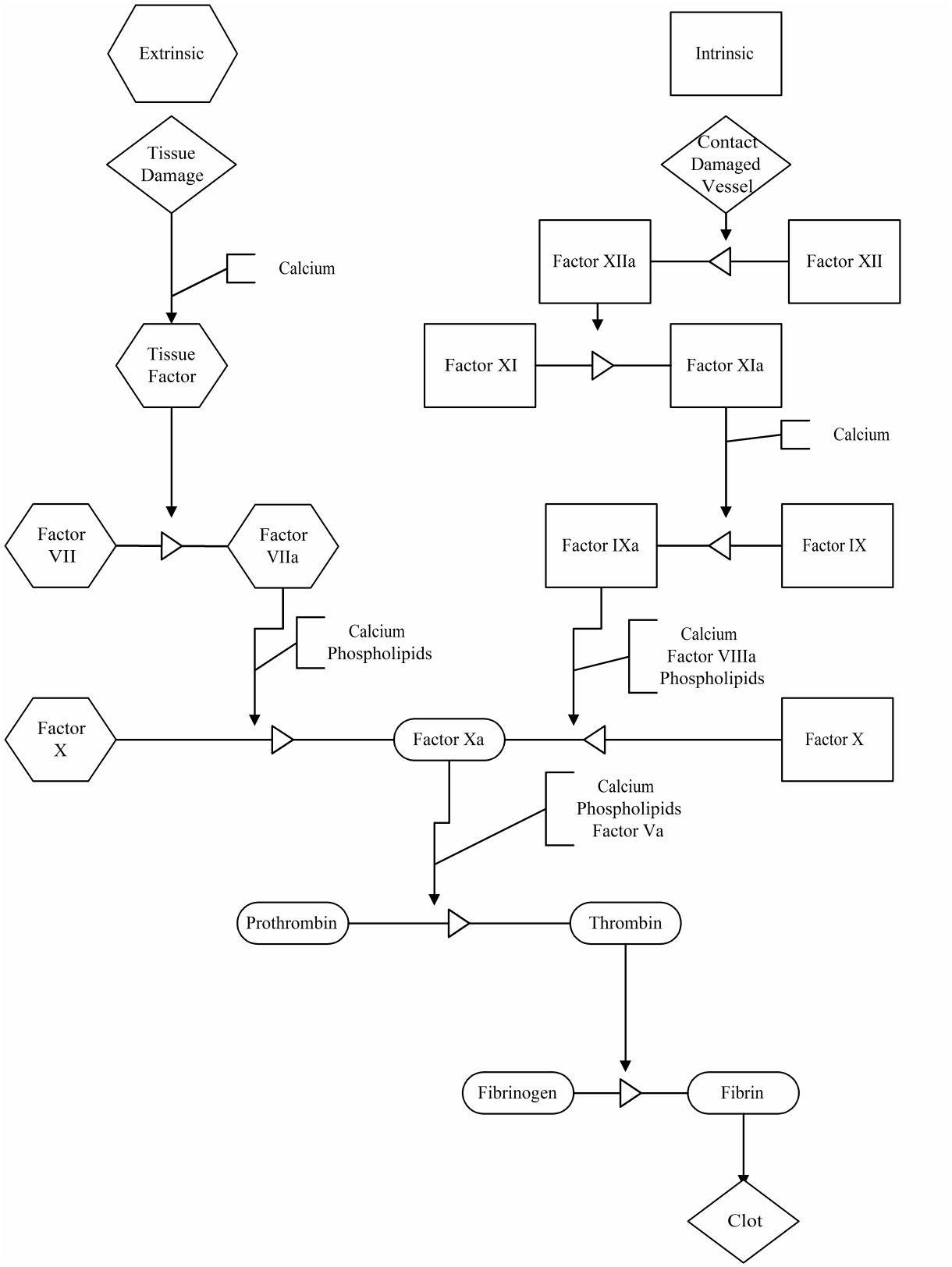

Figure 1-10. Schematic of the Extrinsic & Intrinsic Coagulation Cascades Leading to Clot Formation.

The link between inflammation and coagulation does not only work in one direction; coagulation is able to induce inflammation. Activation of the coagulation cascade results in the formation of several proteases, some of which are able to activate their own receptors. Thrombin, factor Xa (FXa) and the TF-factor VIIa (TF-FVIIa) complex have all been demonstrated to activate pro-inflammatory processes via the protease-activated receptors (PARs) (Cirino *et al.*, 2000). The PARs are GPCRs that possess a sequestered integral ligand that is tethered to the amino-terminus of its extracellular domain. Thrombin is able to cleave and activate PAR_1, PAR_3 and PAR_4, whereas FXa and TF-FVIIa can activate PAR_2 (Ossovskaya *et al.*, 2004). Activation of cells by these coagulation factors has been observed to increase proinflammatory cytokine production (IL-1, IL-6, MCP-1) and iNOS (Opal, 2003). Loss of PAR_1 has been observed to result in a reduction of arthritis severity, reduced inflammation in glomerulonephrtis and carrageenan models and impaired thrombin induced pulmonary vascular leakage (Cunningham *et al.*, 2000; Vogel *et al.*, 2000; Yang *et al.*, 2005). Furthermore loss of PAR_2 has been observed to reduce oedema and infiltration of inflammatory cells in models of allergic dermatitis (Kawagoe *et al.*, 2002), reduce eosinophil infiltration and hypereactivity in allergic airway inflammation (Schmidlin *et al.*, 2002) and protect against adjuvant induced arthritis (Ferrell *et al.*, 2003).

1.2.4 Pathogen Clearance

Invading pathogens are required to be removed from the blood and tissues in order to halt inflammation and further cellular damage. Phagocytosis is the process by which leukocytes recognise and ingest particles and pathogens and is critical for innate immunity. Macrophages upon recognition of an invading pathogen will undergo cytoskeletal changes in order to engulf an evading microbe and trap it within a phagosome which will rapidly become a digestive organelle resulting in the death of the invading pathogen (Greenberg *et al.*, 2002). Killing of this entrapped pathogen can occur via oxygen independent and dependent processes. The oxygen independent process involves fumigating the pathogen with toxic proteases and enzymes. The oxygen dependent method involves pathogen killing by reactive oxygen and nitrogen species (ROS and RNS). The major generator of these metabolites in phagocytic cells is NADPH Oxidase 2 (NOX2) which is able to generate superoxide (O_2^-). O_2^- is then available to react with NO to form peroxynitrite ($ONOO^-$) or to be converted to hydrogen peroxide (H_2O_2). H_2O_2 in combination with chloride ions is able to form the very cytotoxic product hypochlorous acid (HOCl) when in the presence of myeloperoxidase (MPO).

1.2.5 Apoptosis and Clearance of Infected/Damaged Host Cells

During inflammation cell damage and death occurs, depending on the type of cell death initiated the outcome can be either non-inflammatory or pro-inflammatory. Apoptotic cell death is a controlled and non-inflammatory form of cell death. Dramatic biochemical and cell biological events occur within an apoptotic cell and ultimately results in its recognition and removal by phagocytes prior to it becoming necrotic and its inflammatory contents spilling into surrounding tissues. Apoptosis can be initiated by two main pathways the death receptor (extrinsic) pathway and the mitochondrial (intrinsic) pathway (Figure 1-11). Both pathways result in the activation of caspases that are able to cleave specific target proteins resulting in the morphological and biochemical changes associated with apoptosis. For example DNA laddering a classic marker of apoptosis occurs by cleavage of genomic DNA between nucleosomes by the nuclease caspase-activated DNase (CAD). CAD is usually present in living cells bound to its inhibitor (ICAD), caspase-3 and caspase-7 can cleave off ICAD, therefore resulting in the release and activation of CAD (Enari *et al.*, 1998; Fink *et al.*, 2005). Furthermore caspases have been reported to be involved in the process of allowing the recognition and ultimately removal of this dying cell. This involves the translocation of the anionic phospholipid phosphatidylserine (PS) from the inner to the outer leaflet of the plasma membrane. PS is not expressed on resting cells and therefore provides a cell surface marker for discrimination of "self" vs. other by phagocytes (Naito *et al.*, 1997).

1.2.6 The Innate Immune System and Disease

The innate immune system plays a vital role in the elimination of pathogens. However aberrant activation can result in severe consequences including the induction of chronic inflammatory diseases, neurodegeneration and cancer. An important part of the innate immune system is the production and secretion of the IL-1 cytokines and the activation of caspases. Both of these play important roles in the body's response to pathogen invasion. IL-1β has been implicated to have a role in many diseases including RA (Dayer *et al.*, 2001; Eastgate *et al.*, 1988), atherosclerosis (Kirii *et al.*, 2003), Alzheimer's disease (Deniz-Naranjo *et al.*, 2008), multiple sclerosis (Yiangou *et al.*, 2006) and neuropathic pain (Sommer *et al.*, 2004). Caspase-1 has been implicated to play a role in Huntington's chorea (Wang *et al.*, 2005), amyotrophic lateral sclerosis (Li *et al.*, 2000) and Parkinson's disease (Kahns *et al.*, 2003). Mutations leading to overactivation of the caspase-1 activator;

NALP3 have been observed to cause autoinflammatory disorders (Neven *et al.*, 2004), which are associated with recurrent inflammatory episodes generally associated with fever, arthralgia and urticaria.

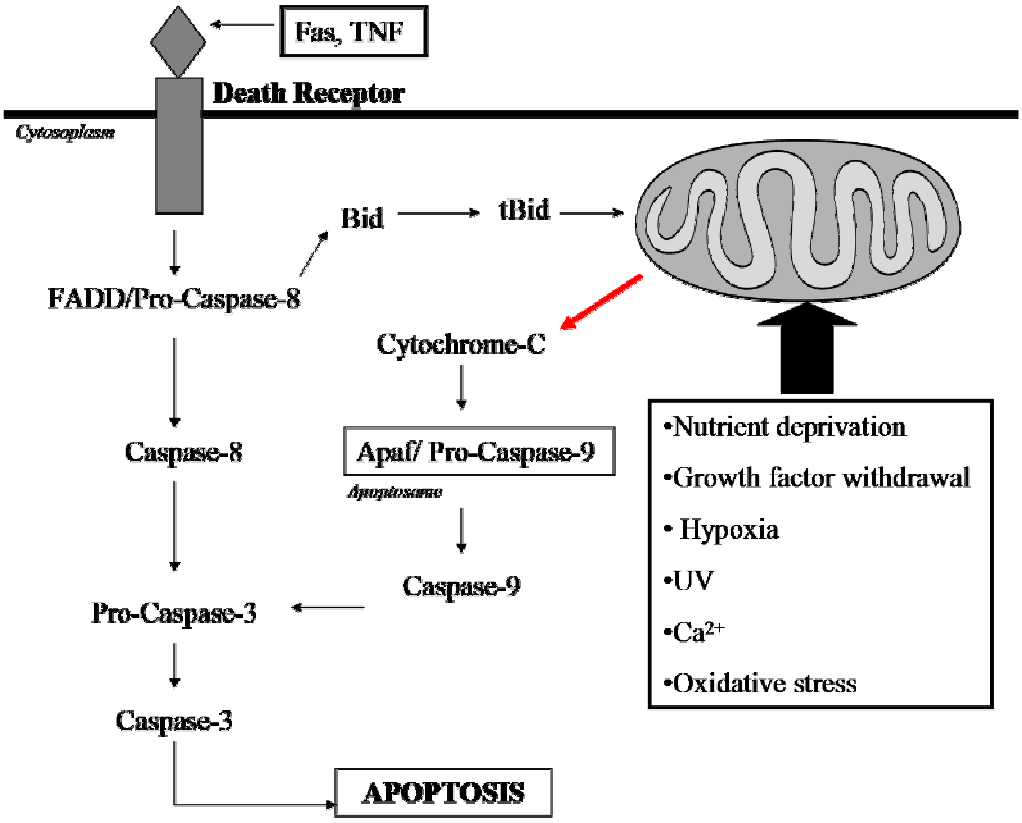

Figure 1-11. Simplified Model of Extrinsic and Intrinsic Apoptotic Cell Death. Intrinsic apoptosis involves the integration and propagation of death signals originating inside the cell by the mitochondria (Sitailo *et al.*, 2002). Cytochrome-c will be released (red arrow) from the mitochondria resulting in the formation of the Apaf containing apoptosome, which will recruit and activate caspase-9 (Li *et al.*, 1997b). Caspase-9 is then able to directly cleave/activate caspase-3. Extrinsic apoptosis is initiated when a death receptor ligand (TNF, Fas etc) binds to and activates a death receptor. This induces receptor oligomerization and recruitment of adaptor/scaffold proteins including pro-caspase-8 and FADD. Caspase-8 will undergo oligomerization and autoactivation, resulting in either direct cleavage/activation of caspase-3 or truncation of Bid (tBid) (Yin *et al.*, 1999) which can translocate to the mitochondria and induce cytochrome-c/caspase-9 induced caspase-3 activation.

1.3 AIMS

The overall idea behind my work was to examine the role and mechanisms of purinergic signaling in macrophages leading to the propagation, mediation and amplification of innate immune and inflammatory responses. Based on this idea and the previous literature a series

of aims where formulated and are listed below, further detail in to each of the aims and reasoning for them can be found at the beginning of each results chapter.

- Pharmacology of the $P2X_7R$ on macrophages and the effect of the extracellular milieu on $P2X_7R$ function.
- Role of extracellular ATP on induction of morphological changes and cell death.
- Role of extracellular ATP in evoking pro-coagulant responses.
- Characterisation of ATP evoked generation of ROS.
- Investigation of the signaling pathway/s from $P2X_7R$ activation to the generation of pro-inflammatory cytokines.

CHAPTER 2

MATERIALS AND METHODS

2.1 MATERIALS

2.1.1 General Reagents

REAGENT	SUPPLIER
Acetone	Sigma-Aldrich®, UK
Acrylamide Mix (30 %, Protogel)	Fisher Scientific UK
Albumin from Bovine Serum (BSA)	Sigma-Aldrich®, UK
Ammonium Persulfate	Acros Organics
Apyrase Grade VI	Sigma-Aldrich® UK
ATP Di-Sodium Salt Grade II	Sigma-Aldrich® UK
BzATP	Sigma-Aldrich® UK
Cadmium Chloride ($CdCl_2$)	Sigma-Aldrich® UK
Calcium Chloride Dihydrate ($CaCl_2$)	Sigma-Aldrich® UK
Copper (II) Chloride ($CuCl_2$)	Sigma-Aldrich® UK
Cut-Off Filters 3K Nanosep	Pall (VWR UK)
D-(+)-Glucose	Sigma-Aldrich® UK
Digitonin	Sigma-Aldrich® UK
EDTA	Fisher Scientific UK
EGTA	Sigma-Aldrich® UK
Enhanced Chemiluminescent Advance™ (ECL)	GE Healthcare Life Sciences UK
Formaldehyde (37 %)	Sigma-Aldrich®, UK
Glutaraldehyde	Sigma-Aldrich®, UK
Glycine	Fisher Scientific UK
Griess Reagent	Sigma-Aldrich®, UK
HEPES	Sigma-Aldrich® UK
Magnesium Chloride ($MgCl_2$)	Sigma-Aldrich® UK
Mercury (II) Chloride ($HgCl_2$)	Sigma-Aldrich® UK
Methanol (MeOH)	Fisher Scientific UK
Nitrocellulose Membrane (0.2 μm)	BIO-RAD UK
Osmium Tetroxide	Sigma-Aldrich®, UK
Phosphate Buffered Saline (PBS)	Sigma-Aldrich® UK
Pluronic Acid F-127	Invitrogen™ UK

Potassium Chloride (KCl)	Sigma-Aldrich® UK
Precision Plus Protein Kaleidoscope Standards	BIO-RAD UK
Probenecid	Sigma-Aldrich® UK
Protease Inhibitor Cocktail General Use (PIC)	Sigma-Aldrich® UK
Skimmed Milk Powder	OXOID (Sigma-Aldrich® UK)
Sodium Chloride (NaCl)	Sigma-Aldrich® UK
Sodium Dodecyl Sulfate (SDS)	Fisher Scientific UK
Sodium Hydroxide (NaOH)	Sigma-Aldrich® UK
Sodium Nitrite	Sigma-Aldrich®, UK
TEMED	Fisher Scientific UK
Tris-HCl	Fisher Scientific UK
Triton-X 100	Sigma-Aldrich® UK
Zinc Chloride ($ZnCl_2$)	(FLUKA) Sigma-Aldrich® UK

2.1.2 Antibodies

ANTIBODY	SUPPLIER
Alexa 488-conjugated $(Fab)_2$ fragments of goat anti-rabbit IgG	Invitrogen™, UK
Anti-$P2X_7R$	Alamone Labs, Jerusalem, Israel
Caspase-1 p10 (M-20) PAb	Santa-Cruz Biotechnology, UK
Mouse IL-1β MAb	Thermo Scientific, UK
Polyclonal Rabbit Anti-Mouse IgG/HRP	DakoCytomation, UK
Polyclonal Swine Anti-Rabbit IgG/HRP	DakoCytomation, UK
Rabbit Anti- Mouse anti-TF Antibody	Axis-Shield, UK
Rabbit IgG	Invitrogen™, UK

2.1.3 Cell Culture

REAGENT	SUPPLIER
Dulbecco's Modified Eagle Medium: Nutrient Mixture F-12 1:1 (DMEM-F12)	Invitrogen™ UK
Foetal Bovine Serum (FBS)	Invitrogen™ UK
FuGENE 6	Roche UK

LPS from *Escherichia coli* 055:B5	Sigma-Aldrich® UK
Murine Macrophage Colony Stimulating Factor (MCSF)	Sigma-Aldrich® UK
Penicillin-Streptomyosin	Invitrogen™ UK
RPMI-1640	Sigma-Aldrich® UK
Trypsin 0.05 % with EDTA	Invitrogen™,UK

2.1.4 Fluorescent Indicators

REAGENT	SUPPLIER
2,7 Dichlorodihydrofluorescein diacetate (H_2DCF-DA)	Invitrogen™ UK
4',6-diamidino-2-phenylindole (DAPI)	Invitrogen™, UK
Annexin-V-Alexa Fluor® 488	Invitrogen™, UK
Ethidium Bromide (EtBr)	Fisher Scientific UK
Fluo-4 AM	Invitrogen™ UK
L-Glutamine (200mM)	Invitrogen™ UK
Phalloidin-Alexa Fluor® 546	Invitrogen™, UK

2.1.5 Inhibitors

REAGENT	SUPPLIER
2,4-Dinitrochlorobenzene (DNCB)	Sigma-Aldrich® UK
3-Morpholinosydnonimine, HCl (SIN-1)	Calbiochem® UK
A438079-HCl	Tocris Bioscience UK
Allopurinol	Sigma-Aldrich® UK
Apocynin	Sigma-Aldrich® UK
Auranofin	BIOMOL® International UK
Brilliant Blue G (BBG)	Sigma-Aldrich® UK
Carbenoxolone	Sigma-Aldrich® UK
CGS 15943	Tocris Bioscience UK
Diphenyleneiodonium (DPI)	Sigma-Aldrich® UK
KN-62	Calbiochem® UK
Mn-cpx 3	Calbiochem® UK
Myxothiazol	Sigma-Aldrich® UK

Rotenone	Sigma-Aldrich® UK
Superoxide Dismutase, Bovine (SOD)	Sigma-Aldrich® UK
Suramin Sodium Salt	Sigma-Aldrich® UK
Z-YVAD-FMK	Cambridge Bioscience UK

2.1.6 Coagulation Factors and Reagents

REAGENT	SUPPLIER
Annexin V from human placenta	Sigma-Aldrich®, UK
Bovine FVa	Cambridge Bioscience, UK
Bovine FX	Cambridge Bioscience, UK
Bovine FXa	Cambridge Bioscience, UK
Human FVIIa	Cambridge Bioscience, UK
Human Prothrombin	Cambridge Bioscience, UK
S2238™	Instrumentation Laboratories, UK
S2765™	Instrumentation Laboratories, UK

2.1.7 Kits

KIT	SUPPLIER
CytoTox-96™	Promega, UK
Cytotoxicity Detection Kit	Roche, UK
CytoTox-One™	Promega, UK

2.2 EXTERNAL SOLUTIONS[2]

2.2.1 Physiological Salt Solution

Reagent	Concentration (mM)
NaCl	147
HEPES	10
Glucose	12
$CaCl_2$	2
KCl	2

[2] ATP was made up as a 50mM stock in the different external solutions and the pH readjusted to 7.3 using NaOH.

$MgCl_2$	1

Used for the majority of assays unless stated. pH 7.3 with NaOH

2.2.2 Calcium-Free Salt Solution[3]

Reagent	Concentration (mM)
NaCl	147
HEPES	10
Glucose	12
EGTA	1
KCl	2
$MgCl_2$	1

pH 7.3 with NaOH

2.2.3 Nominal Calcium/Magnesium Salt Solution[4]

Reagent	Concentration (mM)
NaCl	147
HEPES	10
Glucose	12
KCl	2

pH 7.3 with NaOH

2.3 CELL CULTURE

2.3.1 RAW264.7 Murine Macrophage Culture

RAW264.7 cells (ATCC, Manassas, VA) were maintained in DMEM:F12 containing 10 % heat inactivated FBS, 2 mM L-glutamine, 100 U ml^{-1} penicillin and 100 µg ml^{-1} streptomycin (complete culture medium) at 37 °C in a humidified atmosphere of 5 % CO_2 and 95 % air. Cells were subcultured by mechanically scrapping cells in to culture medium and resuspended into fresh complete medium at a subcultivation ratio of 1:3 to 1:6 with medium being replaced every 2 to 3 days. Cells for experimental assays were mechanically scraped in to culture medium and subsequently centrifuged at 240 *x*g (S4180 rotor,

[3] Potentially nM levels of Ca^{2+} present in Calcium-free Salt Solution
[4] Potentially µM levels of Ca^{2+} and Mg^{2+} present in Nominal Ca^{2+}/Mg^{2+} Salt Solution

Beckman GS-15R) for 4 minutes at room temperature (RT). Waste medium was aspirated off and cells resuspended into fresh complete medium for counting and re-seeding.

2.3.2 HEK293 Cell Culture

Human embryonic kidney (HEK) 293 cells (ECACC, UK) were maintained in complete culture medium at 37 °C in a humidified atmosphere of 5 % CO_2 and 95 % air. Cells were harvested for subculture and experimental assays by rinsing cells in sterile PBS followed by incubation with 0.05 % Trypsin/EDTA for 5 minutes (37 ^{o}C). Trypsin/EDTA was stopped by addition of complete medium and cells were harvested from the culture vessel surface by pipetting up and down. Cells were subsequently centrifuged at 240 *x*g (S4180 rotor, Beckman GS-15R) for 4 minutes (RT). Waste medium was aspirate off and cells re-suspended into fresh complete medium for counting and re-seeding. Cells were seeded at 3- 5 x 10^5 cells/cm^2 for maintenance and split upon reaching 70-80 % confluence.

2.3.3 HEK293 Transient Transfections

Plasmid DNA	Accession Number	Source
mP2X7R-pcDNA3 (P451)	AJ489297	Prof A Surprenant
rP2X7R-pcDNA3	CAA65131	Prof A Surprenant

HEK293 cells were seeded at a density of 1.5 x 10^4 cells ml^{-1} in to a sterile black-walled cell-culture treated 96 well plate and maintained in complete medium overnight. Complete medium was removed from cells and replaced with antibiotic free complete culture medium. Cells were transfected with plasmid DNA using FuGENE-6 at a 6:1 ratio (FuGENE-6:DNA) following the manufacturer's protocol. Mock transfectants, omitting DNA were used as controls. Transfection reagent was removed 24 hours post-transfection and cells used in experimental assays within 24 hours after reagent removal.

2.3.4 J774.2 Murine Macrophage Culture

J774.2 cells (ECACC, UK) were maintained between 3 – 9 x 10^5 cells ml^{-1} in complete culture medium at 37 °C in a humidified atmosphere of 5 % CO_2 and 95 % air. Cells were subcultured by mechanically scrapping cells in to culture medium and resuspended into fresh complete medium at a subcultivation ratio of 1:3 to 1:6 with medium being replaced every 2 to 3 days. Cells for experimental assays were mechanically scraped in to complete

culture medium and subsequently centrifuged at 240 *x*g (S4180 rotor, Beckman GS-15R) for 4 minutes (RT). Waste medium was aspirated off and cells resuspended into fresh complete medium for counting and re-seeding. For LPS priming[5], cells plated overnight in complete culture medium were incubated for 4-6 hours at 37 ^{o}C with 1 μg ml^{-1} LPS.

2.3.5 Isolation, Generation and Culture of Murine Bone-Marrow Derived Macrophages

Mouse bone marrow cells were collected from femurs of C57BL/6 mice (8-12 wks) by flushing with 2 ml of bone marrow medium consisting of RPMI-1640 containing 15 % (v/v) heat inactivated FBS, 2 mM L-glutamine, 100 U ml^{-1} penicillin and 100 μg ml^{-1} streptomycin using a 25-gauge needle. Cell suspensions were centrifuged at 240 *x*g (S4108 rotor, Beckman GS-15R) for 10 minutes at RT. Cells were resuspended in bone marrow medium (10 ml / mouse) and passed up and down six times through a 19-gauge needle to disperse cell clumps. Adherent bone marrow cells were removed by incubation at 37 ^{o}C for 4 – 6 hours in T25 flasks (5 ml cell suspension / flask). The non-adherent bone marrow cells were placed in fresh T25 flasks and M-CSF added to give a final concentration of 10 ng ml^{-1} (Lin *et al.*, 2001). Cells were maintained in culture at 37 °C in a humidified atmosphere of 5 % CO_2 and 95 % air. Media and M-CSF was completely changed on day five and experimental assays performed on day seven. For LPS[3] priming, cells plated overnight in bone marrow medium with M-CSF were incubated for 4-6 hours at 37 ^{o}C with 1 μg ml^{-1} LPS. Bone-marrow cells from gp91phox$^{-/-}$ and p47phox$^{-/-}$ mice (C57BL/6) were a generous gift from Dr A Cave and Professor A Shah (Cardiovascular Division, Kings College London, UK) (Bendall *et al.*, 2002; Li *et al.*, 2004; Pollock *et al.*, 1995).

2.3.6 Freezing[6]

Harvested cells were resuspended at 1 x 10^{6} cells ml^{-1} in complete medium containing 10 % DMSO (RAW264.7, J774.2) or glycerol (HEK293) and an additional 10 % FBS. 1 ml volumes were aliquoted into cryotubes which were subsequently placed into a 'Mr. Frosty' (filled with 250 ml propan-2-ol). Cells were incubated at -80 ^{o}C overnight before long-term storage in liquid nitrogen.

[5] For Chapters 6 and 7 where ROS generation and its role in the processing and release of IL-1β were examined, cells were required to be activated with LPS to induce the expression of pro-IL-1β.

[6] Cell line integrity was maintained by freezing down low passage stocks (<2 subcultures) which were thawed for use once cells in current use reached passaged 10.

2.3.7 Thawing

Cryotubes were removed from liquid nitrogen and thawed at 37 ^{o}C. Cells were removed from cryotubes and diluted into 5 ml of complete culture medium in a drop-wise manner. Cells were centrifuged at 240 *x*g (S4180 rotor, Beckman GS-15R) for 4 minutes (RT) to removed cell freezing medium and resuspended in 5ml of complete medium and seeded into a T25 flask.

2.4 PURINERGIC RECEPTOR FUNCTION

2.4.1 Intracellular Calcium Concentrations

Cell seeding conditions -

Density: 1.5 x 10^6 cells ml^{-1}

Culture Vessel: Sterile black-walled cell-culture treated 96 well plates

Media: 100 µl complete culture medium

Duration: 17 – 24 hours

Cells (1.5 x 10^5) were loaded with 5 µM Fluo-4AM (DMEM:F12) in the presence of probenecid (2.5 mM) to inhibit dye leakage and sequestration via organic anion transporters (Di Virgillio *et al.,* 1990), apyrase (0.32 U ml^{-1}) to breakdown ATP/ADP released by cells in order to inhibit desensitisation of P2 receptors and pluronic acid (0.2 %) to enhance dye solubility and dye uptake for 30 minutes at 37 ^{o}C, under limited light conditions. Excess Fluo-4AM was aspirated from the cells and replaced with external solution containing probenecid (2.5 mM). Cells were left to rest for 10 minutes (37 ^{o}C). Antagonists were added 5 minutes prior to ATP application. ATP was applied using Fluostar optima injection system and Fluo-4 excited at 485 nm with fluorescence collected at 520 nm every 3-10 s using a multimode platereader (Fluostar Optima, BMG Labtech, UK). At the end of each test run 15 µM digitonin was applied to lyse cells and therefore obtain maximum Fluo-4 fluorescence readings.

Each experimental sample was performed in duplicate and values were normalized to baseline and maximum fluorescence readings (Equation 1). Peak responses were used to construct individual concentration-response curves. Final concentration-response curves were constructed by normalizing individual curves to maximum ATP evoked responses

(Equation 2). Curve fitting was performed using Prism Version 4 (GraphPad Software, San Diego CA) using a four parameter logistic equation (Equation 3).

$$(1) \qquad y = \left(\frac{F - F_0}{F_{\max}} \right) \times 100$$

Where F is fluorescence, F_0 is fluorescence at time 0 and F_{max} is maximum fluorescence.

$$(2) \qquad y = \left(\frac{R}{R_{\max}} \right) \times 100$$

Where R is the response and R_{max} is the maximal response evoked by the agonist in control conditions.

$$(3) \qquad y = baseline + \frac{\alpha}{1 + 10^{(LogA_{50} - x)n_H}}$$

Where x is the logarithm of the molar concentration of the drug, α is the maxima (max - baseline), $logA_{50}$ is the half maximal response and n_H is the Hill slope.

2.4.2 Pore Formation

Cell seeding conditions -

Density: 1.5 x 10^6 cells ml^{-1}
Culture Vessel: Sterile black-walled cell-culture treated 96 well plates
Media: 100 µl complete culture medium
Duration: 17 – 24 hours

Pore formation as a result of prolonged $P2X_7R$ activation was measured by assessing the influx of EtBr (394 Da). EtBr upon entry in to the cell is able to bind nucleic acids and produce a fluorescent signal. Cells were washed in to external solution (37 ^oC) containing 25 µM EtBr and divalent cations/inhibitors where appropriate. Cells were left to rest for 5 minutes (37 ^oC) prior to ATP application. EtBr was excited at 544 nm with fluorescence

collected at 590 nm using a multimode platereader (Fluostar Optima, BMG Labtech, UK). At the end of each test run 0.2 % Triton-X 100 was applied in order to obtain maximum permeabilisation (EtBr fluorescence) readings.

Each experimental sample was performed in triplicate and values were normalized to baseline and maximum fluorescence readings (Equation 1). Linear regression between t = 0 and t = 15 minutes of agonist application was used to determine rates of EtBr influx (Prism Version 4, GraphPad Software, San Diego CA). Final concentration-response curves were constructed by normalizing individual curves to maximum ATP evoked responses (Equation 2) in the control salt solution. Curve fitting was performed using Prism Version 4 (GraphPad Software, San Diego CA) using a four parameter logistic equation (Equation 3).

Where addition of divalent cations to the external solution resulted in an increase in ATP/BzATP pEC_{50} values, ATP^{4-} concentrations were calculated in order to assess effects of the test cation independently from those due to chelation of ATP^{4-}. ATP^{4-} concentrations were calculated from total ATP concentrations using Webmaxc Standard (Stanford, USA) (Patton *et al.*, 2004). The K_d value of BzATP was assumed to be the same as ATP (Virginio *et al.*, 1997) for calculation of free $BzATP^{4-}$ concentrations.

2.4.3 Cytotoxicity

Cell seeding conditions -

Density: 1.5 x 10^6 cells ml^{-1}
Culture Vessel: Sterile clear-walled cell-culture treated 96 well plates
Media: 100 µl complete culture medium
Duration: 17 – 24 hours

Cell death determined as total and irreversible loss of cell membrane integrity was evaluated by measuring the release of cytosolic lactate dehydrogenase (LDH) from cells (1.5 x 10^5 cells) using either the Cytotox-96™ assay (Promega, UK), Cytotox One™ assay (Promega, UK) or Roche Cytotoxicity Detection Kit (Roche, UK) following the manufacturers protocol. Cells were washed into external solution (37 ^oC) containing

divalent cation/inhibitors where appropriate. ATP was applied and cells incubated for various times (37 ^{o}C). Supernatant was removed and incubated with LDH substrate and read using a multimode platereader (Fluostar Optima, BMG Labtech, UK) (Cytotox-96™ and Roche Cytotoxicity at 490nm absorbance, Cytotox One™ at Ex/Em of 560nm/590nm). Total cellular LDH was determined by the addition of Triton-X 100 (0.2 %) to untreated cells. Each experimental sample was performed in triplicate and values were normalized to zero LDH release (cell-free external solution) and expressed as a percentage of total cellular LDH.

2.5 CELL MORPHOLOGY

2.5.1 Scanning Electron Microscopy[7]

Cell seeding conditions -

Cell No: 30,000 cells
Culture Vessel: VWR® Micro 13 mm Round No.1 Cover Glass
Media: Standard culture medium
Duration: 17 – 24 hours

RAW264.7 cells (3 x 10^5 ml^{-1}) in standard culture medium were pipetted (100 µl) on to VWR® Micro 13 mm Round No.1 Cover Glass sat in sterile cell walled cell culture treated 24-well plates. Cells were left to adhere for 1 hour (37 ^{o}C) before flooding the well with standard culture medium and leaving in the incubator overnight. Standard culture medium was aspirated from cells and cells washed with external solution. Cells were then incubated (37 ^{o}C) in external solution in the absence or presence of ATP (1 mM, 10 minutes) before fixing with 1 % glutaraldehyde for 30 minutes at RT. Cover glass was washed (x3) with PBS and post-fixed in 1 % osmium tetroxide in PBS. Cells were then sequentially dehydrated in increasing concentrations of acetone (50–100 % in dH_20) and critical point dried for 15 minutes. Cover glasses were mounted on SEM holders and sputter-coated with gold before being viewed using a JEOL JSM-6480-LV electron microscope.

2.5.2 Live Cell Tracking of ATP Induced Morphological Changes

Cell seeding conditions –

Cell No: 30,000 cells

[7] Samples preparation and image capture performed in University of Bath CEOS with help of Dr U.J. Potter

Culture Vessel: VWR® Micro 13 mm Round No.1 Cover Glass
Media: Standard culture medium
Duration: 17 – 24 hours

RAW264.7 cells plated on VWR® Micro 13 mm Round No.1 Cover Glass[8] were visualised using a laser scanning confocal microscope (FV300-SU, Olympus, Japan) with an oil immersion x 60 objective and images recorded with Fluoview software (Olympus, USA). External solutions were continuously applied to cells via a gravity driven superfusion system. Images were recorded for 100 seconds before application of ATP (600 seconds). To assess reversal of morphological changes recordings were taken for a further 1800 seconds after ATP application had ceased. All experiments were carried out using external solutions warmed to 37 ^{o}C.

Annexin-V-Alexa Fluor® 488 (AnV-488 50 μl ml^{-1}) was used to assess ATP-induced phosphatidylserine translocation in RAW 264.7 cells. Cells were visualised using a laser scanning confocal microscope (FV300-SU, Olympus, Japan, excitation 488 nm and emission 505 nm) enabling simultaneous fluorescence and brightfield imaging, with a water immersion x 40 objective and images recorded with Fluoview software (Olympus, USA). Recordings of cells bathed in warmed physiological salt solution (37 ^{o}C) in the presence of AnV-488 (50 μl ml^{-1}) were taken for 100 seconds before a 600 seconds application of ATP.

Time-lapse images collected at 20-25 second intervals were sequenced together at three images per second using NIH Image J Software (W. Rasband, National Institutes of Health, Bethesda, MD). To assess membrane blebbing the number of cells blebbing were counted (≥1 bleb/cell) and expressed as a percentage of the total number of cells within the image. To evaluate filopodia retraction, filopodia were measured and values expressed as a percentage change in filopodia length from control (t = 0 seconds).

2.5.3 Staining and Visualization of F-Actin with Phalloidin

Cell seeding conditions -

Cell No: 30, 000 cells

[8] Cell seeding conditions as *Scanning Electron Microscopy*

Culture Vessel: 4 well, NUNC™ Lab-Tek™ Chamber Slide™ System
Media: 600 µl standard culture medium
Duration: 17 – 24 hours

Standard culture medium was aspirated off cells which were subsequently washed in external solution. RAW264.7 cells were stimulated with ATP (1 mM, 10 minutes, 37 ^{o}C) and fixed by the direct addition of 3.7 % formaldehyde in PBS (10 minutes, RT). Cells were washed (x 2) in PBS and incubated for 30 minutes (RT, reduced light conditions) with the high affinity F-actin probe; phalloidin-Alexa Fluor® 546 (Phalloidin-546, 20 µl ml^{-1}, RT) in PBS containing 0.1 % Triton-X 100. Cells were washed (x2) with PBS and with (x1) dH_2O to prevent salt crystals. The media chamber and gasket were removed from the slide and cover glass mounted and sealed onto the cover slide using anti-fade and nail varnish. Cells were visualised using a laser scanning confocal microscope (FV300-SU, Olympus, Japan, excitation 546 nm and emission 573 nm) enabling simultaneous fluorescence and brightfield imaging, with a water immersion x 40 objective and images recorded with Fluoview software (Olympus, USA).

2.5.4 Total Cellular F-Actin Measurements

Cell seeding conditions -

Density: 1.5 x 10^6 cells ml^{-1}
Culture Vessel: Sterile black-walled cell-culture treated 96 well plates
Media: 100 µl standard culture medium
Duration: 17 – 24 hours

Standard culture medium was aspirated off cells which were subsequently washed in physiological salt solution. RAW264.7 cells were stimulated in physiological salt solution in the absence or presence of ATP (1 mM, 10 minutes, 37 ^{o}C) and fixed by the direct addition of 3.7 % formaldehyde in PBS (30 minutes, RT). Cells were washed (x 3) in PBS and incubated for 30 minutes (RT, reduced light conditions) with the high affinity F-actin probe; phalloidin-Alexa Fluor® 546 (Phalloidin-546, 20 µl ml^{-1}, RT) in PBS containing 0.1 % Triton-X 100. For the final 5 minutes of the incubation the nucleic acid stain DAPI

(100 nM) was applied to the cells. Subsequently cells were washed (x2) in PBS. Fluorescence readings were recorded using a multimode plate-reader (Fluostar Optima, BMG Labtech, UK). Phalloidin was excited at 544 nm and fluorescence collected at 590 nm. DAPI was excited at 355 nm and fluorescence collected at 460 nm. Each experimental sample was performed in triplicate and values were expressed as a ratio of phalloidin fluorescence over DAPI fluorescence.

2.6 COAGULATION

2.6.1 Tissue Factor Activity

Cell seeding conditions: -

Density: 1.5 x 10^6 cells ml^{-1}

Culture Vessel: Sterile clear-walled cell-culture treated 96 well plates

Media: 100 µl standard culture medium

Duration: 17 – 24 hours

TF activity was assessed by measuring the presence of active factor X (FXa) using the chromogenic substrate S-2765™. S-2765™ undergoes Reaction 1 when FXa is present. The method for the determination of FX activity is based on the difference in absorbance between the pNA formed and the original substrate. The rate of pNA formation is proportional to the activity of FX.

Reaction 1: N-α-Z-D-Arg-Gly-Arg-pNA ➔ N-α-Z-D-Arg-Gly-Arg·OH + pNA

RAW264.7 cells were bathed in physiological salt solution in the absence or presence of extracellular ATP (37 ^oC). Cells were washed into physiological salt solution and incubated with bovine factor X (FX, 150 nM) and human factor VIIa (FVIIa, 5 nM) for 15 minutes at 37 ^oC before addition of S-2765™ (0.5 mM). Absorbance was measured continuously at 405 nm using a multimode plate-reader (Fluostar Optima, BMG Labtech, UK). Each experimental sample was performed in triplicate and values were normalized to a cell-free control. Linear regression was used to determine the rate of conversion of pNA formation (Prism Version 4, GraphPad Software, San Diego CA).

2.6.2 Tissue Factor Expression

Cell seeding conditions -

Density: 3 x 10^6 cells

Culture Vessel: Sterile cell-culture treated T25 flask

Media: 5 ml standard culture medium

Duration: 17 – 24 hours

Blocking Buffer

Reagent	Concentration
PBS	
BSA	1 % (w/v)
FBS	10 % (v/v)

FACS Buffer

Reagent	Concentration
PBS	
FBS	5 % (v/v)

RAW264.7 cells were washed with physiological salt solution and bathed in physiological salt solution in the absence or presence of ATP (3 mM, 5 minutes, 37 ^oC). Cells were harvested by mechanical scrapping and centrifuged at 240 *x*g (4 ^oC, S4180 rotor, Beckman GS-15R). Cells were re-suspended at 1 x 10^6 cells ml^{-1}in blocking buffer and incubated for 1 hour at 4 ^oC. Blocking buffer was removed by spinning down cells at 5000 rpm for 30 seconds (ProFuge^{TM}, Microcentrifuge 2400). Cells were incubated in FACS buffer in the absence or presence of either rabbit anti-mouse TF IgG (25 μg ml^{-1}) or non-relevant rabbit IgG (25 μg ml^{-1}) for 1 hour at 4 ^oC. Primary antibody was removed by spinning down cells at 5000 rpm for 30 seconds (ProFuge^{TM}, Microcentrifuge 2400) and washing with FACS buffer (x2). Cells were incubated in FACS buffer containing Alexa 488-conjugated $(Fab)_2$ fragments of goat anti-rabbit IgG (10 μg ml^{-1}) for 1 hour at 4 ^oC. Cells were then washed (x3) in FACS buffer and re-suspended in 1 ml of FACS buffer before being analysed using a FACSCanto^{TM} flow cytometer (Becton Dickinson). Data were analysed using WINMDI 2.8 software (Microsoft). At least 10,000 viable cells per condition were analysed for the determination of percentage of positive cells.

2.6.3 Microvesicle Generation and Collection

Cell seeding conditions -

Density: 3 x 10^6 cells
Culture Vessel: Sterile cell-culture treated T25 flask
Media: 5 ml standard culture medium
Duration: 17 – 24 hours

RAW264.7 cells were washed with external solution and incubated in external solution in the absence or presence of ATP (10 minutes, 37 ^oC). Supernatants was collected and clarified by centrifugation at 240 *x*g (S4180 rotor, Beckman GS-15R) for 4 minutes at 4 ^oC. Microvesicles were collected by ultracentrifugation of the clarified supernatants (100, 000 *x*g, Type 70.1 Ti rotor, Beckman L8-70M) for 90 minutes at 4 ^oC. The microvesicle fraction (pellet) was collected and re-suspended in 150 μl physiological salt solution.

2.6.4 Whole Cell Stimulation for Prothrombinase Complex Assay

Cell seeding conditions -

Density: 1.5 x 10^6 cells ml^{-1}
Culture Vessel: Sterile clear-walled cell-culture treated 96 well plates
Media: 100 μl standard culture medium
Duration: 17 – 24 hours

RAW264.7 cells were bathed in physiological salt solution in the absence or presence ATP (10 minutes, 37 ^oC). Cells were washed into physiological salt solution containing grade VI apyrase (1.28 U ml^{-1}).

2.6.5 Prothrombinase Complex Activity

Prothrombinase complex activity was assessed by measuring the generation of thrombin using the chromogenic substrate S-2238™. S-2238™ undergoes Reaction 2 when thrombin is present. The method for determination of thrombin activity is based on the difference in absorbance between the pNA formed and the original substrate. The rate of pNA formation is proportional to enzyme activity.

Reaction 2: H-D-Phe-Pip-Arg-pNA ➔ H-D-Phe-Pip-Arg-OH + pNA

RAW264.7 cells or RAW264.7 derived microvesicles in physiological salt solution were incubated with bovine FXa (6 nM), bovine factor Va (FVa, 3 nM), and S-2238™ (0.5 mM). The generation of thrombin was initiated by the addition of human prothrombin (15 nM). Absorbance was measured continuously at 405 nm using a multimode plate-reader (Fluostar Optima, BMG Labtech, UK). Each experimental sample was performed in triplicate and values were normalized to a cell-free control. Linear regression was used to determine the rate of conversion of pNA formation (Prism Version 4, GraphPad Software, San Diego CA). Data was expressed as the fold-change in the rate of thrombin generation from control.

2.7 OXIDATIVE STRESS

2.7.1 Detection of Reactive Oxygen Species

Cell seeding conditions -

Density: 1 x 10^6 cells ml^{-1}

Culture Vessel: Sterile black-walled cell-culture treated 96 well plates

Media: 100 μl complete culture medium

Duration: 17 – 24 hours

The accumulation of intracellular reactive oxygen and nitrogen species (ROS) was estimated by using 2', 7'-dichlorodihydrofluorescein diacetate (H_2DCF-DA). H_2DCFDA readily diffuses into cells where intracellular esterases cleave the acetate group of H_2DCF-DA from the molecule to yield H_2DCF, which is trapped within the cells. Intracellular ROS oxidises H_2DCF to form the highly fluorescent compound DCF. Culture medium was removed from LPS primed cells and cells incubated with 10 μM H_2DCF-DA in DMEM:F12 (1:1) with 2.5 mM probenecid[9] for 40 minutes at RT, under limited light conditions. Excess H_2DCF-DA was aspirated from the cells and replaced with physiological salt solution containing probenecid (2.5 mM) and antagonist where appropriate. Cells were left to rest for 5 minutes (37 ^oC) prior to agonist application. DCF fluorescence was excited at 485nm and emission collected at 520 nm using a multimode plate reader (Fluostar Optima, BMG Labtech, UK).

[9] Used for inhibiting dye secretion and sequestration via organic anion transporters.

Each experimental sample was performed in triplicate and values were normalized to baseline. Linear regression between t = 0 and t ≈ 5 minutes of agonist application was used to determine rates of DCF generation (rate of ROS generation) (Prism Version 4, GraphPad Software, San Diego CA). Final concentration-response curves were constructed by normalizing individual curves to maximum ATP evoked responses (Equation 2) in the control conditions. Curve fitting was performed using Prism Version 4 (GraphPad Software, San Diego CA) using a four parameter logistic equation (Equation 3).

2.7.2 Saville-Greiss Assay

Cell seeding conditions -

Density: 1 x 10^6 cells ml^{-1}
Culture Vessel: Sterile cell-culture treated 24 well plates
Media: 1 ml standard culture medium
Duration: 17 – 24 hours

The Saville-Greiss assay is used to measure the non-volatile metabolite nitrite (NO_2) as an indicator of NO formation. This assay was used in this study as a positive control for the effect of the NOS inhibitor L-NAME on ROS generation. J774.2 cells were primed for with 1 μg ml^{-1} LPS (6 hours) in the absence or presence of L-NAME. Cells were washed in physiological salt solution and ATP was applied to cells for the final 30 minutes (37 ^oC). Cells were lysed in ice-cold lysis buffer containing 1 % nonidet P-40 and PIC. Griess reagent was incubated with the samples (1:1) and nitrite concentrations were determined from sodium nitrite standard curves quantified on a multimode plate reader (Fluostar Optima, BMG Labtech, UK) at 544 nm.

2.8 PROTEIN EXPRESSION ANALYSIS

2.8.1 Sample Generation for Receptor Expression

Cell seeding conditions -

Density: 1.0 x 10^6 cells ml^{-1}
Culture Vessel: Sterile cell-culture treated 24 well plates
Media: 1 ml standard culture medium
Duration: 17 – 24 hours

Media was aspirated from cells and cells washed with physiological salt solution (1 ml) before lysis using 1 % Triton-X 100 in PIC (75 µl, 4 ^{o}C). Samples were cleared by centrifugation at 1500 *x*g (F3601 rotor, Beckman GS-15R) for 10 minutes at 4 ^{o}C. Samples were diluted with 2x sample buffer and boiled for 5 minutes before storage at -80 ^{o}C.

2.8.2 Sample Generation for IL-1β and Caspase-1

Cell seeding conditions -

Density: 1.0 x 10^6 cells ml^{-1}
Culture Vessel: Sterile cell-culture treated 24 well plates
Media: 1 ml standard culture medium
Duration: 17 – 24 hours

Media was aspirated from LPS primed cells and cells washed with physiological salt solution (1 ml) before incubation in physiological salt solution (250 µl) in the absence or presence of ATP (37 ^{o}C). For analysis of the release of IL-1β, secreted protein fractions were collected and placed on ice before washing cells in physiological salt solution (1 ml, 4 ^{o}C) and cells lysed using 1 % Triton-X 100 in PIC (75 µl, 4 ^{o}C)[10]. For analysis of caspase-1 activation cells were lysed by adding 10 % Triton-X 100 in 10x PIC (25 µl, 4 ^{o}C) directly to the cells and supernatant. Samples were cleared by centrifugation at 1500 *x*g (F3601 rotor, Beckman GS-15R) for 10 minutes at 4 ^{o}C. Secreted protein fractions were concentrated (x6) using 3K Nanosep cut-off filters according to the manufacturers' protocol. Samples were diluted with 2x sample buffer and boiled for 5 minutes before storage at -80 ^{o}C.

2.8.3 SDS-PAGE

12 % Resolving Gel (5 ml – 1 Gel)

Solution Components	Volume (ml)
H_2O	1.6
30 % Acrylamide Mix	2.0
1.5 M Tris (pH 8.8)	1.3
10 % SDS (w/v)	0.05

[10] Triton-X 100 and PIC were at a final concentration of 1% and 1x respectively after addition to the well.

10 % Ammonium Persulfate (w/v)	0.05
TEMED	0.002

5 % Stacking Gel (1 ml – 1 Gel)

Solution Components	Volume (ml)
H_2O	0.68
30 % Acrylamide Mix	0.17
1 M Tris (pH 6.8)	0.13
10 % SDS (w/v)	0.01
10 % Ammonium Persulfate (w/v)	0.01
TEMED	0.001

Running Buffer

Solution Components	Concentration
Glycine	192 mM
SDS	0.1 % (w/v)
Tri-HCl	25 mM

Solubilised proteins were loaded on to an SDS-PAGE gel composed of a 5 % stacking and 12 % resolving gel. Samples were electrophoresed at 200 V in running buffer for approximately 40 minutes using the Bio-Rad Mini Protean II system (Bio-Rad, UK). A protein standard was run in one lane per gel to estimate protein size during analysis.

2.8.4 Immunoblotting

Transfer Buffer

Solution Components	Concentration
Glycine	192 mM
SDS	0.1 % (w/v)
Tri-HCl	25 mM
Methanol	20 % (v/v)

Wash Buffer

Solution Components	Concentration
PBS	
Tween	0.5 % (v/v)

Blocking Buffer

Solution Components	Concentration
PBS	
Tween	0.5 % (v/v)
Skimmed Milk	5 % (w/v)

Proteins were transferred by electroblotting in transfer buffer for 2 hours at 150 mA onto nitrocellulose membrane (0.2 μm) using the Bio-Rad Mini Trans-Blot cell (Bio-Rad, UK). Membranes were incubated for 60 minutes at RT in blocking buffer under constant agitation. The membrane was then incubated overnight at 4 ^{o}C under constant agitation in blocking buffer containing primary antibody[11]. The membrane was washed (x3, 5 minutes) in wash buffer and incubated in secondary antibody[12] for 60 minutes at RT under constant agitation. The membrane was washed (x6, 5 minutes) in wash buffer and protein visualised using the Amersham™ ECL Advance™ western blotting detection agent.

2.9 STATISTICAL ANALYSES

Average results are expressed as the mean ± s.e.m from the number of assays indicated. Statistical analysis on experiment and control groups were performed using either Student's t-test or one-way analyses of variance (ANOVA) with Dunnett's post-hoc analysis where appropriate using the statistical software package Prism version 4 (GraphPad Software, San Diego CA). Significance was reached when $p<0.05$.

[11] Primary Ab dilutions: Mouse IL-1β MAb 1:5000 / Caspase-1 p10 (M-20) 1:500 / $P2X_7R$ 1:2500

[12] Secondary Ab dilutions at 1:5000: IL-1β - Polyclonal Rabbit Anti-Mouse IgG/HRP, Caspase-1/$P2X_7R$ – Polyclonal Swine Anti-Rabbit IgG/HRP

CHAPTER 3

GENERAL PHARMACOLOGY & THE EFFECT OF DIVALENT CATIONS AT THE MURINE $P2X_7$ RECEPTOR

Portions of this chapter have been published in Cellular Signaling (2008), 19(4)
Portions of this chapter are in press with Biochemical Pharmacology

3.1 INTRODUCTION

In this portion of the study the general pharmacology of an endogenously expressed murine macrophage $P2X_7R$ was investigated. Furthermore the ability of divalent metal cations to modulate $P2X_7R$ function was also assessed. Examining the properties of the mouse $P2X_7R$ and determining differences between species could be of importance for two major reasons:

1. Increasing use of $P2X_7R$ KO mice and the use of animal models of disease drives the need to acquire knowledge of the mouse $P2X_7R$.
2. Prior to conducting this study much of the pharmacological characterisation of the $P2X_7R$ had been carried out using the rat orthologue, which may not be comparable to the mouse or human orthologue.

Activation of the $P2X_7R$ by ATP will lead to the opening, within milliseconds of a non-selective cation channel, allowing the entry of ions such as Na^+ and Ca^{2+} into the cell (Figure 3-1). Prolonging this activation leads to the opening of a large pore within seconds to minutes, allowing the entry of dyes <900Da into the cell. The dye permeation pathway is not fully understood, but appears to involve increases in intracellular Ca^{2+}, the MAPK second messenger system (Faria *et al.*, 2005) and pannexin-1 hemichannels (Pelegrin *et al.*, 2006). Prolonging activation of the $P2X_7R$ (≈ 30 minutes) will eventually lead to cytolytic cell death (Ferrari *et al.*, 1997a; Mackenzie *et al.*, 2005), however it is generally accepted that the dye permeation pathway is a separate event to cell death. These $P2X_7R$ functional responses led to the selection of three assays to assess the pharmacology of the mouse $P2X_7R$; changes in $[Ca^{2+}]_i$, accumulation of the large molecular weight dye ethidium bromide (372Da) and the release of cellular lactate dehydrogenase, indicative of cell death.

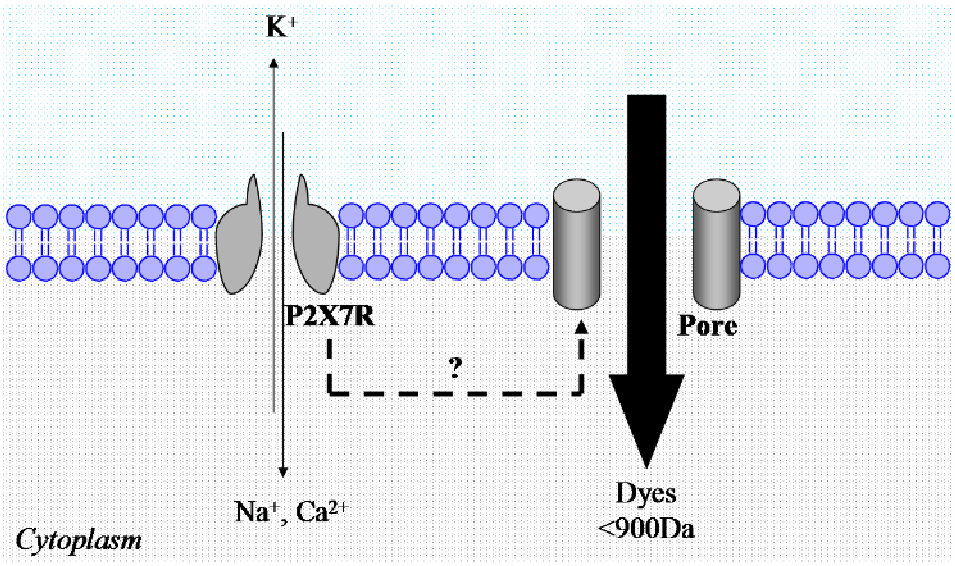

Figure 3-1. Schematic of the Two Permeation States Induced by Activation of the P2X$_7$R. The first permeation pathway is the opening on the non-selective cation ion channel. The second permeation pathway occurs with prolonged activation of the P2X$_7$R and allows the uptake of large molecular weight dyes. The above diagram is based on the concept that the P2X$_7$R couples to a separate pore forming protein recently elucidated to be pannexin-1 (Pelegrin *et al.*, 2006). However a number of other models have been proposed including dilation of the channel itself (Khakh *et al.*, 1999; Virginio *et al.*, 1999). Potentially there are in fact three permeation states; opening of the non-selective cation channel, coupling to a second membrane protein for dye uptake and dilation of the P2X ion channel allowing the entry of larger cations such as NMDG (Jiang *et al.*, 2005; Yan *et al.*, 2008).

Pharmacologically the P2X$_7$R is the most distinct of the P2X receptors due to it being unusually insensitive to ATP (EC_{50} range of 0.1 – 1.8 mM), whilst the ATP-analogue BzATP is around 10-fold more potent than ATP (EC_{50} range of 3 - 300μM). Furthermore there are clear species differences in P2X$_7$R pharmacology. For instance mouse P2X$_7$Rs display markedly lower sensitivity to ATP and BzATP compared to the rat P2X$_7$Rs (Table 3-1A). By contrast the human P2X$_7$R has a comparable sensitivity to BzATP but a lower ATP sensitivity. Mutagenesis studies have identified amino-acids (K127A and N284D) in the ectodomain of the P2X$_7$R which are responsible for the differences in ATP and BzATP sensitivity between rat and mouse P2X$_7$Rs (Young *et al.*, 2007).

In addition to the differences in potency of P2X$_7$R agonists at different species of receptor, there are also differences in antagonist potency. Although IC_{50} values of P2X$_7$R antagonists cannot always be accurately compared due to differences between studies on agonist concentration, agonist used (ATP versus BzATP), buffer composition, cell

background and assay used; it is generally accepted that the isoquinolines KN-62 and KN-04 potently block human $P2X_7Rs$ with higher concentrations required to block rat $P2X_7Rs$ (Humphreys *et al.*, 1998), whereas the opposite is true for Brilliant Blue G (BBG) (Jiang *et al.*, 2000) (Table 3-1B). The newer highly selective $P2X_7R$ antagonists are also observed to have major differences in potency at different species of receptor. AZ11645373 is a highly selective and potent human $P2X_7R$ antagonist (IC_{50} = 10 – 100 nM) and is observed to be 500-fold less potent at blocking the rat $P2X_7R$ (Stokes *et al.*, 2006). GSK314181A has an IC_{50} range of between 18 – 85 nM at the human receptor whereas at the rat receptor it has an IC_{50} range of 29 – 980 nM (Broom *et al.*, 2008). The Abbott Laboratories antagonists A-438079 and A-740003 however are reported to be highly selective and potent blockers at both the human and rat $P2X_7Rs$ (Donnelly-Roberts *et al.*, 2007a).

EC_{50} (μM)	MOUSE	RAT	HUMAN
ATP	900	120	1800
BzATP	300	3	210

Table 3-1A. Summary of EC_{50} of ATP and BzATP at the Mouse, Rat and Human $P2X_7Rs$. Values are based on the findings from (Moore *et al.*, 2007; Stokes *et al.*, 2006; Surprenant *et al.*, 1996; Young *et al.*, 2007)

IC_{50} (nM)	RAT	HUMAN
KN-62/KN-04	> 3000	30 - 100
BBG	10	200

Table 3-1B. Summary of IC_{50} of KN-62/KN-04 and BBG at the Rat and Human $P2X_7Rs$. Values are based on the findings from (Humphreys *et al.*, 1998; Jiang *et al.*, 2000).

$P2X_7Rs$ along with other P2XRs, are modulated by the presence of extracellular divalent cations, this phenomenon is also observed with other ligand-gated ion channels such as the glutamate receptors, $GABA_A$ receptors and nicotinic receptors (Huidobro-Toro *et al.*, 2008). The effects of different divalent cations are specific to each P2XR subtype (Table 3-2). For example extracellular Zn^{2+} is observed to have no effect at the $P2X_1$ and $P2X_3$ receptors (Nakazawa *et al.*, 1997), potentiates responses at the $P2X_2$ (< 100 μM) and $P2X_4$ (< 300 μM) receptors (Coddou *et al.*, 2003; Lorca *et al.*, 2005) and inhibits the $P2X_7R$

(Virginio *et al.*, 1997). Whereas extracellular Cu^{2+} inhibits at $P2X_4$ and $P2X_7$ and potentiates at $P2X_2$. The mechanism for the action of the effects of these different divalent cations is proposed for each receptor to be a binding of the cation to specific metal binding sites within the receptors (Huidobro-Toro *et al.*, 2008).

	P2X1	P2X2	P2X3	P2X4	P2X5	P2X6	P2X7
Ca^{2+}	No effect	⬇	No effect	-	⬇	-	⬇
Mg^{2+}	No effect	-	⬇	⬇	-	-	⬇
Cu^{2+}	-	⬆	-	⬇	-	-	⬇
Zn^{2+}	No effect	⬆	No effect	⬆	⬆	-	⬇
Cd^{2+}	No effect	⬆ (weak)	No effect	⬆	-	-	⬇
Hg^{2+}	-	⬆	-	⬇	-	-	-

Table 3-2. Effects of Increasing the Concentration of Extracellular Divalent Cations on P2XRs. Data based on (Evans *et al.*, 1996; Giniatullin *et al.*, 2003; Lorca *et al.*, 2005; Nakazawa *et al.*, 1997; Negulyaev *et al.*, 2000; Seyffert *et al.*, 2004; Virginio *et al.*, 1997; Virginio *et al.*, 1998; Wildman *et al.*, 2002; Wildman *et al.*, 1999a; Wildman *et al.*, 1999b; Xiong *et al.*, 1999). The majority of the data is for the rat orthologue of the receptor. Overall affects observed were not always the same between studies which maybe due to species of receptor used, pre-incubation time with divalent cation, cell background, concentration of agonist and functional response measured. ⬆ denotes potentiation, ⬇ denotes inhibition.

The majority of the studies performed to investigate the effects of divalent cations at P2X receptors have been performed using the rat orthologues of the receptor expressed in HEK293 cells or *Xenopus* oocytes. Considering the clear species differences between the $P2X_7$ receptors observed with agonists and antagonists, it could be hypothesized that species differences in the binding and modulation of the receptor by divalent cations may also occur.

Another reason why it maybe of interest to study the effects of divalent cations at the $P2X_7R$ is that inhibition by physiological concentrations of Ca^{2+} and Mg^{2+} (Virginio *et al.*, 1997) would suggest that activation of the $P2X_7R$ is suppressed under physiological conditions, thus preventing/reducing any unwanted effects of receptor over-activation (potentially leading to cytolysis) whilst maintaining low level activation required for physiological responses (cell proliferation) (Jiang, 2008). Although ion concentrations in the blood are highly regulated; most cell types are not in direct contact with blood and

therefore there is potential for tissue specific and localised differences in ion concentrations (Bosher *et al.,* 1978, Silver *et al.,* 1988). Furthermore there is thought to be a relationship between intracellular Ca^{2+} signalling events and changes to extracellular Ca^{2+} concentration with the outward and inward exchange of Ca^{2+} potentially causing local elevations or depletions in the extracellular Ca^{2+} concentration (Hofer *et al.,* 2003). Therefore under pathophysiological conditions the local extracellular concentration of Ca^{2+} and Mg^{2+} could possibly be reduced leading to an enhancement of $P2X_7R$ activation and therefore initiating some of the functional $P2X_7R$ responses associated with an immune response including the processing and secretion of IL-1β.

The effects of Zn^{2+} and Cu^{2+} are of particular interest; both of these divalent ions are essential trace metal nutrients where imbalances have been observed to provoke a range of different effects. Both cations are required for the action of various enzymes, including superoxide dismutase, tyrosine and tryptophan hydroxylases. Zn^{2+} plays an important signaling role in the immune system, whereby treatment with oral Zn^{2+} has profound effects on immune response and acts as an anti-inflammatory therapeutic (Dardenne, 2002; Fraker *et al.*, 2000). Cu^{2+} deficiencies have been related to neurological disturbances, anaemia and hair changes (Cerpa *et al.,* 2005).

Therefore a study on the regulation of the mouse $P2X_7R$ by divalent cations could potentially:

- Reveal species differences in metal binding sites and increase our knowledge about P2XR regulation by divalent cations.
- Increase our understanding on how $P2X_7R$ function maybe regulated under physiological and pathophysiological conditions.

When examining if the $P2X_7R$ is modulated by divalent cations it is important to account for free ATP^{4-} concentrations, this form of ATP has been reported to be the active ligand at this receptor (Cockcroft *et al.*, 1979; Cockcroft *et al.*, 1980; Dahlquist *et al.*, 1974). ATP has multiple ionisable groups with different acid dissociation constants. In a neutral solution ATP is ionized and exists mostly as ATP^{4-} with a small proportion of ATP^{3-}. As ATP has several negatively charged groups in neutral solution it is able to chelate metals with very high affinity. Example binding constants for various metal ions (per mole) are

Mg^{2+}, 9554; Na^{+}, 13; Ca^{2+}, 3722 and K^{+}, 8. Due to the strength of these interactions, ATP exists in the cell mostly in a complex with Mg^{2+}. Therefore increasing the concentration of divalent metal cations will lead to a reduction in the concentration of the free active ATP^{4-} ligand.

The key findings of this study were:

1. ATP elicits increases in $[Ca^{2+}]_i$ (seconds), uptake of EtBr (minutes) and cell death (>30 minutes) in the RAW264.7 murine macrophage cell line.
2. Ca^{2+}, Mg^{2+} and Cd^{2+} primarily inhibit EtBr uptake in RAW264.7 cells by reducing the concentration of the active $P2X_7R$ ligand ATP^{4-}.
3. Hg^{2+} potentiates EtBr uptake in RAW264.7 cells
4. Cu^{2+} inhibits the EtBr uptake in RAW264.7 cells, HEK293/mP2X7R, HEK293/rP2X7R
5. Zn^{2+} has differential effects at the $P2X_7R$ depending on species, cell background and agonist used.

3.2 RESULTS

3.2.1 ATP Evokes an Increase in Intracellular Calcium in RAW264.7 Murine Macrophages

Application of extracellular ATP on to RAW264.7 cells loaded with Fluo-4 AM in the presence of 2 mM Ca^{2+} was observed to trigger an increase in Fluo-4 fluorescence (Figure 3-2A, Figure 3-2B) indicative of an increase in $[Ca^{2+}]_i$. Concentrations of ATP < 1mM induced a rapid transient increase whereas concentrations ≥ 1 mM gave a sustained response (> 1 minute). Plotting peak responses established that ATP evoked a concentration-dependent response (Figure 3-2C) with an EC_{50} value of 380 μM (n = 8 ± s.e.m, pEC_{50} = 3.42 ± 0.05, n_H = 0.94 ± 0.08). In the absence of external Ca^{2+} (calcium-free external salt solution containing 1mM EGTA); responses evoked by 1 mM ATP were reduced, with the peak $[Ca^{2+}]_i$ rise decreased by 82.83 ± 4.32 % and the sustained component by 92.80 ± 2.6 % (n = 6 ± s.e.m, $p < 0.001$) (Figure 3-2D).

Pre-addition of the generic P2X receptor antagonist suramin (10 and 100 μM) failed to significantly inhibit ATP (0.03, 0.3 and 3 mM) induced increases in $[Ca^{2+}]_i$ in RAW264.7 cells (n = 6, Figure 3-3A, Figure 3-3B). Addition of 1 mM ATP in the presence of the potent human $P2X_7R$ antagonist KN-62 (Figure 3-3C) was observed to reduce increases in $[Ca^{2+}]_i$. Comparing peak and sustained responses in the presence and absence of KN-62 determined that 10 μM KN-62 significantly inhibited ATP triggered rises in peak and sustained $[Ca^{2+}]_i$ by 46.31 ± 11.78 % and 58.02 ± 3.97 % respectively (n = 6 ± s.e.m; $p<0.05$) (Figure 3-3D). Addition of 1 mM ATP in the presence of the potent rat $P2X_7R$ antagonist BBG (0.3 – 10 μM) yielded a dose-dependent block in ATP triggered rises in $[Ca^{2+}]_i$ (n = 6, Figure 3-3E). 10 μM BBG was observed to inhibit the peak and sustained $[Ca^{2+}]_i$ response induced by 1 mM ATP (Figure 3-3F) by 67.99 ± 5.03 % and 87.48 ± 4.12 %, respectively (n = 6 ± s.e.m; $p<0.01$).

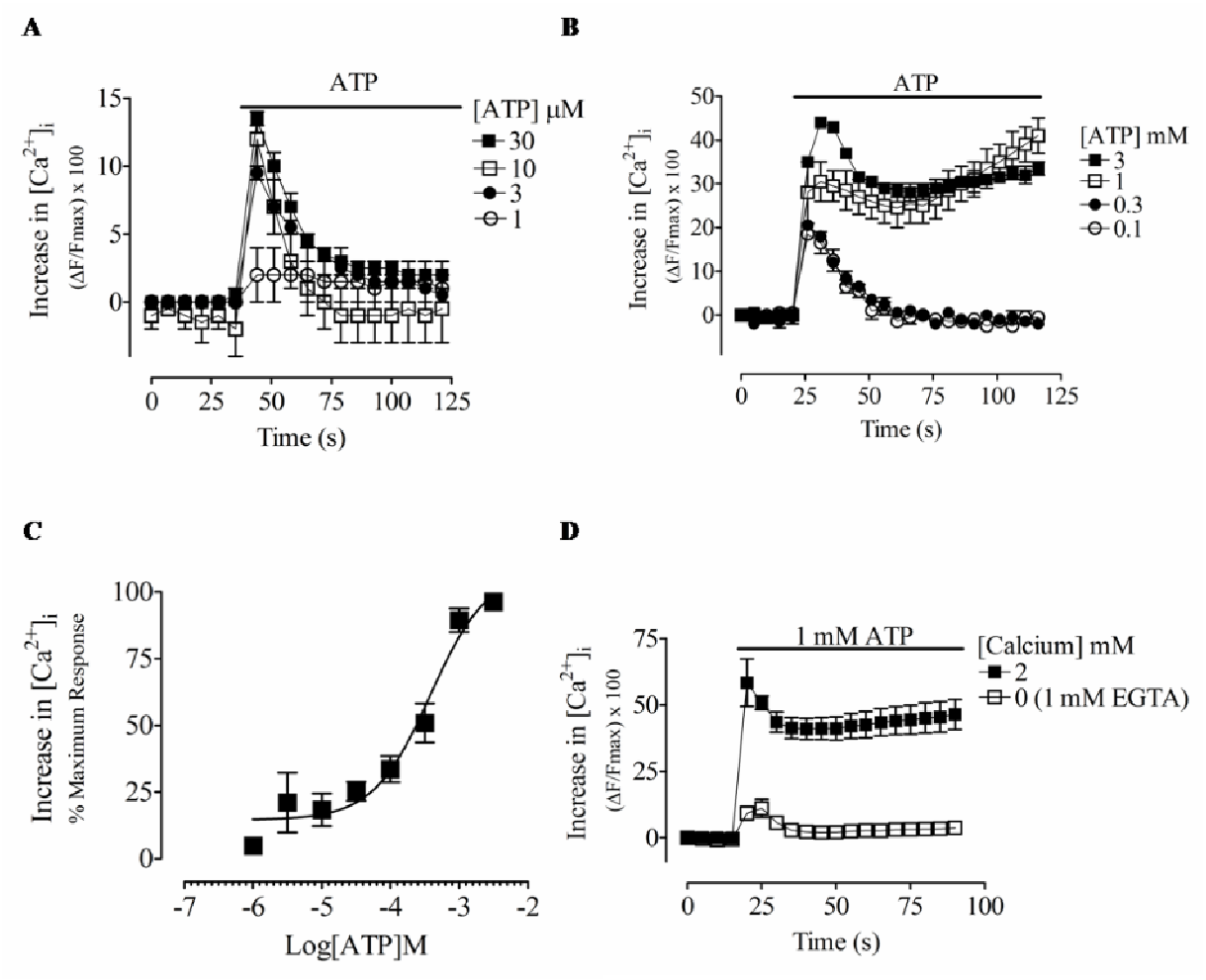

Figure 3-2. ATP Evokes Transient and Sustained Increases in $[Ca^{2+}]_i$ in RAW264.7 Macrophages. A, Representative trace of rapid transient ATP (1 – 30 µM) induced increases in $[Ca^{2+}]_i$. B, Representative trace of transient ATP (0.1 & 0.3 mM) and sustained ATP (1 & 3 mM) induced increases in $[Ca^{2+}]$. C, Concentration-response curve of the effect of ATP on $[Ca^{2+}]_i$ (n = 8 ± s.e.m, pEC_{50} of 3.42 ± 0.05). D, Kinetic trace comparing the effect of ATP (1 mM) on increases in $[Ca^{2+}]_i$ in the presence (2 mM) and absence (1 mM EGTA) of Ca^{2+} (n = 6 ± s.e.m).

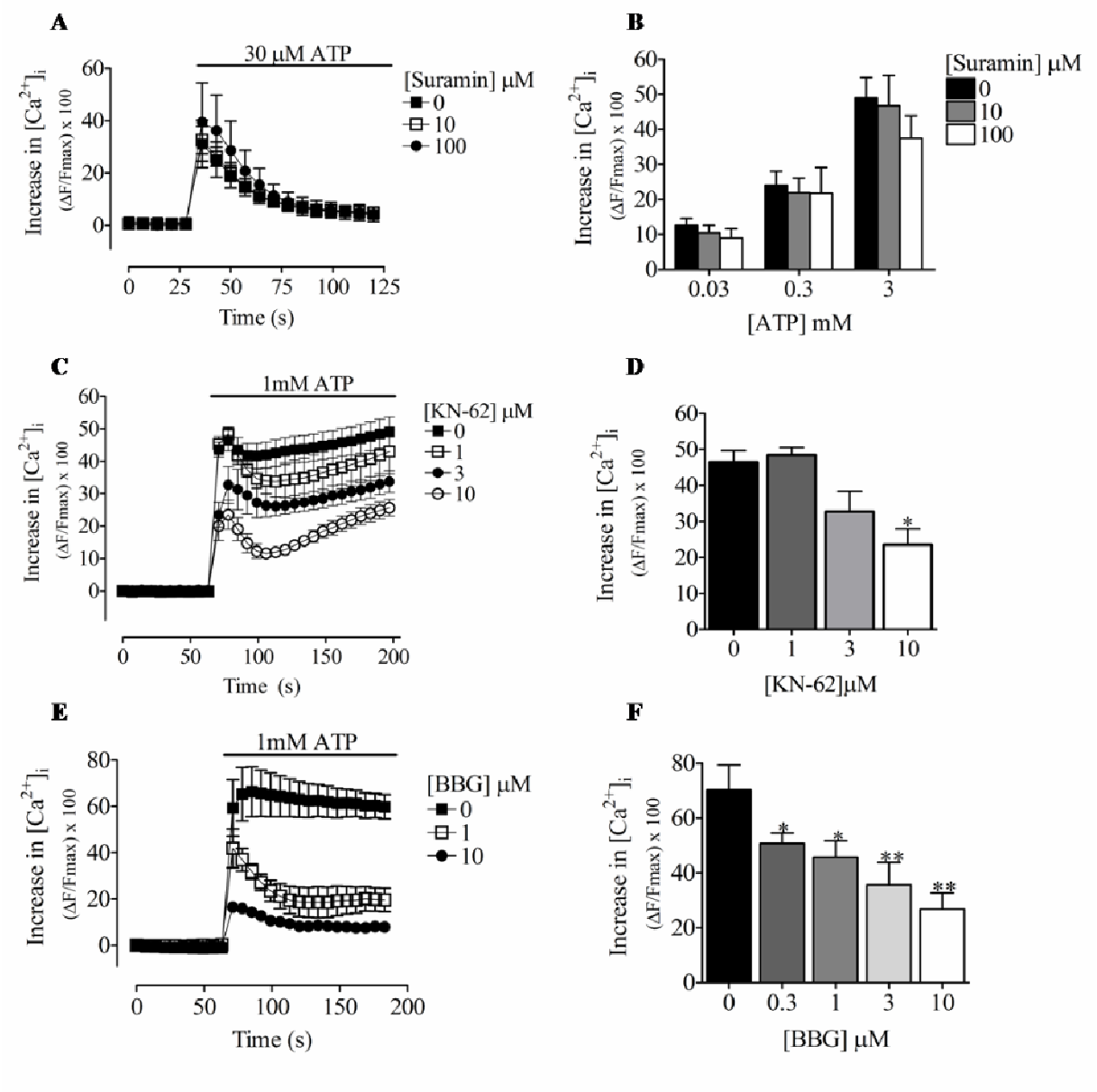

Figure 3-3. ATP Induced Increases in $[Ca^{2+}]_i$ are Inhibited by P2X7R Antagonists. A, Kinetic trace and B, histogram of the effects of suramin on ATP evoked increases in $[Ca^{2+}]_i$ (n = 6 ± s.e.m). C, Kinetic trace and D, histogram of the effects of KN-62 on ATP evoked increases in $[Ca^{2+}]_i$ (n = 6 ± s.e.m). E, Kinetic trace and F, histogram of the effects of BBG on ATP evoked increases in $[Ca^{2+}]_i$ (n = 6 ± s.e.m). One-way ANOVA with Dunnett's post-hoc test, *: $p<0.05$, **: $p<0.01$.

3.2.2 ATP Induces the Uptake of EtBr into RAW264.7 Murine Macrophages

Application of 3 mM ATP on to RAW264.7 cells bathed in a physiological salt solution containing 25 μM EtBr (37 ^{o}C) was observed to induce a continuous increase in EtBr fluorescence above an ATP-free control (Figure 3-4A). Using a range of ATP concentrations and calculating rates of increase in EtBr fluorescence (0-15 minutes ATP application) established that a concentration ≥ 1 mM ATP was required to induce EtBr uptake above an ATP-free control with a peak rate of uptake achieved with 3 – 5 mM ATP. Plotting a concentration-response curve (Figure 3-4B) determined that ATP evoked EtBr uptake with an EC_{50} of 1.55 mM (n = 29 ± s.e.m, pEC_{50} = 2.81 ± 0.02, n_H = 5.81 ± 0.46). Pre-application of KN-62 was observed to inhibit ATP (3 mM) evoked EtBr uptake (Figure 3-4C). This inhibition was observed to be concentration-dependent with an IC_{50} of 1.32 μM (n = 9 ± s.e.m, pIC_{50} = 5.88 ± 0.20, n_H = -0.98 ± 0.30) (Figure 3-4D). Preliminary experiments determined that BBG quenched and suramin increased the basal fluorescence of the recorded EtBr signal (data not shown) and where therefore not tested in these experiments.

3.2.3 Prolonged ATP Stimulation Induces Cell Death

Cell viability was determined by measuring the retention of the cytosolic enzyme LDH. An application of 3 mM ATP onto RAW264.7 cells bathed in physiological salt solution for > 30 minutes (37 ^{o}C) was observed to induce a significant release of LDH into the external medium (Figure 3-5A, n = 9). Pre-addition of KN-62 was observed to block ATP (3 mM, 60 minutes) induced LDH release with an IC_{50} of 407 nM (Figure 3-5B, n = 9 ± s.e.m, pIC_{50} = 6.39 ± 0.18, n_H = -1.47 ± 0.73, α = -36.93 ± 4.86).

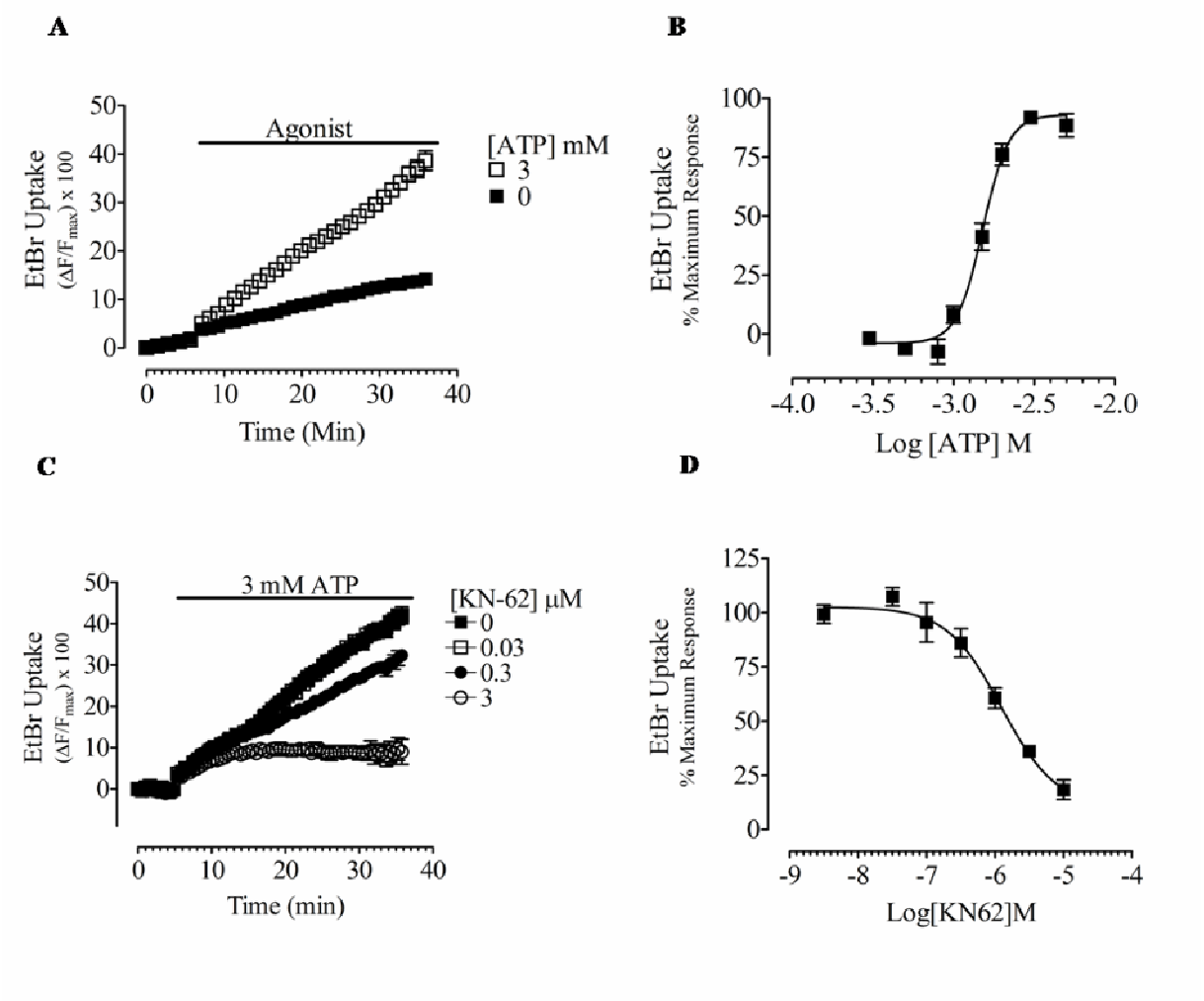

Figure 3-4. ATP Induced EtBr Uptake is Inhibited by KN-62. A, Representative trace of ATP induced increase in EtBr fluorescence indicative of pore formation. B, Concentration-response curve of the effect of ATP on inducing pore formation (n = 29 ± s.e.m, pEC_{50} of 2.81 ± 0.02). C, Representative trace and D, concentration-inhibition curve of the effect of KN-62 on ATP evoked pore-formation (n = 9 ± s.e.m, pIC_{50} of 5.88 ± 0.20).

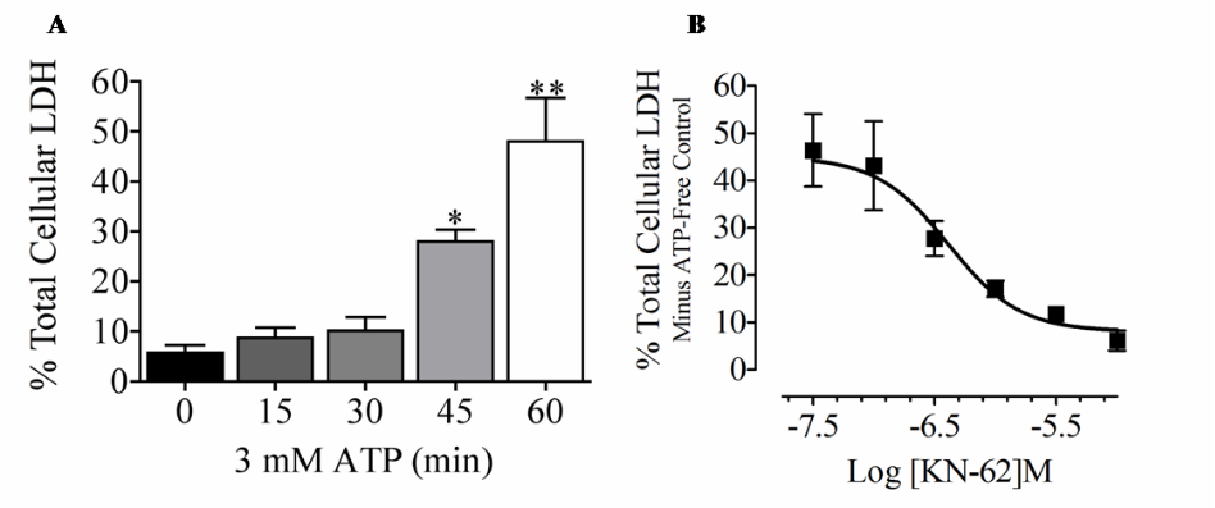

Figure 3-5. ATP Induced Cell Death is Inhibited by KN-62. A, Histogram demonstrating that incubating cells with 3 mM ATP for 45 or 60 minutes induced a significant release of LDH (n = 9 ± s.e.m). B, Concentration-response curve of the effect of stimulating RAW264.7 cells with ATP in the presence of KN-62 (n = 9 ± s.e.m, pIC_{50} = 6.39 ± 0.18, n_H = -1.47 ± 0.73, α = -36.93 ± 4.86). One-way ANOVA with Dunnett's post-hoc test, *: $p<0.05$, **: $p<0.01$.

3.2.4 Reducing Extracellular [Ca^{2+}] and [Mg^{2+}] Enhances EtBr Uptake by Increasing [ATP^{4-}]

In the presence of extracellular Ca^{2+} (2 mM) and Mg^{2+} (1 mM) (described as physiological) an application of ATP on to RAW264.7 cells was observed to trigger the uptake of EtBr with an EC_{50} of 1.55 mM (n = 29). Removal of both extracellular Ca^{2+} and Mg^{2+} (described as nominal) was observed to cause an increase in the rate of dye uptake induced by ATP above an ATP-free control (Figure 3-6A). Constructing concentration-response curves revealed that removal of extracellular Ca^{2+} and Mg^{2+} significantly decreased the EC_{50} to 309 μM (n = 29, $p<0.001$) (Figure 3-6B, Table 3-3). No significant change in n_H or α was observed ($p>0.05$). Taking in to account changes in the concentration of ATP^{4-} abolished the significant decrease in EC_{50} obtained by reducing extracellular [Ca^{2+}] and [Mg^{2+}] (Figure 3-6C).

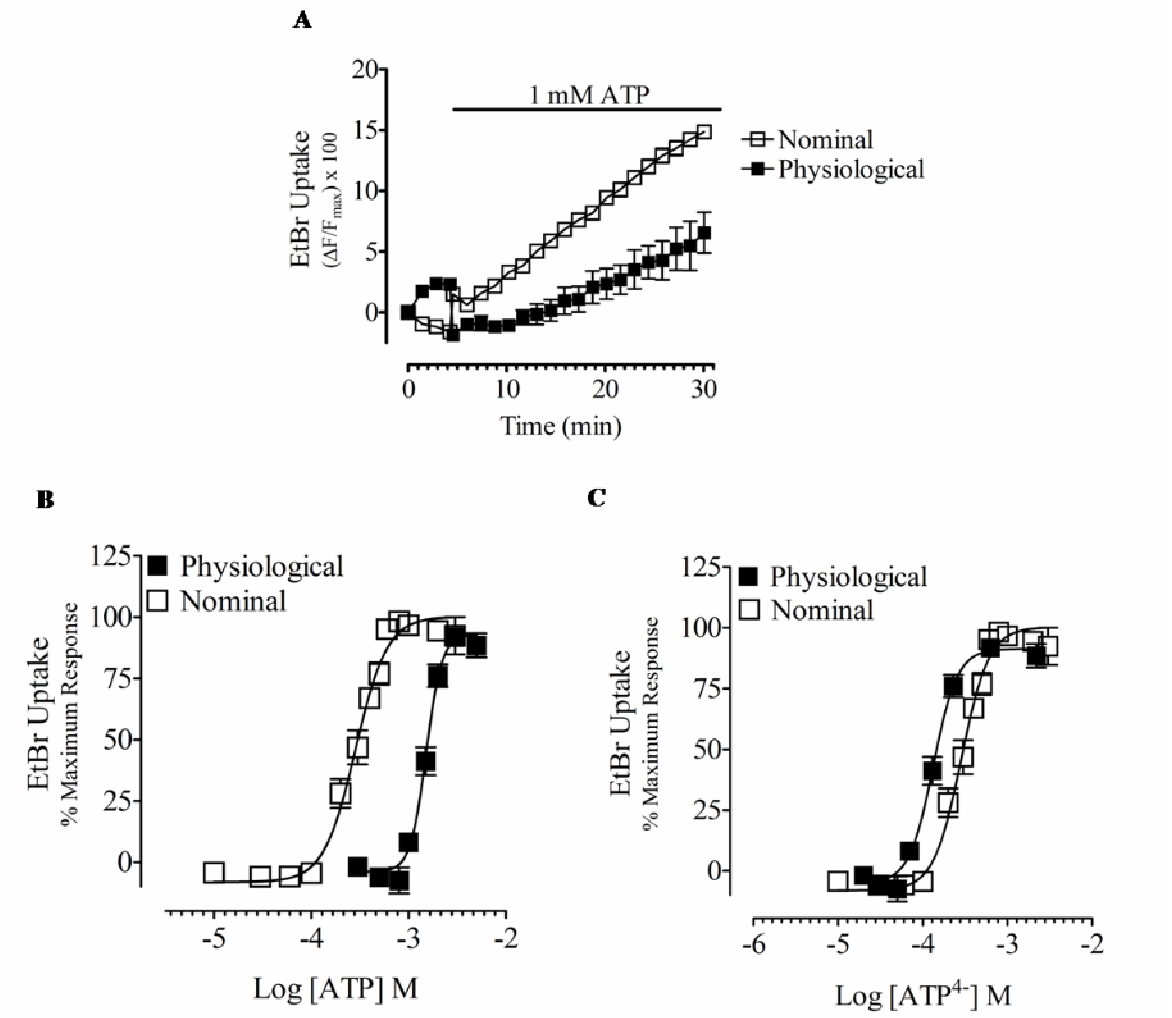

Figure 3-6. Removal of Extracellular Ca^{2+} & Mg^{2+} Potentiates EtBr Uptake by Increasing Free [ATP^{4-}]. A, Representative trace of the effect of removal of Ca^{2+}/Mg^{2+} from the external solution on ATP (1 mM) induced EtBr uptake. B, Concentration-response curve of the effect of removal of Ca^{2+}/Mg^{2+} from the external solution on ATP induced pore formation. C, Re-plotted ATP^{4-} concentration-response curves. (n = 29 ± s.e.m).

	pEC_{50} ± s.e.m	**n_H ± s.e.m**	**α ± s.e.m**
Physiological	2.81 ± 0.02	5.81 ± 0.46	102 ± 4
Nominal	3.51 ± 0.03***	5.88 ± 1.14	113 ± 5

Table 3-3. ATP Concentration-Response Curve Parameters for EtBr Uptake in Physiological Salt Solution and Nominal Ca^{2+}/Mg^{2+} Solution. n = 29 ± s.e.m, Student's two-tailed t-test ***:p<0.001.

3.2.5 Effect of Increasing Extracellular Ca^{2+} or Mg^{2+} on EtBr Uptake

Increasing the concentration of external Ca^{2+} in the physiological salt solution was found to inhibit ATP evoked EtBr uptake, as demonstrated with a rightward shift in ATP concentration response curve (Figure 3-7A). A significant increase in the EC_{50} from 1.41 mM to 2.88 mM was obtained in the presence of 10 mM Ca^{2+} (n = 4, $p<0.001$) (Table 3-4A). The hill-slope (n_H) was also observed to increase with increasing concentrations of Ca^{2+} however this increase was not found to be statistically significant (n = 4, $p>0.05$). Taking in to account changes in the concentration of ATP^{4-} abolished the significant increase in EC_{50} obtained by increasing Ca^{2+} to 10 mM (Figure 3-7B, Table 3-4B).

Increasing the concentration of external Mg^{2+} in the physiological salt solution from 1 to 3 or 10 mM was found to inhibit ATP evoked EtBr uptake (Figure 3-8A.). A significant increase in the EC_{50} from 1.45 mM to 2.40 mM was obtained in the presence of 3 mM Mg^{2+} (n = 5, $p<0.05$) (Table 3-5A). No significant change in n_H or α was observed ($p>0.05$). Concentration-response curve fitting for ATP evoked EtBr uptake in the presence of 10 mM Mg^{2+} was not achieved due to responses being obtained at only two of the ATP concentrations tested; therefore pEC_{50}, n_H and α parameters could not be calculated and compared to responses in the physiological salt solution. Taking in to account changes in the concentration of ATP^{4-} abolished the significant increase in EC_{50} obtained by increasing Mg^{2+} to 3 mM (Figure 3-8B, Table 3-5B).

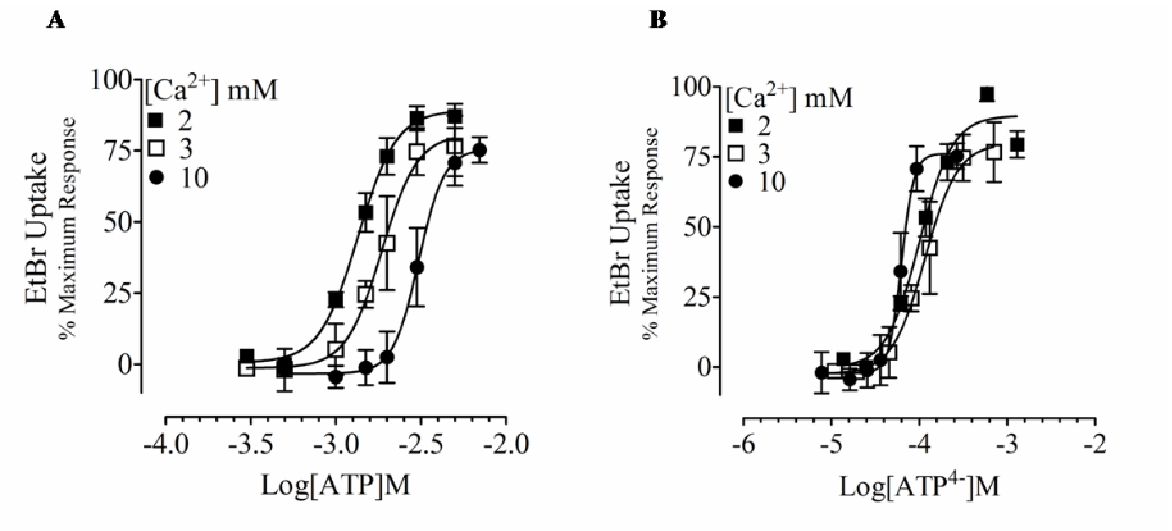

Figure 3-7. Increasing External Ca^{2+} Inhibits EtBr Uptake by Decreasing [ATP^{4-}]. ATP was injected on to RAW264.7 cells (1.5 x 10^5) bathed in physiological salt solution containing either 2, 3 or 10 mM Ca^{2+} and 25 μM EtBr (37 °C). A, Concentration-response curves demonstrating the effect of ATP on EtBr uptake in the presence of increasing [Ca^{2+}]. B, Re-plotted ATP^{4-} concentration response curves. (n = 4 ± s.e.m).

A

[Ca^{2+}] mM	**pEC_{50} ± s.e.m**	**n_H ± s.e.m**	**α ± s.e.m**
2	2.85 ± 0.07	3.86 ± 0.77	83 ± 2
3	2.83 ± 0.11	4.13 ± 1.84	101 ± 14
10	2.54 ± 0.04**	5.77 ± 3.38	76 ± 7

B

[Ca^{2+}] mM	**pEC_{50} ± s.e.m**
2	4.03 ± 0.09
3	3.87 ± 0.12
10	4.21 ± 0.07

Table 3-4. ATP Concentration-Response Curve Parameters for EtBr Uptake in the Presence of Increasing [Ca^{2+}]$_e$. A, ATP concentration-response curve parameters. B, ATP^{4-} pEC_{50} values. n = 4 ± s.e.m, One-Way ANOVA **:$p<0.001$.

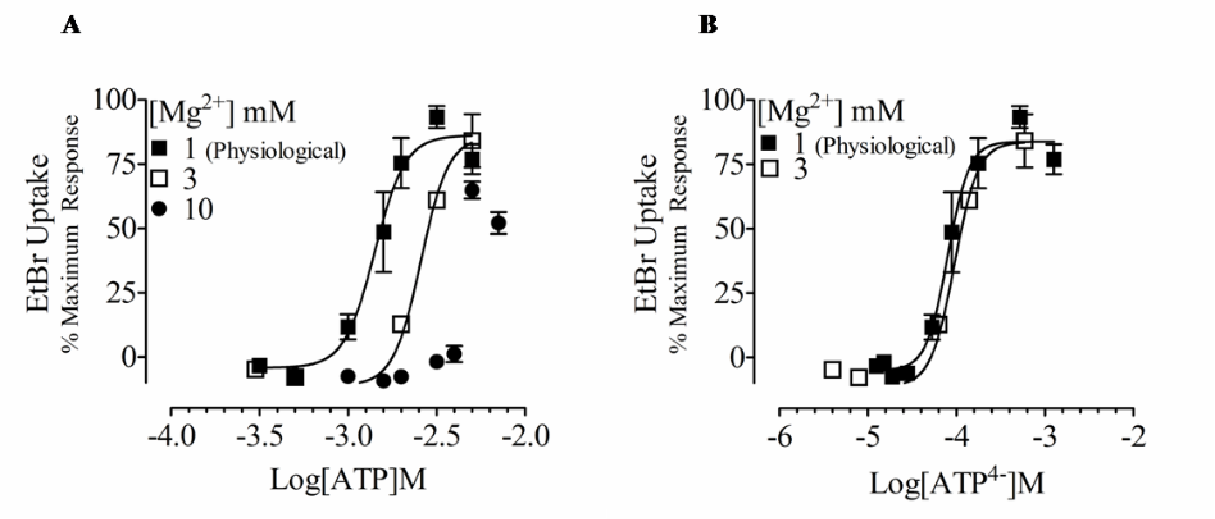

Figure 3-8. Increasing External Mg^{2+} Inhibits EtBr Uptake by Decreasing $[ATP^{4-}]$. ATP was injected on to RAW264.7 cells (1.5 x 10^5) bathed in physiological salt solution containing either 1 (physiological), 3 or 10 mM Mg^{2+} and 25 μM EtBr (37 °C). A, Concentration-response curves demonstrating the effect of ATP on EtBr uptake in the presence of increasing $[Mg^{2+}]$. B, Re-plotted ATP^{4-} concentration response curves. (n = 5 ± s.e.m).

A

$[Mg^{2+}]$ mM	**pEC_{50} ± s.e.m**	**n_H ± s.e.m**	**α ± s.e.m**
1	2.84 ± 0.05	5.04 ± 1.35	94 ± 8
3	2.62 ± 0.05*	5.59 ± 1.15	95 ± 14
10	NA	NA	NA

B

$[Mg^{2+}]$ mM	**pEC_{50} ± s.e.m**
1	4.01 ± 0.10
3	4.06 ± 0.07
10	NA

Table 3-5. ATP Concentration-Response Curve Parameters for EtBr Uptake in the Presence of Increasing $[Mg^{2+}]_e$. A, ATP concentration-response curve parameters. B, ATP^{4-} pEC_{50} values. n = 5 ± s.e.m, One-Way ANOVA with Dunnett's post-hoc test **:p<0.01.

3.2.6 Effect of Heavy Metal Cations Cadmium and Mercury of EtBr Uptake

Addition of Hg^{2+} at concentrations ≤ 3 μM into the external physiological salt solution was observed to have no significant effect on ATP evoked EtBr uptake into RAW264.7 cells (n = 4) (Figure 3-9A, Table 3-6). An addition of 10 μM Hg^{2+} however was observed to increase the maximal rate of EtBr uptake evoked by ATP by 118 ± 54 % (n = 4). This was observed to occur with no significant change in n_H or EC_{50} (n = 4, $p>0.05$) and in the absence of any significant change in the release of lactate dehydrogenase (n = 3, $p>0.05$) (Figure 3-9B).

Addition of Cd^{2+} at a concentration of 1 mM was observed to rightward shift the ATP EtBr concentration-response curve resulting in a significant increase in the EC_{50} from 1.58 mM to 2.29 mM (n = 4, $p<0.01$) (Figure 3-10A, Table 3-7A). The n_H was observed to decrease with increasing concentrations of Cd^{2+} however this decrease was not found to be statistically significant (n = 4, $p>0.05$). Taking in to account changes in the concentration of ATP^{4-} abolished the significant increase in EC_{50} obtained by evoking EtBr uptake in the presence of Cd^{2+} (Figure 3-10B, Table 3-7B).

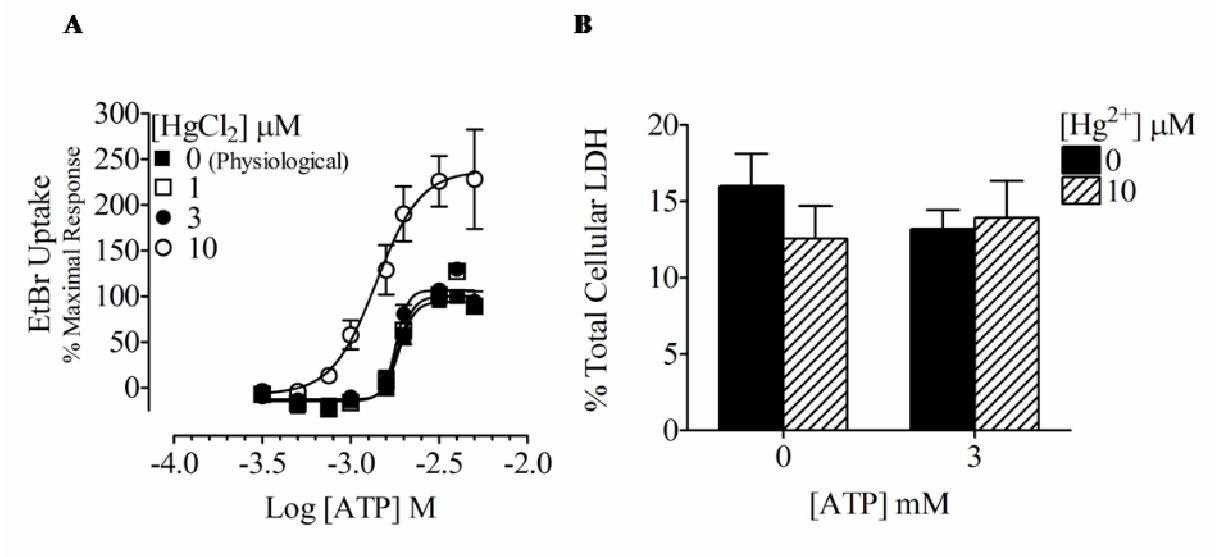

Figure 3-9. Extracellular $HgCl_2$ Potentiates EtBr Uptake in the Absence of Cell Death. A, Concentration-response curves demonstrating the effect of the presence of Hg^{2+} on ATP evoked EtBr uptake (n = 4 ± s.e.m). B, Histogram of the effect of Hg^{2+} on RAW264.7 cell death in the absence and presence of an ATP stimulation (15 minutes) (n = 3 ± s.e.m).

$[Hg^{2+}]$ µM	**pEC_{50} ± s.e.m**	**n_H ± s.e.m**	**α ± s.e.m**
0	2.74 ± 0.03	5.25 ± 1.12	109 ± 4
1	2.74 ± 0.04	6.05 ± 1.98	114 ± 8
3	2.75 ± 0.04	6.49 ± 2.29	120 ± 11
10	2.85 ± 0.08	3.45 ± 1.34	232 ± 50*

Table 3-6. ATP Concentration-Response Curve Parameters for EtBr Uptake in the Presence of Hg^{2+}. n = 4 ± s.e.m, One-Way ANOVA with Dunnett's post-hoc test **:$p<0.05$.

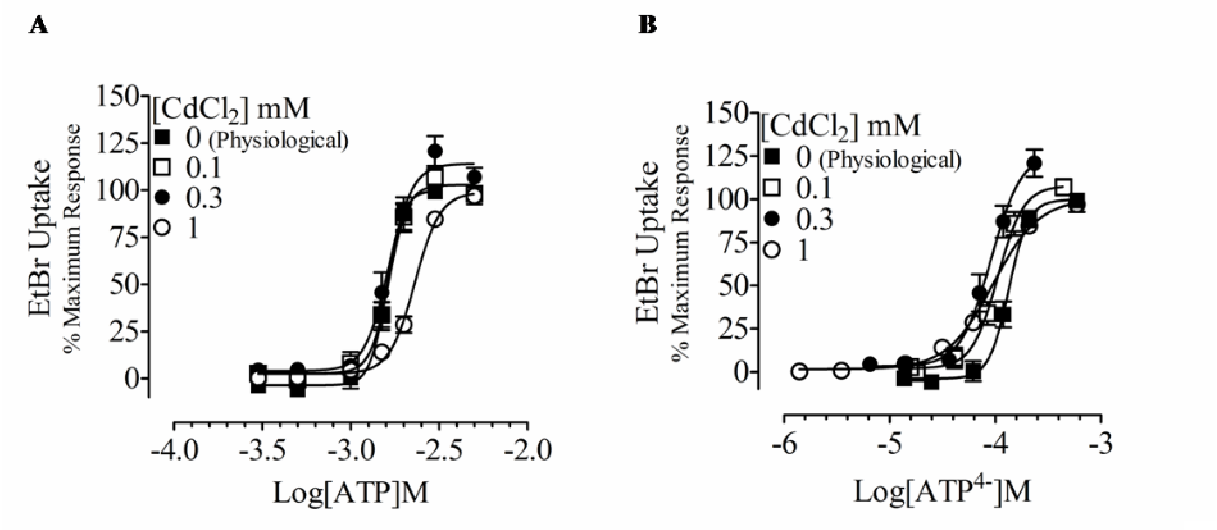

Figure 3-10. Extracellular Cd^{2+} Inhibits EtBr Uptake by Decreasing $[ATP^{4-}]$. A, Concentration-response curves demonstrating the effect of ATP on EtBr uptake in the presence of Cd^{2+}. B, Re-plotted ATP^{4-} concentration response curves. ($n = 4 \pm$ s.e.m).

A

$[Cd^{2+}]$ mM	**pEC_{50} ± s.e.m**	**n_H ± s.e.m**	**α ± s.e.m**
0	2.80 ± 0.01	5.15 ± 1.23	97 ± 4
0.1	2.78 ± 0.02	5.38 ± 1.31	100 ± 10
0.3	2.79 ± 0.04	6.25 ± 0.37	110 ± 10
1	2.64 ± 0.02**	5.07 ± 0.91	99 ± 8

B

$[Cd^{2+}]$ mM	**pEC_{50} ± s.e.m**
0	3.88 ± 0.02
1	4.01 ± 0.07

Table 3-7. ATP Concentration-Response Curve Parameters for EtBr Uptake in the Presence of Cd^{2+}. A, ATP concentration-response curve parameters. B, ATP^{4-} pEC_{50} values. $n = 4 \pm$ s.e.m, One-Way ANOVA or Student's two-tailed t-test **:$p<0.01$.

3.2.7 Effect of the Trace Metal Ions Zinc and Copper on ATP Evoked EtBr Uptake

Stimulating RAW264.7 cells with ATP in presence of ≥ 300 μM Zn^{2+} was observed to inhibit EtBr uptake. Concentration-response curves were observed to be rightward shifted when extracellular Zn^{2+} was present (Figure 3-11A and B), with an increase in the EC_{50} from 1.51 mM to 2.57 mM (1 mM $ZnCl_2$). Significant differences in the pEC_{50} values of ATP were calculated when in the presence of 0.3 and 1 mM Zn^{2+} (n = 9, $p<0.01$) (Table 3-8A). A significant difference in the n_H of the ATP concentration-response curve was calculated when 1 mM Zn^{2+} was present (n = 9, $p<0.01$). No significant change in α was observed with increasing concentrations of Zn^{2+} (n = 9, $p>0.05$), however it is debatable whether a true maxima for the ATP concentration-response curve in the presence of 1 mM $ZnCl_2$ was reached. Taking in to account changes in the concentration of ATP^{4-} abolished the significant decrease in pEC_{50} values obtained by evoking EtBr uptake in the presence of Zn^{2+} (Figure 3-11C and D, Table 3-8B).

Evoking ATP induced EtBr uptake in the presence of Cu^{2+} was observed to inhibit EtBr uptake. Plotting concentration-response curves demonstrated that 10 and 30 μM Cu^{2+} decreased the maximum rate of EtBr uptake (Figure 3-12A). A significant reduction in α was determined in the presence of 30 μM Cu^{2+} by 67 ± 18 % (n = 4 ± s.e.m, $p<0.01$) (Table 3-9). No significant change in pEC_{50} or n_H was observed with any of the concentrations of Cu^{2+} (n = 4, $p>0.05$).

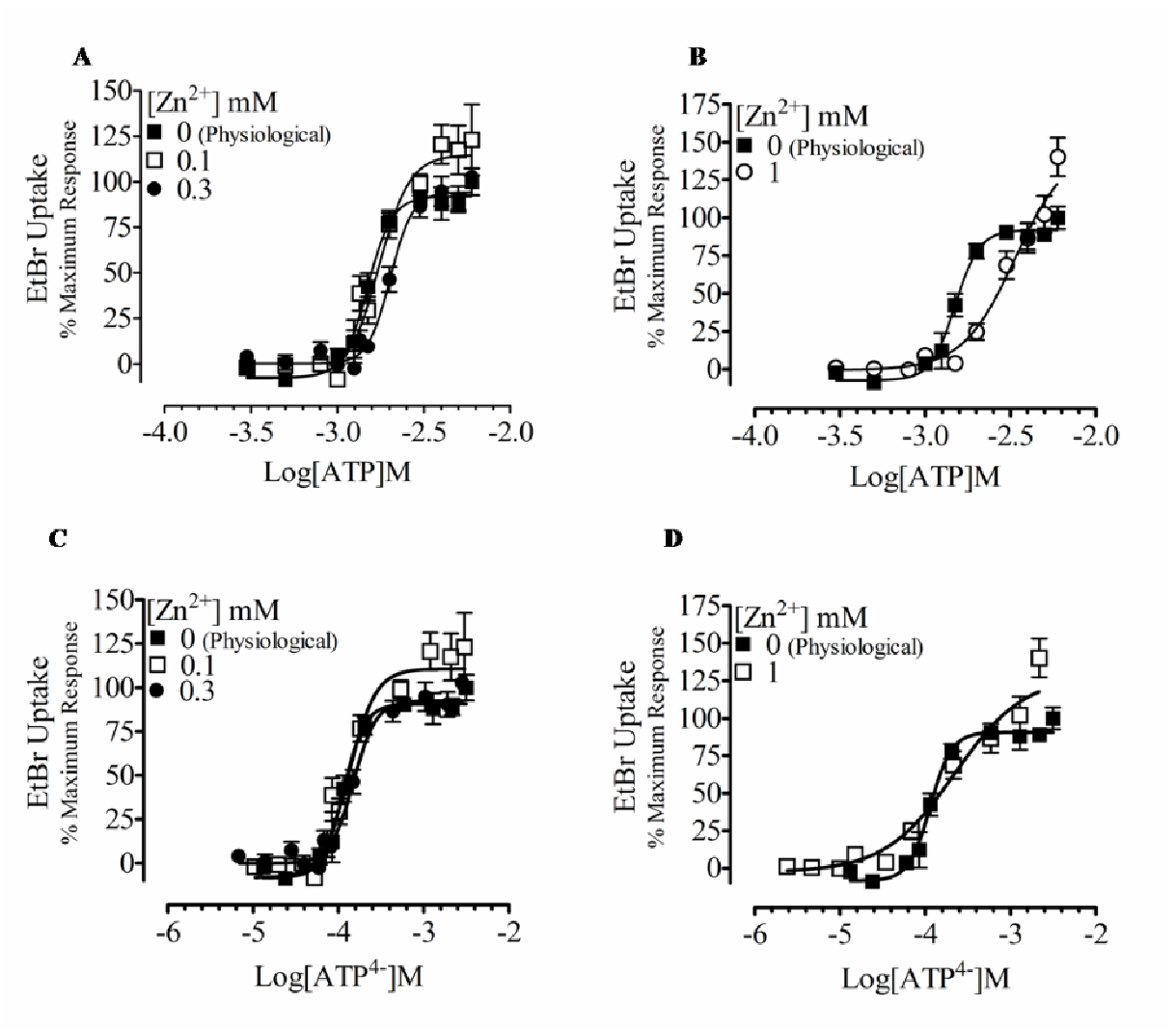

Figure 3-11. Extracellular Zn^{2+} Modulates EtBr Uptake Induced by ATP. A, Concentration-response curves demonstrating the effect of ATP on EtBr uptake in the presence of 100 and 300 μM Zn^{2+}. B, Concentration-response curves demonstrating the effect of ATP on EtBr uptake in the presence of 1 mM Zn^{2+}. C, Re-plotted ATP^{4-} concentration response curves demonstrating the effect of 100 and 300 μM Zn^{2+}. D, Re-plotted ATP^{4-} concentration response curves demonstrating the effect of 1 mM Zn^{2+}. (n = 9 ± s.e.m).

A

$[Zn^{2+}]$ mM	**pEC_{50} ± s.e.m**	**n_H ± s.e.m**	**α ± s.e.m**
0	2.82 ± 0.04	6.10 ± 1.19	111 ± 7
0.1	2.76 ± 0.04	4.87 ± 0.99	117 ± 9
0.3	2.63 ± 0.04**	6.77 ± 1.71	119 ± 8
1	2.59 ± 0.05**	2.8 ± 1.08**	117 ± 25

B

$[Zn^{2+}]$ mM	**pEC_{50} ± s.e.m**
0	3.96 ± 0.06
0.1	3.79 ± 0.10
0.3	3.67 ± 0.10
1	3.53 ± 0.32

Table 3-8. ATP Concentration-Response Curve Parameters for EtBr Uptake in the Presence of Zn^{2+}. A, ATP concentration-response curve parameters in the presence of Zn^{2+}. B, ATP^{4-} pEC50 values in the presence of Zn^{2+}. $n = 9 \pm$ s.e.m, One-Way ANOVA with Dunnett's post-hoc test **:$p<0.01$.

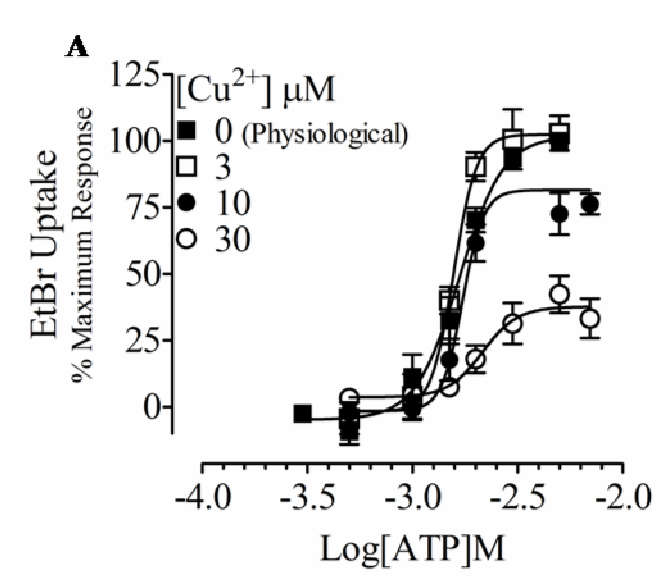

Figure 3-12. Extracellular Cu^{2+} Inhibits EtBr Uptake Induced by ATP. Concentration-response curve demonstrating the effect of ATP on EtBr uptake in the presence of 3, 10 and 30μM Cu^{2+}. (n = 4 ± s.e.m).

$[Cu^{2+}]$ μM	**pEC_{50} ± s.e.m**	***nH* ± s.e.m**	**α ± s.e.m**
0	2.79 ± 0.03	4.19 ± 0.92	108 ± 6
3	2.82 ± 0.01	7.99 ± 2.68	101 ± 22
10	2.77 ± 0.03	8.66 ± 2.12	85 ± 3
30	2.65 ± 0.08	5.23 ± 3.14	32 ± 11**

Table 3-9. ATP Concentration-Response Curve Parameters for EtBr Uptake in the Presence of Cu^{2+}. n = 4 ± s.e.m, One-Way ANOVA with Dunnett's post-hoc test **:$p<0.01$.

3.2.8 Effect of Zinc on Recombinant Mouse and Rat P2X7 Receptors

The effect of Zn^{2+} on the recombinant mouse $P2X_7R$ expressed in HEK293 cells was studied to determine whether the lack of effect of Zn^{2+} on the mouse $P2X_7R$ endogenously expressed on RAW264.7 cells was due to a fault in either the expression system or assay used. In addition the effect of Cu^{2+} on the recombinant mouse $P2X_7R$ receptor expressed in HEK293 cells was studied. Furthermore control experiments observing the effect of Zn^{2+} and Cu^{2+} on the recombinant rat $P2X_7$ receptor were also performed, which has previously been demonstrated to be inhibited by these ions (Virginio *et al.*, 1997).

An application of 5 mM ATP onto HEK293 cells transfected with the mouse $P2X_7$ receptor was observed to evoke uptake of EtBr above control (Figure 3-13A). Uptake of EtBr was observed to be increased when 300 μM $ZnCl_2$ was added to the physiological salt solution (Figure 3-13B). Constructing dose-response curves demonstrated that 300 μM Zn^{2+} decreased the EC_{50} of ATP from 2.64 mM to 1.68 mM (n = 5) (Figure 3-13C, Table 3-10A), pEC_{50} values were found to be significantly increased (n = 5, $p<0.01$) with no significant changes in n_H or α observed (n = 5).

ATP was observed to elicit a dose-dependent increase in EtBr uptake in HEK293 cells expressing the rat $P2X_7R$ with an EC_{50} of 955 μM (n = 7) (Figure 3-13D), which was observed to be lower than the EC_{50} values obtained at the $P2X_7R$ in both RAW 264.7 and HEK293/m$P2X_7R$ cells (1.55 mM and 2.64 mM respectively). Addition of 100 μM Zn^{2+} to the physiological salt solution was observed to significantly inhibit EtBr uptake. This inhibition was due to a significant decrease in the maximal rate of EtBr uptake by 63 ± 10 % (n = 7 ± s.e.m, $p<0.01$) (Table 3-10B). No significant changes in pEC_{50} or n_H were observed (n = 7).

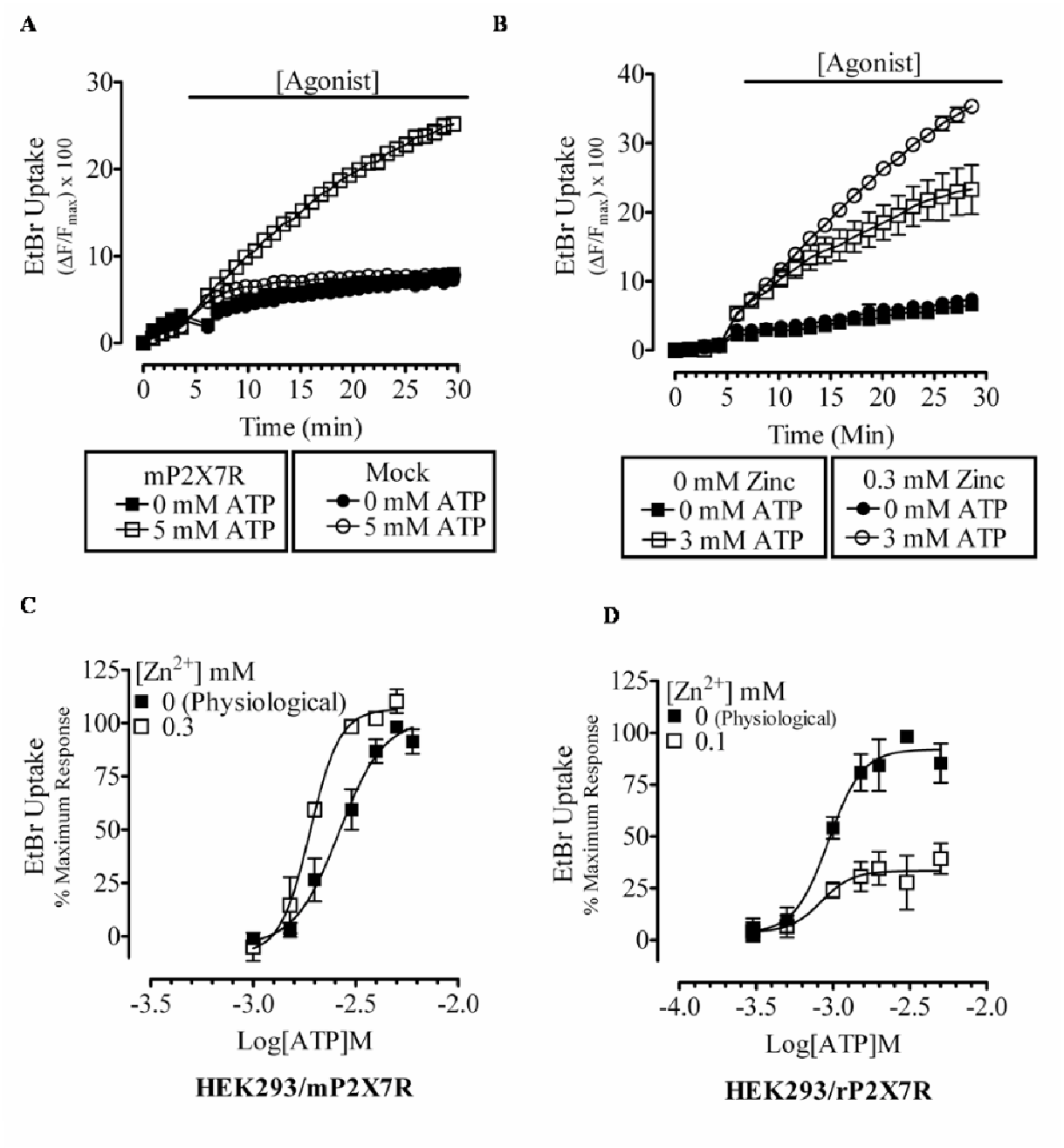

Figure 3-13. EtBr Uptake Modulation by Zn^{2+} at mP2X$_7$R and rP2X$_7$R Expressed in HEK293 cells. A, Representative kinetic graph demonstrating EtBr uptake occurring only when ATP is injected onto HEK293 cells expressing the mP2X$_7$R. B, Representative kinetic graph demonstrating an increase in the rate of EtBr uptake when ATP stimulation of HEK293/mP2X$_7$R cells occurs in the presence of 300 μM Zn^{2+}. C, HEK293/mP2X$_7$R concentration-response curve demonstrating a leftward shift in EtBr uptake when 300 μM Zn^{2+} is present (n = 5 ± s.e.m). D, HEK293/rP2X$_7$R concentration-response curve demonstrating a decrease in maximal EtBr uptake when 100 μM Zn^{2+} is present (n = 7 ± s.e.m).

A

HEK293/mP2X7R

$[Zn^{2+}]$ μM	**pEC_{50} ± s.e.m**	**n_H ± s.e.m**	**α ± s.e.m**
0	2.58 ± 0.05	3.97 ± 1.15	102 ± 7
300	2.78 ± 0.07*	5.96 ± 1.76	118 ± 6

B

HEK293/rP2X7R

$[Zn^{2+}]$ μM	**pEC_{50} ± s.e.m**	**n_H ± s.e.m**	**α ± s.e.m**
0	3.02 ± 0.03	3.93 ± 1.69	96 ± 1
100	3.13 ± 0.12	4.32 ± 5.51	36 ± 9**

Table 3-10. ATP Concentration-Response Curve Parameters for EtBr Uptake at the Mouse and Rat $P2X_7R$ in the Absence and Presence of Zn^{2+}. A, ATP concentration-response curve parameters in the presence of Zn^{2+} for HEK293/mP2X7R. n = 5 ± s.e.m. B, ATP concentration-response curve parameters in the presence of Zn^{2+} for HEK293/rP2X7R. n = 7 ± s.e.m. Student's two-tailed t-test *:$p<0.05$, **:$p<0.01$.

3.2.9 Effect of Copper on Recombinant Mouse and Rat $P2X_7$ Receptors

In a physiological salt solution ATP evoked EtBr uptake into HEK293 cells expressing either the $mP2X_7R$ or $rP2X_7R$ was inhibited by Cu^{2+} (Figure 3-14A and B). A true maximum for the ATP concentration-response curves at the recombinant mouse $P2X_7R$ was not reached therefore curve fitting parameters are not given. Rate of EtBr uptake induced by 5 mM ATP was reduced by 35 ± 17 % (n = 5 ± s.e.m) when 30 μM Cu^{2+} was present. A true maximum for ATP concentration-response curves at the recombinant rat $P2X_7R$ was not reached, therefore curve fitting parameters are not given. Rate of EtBr uptake induced by 3 mM ATP was reduced by 37 ± 12 % (n = 4 ± s.e.m) when 30 μM Cu^{2+} was present.

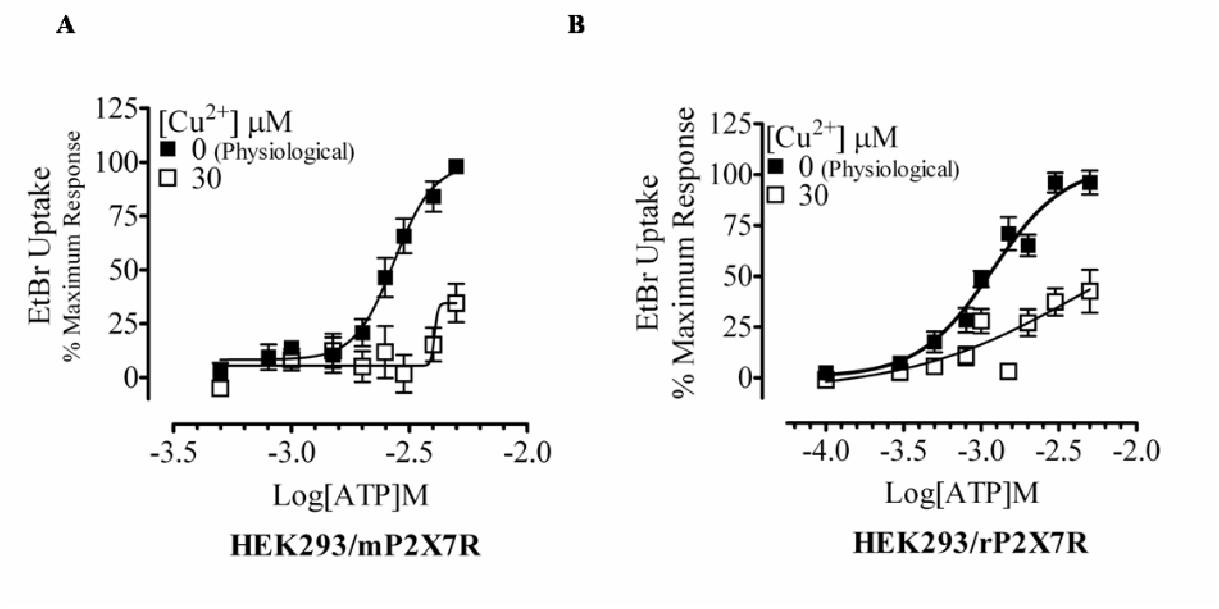

Figure 3-14. EtBr Uptake is Inhibited by Cu^{2+} at mP2X$_7$R and rP2X$_7$R Expressed in HEK293 cells. A, HEK293/mP2X7R concentration-response curve demonstrating a reduction in the maximum response when 30 µM Cu^{2+} is present (n = 5 ± s.e.m). B, HEK293/rP2X7R concentration-response curve demonstrating a decrease in the maximum response when 30 µM Cu^{2+} is present (n = 4 ± s.e.m).

3.2.10 Reducing Extracellular $[Ca^{2+}]$ and $[Mg^{2+}]$ Enhances EtBr Uptake by Increasing $[BzATP^{4-}]$

In addition to the different efficacies of antagonists between species of $P2X_7R$, it has also been noted that antagonists can have differing efficacy at the same species of receptor when different agonists are used. Many studies of the $P2X_7R$ use the ATP analogue BzATP, which is regarded by some as a selective agonist of the $P2X_7R$. This however is untrue. BzATP is known to activate other P2X receptors with either comparable or lower EC_{50}s (Table 1-1). Therefore as part of the study into divalent cation modulation of the $P2X_7R$, the effect of metal ions on BzATP evoked responses was examined.

Using RAW264.7 cells an application of the non-physiological but more potent $P2X_7R$ agonist, BzATP was found to elicit EtBr uptake in the physiological salt solution at lower concentrations than ATP. However a maximal response was not reached despite using up to 1 mM BzATP (n = 8, Figure 3-15A). Removal of both extracellular Ca^{2+} and Mg^{2+} (nominal) was observed to cause an increase in the rate of dye uptake induced by BzATP with a maximal response reached using ≈ 300 μM BzATP and an EC_{50} of 89 μM calculated (n = 8, Figure 3-15A, Table 3-11). Comparing the responses of BzATP and ATP in the nominal Ca^{2+}/Mg^{2+} solution revealed that BzATP evoked EtBr uptake into RAW264.7 cells with a significantly lower EC_{50} (n = 8, $p<0.001$) (Table 3-11.). No significant change in n_H or α was observed ($p>0.05$). Taking in to account changes in the concentration of $BzATP^{4-}$ revealed that BzATP induced concentration-response curves evoked in a physiological salt solution and a nominal Ca^{2+}/Mg^{2+} salt solution were now overlapping (Figure 3-15B).

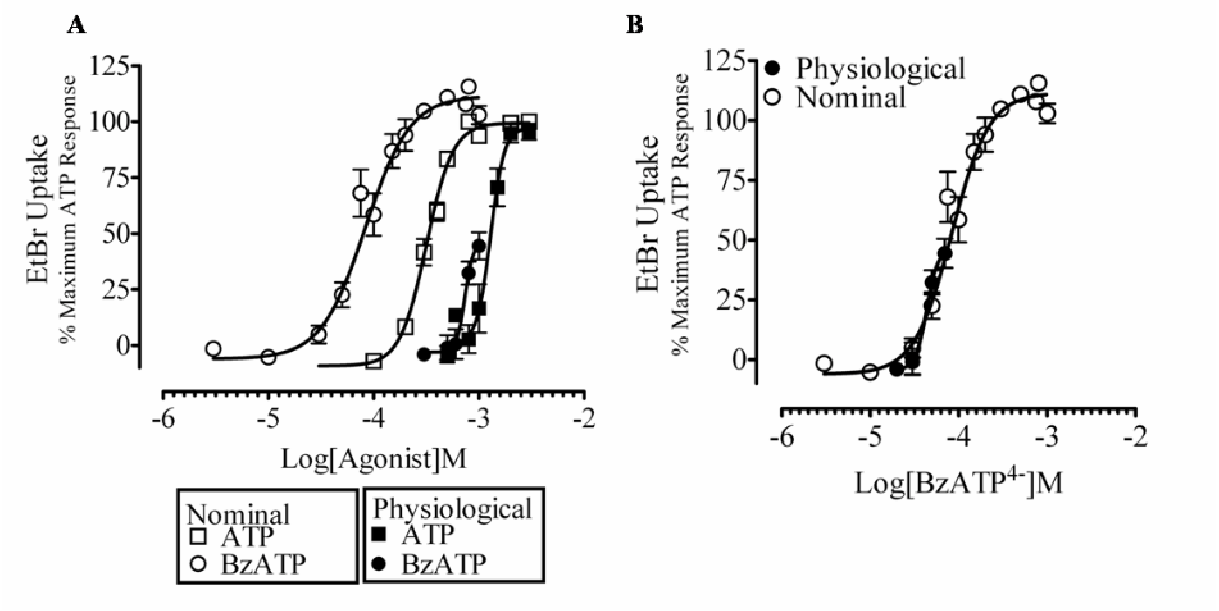

Figure 3-15. Removal of Extracellular Ca^{2+} & Mg^{2+} Potentiates EtBr Uptake by Increasing Free [$BzATP^{4-}$]. A, Concentration-response curves demonstrating the effect of ATP and BzATP on EtBr uptake in the presence and absence of Ca^{2+}/Mg^{2+}. B, Re-plotted $BzATP^{4-}$ concentration response curves. (n = 8 ± s.e.m).

	pEC_{50} ± s.e.m	n_H ± s.e.m	α ± s.e.m
ATP	3.56 ± 0.06	5.16 ± 1.19	119 ± 12
BzATP	4.05 ± 0.10***	6.31 ± 1.36	121 ± 10

Table 3-11. ATP and BzATP Concentration-Response Curve Parameters for EtBr uptake in Nominal Ca^{2+}/Mg^{2+} Salt Solution. n = 8 ± s.e.m, Student's two-tailed t-test where ***:p<0.001.

3.2.11 Effect of Zinc on ATP Evoked EtBr Uptake in the Absence of Ca^{2+} and Mg^{2+}

In order to assess and compare the effect of Zn^{2+} on BzATP activation of the P2X$_7$R, the study would require responses to be elicited in a nominal Ca^{2+}/Mg^{2+} solution to construct full concentration-response curves. Initially I determined the effect of Zn^{2+} on modulating ATP evoked EtBr uptake in a nominal Ca^{2+}/Mg^{2+} solution.

Stimulating RAW264.7 cells with ATP in the presence of 100 μM or 300 μM Zn^{2+} was observed to inhibit EtBr uptake. Construction of concentration-response curves demonstrated that curves were rightward shifted in the presence of Zn^{2+} (n = 6, Figure 3-16A). The EC_{50} value of ATP was found to increase from 302 μM to 575μM and 603 μM in the presence of 100 and 300 μM Zn^{2+} respectively (Table 3-12A). No significant change in n_H or α was observed ($p>0.05$). Taking in to account changes in the concentration of ATP^{4-} abolished the significant increase in EC_{50} obtained by evoking EtBr uptake in the presence of Zn^{2+} (Figure 3-16B).

Stimulating the HEK293/mP2X$_7$R with ATP in the presence of 300 μM Zn^{2+} was observed to potentiate EtBr uptake (n = 3). This potentiation was observed as an increase in the maximal response ($p<0.05$) without significant change in EC_{50} or n_H (Figure 3-16C, Table 3-12B).

Stimulating the HEK293/rP2X$_7$R with ATP in the presence of 100 μM Zn^{2+} was observed to inhibit EtBr uptake (n = 3, Figure 3-16D). This inhibition was observed as a significant increase in the EC_{50} from 339 μM to 871 μM ($p<0.01$, Table 3-12C). No significant change in n_H or α was observed ($p>0.05$). Taking in to account changes in $[ATP^{4-}]$ I still observed a significant increase in the EC_{50} of ATP induced EtBr uptake in the presence of Zn^{2+} when compared to control responses ($p<0.01$, Figure 3-16E).

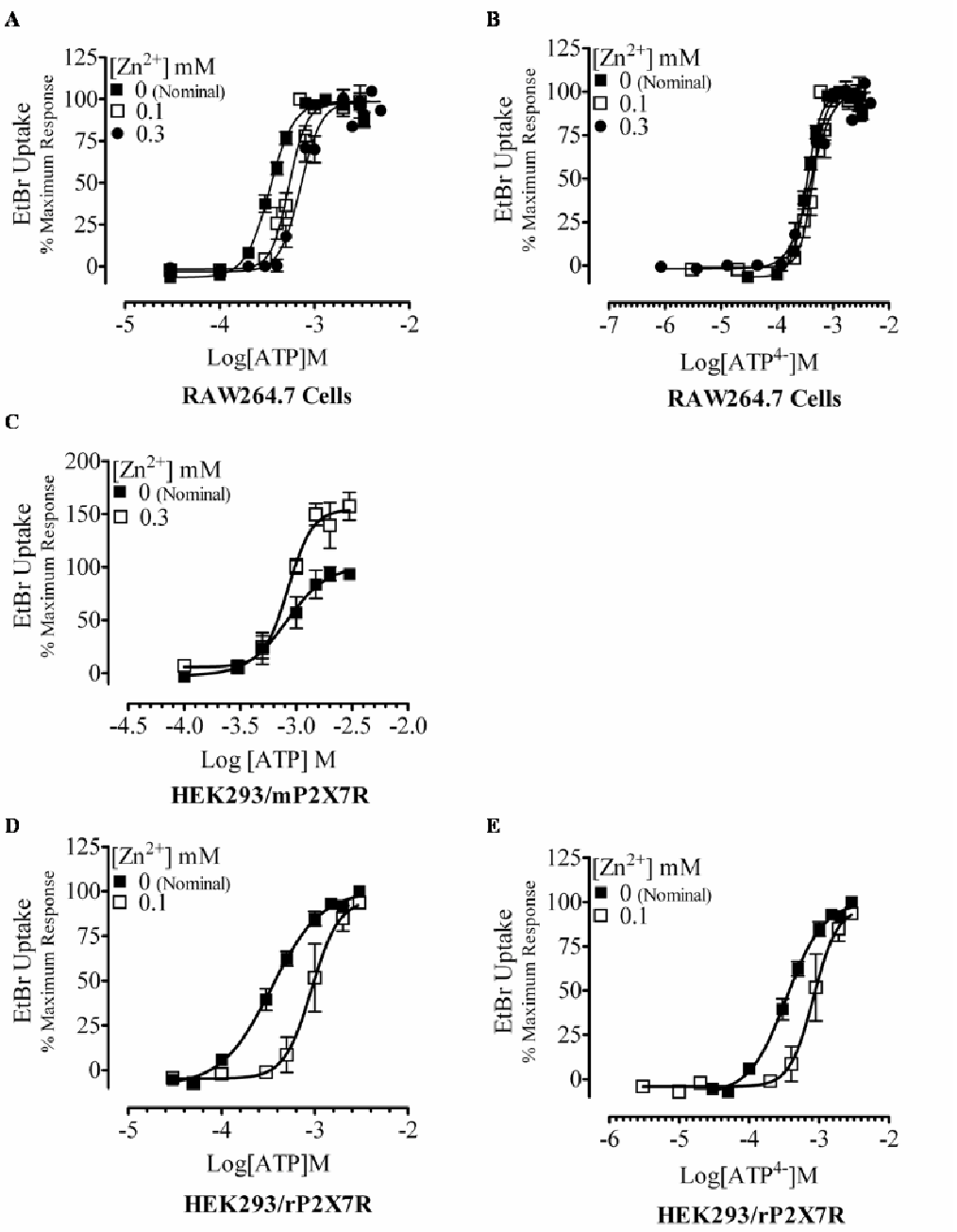

Figure 3-16. Modulation of EtBr Uptake by Zn^{2+} in the Absence of Ca^{2+} and Mg^{2+}. A, Concentration-response curve demonstrating the effect of Zn^{2+} on EtBr uptake into RAW264.7 cells (n = 6 ± s.e.m). B, Re-plotted ATP^{4-} concentration response curves demonstrating the effect of 100 and 300 μM Zn^{2+}. C, Concentration-response curve demonstrating the effect of Zn^{2+} on EtBr uptake into HEK293/mP2X$_7$R cells (n = 3 ± s.e.m). D, Concentration-response curve demonstrating the effect of Zn^{2+} on EtBr uptake into HEK293/rP2X$_7$R cells (n = 3 ± s.e.m). E, Re-plotted ATP^{4-} concentration response curves demonstrating the effect of 100 μM Zn^{2+}.

A

RAW264.7 Cells

$[Zn^{2+}]$ mM	**pEC_{50} ± s.e.m**	**n_H ± s.e.m**	**α ± s.e.m**
0	3.52 ± 0.18	3.39 ± 0.41	114 ± 10
0.1	3.24 ± 0.11*	4.67 ± 0.94	89 ± 11
0.3	3.22 ± 0.23**	3.94 ± 0.64	97 ± 9

B

HEK293/$mP2X_7R$

$[Zn^{2+}]$ mM	**pEC_{50} ± s.e.m**	**n_H ± s.e.m**	**α ± s.e.m**
0	3.10 ± 0.11	3.31 ± 0.40	100 ± 8
0.3	3.09 ± 0.06	4.19 ± 0.34	151 ± 14*

C

HEK293/$rP2X_7R$

$[Zn^{2+}]$ mM	**pEC_{50} ± s.e.m**	**n_H ± s.e.m**	**α ± s.e.m**
0	3.47 ± 0.05	1.82 ± 0.23	114 ± 6
0.1	3.06 ± 0.01**	2.97 ± 1.2	90 ± 7

Table 3-12. ATP Concentration-Response Curve Parameters for EtBr Uptake in the Presence of Zn^{2+} in a Nominal Ca^{2+}/Mg^{2+} Salt Solution. A, RAW264.7 cells (n = 6 ± s.e.m). B, HEK293/$mP2X_7R$ cells (n = 3 ± s.e.m). C, HEK293/$rP2X_7R$ cells (n = 3 ± s.e.m). One-Way ANOVA or two-tailed Student's t-test *:$p<0.05$, **:$p<0.01$.

3.2.12 Effect of Zinc on BzATP Evoked EtBr Uptake

As a maximum response to BzATP was not observed in a physiological salt solution using concentrations up to 1 mM, the action of extracellular Zn^{2+} was studied in a nominal Ca^{2+}/Mg^{2+} salt solution. In RAW264.7 cells extracellular Zn^{2+} was observed to inhibit EtBr uptake with 100 μM Zn^{2+} shifting the EC_{50} to 796 μM from 91 μM ($p<0.001$, $n = 3$) (Figure 3-17A, Table 3-13A). No significant change in n_H or α was observed ($p>0.05$). Taking into account changes in [$BzATP^{4-}$] I still observed a significant rightward shift in the BzATP evoked concentration-response curve in the presence of Zn^{2+} ($p<0.001$, Figure 3-13B).

BzATP stimulations of HEK293/mP2X$_7$R cells evoked EtBr uptake, however a maximal response was not reached using up to 1 mM BzATP ($n = 3$, Figure 3-17C). Application of 300 μM Zn^{2+} was observed to reduce maximal EtBr uptake evoked by BzATP ($n = 3$). For HEK293/rP2X$_7$R cells BzATP evoked EtBr uptake with an EC_{50} of 13.2 μM (pEC_{50} = -4.88 ± 0.007, $n = 3$ ± s.e.m). An addition of 100 μM Zn^{2+} or 300 μM Zn^{2+} was observed to significantly inhibit BzATP evoked responses ($n = 3$) where the EC_{50} value increased to 224 μM in the presence of 100 μM Zn^{2+} ($p<0.001$, Figure 3-17D, Table 3-13B). Taking into account changes in [$BzATP^{4-}$] I still observed a significant rightward shift in the BzATP evoked concentration-response curve in the presence of Zn^{2+} ($p<0.01$, Figure 3-17E).

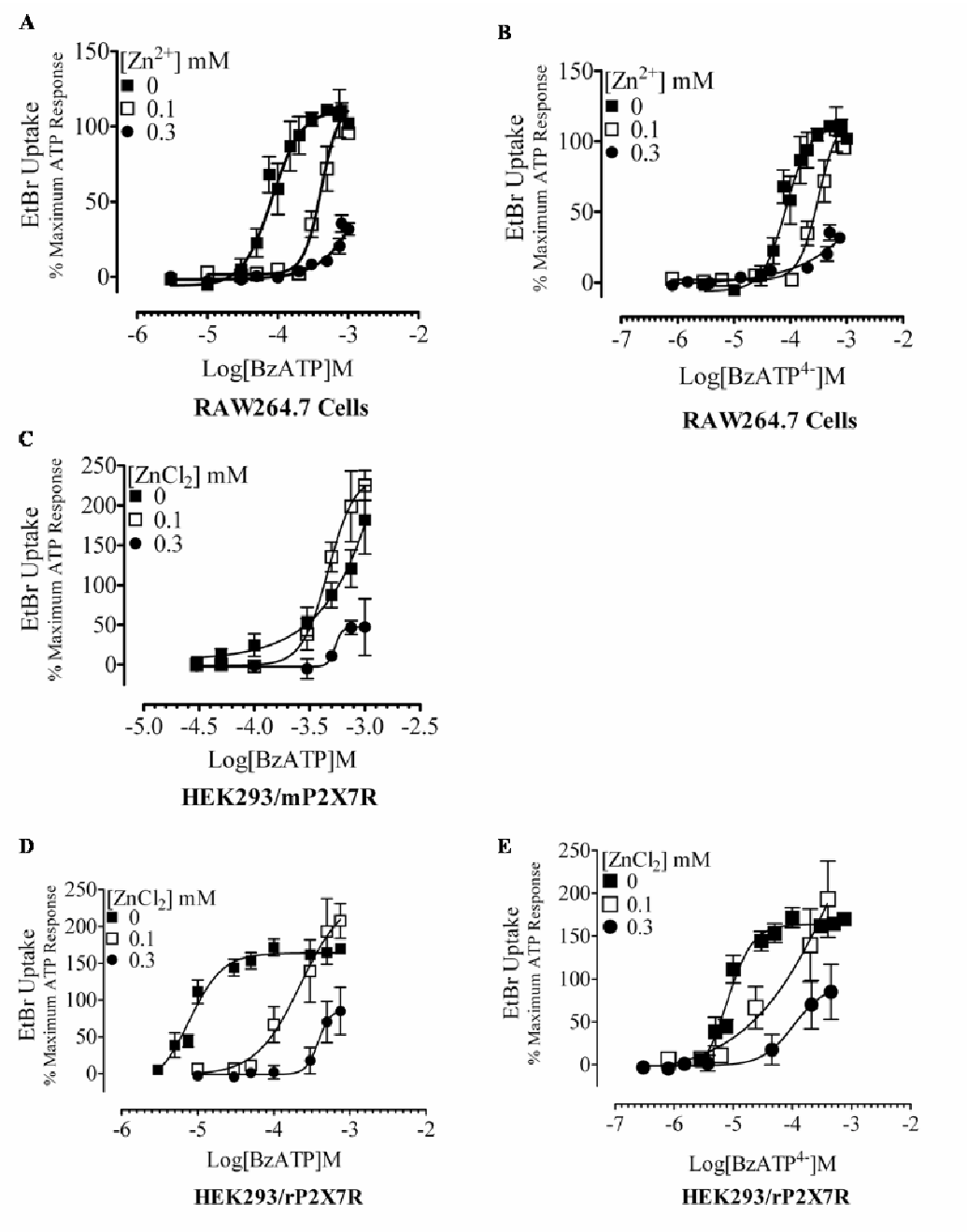

Figure 3-17. Modulation of BzATP evoked EtBr Uptake by Zn^{2+} in the Absence of Ca^{2+} and Mg^{2+}. A, Concentration-response curve demonstrating the effect of Zn^{2+} on EtBr uptake into RAW264.7 cells (n = 3 ± s.e.m). B, Re-plotted $BzATP^{4-}$ concentration response curves demonstrating the effect of 100 and 300 μM Zn^{2+}. C, Concentration-response curve demonstrating the effect of Zn^{2+} on EtBr uptake into HEK293/mP2X$_7$R cells (n = 3 ± s.e.m). D, Concentration-response curve demonstrating the effect of Zn^{2+} on EtBr uptake into HEK293/rP2X$_7$R cells (n = 3 ± s.e.m). E, Re-plotted $BzATP^{4-}$ concentration response curves demonstrating the effect of 100 μM Zn^{2+}.

A

RAW264.7 Cells

$[Zn^{2+}]$ mM	**pEC_{50} ± s.e.m**	**n_H ± s.e.m**	**α ± s.e.m**
0	4.04 ± 0.10	2.09 ± 0.67	117 ± 11
0.1	3.10 ± 0.14***	3.43 ± 1.32	114 ± 8

B

HEK293/$rP2X_7R$

$[Zn^{2+}]$ mM	**pEC_{50} ± s.e.m**	**n_H ± s.e.m**	**α ± s.e.m**
0	4.88 ± 0.05	1.82 ± 0.23	163 ± 11
0.1	3.65 ± 0.26**	2.97 ± 1.2	214 ± 23

Table 3-13. BzATP Concentration-Response Curve Parameters for EtBr Uptake in the Presence of Zn^{2+} in a Nominal Ca^{2+}/Mg^{2+} Salt Solution. A, RAW264.7 cells (n = 3 ± s.e.m). B, HEK293/$rP2X_7R$ cells (n = 3 ± s.e.m). One-Way ANOVA or two-tailed Student's t-test *:$p<0.05$, **:$p<0.01$.

3.3 DISCUSSION

In this study I determined (i) the pharmacological properties of the murine $P2X_7R$ expressed endogenously in the RAW264.7 cell line, (ii) that metal ions such as Mg^{2+}, Ca^{2+} Cd^{2+} and Zn^{2+} inhibit the activation of this receptor by ATP by reducing the concentration of ATP^{4-}, (iii) Hg^{2+} can potentiate ATP evoked EtBr uptake, (iv) Cu^{2+} inhibits the activation of the $P2X_7R$ potentially through direct binding to the receptor and (v) Zn^{2+} modulation of the $P2X_7R$ is dependent on species, cell background and agonist.

3.3.1 General Pharmacology

The RAW264.7 murine macrophage cell line has previously been determined to express the $P2X_7R$ (Hiken *et al.*, 2004; Pfeiffer *et al.*, 2004) and this was confirmed by western blot and immunohistochemistry (Figure A-1[13]). Extracellular ATP in the presence of 2 mM Ca^{2+} was observed to evoke a concentration-dependent increase in $[Ca^{2+}]_i$ (Figure 3-2A). In order to assess the contribution of Ca^{2+} influx versus Ca^{2+} release from intracellular stores towards evoking this response, ATP was applied in Ca^{2+} free conditions. The results determined that a substantial part of the ATP evoked response is due to the uptake of Ca^{2+} into the cells probably through the activation of multiple types of P2Rs (Figure 3-2D). Three points indicated that part of this response is $P2X_7R$ mediated (i) an EC_{50} value of 380 μM is unlikely to be able to be accounted for by activation of P2Y or $P2X_{1\text{-}6}$ receptors alone (ii) the responses evoked by ATP concentrations of 1 and 3 mM were sustained and (iii) both peak and sustained parts of the response were inhibited by BBG and KN-62 (Figure 3-3). However the response is unlikely to be solely $P2X_7R$ mediated. Inhibition by BBG and KN-62 was only partial and the EC_{50} value of 380 μM obtained for ATP evoked increases in $[Ca^{2+}]_i$ was lower than that observed for the membrane currents mediated by cloned $mP2X_7Rs$; EC_{50} = 734 μM (Chessell *et al.*, 1998) and Ca^{2+} dependent IL-1β release from Bac1 macrophages; EC_{50} = 800 μM (Verhoef *et al.*, 2005).

ATP evoked pore formation with EC_{50}'s ranging from 1.41 to 1.82 mM, was completely blocked by KN-62 (IC_{50} = 1.32 μM) (Figure 3-4D) suggesting $P2X_7$ receptors alone stimulate EtBr uptake. Pore formation was found to occur within minutes of ATP application whereas prolonging ATP (3 mM) stimulation to 45 – 60 minutes was observed to evoke a significant release of the large cytosolic enzyme LDH, indicating a breakdown

[13] Figures A-1 to A7 are to be found within the I: Appendix

in the integrity of the cell membrane and therefore cell death. Release of LDH initiated by ATP could be completely blocked by pre-treating and stimulating cells in the presence of KN-62 (IC_{50} = 407 nM). This suggests and also agrees with other studies that $P2X_7R$ pore formation and potentially other $P2X_7R$ mediated apoptotic events can occur in the absence of cell death (MacKenzie *et al.*, 2001; Mackenzie *et al.*, 2005).

In order to assess the role of divalent cations on regulating the $mP2X_7R$ I employed the use of RAW264.7 cells (endogenous) and HEK293 cells expressing either the recombinant mouse or rat $P2X_7R$. This also gave us a more direct comparison of the sensitivity of the $mP2X_7R$ compared to the $rP2X_7R$ for ATP (in physiological salt solution). The endogenous and recombinant $mP2X_7R$ was observed to be less sensitive to ATP than the rat $P2X_7R$ (Table 3-14A). This pattern correlates with the literature (Young *et al.*, 2007), although our EC_{50} values are higher than those previously reported and expression system/cell background seemed to play a role in regulating sensitivity of the $P2X_7R$ to ATP. The differences between our EC_{50} values and those reported may reflect the choice of assay used to assess $P2X_7R$ activation. I also established that the $mP2X_7R$ could be blocked using KN-62 with an IC_{50} range of 407 – 1320 nM, making the receptor more sensitive to blockade to KN-62 than the rat receptor but less so than the human (Table 3-14B).

EC_{50} (mM)	MOUSE	RAT	HUMAN
Our Study	1.41 – 1.82 (E) 2.64 – 2.69 (R)	0.95 – 1.20	N/A
Reported	0.90	0.12	1.8

Table 3-14A. Summary of EC_{50} of ATP at the Mouse, Rat and Human $P2X_7Rs$. Values are based on the findings from (Moore *et al.*, 2007; Stokes *et al.*, 2006; Surprenant *et al.*, 1996; Young *et al.*, 2007). E = endogenous, R = recombinant.

IC_{50} (nM)	MOUSE	RAT	HUMAN
KN-62/KN-04	407 - 1320	> 3000	30 - 100

Table 3-14B. Summary of IC_{50} of KN-62/KN-04 at the Mouse, Rat and Human $P2X_7Rs$. Values are based on the findings from (Humphreys *et al.*, 1998; Jiang *et al.*, 2000; Moore *et al.*, 2007).

The nature of the $P2X_7R$ "pore" has been controversial. A number of models have been proposed including the dilation of the P2X ion channel protein and coupling to a second membrane protein. Dye uptake could be occurring via a conformational change of the receptor itself, allowing dilation and uptake of larger molecules similar to that seen with the $P2X_2$ and $P2X_4$ receptors (Khakh *et al.*, 1999; Virginio *et al.*, 1999); or the receptor opens a distinct channel protein which is permeable to these dyes, similar to the maitotoxin induced pore (Schilling *et al.*, 1999). There are a number of factors favouring either interpretation, for the former the increase in permeability is progressive, is observed in a range of host cells and factors which block the initial current also block dye uptake (North, 2002). For the latter; calmidazolium is able to block the initial current but not dye uptake (Virginio *et al.*, 1997) and in some oocyte expression systems, activation of the $P2X_7R$ has been observed to only induce the initial current and not dye uptake (North, 2002).

During this study a candidate for the $P2X_7R$ pore was suggested; this was the hemi-channel protein pannexin-1 (Locovei *et al.*, 2007; Pelegrin *et al.*, 2007; Pelegrin *et al.*, 2006). I carried out initial experiments using the reported pannexin-1 current ($P2X_7R$ dye uptake) blockers carbenoxolone (CBX) (Bruzzone *et al.*, 2005) and probenecid (Silverman *et al.*, 2008). However I failed to observe any inhibition with either of these blockers; furthermore in the case of CBX a dose-dependent facilitation of dye uptake occurred (Figure A-2). Other groups have observed different responses when treating cells with reported pannexin-1 blockers (CBX, Mefloquine; MFQ, peptide pannexin-1 mimetic; $_{10}$Pnx). For example; CBX failed to inhibit EtBr uptake into ATP stimulated 2BH4 cells (Faria *et al.*, 2005), MFQ, CBX and $_{10}$Pnx failed to inhibit dye-uptake into HEK293/$P2X_7R$ cells (Schachter *et al.*, 2008), CBX inhibited YO-PRO uptake and Ca^{2+} transients in astrocytes (Suadicani *et al.*, 2006) but only inhibited YO-PRO uptake in HEK293/$P2X_7R$ cells (Pelegrin *et al.*, 2006). My data does not support the involvement of pannexin-1 in ATP mediated uptake of large molecular weight dyes; however further

experiments would be required to either ultimately accept or reject a role potential for pannexin-1 in P2X$_7$R mediated dye uptake.

3.3.2 Mg^{2+}, Ca^{2+} Cd^{2+} and Zn^{2+} Inhibits mP2X$_7$R Activation by Reducing [ATP^{4-}]

When investigating if the mouse P2X$_7$R could be modulated by changing divalent cation concentrations in the extracellular solution, I hypothesized three potential outcomes based on previous literature (i) inhibition due to a reduction in [ATP^{4-}] (Klapperstück *et al.*, 2001; Michel *et al.*, 1999), (ii) inhibition or potentiation due to a direct interaction with the P2X$_7$R (Virginio *et al.*, 1997), or (iii) no effect.

I decided to use "pore formation" (EtBr uptake assay) as a measure of P2X$_7$R activation; as I had already established that the effect of ATP could be completely blocked by KN-62 and therefore was potentially mediated primarily by the P2X$_7$R. Furthermore within the literature it has been established that ATP-evoked dye uptake and ATP-evoked ionic current properties resemble each other. For example the efficacies of ATP and BzATP are comparable, as is the sensitivity to block by ions and antagonists (Surprenant *et al.*, 1996; Virginio *et al.*, 1997) and species differences are observed both with dye uptake and ionic currents (North, 2002).

In the case of Mg^{2+}, Ca^{2+}, Cd^{2+} and Zn^{2+} I determined that EtBr uptake was inhibited when these ions were present. This inhibition was observed as a rightward shift in the ATP concentration-response curve with a subsequent increase in the EC_{50}. On conversion of [ATP] into [ATP^{4-}] the ATP concentration-responses curves in the presence of Mg^{2+}, Ca^{2+}, Cd^{2+} and Zn^{2+} were observed to now overlap abolishing the apparent increase in the EC_{50}. Therefore I concluded that these ions inhibit P2X$_7$R activation by chelating and therefore reducing the concentration of the P2X$_7$R ligand ATP^{4-}. These results were similar to those obtained in studies where the effect of divalent cations on the human P2X$_7$R (Klapperstück *et al.*, 2001; Michel *et al.*, 1999) were examined but did not correlate with studies where divalent cations were observed to inhibit rat P2X$_7$R activation irrespective of there action on ATP^{4-} chelation (Virginio *et al.*, 1997).

3.3.3 Hg^{2+} Potentiates $mP2X_7R$ Activation

Stimulating RAW264.7 cells in the presence of 10 μM Hg^{2+} was observed to increase the maximal rate of ATP evoked EtBr uptake (Figure 3-9). Hg^{2+} has been demonstrated to increase $P2X_2R$ activation and inhibit $P2X_4R$ activation. ATP evoked currents were observed to be increased 10 – 20 fold when Hg^{2+} was pre-incubated with oocytes expressing the $rP2X_2R$ (Lorca *et al.*, 2005). It has been proposed that divalent ion potentiation of $P2X_2R$ currents was due to the ability of the metal ions to bind to extracellular histidines (H120, H192, H213), forming a high-affinity metal coordination complex. Furthermore it was hypothesised that this metal "allosteric pocket" is separate and independent of the ATP binding site. In the extracellular domain of the $mP2X_7R$ there are seven histidines, five of which are conserved in rat (H62, H85, H201, H219, H267) and six of which are conserved in human (H62, H85, H201, H219, H267, H268) (Figure 3-18). These histidines could potentially play a role in Hg^{2+} binding and modulation of the $P2X_7R$.

In contrast $P2X_4R$ mediated currents are inhibited by Hg^{2+} with an IC_{50} of 9.2 μM, and mutation of extracellular histidines failed to abolish this effect (Coddou *et al.*, 2005). They hypothesised that Hg^{2+} could interact at a metal binding site distal to the ATP binding site and potentially interact with amino acids located intracellularly or in the transmembrane domain of the receptor due to the reported high permeability of $HgCl_2$ through lipid bilayer membranes.

Figure 3-18. Alignment of Mouse, Rat and Human P2X7R Extracellular Domains. Mouse histidines highlighted.

3.3.4 Cu^{2+} Inhibits mP2X7R and rP2X7R Activation Directly

In contrast to other divalent cations tested Cu^{2+} was observed to inhibit dye uptake independently of a reduction in [ATP^{4-}] (Figure 3-12). This inhibition was observed as a reduction in the maxima of the ATP concentration-response curve for RAW264.7 cells, HEK293/mP2X7R and HEK293/rP2X7R cells. This inhibition correlates with previous reports where Cu^{2+} has been observed to inhibit both rat and human P2X7R mediated responses independently of [ATP^{4-}] (Michel *et al.*, 1999; Virginio *et al.*, 1997). In addition, during the course of this study two papers were published, which elucidated the potential binding site of Cu^{2+} to the recombinant rat P2X7R (Acuña-Castillo *et al.*, 2007; Liu *et al.*, 2008). However each of these papers proposed a different model.

In the study by Liu *et al.*, 2008 mutagenesis of H62 and D197 either alone or in combination abolished inhibition by Cu^{2+} when ATP or BzATP was the activating ligand. Furthermore mutation of H201 or H267 paritally attenuated Cu^{2+} inhibiton of ATP but not BzATP evoked responses. The study by Acuña-Castilio *et al.,* 2007 identified H267 with contribution from H130 and H201 to be involved in the binding of Cu^{2+} to the P2X7R. Both of these studies used alanine screening to identify these residues. Based on functional studies, it could be suggested that a common metal binding site for Cu^{2+} at the human, mouse and rat P2X7R exists. H62, H201 and H267 are all conserved between the mouse, human and rat. However D197 although conserved in human is a histidine in mouse and

H130 is a serine in both human and mouse (Figure 3-19). Both papers also implicate that the residues involved in Cu^{2+} binding respective of each study are important binding sites for Zn^{2+} to the recombinant P2X$_7$R. Liu *et al.*, 2008 implicated a common binding site for Zn^{2+} and Cu^{2+} whereas Acuña-Castilio *et al.,* 2007 implicate H267 and H219 as important residues; this would indicate different but overlapping sites for the binding of Cu^{2+} and Zn^{2+}. H267 and H219 are conserved in the rat, mouse and human P2X$_7$R sequences and therefore it would be predicted that Zn^{2+} would inhibit all three receptors in a similar way. However as already discussed Zn^{2+} failed to cause a direct inhibit RAW264.7 cell dye uptake.

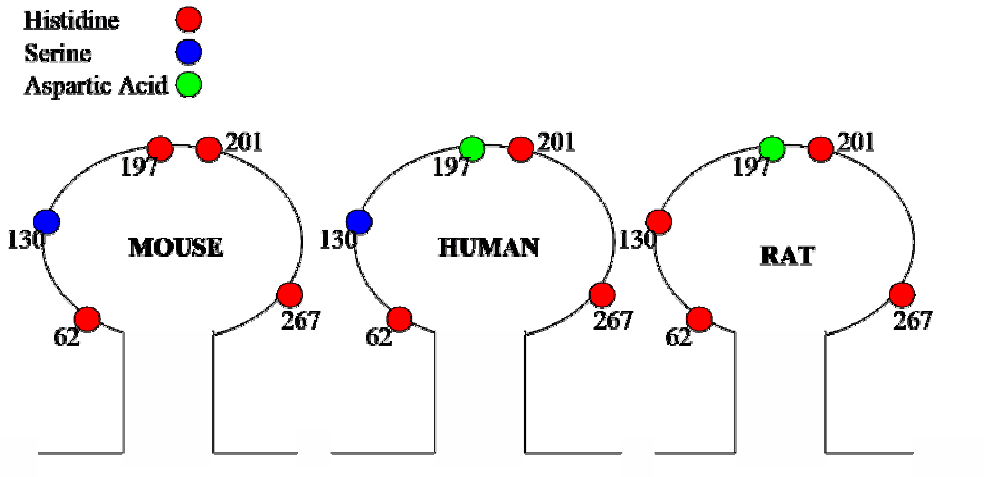

Figure 3-19. Residues Indicated to be Important in Cu^{2+} Binding to the Recombinant rP2X$_7$R. (Acuña-Castillo *et al.*, 2007; Liu *et al.*, 2008)

3.3.5 Zn^{2+} Modulation of the P2X$_7$R is Dependent on Species, Cell Background and Agonist

In order to rule out the lack of effect of Zn^{2+} on the mouse P2X$_7$ receptor in RAW264.7 cells being due to the expression system used or the assay design; the effect of Zn^{2+} on the recombinant mouse and rat P2X$_7$R receptor expressed in HEK293 cells was studied. In correlation with the literature (Virginio *et al.,* 1997), Zn^{2+} was observed to inhibit ATP evoked dye uptake in HEK293/rP2X$_7$R cells (Figure 3-13), this inhibition could not be accounted for by a reduction in [ATP^{4-}] alone. In contrast Zn^{2+} was observed to potentiate ATP evoked dye uptake in HEK293/mP2X$_7$R cells (Figure 3-13). This therefore indicated that mouse P2X$_7$Rs are insensitive to direct block by extracellular Zn^{2+}. Furthermore

depending on the cell expression system used I observed two different effects of Zn^{2+} at the mP2X$_7$R (i) inhibition due to chelation of ATP^{4-} and (ii) potentiation (Table 3-15).

In the study by Liu *et al.,* 2008 different residues were observed to be involved in the inhibition of either ATP or BzATP evoked responses by Zn^{2+} at the rat P2X$_7$R. It has already been demonstrated that rat P2X$_7$R's are 100 times more sensitive to BzATP than the mouse P2X$_7$R and that this is attributed to two residues in the ectodomain K127 and N284 (also involved in ATP sensitivity) which are A127 and D284 in mouse (Young *et al.*, 2007) (Figure 3-20). I therefore investigated whether BzATP evoked responses at the mouse P2X$_7$R were modulated by extracellular Zn^{2+}. Due to BzATP being unable to evoke maximal dye uptake at concentrations of 1 mM at the mouse P2X$_7$R (Figure 3-20), I had to perform this part of the study in the absence of Ca^{2+} and Mg^{2+}.

I initially re-tested the effect of Zn^{2+} against ATP evoked dye-uptake in a nominal Ca^{2+}/Mg^{2+} -free salt-solution[14], correlating with our previous results Zn^{2+} inhibited RAW264.7 cells dye uptake by reducing [ATP^{4-}], potentiated HEK293/mP2X$_7$R dye uptake and directly inhibited HEK293/rP2X$_7$R dye uptake. However the form of this inhibition was different to that observed in the physiological salt solution, instead of seeing a significant reduction in the maxima I observed a rightward shift in the concentration-response curve (Table 3-15).

As predicted Zn^{2+} caused a direct inhibition of BzATP evoked dye uptake in HEK293 cells expressing the rat P2X$_7$R. Furthermore Zn^{2+} caused inhibition of BzATP evoked dye uptake mediated by the endogenous and recombinant mouse P2X$_7$R, this inhibition could not be accounted for by a reduction in [$BzATP^{4-}$] alone. Based on these results I could hypothesize (i) that Zn^{2+} could bind to multiple sites at the P2X$_7$R allowing selective inhibition of BzATP at mP2X$_7$Rs without inhibiting ATP responses while both responses are inhibited at rat P2X$_7$Rs or (ii) that the Zn^{2+} bind site is structurally altered in the mP2X$_7$R allowing inhibition of BzATP but not ATP evoked responses.

[14] Effect of Cu^{2+} on ATP evoked responses in the nominal Ca^{2+}/Mg^{2+} salt solution were also re-tested. Cu^{2+} was observed to still inhibit at all three cell type, observed as a reduction in the maxima of the concentration-response curve. See Figure A-3

Solution	RAW264.7	HEK293/m$P2X_7$	HEK293/r$P2X_7$
Physiological	⬇ ATP^{4-}	⬆	⬇ Direct (↓maxima)
Nominal Ca^{2+}/Mg^{2+}	⬇ ATP^{4-}	⬆	⬇ Direct (↑EC_{50})

Table 3-15. Effect of Extracellular Zn^{2+} on ATP Evoked Responses. ⬆ denotes potentiate and ⬇ denotes inhibition.

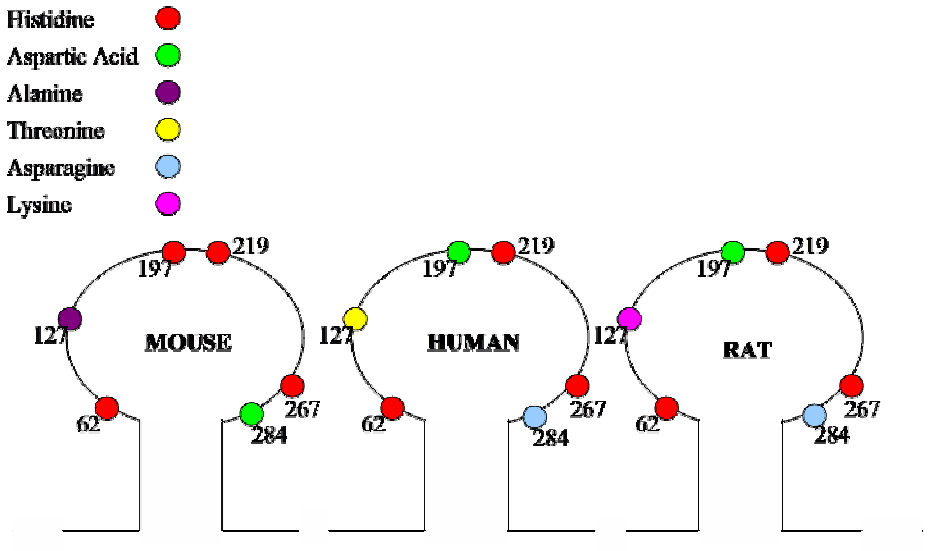

Figure 3-20. Residues Indicated to be Important in Zn^{2+} Binding to the Recombinant r$P2X_7R$. (Acuña-Castillo *et al.*, 2007; Liu *et al.*, 2008). Residues 127 and 284 indicated by Young *et al.,* 2007 to be important in the increased sensitivity of BzATP at the rat $P2X_7R$.

3.3.6 Concluding Remarks

Here I demonstrated the differences and similarities in the mechanisms of regulation of the mouse and rat $P2X_7Rs$ by metal divalent cations. These results remind us of the critical differences in receptor pharmacology between species of P2X receptors. Furthermore differences in modulation occurred depending on the cell background, assay solution and agonists used to evoke the response. The findings therefore suggest that caution should be exercised in cross-species extrapolation on studies of $P2X_7Rs$ and on the selection of the conditions of the assay used to examine $P2X_7R$ activation. However irrespective of mechanism my results suggest that divalent cations can reduce activation of the $P2X_7R$, supporting the hypothesis that under physiological conditions $P2X_7R$ activation is suppressed by the local extracellular environment.

CHAPTER 4

ATP INDUCES APOPTOTIC-LIKE EVENTS IN THE ABSENCE OF CELL DEATH

Portions of this chapter have been published in *Cellular Signaling*, **19**(4)

4.1 INTRODUCTION

In the previous section I determined that a short exposure to ATP (1 – 5 minutes) could evoke dye influx and extension of ATP exposure (> 30 minutes) could lead to the release of the large cytosolic enzyme LDH indicative of cell death. Activation of $P2X_7Rs$ heterologously expressed in HEK293 cells, have been observed to evoked gross changes in cellular morphology often associated with various forms of cell death (MacKenzie *et al.*, 2001; Mackenzie *et al.*, 2005). These events include externalisation of PS, mitochondrial swelling, reorganisation of F-actin, large membrane blebbing (>2 μm) and microvesicle shedding (<1 μm). I decided to investigate whether these morphological events occurred when RAW264.7 macrophages were stimulated with ATP.

The most obvious potential outcome of host pathogen interactions is the death of host cells; however the way in which cell death may occur can happen via a variety of mechanisms. Cell death is typically discussed as either apoptotic/programmed or necrotic/accidental. There are in fact many forms of cell death which can be defined by their biochemical features, and a better way to class forms of cell death is probably non-inflammatory and pro-inflammatory. Apoptosis and autophagy are non inflammatory forms of cell death, whereas oncosis (early phase necrosis[15]), pyroptosis and pyronecrosis are pro-inflammatory. These different forms of cell death cause a series of distinct morphological changes as well as biochemical ones to the dying cell (Table 4-1). For example apoptotic cells are observed to shrink and round up, have condensed chromatin, bleb and finally form apoptotic bodies which can be cleared by phagocytosis. Whereas oncotic cells and their organelles swell, plasma membrane integrity is lost and the cellular contents are released.

[15] Necrosis is probably a final common pathway of cell death, cells undergoing oncosis will end up necrotic however apoptotic cells (*in vitro*) can end up necrotic due to the loss of coordinated metabolic activity and compartmentalisation of the cell.

	Pro-Inflammatory	Morphological Features
Apoptosis	No	Cell shrinkage and rounding-up, PS exposure, Membrane blebbing (zeiotic), Chromatin condensation, Apoptotic bodies
Autophagy	No	Vacuolisation, Degradation of cytoplasmic contents, Slight chromatin condensation
Oncosis	Yes	Cell swelling, Mitochondria/organelle swelling, Disruption of plasma membrane, Membrane blebbing
Pyroptosis	Yes	Disruption of plasma membrane, Plasma membrane pore formation, membrane vesicles
Pyronecrosis	Yes	Disruption of plasma membrane

Table 4-1. Summary of Morphological Changes Associated with Different Forms of Cell Death. Data based on information from (Fernandes-Alnemri *et al.*, 2007; Fink *et al.*, 2005; Ting *et al.*, 2008)

4.1.1 Plasma Membrane Pore Formation

I demonstrated in the previous chapter that activation of the $P2X_7R$ will lead to the uptake of EtBr, indicative of pore formation. Formation of a "pore" has also been reported to occur during pyroptosis that is a caspases-1 dependent form of apoptosis. *S.Typhimurium* infected macrophages were observed to become permeable to EtBr (394Da) whilst excluding a larger dye; ethidium homodimer-2 (1293Da) which was suggested to be consistent with the formation of discrete membrane lesions allowing passage of smaller molecules but exclusion of larger ones (Fink *et al.*, 2006). This process was observed to be dependent on caspases-1 and actin polymerisation. Furthermore the pore was determined to induce dissipation of ionic gradients, influx of water, cell swelling and finally cell lysis. Activation of the $P2X_7R$ has also been observed to induce cell swelling and ultimately lysis in lymphocytes[16] (Taylor *et al.*, 2008), dopaminergic neurones (Jun *et al.*, 2007), macrophages (Murgia *et al.*, 1992) and HEK293 cells expressing the $P2X_7R$ (Ferrari *et al.*, 2007).

4.1.2 Exposure of Phosphatidylserine

Activation of the $P2X_7R$ in transfected HEK293 cells (Mackenzie *et al.*, 2005), T-Lymphocytes (Elliott *et al.*, 2005), erythrocytes (Sluyter *et al.*, 2007) and macrophages

[16] Cell shrinkage initially occurred in this study but was followed by cell swelling after a period of 2 minutes.

(Wilson *et al.*, 2004) has been observed to induce the rapid movement of PS from the inner to the outer leaflet of the plasma membrane. This phenomenon is associated with apoptotic cell death. In viable/non-apoptotic cells, phospholipids are asymmetrically distributed across the plasma membrane, with the majority of anionic phospholipids (e.g. PS, phosphoethanolamine PE) localised on the inner leaflet (Bevers *et al.*, 1999). The exposure of PS on the outer leaflet of the plasma membrane allows the recognition of apoptotic cells/bodies by phagocytes and ensures the safe clearance of apoptotic waste without the induction of inflammation.

At physiological cytoplasmic Ca^{2+} concentrations asymmetry for the plasma membrane is maintained by two lipid transporters a "flippase" which catalyses the rapid inward transport aminophospholipids (PS and PE) and a "floppase" which promotes a slower outward transport amino and choline (sphingomyelin and phosphatidylcholine) containing phospholipids (Zwaal *et al.*, 2005). When a substantial rise in the cytoplasmic Ca^{2+} concentration occurs the flippase is inhibited and furthermore a third lipid transporter; "scramblase" is activated (Williamson *et al.*, 1995) (Figure 4-1). This scramblase is able to mix the lipids between the two membrane leaflets (Zwaal *et al.*, 2005), which cannot be corrected and therefore leads to a loss in membrane asymmetry. Providing the flippase is not irreversibly inactivated by the intracellular protease calpain (activated by the rise in $[Ca^{2+}]_i$), efflux of Ca^{2+} will lead to a restoration of lipid asymmetry (Comfurius *et al.*, 1990).

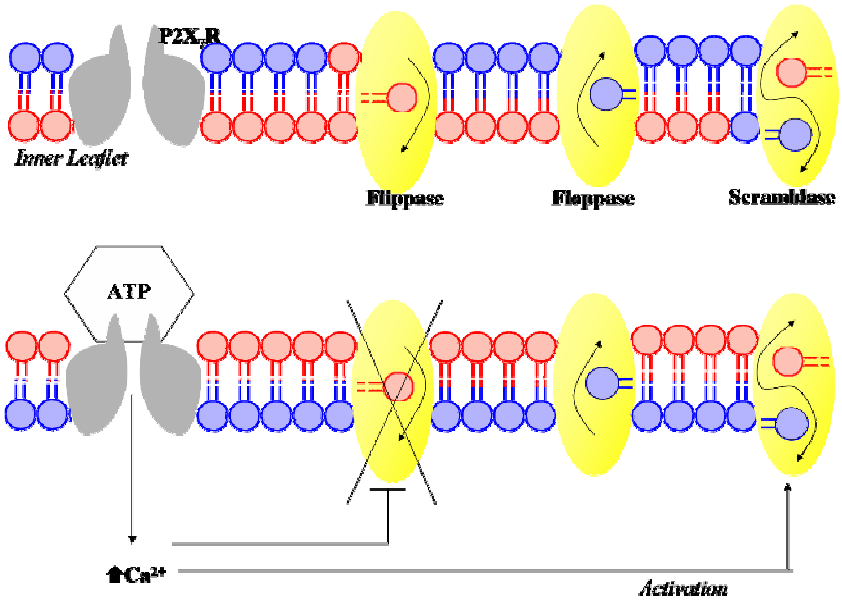

Figure 4-1. Schematic of how $P2X_7R$ activation could lead to the loss of plasma membrane asymmetry. Red phospholipids = aminophospholipids (PS and PE). Blue phospholipids = cholinephospholipids.

4.1.3 Membrane Blebbing & Microvesicle Shedding

Phospholipid asymmetry is commonly observed to be accompanied by cytoskeletal rearrangement, outward blebbing of the plasma membrane (> 2 μm) and the shedding of microvesicles (< 1 μm) in which the phospholipids are randomised over the vesicular membrane (Zwaal *et al.*, 1997). $P2X_7R$ activation in transfected HEK293 cells (Mackenzie *et al.*, 2005; Morelli *et al.*, 2003), macrophages (Pfeiffer *et al.*, 2004) and osteoblasts (Panupinthu *et al.*, 2007) has been observed to evoke membrane blebbing. Furthermore microvesicle shedding has been observed to occur in $P2X_7R$ expressing HEK293 cells (MacKenzie *et al.*, 2001), dendritic cells (Pizzirani *et al.*, 2007), macrophages (MacKenzie *et al.*, 2001) and microglia (Bianco *et al.*, 2005) after stimulation with ATP.

Both apoptotic and oncotic cell death has been observed to evoked membrane blebbing (Fink *et al.*, 2005). Apoptotic blebbing is often distinguished from other types of blebbing by its zeiotic nature that is the process of continuous and dynamic protrusions and retractions. Whereas oncotic blebbing is characterised by blebs that do not retract but gradually enlarge to diameters of 10 – 20 μm (Mackenzie *et al.*, 2005). Little is known about the mechanism behind and the reason for apoptotic membrane blebbing. It has been hypothesised that blebbing is dependent on caspase-mediated cleavage of a cytoskeletal component/regulator such as gelsolin, an actin depolymerising agent (Kothakota *et al.*, 1997) or ROCK I (Rho-activated serine/threonine kinase) which is involved in stabilisation of F-actin, phosphorylation of myosin light chains and coupling of actin-myosin filaments to the plasma membrane (Leverrier *et al.*, 2001). Evidence for the involvement of ROCK I in $P2X_7R$ mediated blebbing is conflicting. Mackenzie *et al.,* 2005 failed to observe inhibition of Ca^{2+}-dependent zeiotic blebbing using the ROCK I inhibitor Y-27632 whereas Pfieffer *et al.,* 2004 and Morelli *et al.,* 2001 did prevent $P2X_7$ evoked blebbing using Y-27632. Blebbing could potentially play a role in the recognition and clearance of apoptotic cells from the immune system, furthermore inhibition of blebbing has been observed to inhibit the relocalisation of fragmented DNA into blebs and apoptotic bodies (Coleman *et al.*, 2001).

PS-rich microvesicles, also described as microparticles or ectosomes are released from a range of cells and support a number of biological responses. Most commonly PS-rich microparticles are observed to be shed from activated platelets through a process thought

to involve the activation of Ca^{2+}-dependent calpain which facilitates the detachment of the vesicles from the plasma membrane via the degradation of cytoskeletal proteins (Zwaal *et al.*, 2005). Recently a study by Fernandes-Alnemri *et al.,* 2007 observed the release of membrane vesicles from cells undergoing pyroptosis. The release of vesicles from cells is thought to be of importance for coagulation, dissemination of an "eat me" signal and signaling between cells. Shedding of microvesicles is also thought to be of importance in the secretion of cytokines. As already stated microvesicle shedding occurs in cells expressing the $P2X_7R$, here they are thought to mediate the secretion of the pro-inflammatory cytokine IL-1β (Bianco *et al.*, 2005; MacKenzie *et al.*, 2001). $P2X_7R$ activation has also been reported to induce the release of exosomes. It was hypothesised that activation of the receptor could couple in to the formation of multivesicular bodies that contained exosomes with entrapped IL-1β, these multivesicular bodies could then fuse with the plasma membrane and release the IL-1β containing exosomes (Qu *et al.*, 2007).

4.1.4 Mitochondrial Changes

A decrease in the mitochondrial membrane potential is considered as an initial and irreversible step towards apoptosis. Other changes to the mitochondria which occur during apoptosis include enhanced membrane permeability and the release of cytochrome-c into the cytosol. ATP activation of HEK293 cells expressing the $hP2X_7R$ is observed to induce a collapse/drop in the mitochondrial membrane potential, fragmentation of the mitochondrial network and mitochondrial swelling (an oncotic rather than apoptotic event) (Adinolfi *et al.*, 2005; Mackenzie *et al.*, 2005). Mackenzie *et al.,* 2005 determined that these events were dependent on Ca^{2+} whereas Adinolfi *et al.,* 2005 determined that mitochondrial fragmentation was blocked in Ca^{2+} free conditions; however mitochondrial swelling and the collapse of the mitochondrial membrane potential where not effected by reducing the extracellular Ca^{2+} concentration.

The $P2X_7R$ has been observed to induce a variety of morphological changes associated with various forms of cell death. In this study I used live cell imaging to assess the kinetics of ATP evoked morphological changes and employed the use of scanning electron microscopy for further detailed investigation of cell surface changes. Furthermore I assessed whether ATP stimulation of RAW264.7 cells ultimately resulted in cell death or whether changes in morphology were reversible. The way in which a cell dies can either be non-inflammatory or pro-inflammatory; therefore examining such morphological changes

could be of importance in understanding the role ATP has during immune/inflammatory responses.

The key findings of this study were:

1. Stimulating RAW264.7 cells with ATP for 10 – 15 minutes and then resting the cells prior to a secondary ATP stimulation does not significantly affect the uptake of EtBr or release of LDH.
2. Extracellular ATP evokes the externalisation of PS.
3. Extracellular ATP does not induce bleb formation or filopodia retraction in RAW264.7 cells in the presence of physiological concentrations of Ca^{2+}
4. Extracellular ATP evoked formation of microvesicles is a Ca^{2+} dependent process.
5. Extracellular ATP evoked externalisation of PS and shedding of microvesicles precedes the release of LDH.

4.2 RESULTS

4.2.1 Prestimulating RAW264.7 Cells with ATP Does Not Effect ATP Evoked Responses

Extracellular ATP (3 mM) was previously determined to evoke pore formation within 1 – 5 minutes and cell death when the application was for > 30 minutes (Moore *et al.*, 2007). Prestimulating RAW264.7 cells with 3 mM ATP for 10 minutes and allowing a 60 minute recovery in standard culture medium, was observed to not significantly change basal (ATP-free) or ATP (3 mM) evoked influx of EtBr compared to controls (10 minutes buffer prestimulation) (Figure 4-2A, $n = 3$, $p>0.05$). Prestimulating RAW264.7 cells with 3 mM ATP for 15 minutes and allowing a 60 minute recovery in standard culture medium was observed to not significantly change basal (ATP-free) or ATP (3 mM, 60 minutes) evoked LDH release compared to control (15 minutes buffer prestimulation) (Figure 4-2B, $n = 3$, $p>0.05$).

4.2.2 High concentrations of ATP stimulate rapid PS translocation

I used live cell imaging and AnV-488 to detect whether ATP induced the translocation of PS from the inner to the outer leaflet of the plasma membrane of RAW264.7 cells. Within 5 minutes of 1 mM ATP addition, AnV-488 was observed to bind to the surface of all RAW 264.7 cells (Figure 4-3A, Figure 4-3B, and Movie 1). AnV-Alexa488 bound in a punctate non-uniform pattern at the surface of the cells and along filopodia projecting from the cell. Addition of 100 μM ATP did not activate PS translocation (Figure 4-3A) thus the receptor sensitivity for extracellular ATP correlates with activation of P2X7 receptors.

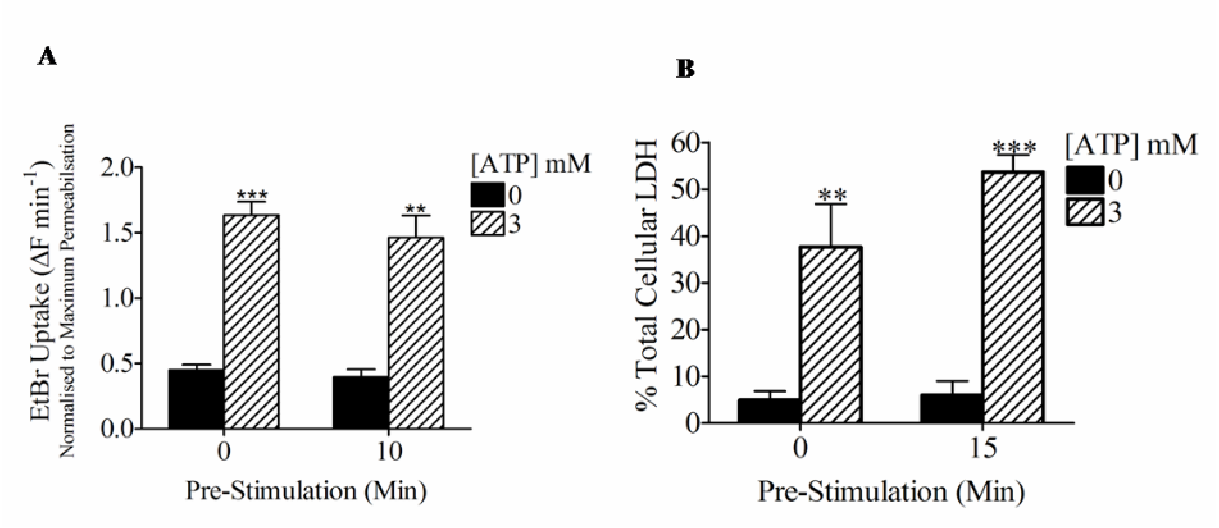

Figure 4-2. ATP Prestimulation Failed to Change Basal and ATP Evoked EtBr Influx or LDH Release. A, Histogram demonstrating that prestimulating RAW264.7 cells with ATP (3 mM) does not significantly change basal or ATP evoked EtBr influx (n = 3 ± s.e.m). B, Histogram demonstrating that prestimulating RAW264.7 cells with ATP (3 mM) does not significantly change basal or ATP evoked LDH release (n = 3 ± s.e.m). Student's t-test, **: $p<0.01$, ***: $p<0.001$.

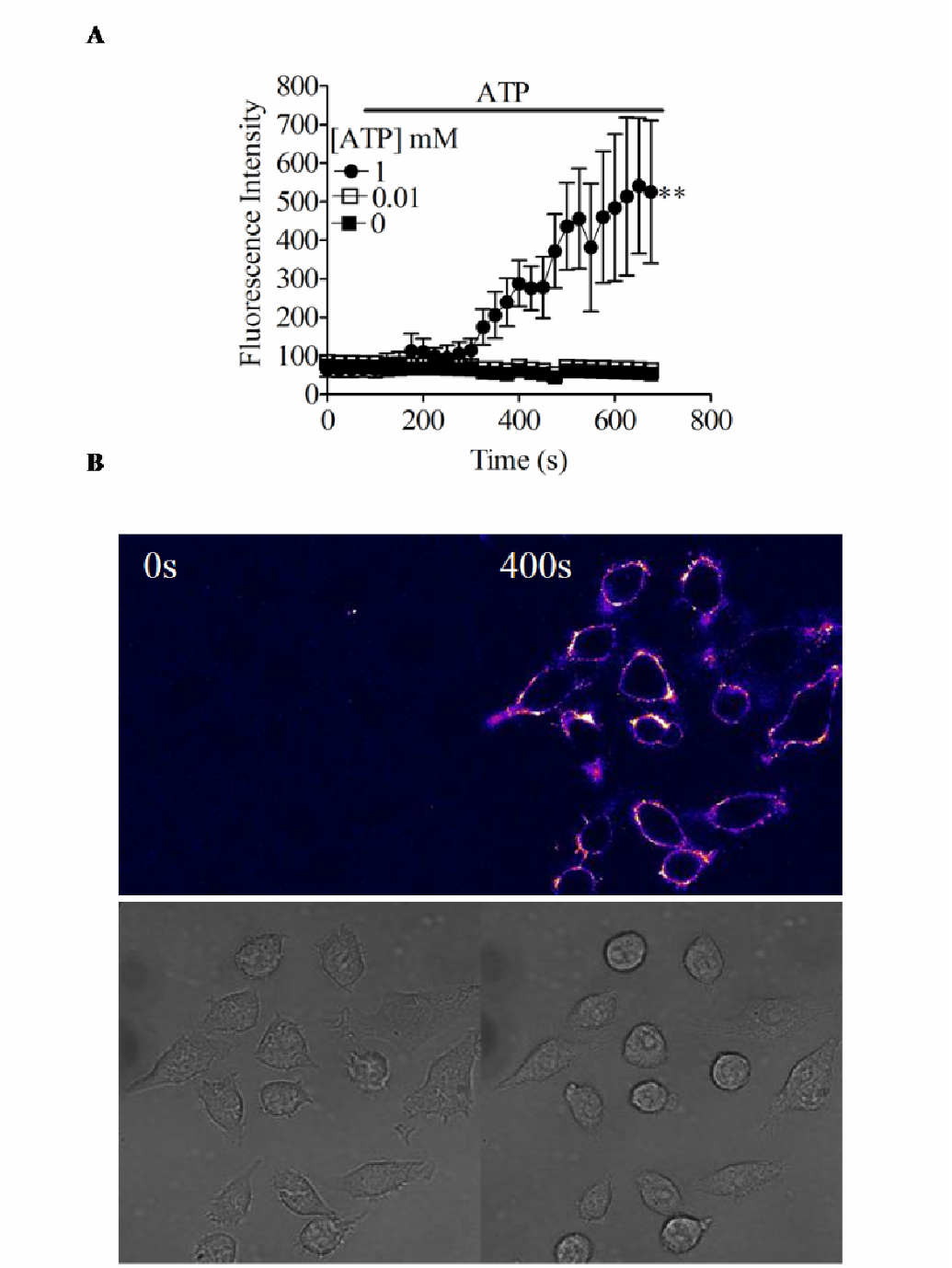

Figure 4-3. P2X$_7$R Activation Evokes the Externalization of PS. A, Kinetic graph demonstrating that 1 mM ATP evoked an increase in AnV-488 binding to RAW264.7 cells (n = 4 ± s.e.m). B, Images demonstrating the localisation of AnV-488 at the plasma membrane and along filopodia of RAW264.7 cells after stimulation with 1 mM ATP for 5 minutes. Above images are representative of 4 experiments, with control images being those collected at t = 0 seconds and ATP images being those collected at t = 400 seconds (5 minutes ATP application). One-way ANOVA with Dunnett's post-hoc test, **: $p<0.01$.

4.2.3 ATP Evokes Membrane Blebbing & Filopodia Retraction in the Absence of Ca^{2+}

Live cell imaging of RAW264.7 cells bathed in a physiological salt solution revealed that a 10 minute application of 3 mM ATP did not evoke any significant changes in cellular morphology (n = 9) (Figure 4-4, Figure 4-5A and B, Movie 2). In contrast imaging of RAW264.7 cells bathed in a Ca^{2+}-free salt solution revealed that ATP (3 mM, 10 minutes) evoked substantial changes in cellular morphology. Cells appeared rounded, had retracted filopodia and large membrane blebs protruding from the cell surface (n = 8, Figure 4-4, Movie 3). Filopodia retraction was observed to occur in 85 ± 4 % of cells whilst membrane blebbing was observed to occur in 83 ± 12 % of cells (n = 8 ± s.e.m) (Figure 4-5A and B). Membrane blebbing was a dynamic and zeiotic event where blebs continued to appear during the washout of the agonist. Membrane blebs however where observed to retract within 15 – 30 minutes following removal of ATP (n = 8, Figure 4-5A, Movie 2).

4.2.4 ATP Mediated Cytoskeletal Reorganisation

Stimulating RAW264.7 cells with ATP (3 mM, 10 minutes) bathed in the presence of Ca^{2+} was observed to not significantly change total levels of F-Actin content (n = 9, $p>0.05$) (Figure 4-5C). Using fixed RAW264.7 cells stained with Phalloidin-546; I determined that ATP (3 mM, 10 minutes) stimulation in the presence of Ca^{2+} induced some changes in the localisation of F-actin with a ring of actin being observed to be localised at the plasma membrane (n = 3) (Figure 4-6A and B). RAW264.7 cells stimulated with ATP (3 mM, 10 minutes) in the absence of Ca^{2+} demonstrated that cells in contrast to controls were rounded, had retracted filopodia and membrane blebs where F-Actin was observed to be localised (Figure 4-6C) (n = 3).

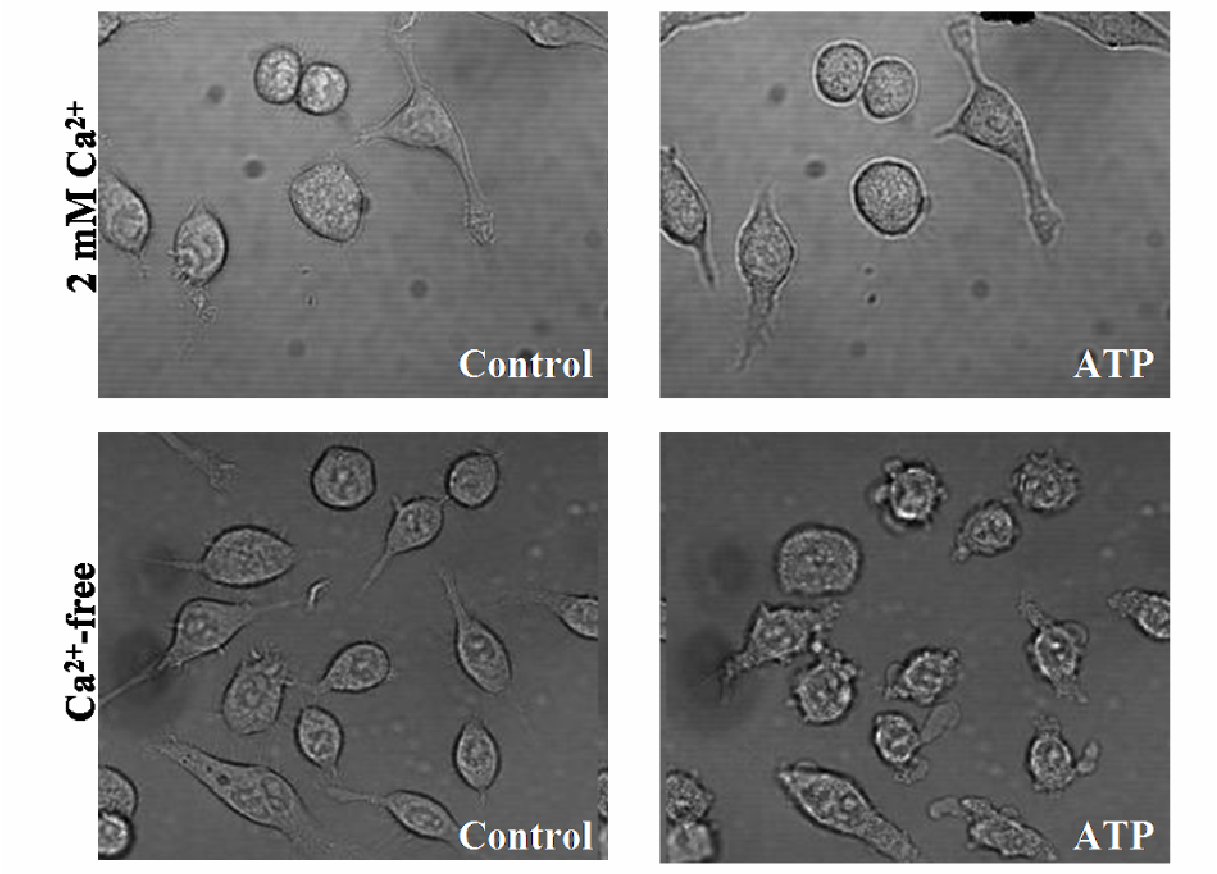

Figure 4-4. ATP Induces Filopodia Retraction and Membrane Blebbing in the Absence of External Ca^{2+}. Cells (30, 000) were bathed in either physiological salt solution or Ca^{2+}-free salt solution (warmed to 37 ^{o}C). Images were collected using a laser scanning confocal microscope (FV300-SU, Olympus, Japan) for 100 seconds before addition of 3 mM ATP (600 seconds). Above images are representative of 8 – 9 experiments, with control images being those collected at t = 0s and ATP images being those collected at t = 700 seconds (10 minutes ATP application).

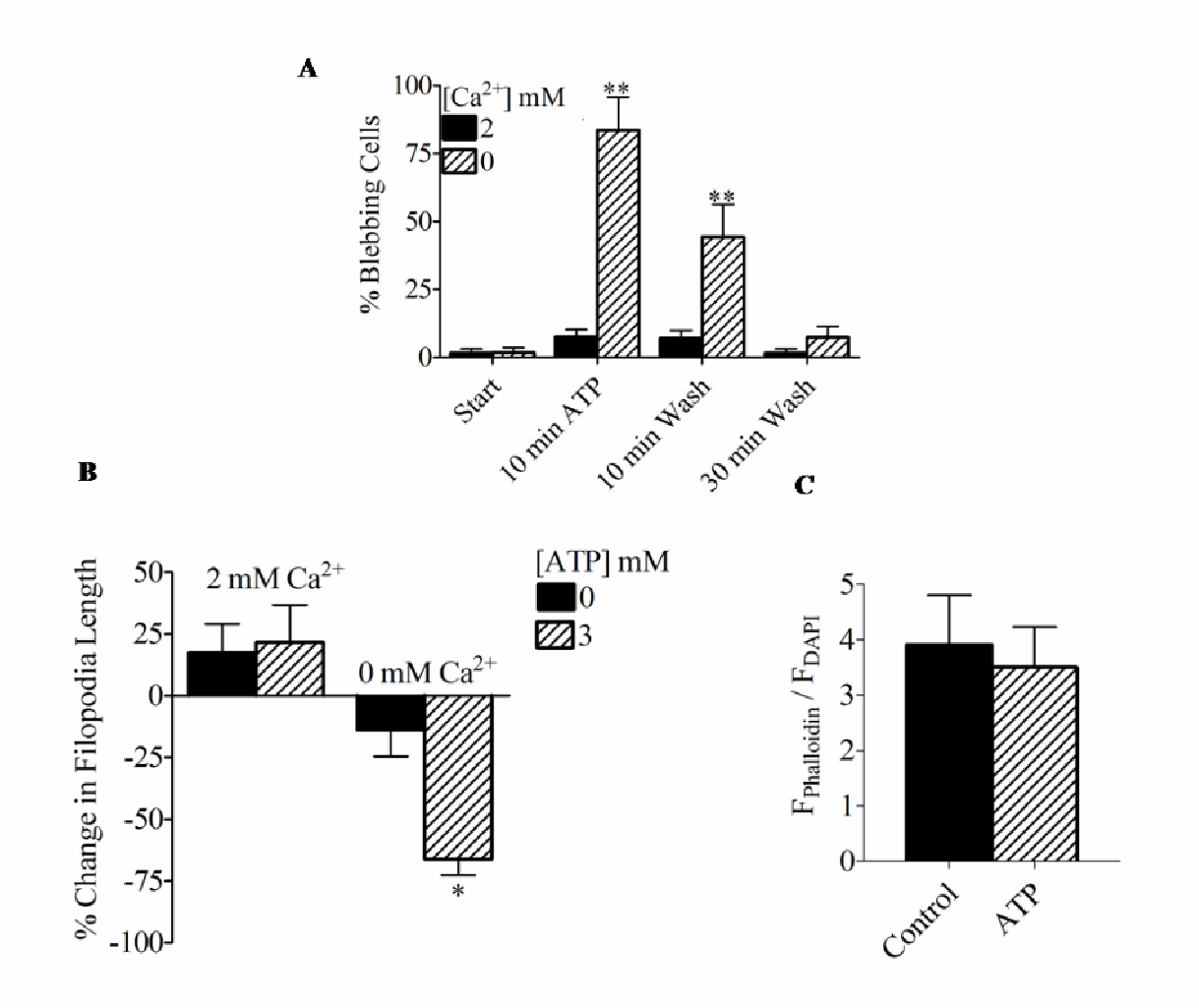

Figure 4-5. ATP Induces Reversible Membrane Blebbing in the Absence of External Ca^{2+}. A, Summarizes the observed total number of cells blebbing as a percentage of the observed total number of cells at t = 0 seconds, t = 700 seconds (10 minutes ATP), t = 1300s (10 minutes wash-out) and t = 2500s (30 minutes wash-out) (n = 8/9 ± s.e.m). B, Summarizes the change in filopodia length normalized to filopodia length at t = 0 seconds whilst bathing cells in the absence or presence of ATP (3 mM) for 10 minutes (n = 8/9 ± s.e.m). C, Total F-Actin content was determined by staining cells stimulated in physiological salt solution in the absence or presence of ATP (3 mM, 10 minutes, 37 ^{o}C) with Phalloidin-546 and DAPI (n = 9 ± s.e.m). Student's two-tailed t-test, *: $p<0.05$, **: $p<0.01$.

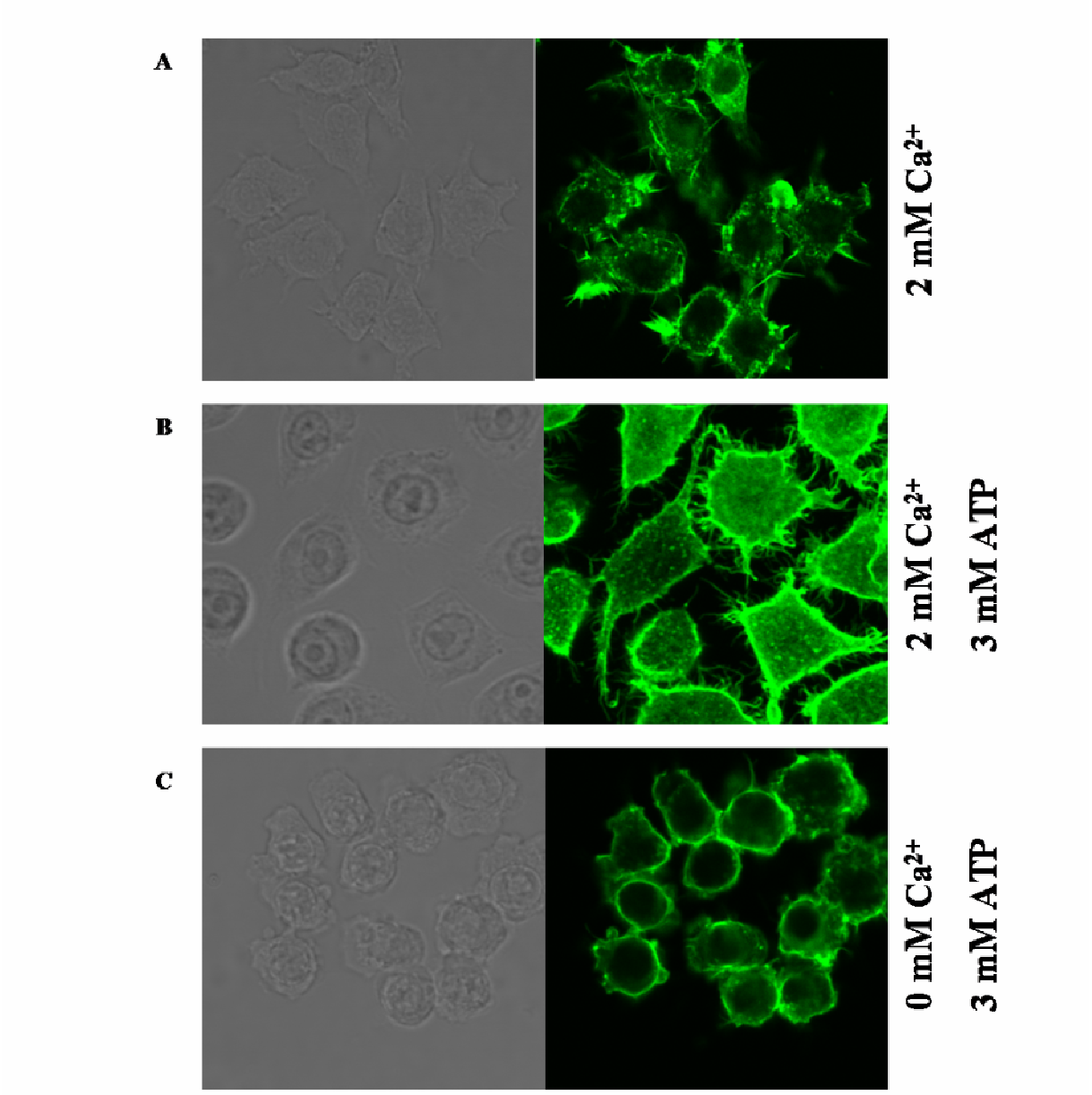

Figure 4-6. ATP Evoked Changes in Cytoskeletal Organisation. A, Cells bathed in physiological salt solution for 10 minutes. B, Cells bathed in physiological salt solution for 10 minutes in the presence of 3 mM ATP. C, Cells bathed in Ca^{2+}-free salt solution for 10 minutes in the presence of 3 mM ATP. Above images are representative of 3 experiments.

4.2.5 Scanning Electron Microscopy Reveals Formation of Microvesicles

In agreement with live cell imaging experiments, ATP stimulated RAW264.7 cells did not display retraction of filopodia or large membrane bleb formation (>2 μM) in scanning electron micrographs (Figure 4-7A, B, C and D). However, it was now apparent that the macrophage surface was covered in small microvesicles (<1 μM) that were not resolved by light microscopy. RAW264.7 cells stimulated with ATP in the absence of Ca^{2+} were observed to have swelled compared to controls (Figure 4-7E and F) and in agreement with live cell imaging had large membrane blebs protruding from the cell surface (Figure 4-7G and H). Furthermore far fewer microvesicles were observed to be present on RAW264.7 cells stimulated with ATP in the absence on Ca^{2+} compared to cells stimulated in the presence of Ca^{2+}. Control RAW264.7 bathed in the absence of Ca^{2+} appeared to a have a flattened morphology compared to control RAW264.7 cells bathed in the presence of Ca^{2+}.

4.2.6 Cell Viability

Cell viability was measured as the retention of cytosolic LDH; release into the external medium indicates a disruption of the plasma membrane and therefore cell death. Application of a range of ATP concentrations (0.3 – 5 mM) for 15 minutes failed to evoke significant release of LDH above control (Figure 4-8A. n = 3, $p>0.05$). Extending the application of ATP to 30 and 60 minutes caused a significant release of LDH with concentrations ≥ 2 mM (Figure 4-8B and C, n = 3, $p<0.01$). ATP evoked LDH release was observed to peak using concentrations between 2 – 3 mM and decreased slightly using a concentration of 5 mM (bell-shaped concentration-response).

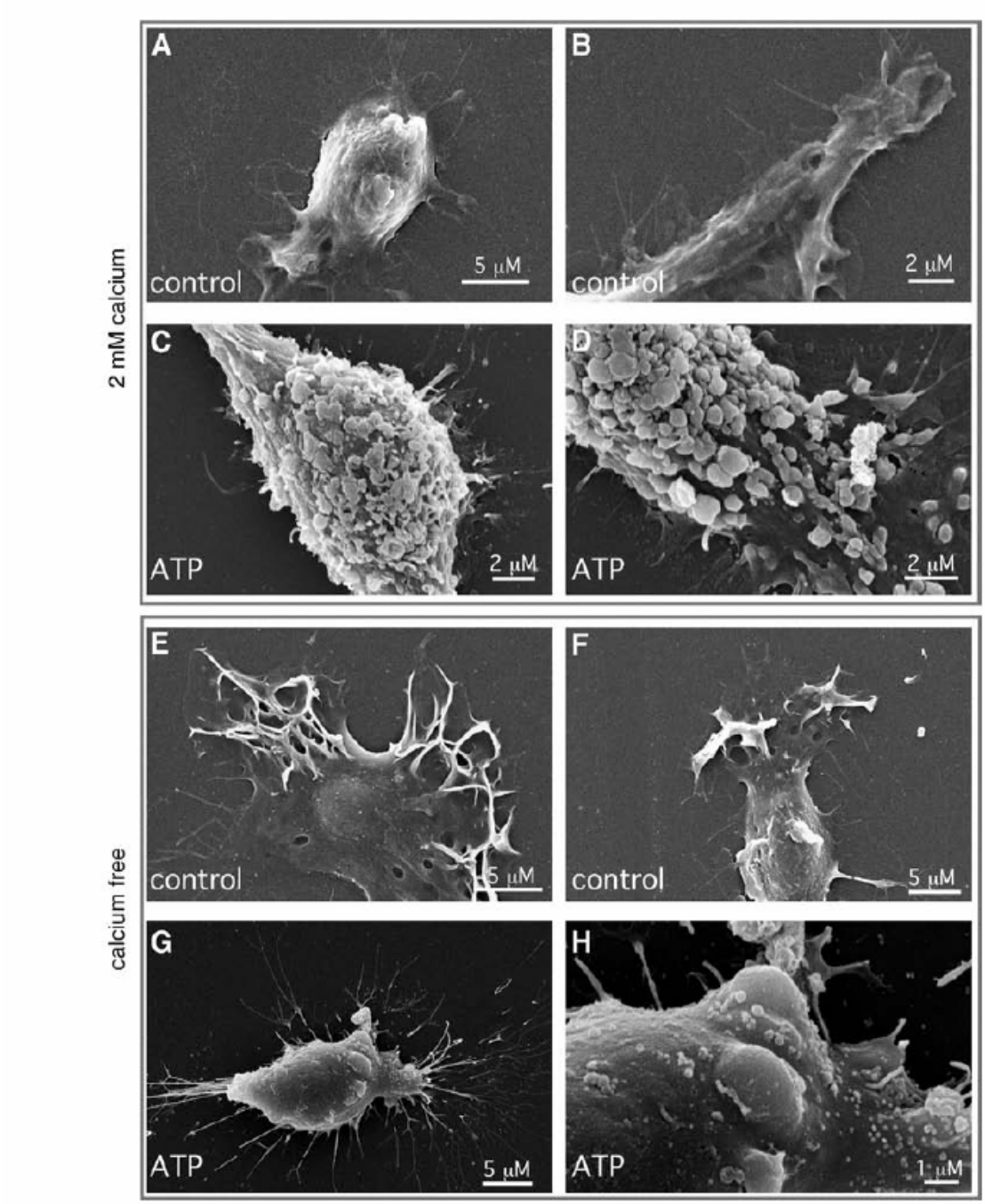

Figure 4-7. ATP Evokes Microvesicle Formation under Physiological Conditions. A & B, Cells bathed in physiological salt solution for 10 minutes. C & D, Cells bathed in physiological salt solution for 10 minutes in the presence of 1 mM ATP. E & F, Cells bathed in Ca^{2+}-free salt solution for 10 minutes. G & H, Cells bathed in Ca^{2+}-free salt solution for 10 minutes in the presence of 1 mM ATP.

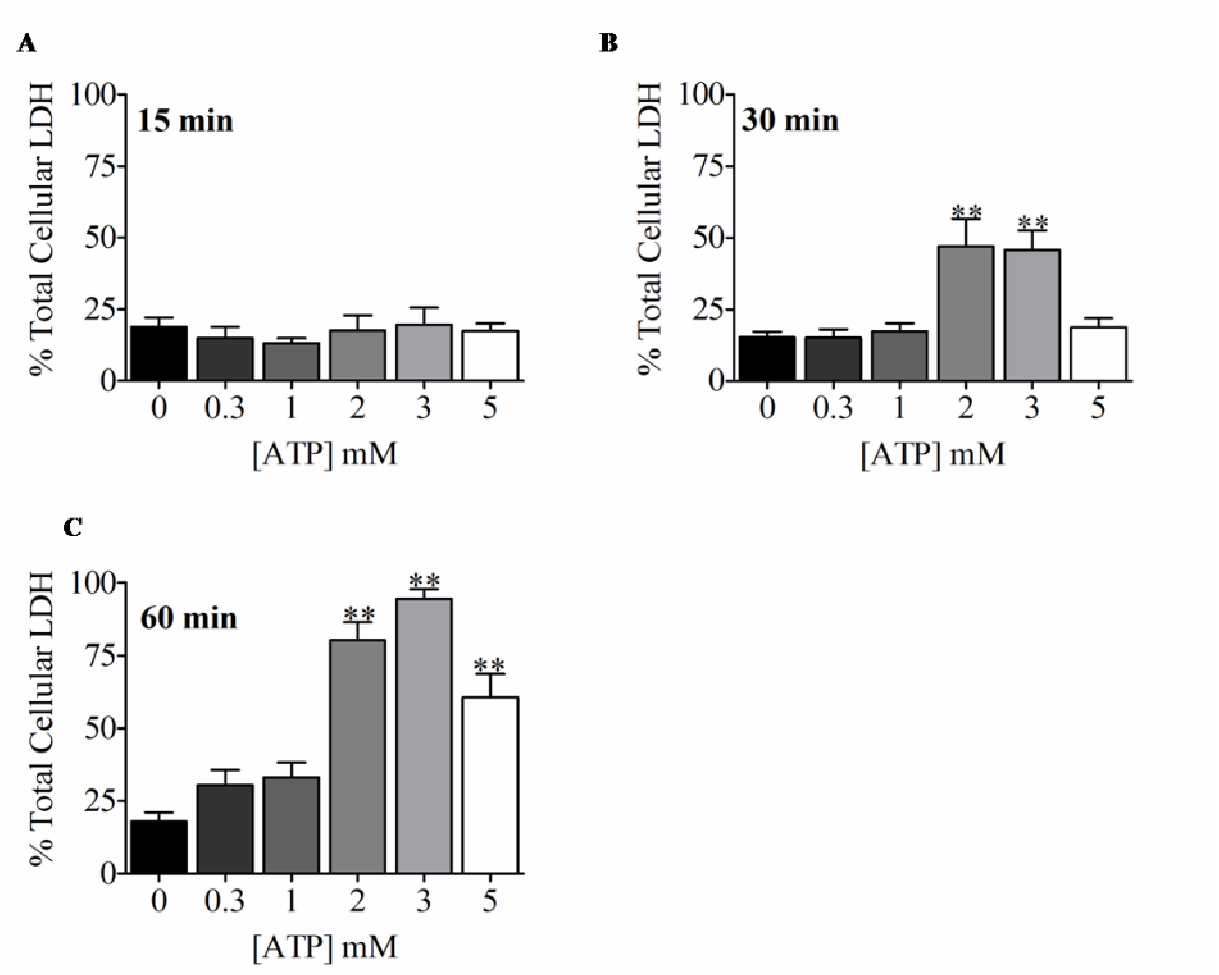

Figure 4-8. Prolonged ATP Stimulation of RAW264.7 Cells Can Evoke LDH Release. A, Histogram demonstrating that a 15 minute application of ATP at various concentrations does not evoke release of LDH above basal release (n = 3 ± s.e.m). B, Histogram demonstrating that a 30 minute application of 2 and 3 mM evokes the release of LDH (n = 3 ± s.e.m). C, Histogram demonstrating that a 60 minute application of ≥ 2 mM ATP evokes the release of LDH (n = 3 ± s.e.m). One-way ANOVA with Dunnett's post-hoc test, *: $p<0.05$, **: $p<0.01$.

4.3 DISCUSSION

In this study I determined (i) brief pre-activation of the $P2X_7R$ does not effect further ATP evoked responses (ii) ATP in physiological conditions rapidly evokes microvesicle shedding and PS exposure in the absence of cell death (iii) ATP in Ca^{2+} free conditions rapidly evokes substantial morphological changes such as cell rounding, filopodia retraction and reversible membrane blebbing.

	Calcium	Calcium Free
Pore Formation	✓	-
PS Exposure	✓	-
Filopodia Retraction	×	✓
Membrane Blebbing	×	✓
Microvesicle Shedding	✓	Reduced
Cell Death	×	×

Table 4-2. Summary of Morphological Changes Observed to be Induced by ATP in RAW264.7 Cells and Whether They Occur in the Absence or Presence of Ca^{2+}.

4.3.1 ATP Induced Morphological Changes in the Presence of Calcium

High concentrations of ATP have long been known to induce cell death in a variety of cells, through the activation of the $P2X_7R$. The exact form of cell death induced though is controversial with reports of apoptotic and oncotic events occurring due to $P2X_7R$ activation. Under physiological conditions I observed that ATP evoked pore formation, PS exposure and microvesicle shedding. Events which are associated with apoptotic and pyroptotic cell death. However these events consistent with the literature where observed to be evoked in the absence of cell death. Evidence for this includes (i) PS exposure and microvesicle shedding was evoked by 1 mM ATP which was observed to not induce LDH release with up to a 60 minute stimulation and (ii) basal and ATP evoked pore formation were not significantly changed by pre-stimulating cells with ATP (10 minutes).

It is possible that this receptor can couple to the same biochemical signaling cascades that are associated with evoking apoptotic and pyroptotic events without ultimately leading to cell death or potentially the receptor may couple to distinct pathways. For example Mackenzie *et al.,* 2005 determined that the $P2X_7R$ could couple to two distinct pathways

(i) Ca^{2+} dependent pathway causing PS exposure, zeiotic membrane blebbing and mitochondrial swelling[17] and (ii) a Ca^{2+} independent ROCK I dependent pathway that was responsible for oncotic blebbing, cytochrome C release and ultimately cell death.

Although PS exposure is considered to be a hallmark of apoptosis, it can be dissociated from other features of the apoptotic process as PS-dependent phagocytic recognition of cells has been observed to occur earlier or independently of later apoptotic events such as caspase activation and DNA fragmentation (Uthaisang *et al.*, 2003; Zhuang *et al.*, 1998). The study by Zhuang *et al.,* 1998 determined that the mitochondrial inhibitors antimycin A and oligomycin blocked increased plasma membrane permeability (assessed using Hoechst 33342, Mwt: 615Da) and externalization of PS but not activation of caspase-3, DNA fragmentation or decreases in the mitochondrial membrane potential.

The translocation of PS on to the outer leaflet of the plasma membrane mediated by the $P2X_7R$ could potentially be involved in the clearance of apoptotic cells; the expression of PS on the surface of both macrophages and their apoptotic targets is required for efficient phagocytosis (Callahan *et al.*, 2003). It could be hypothesised that in areas where inflammatory cell death is occurring, high concentrations of extracellular ATP could accumulate and therefore activate $P2X_7Rs$ expressed on macrophages. This process could potentially lead to the initiation or enhance the phagocytic clearance of cell corpses.

PS exposure could potentially play a role in signal transduction. Elliott *et al.,* 2005 determined that inhibition of PS translocation in T-lymphocytes blocked Ca^{2+} and Na^{+} uptake in response to $P2X_7R$ activation. Their hypothesis was that PS on the intracellular leaflet of the plasma membrane inhibited $P2X_7R$ activity. This however does not appear to fit with my results as increases in $[Ca^{2+}]_i$ were observed to occur prior to the externalisation of PS. Another potential role of $P2X_7R$ mediated PS exposure could simply be for the secretion of cytokines such as IL-1β via microvesicles. As already stated PS exposure is often seen to precede events such as membrane blebbing and shedding of membrane vesicles. Membrane phospholipid asymmetry has been implicated as a mechanism of inducing membrane curvature required for endocytotic vesicles to be pinched off from the plasma membrane. Could PS exposure potentially play a role in the

[17] Attempts to visualise mitochondrial changes in RAW264.7 cells using Mitotracker® probes were made, however results where inconclusive due to the resolution of the images.

formation of and shedding microvesicles? Cells undergoing pyroptotic cell death an event dependent on caspase-1 activation are observed to shed membrane vesicles and release IL-1β and IL-18. This could therefore warrant further investigations to establish whether $P2X_7R$ activation induces pyroptotic cell death, or couples into similar signaling pathways associated with pyroptosis.

4.3.2 ATP Induced Morphological Changes in the Absence of Calcium

Pfeiffer *et al.,* 2004 had previously reported that application of high concentrations of ATP to RAW264.7 cells was able to induce zeiotic membrane blebbing, actin reorganisation and filopodia retraction within 5 minutes. This conflicted with my results where I determined that in physiological concentrations of extracellular Ca^{2+} an application of 3 mM ATP failed to induce zeiotic membrane blebbing and filopodia retraction. However cell rounding; filopodia retraction and large membrane blebbing were observed when ATP stimulations were performed in the absence of extracellular Ca^{2+}. These events are generally viewed as apoptotic events. However consistent with the literature (Mackenzie *et al.*, 2005; Morelli *et al.*, 2003; Verhoef *et al.*, 2003); removal of ATP and washing for 30 minutes; reversed membrane blebbing indicating that the cells were still viable.

4.3.3 Concluding Remarks

Here I demonstrate that in the presence of Ca^{2+} the P2X7R can couple into pathways and induce events (e.g. PS translocation) generally associated with two forms of cell death; apoptosis and pyroptosis. However this does not mean that the cell has to ultimately undergo cell death. For example $P2X_7R$ evoked PS translocation has been reported to be reversible (Mackenzie *et al.*, 2005) and in this and other studies is observed to occur within a timeline were cell lysis is not detected (Figure 4-9). If activation of the $P2X_7R$ is able to induce these cell-death events for signal transduction and/or secretion of cytokines in the absence of cell lysis this would indicate a level of control. Release of microvesicles although a pro-inflammatory event allows the dissemination of pro-inflammatory factors, whereas cell lysis would evoke mass release of all cellular contents in a localised area.

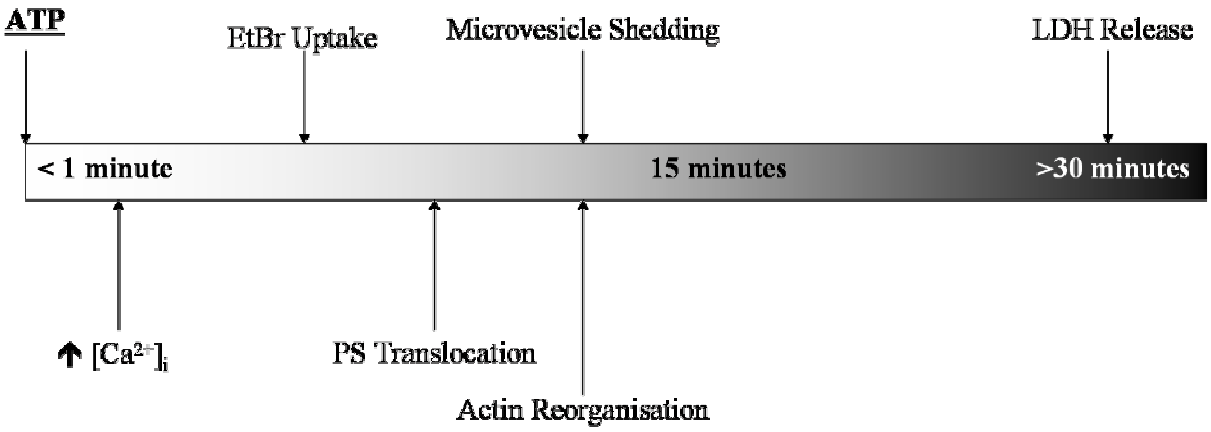

Figure 4-9. Timeline of Extracellular ATP Induced Events. Events are those observed stimulating RAW264.7 cells in the presence of Ca^{2+}.

CHAPTER 5

MURINE MACROPHAGE P2X$_7$ RECEPTORS SUPPORT RAPID PROTHROMBOTIC RESPONSES

Portions of this chapter have been published in *Cellular Signaling*, **19**(4)

5. 1 INTRODUCTION

In the previous chapter I demonstrated that stimulation of RAW264.7 cells with ATP in the presence of Ca^{2+} evoked the translocation of PS from the inner to the outer leaflet of the plasma membrane and the shedding of microvesicles. Exposure of PS is generally associated with cell death and is an important recognition signal for the clearance of apoptotic cells by macrophages. However, PS externalisation also plays an important role in the regulation of the coagulation cascade. Several enzymes of the coagulation cascade require assembly on a receptive membrane surface for full expression of catalytic activity. In the case of the prothrombinase complex; this surface is thought to be one rich in anionic phospholipids such as PS and phosphatidylethanolamine (PE) (Sims *et al.*, 2001). Furthermore activity of TF; the initiator of the extrinsic coagulation cascade is thought to be regulated by the local phospholipid environment (Bach, 2006). I therefore decided to examine whether P2X$_7$R activation on macrophages could be involved in potentially propagating and amplifying pro-coagulant effects. This could be of importance in inflammatory responses/diseases where a dysregulation of coagulation is also observed; such as severe sepsis and atherosclerosis (Opal *et al.,* 2003b).

5.1.1 Induction of Tissue Factor Pro-Coagulant Activity

TF (thromboplastin, FIII or CD142) is a 47 kDa membrane bound glycoprotein with an extracellular domain, transmemembrane domain and a short intracellular domain. It is expressed on a variety of cells, which are not normally exposed to flowing blood unless physical injury or rupture of atherosclerotic plaques occurs. Upon injury and exposure of TF expressing cells; the extrinsic coagulation cascade is initiated. The exposed TF is able to complex with the plasma serine protease, activated Factor VII (FVIIa). This complex is then able to trigger the proteolysis of Factor X (FX) into bioactive Factor Xa (FXa), with the pathway ultimately leading to the formation of thrombin and deposition of fibrin (Figure 5-1) (Key *et al.*, 2007).

In addition to its role as the main initiator of the extrinsic coagulation cascade, TF also participates in inflammatory processes, tumour biology and angiogenesis. For example the TF-FVIIa complex can initiate cellular signaling leading to the production of growth factors and cytokines such as IL-8 (Hjortoe *et al.*, 2004). TF expression can be increased in response a variety of factors such as; endotoxins (LPS), TNFα, IL-1β and oxidized LDL (Liu *et al.*, 2004; Wada *et al.*, 1994). This correlates with the finding that within atherosclerotic plaques TF can be found to be localized on foam-cell macrophages (Landers *et al.*, 1994).

As already stated TF is expressed by cells which are not normally exposed to flowing blood. Therefore it is generally believed that an intact endothelium is the most important factor in preventing TF-initiated coagulation however recent evidence of TF being found in normal blood suggests this is not the complete story (Giesen *et al.*, 1999; Key *et al.*, 1998).

Encryption of TF is now emerging as the primary mechanism of controlling the procoagulant activity of TF. Resting cells which express TF, were observed to express little TF procoagulant activity, therefore it was hypothesized that a stimulus was required to induce this (Bach *et al.*, 1990). Several agents have been observed to induce the activation of TF; for example calcium ionophores have been observed to increase the activity of TF on 'primed' monocytes (Bach *et al.*, 1990; Henriksson *et al.*, 2007).

As previously stated changes in intracellular calcium homeostasis can initiate the translocation by anionic phospholipids from the inner to the outer leaflet of the plasma membrane by activation of scramblase and inhibition of flippase. Therefore it comes of no surprise that increases in TF activity are associated with the exposure of PS on the outer leaflet of the plasma membrane and cell death (Greeno *et al.*, 1996; Henriksson *et al.*, 2007). It is hypothesized that PS can increase the *Vmax* and decrease the *Km* of the conversion of FX to FXa by the TF-FVIIa complex. The increase in *Vmax* has been suggested to be due to (i) PS inducing a change in the TF quaternary structure therefore increasing the number of active catalytic sites and (ii) PS exposure optimizing the orientation of the TF-FVIIa catalytic site (Bach, 2006).

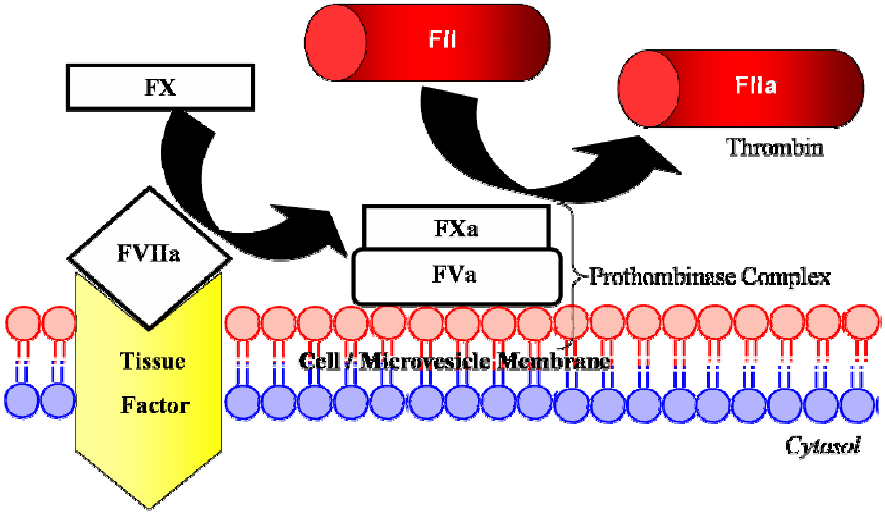

Figure 5-1. Schematic of the extrinsic (TF) coagulation pathway. Translocation of anionic phospholipids (red) from the inner to the outer leaflet of the plasma membrane increase TF pro-coagulant activity leading to the activation of FX. FXa is then able to convert prothrombin (FII) to thrombin (FIIa), a reaction which is catalyzed by the assembly of FXa with its co-factor FVa on a PS-rich membrane surface (prothrombinase complex).

5.1.2 Enhancement of Thrombin Generation

Thrombin (FIIa) is one of the end products of both the intrinsic and extrinsic coagulation cascade. It not only converts soluble fibrinogen to form insoluble strands of fibrin, used to form a haemostatic plug/clot over a wound but is involved in the activation of other factors of the coagulation cascade (FXI, FV and FVIII) and therefore accelerates its own production.

Thrombin is produced by the cleavage of prothrombin (FII). Several proteolytic enzymes can bring about this reaction but under physiological conditions the serine protease factor Xa (FXa) is the activating enzyme. FXa is able to cleave prothrombin at R271 followed by R320 to yield thrombin; this however is a slow process but can be catalysed by the prothrombinase complex. The prothrombinase complex consists of FXa, the cofactor/factor Va (FVa), PS and Ca^{2+} (Figure 5-1). This complex is able to increase the efficiency of prothrombin cleavage by FXa in two ways (Lentz, 2003; Weinreb *et al.*, 2003).

1. The presence of FVa increases the *Vmax* of thrombin formation by forming a complex with FXa allowing the cleavage of prothrombin at R320 followed by R271.

2. Exposure of PS decreases the *Km* of prothrombin by increasing the catalytic efficiency of FXa by triggering a close association of FXa with FVa.

It has been indicated in several studies that monocytes are able to support pro-coagulant responses and the assembly of the prothrombinase complex. Furthermore it has been observed that stimulating monocytes or macrophages for several hours with either lipopolysaccharide (LPS), oxidise LDL or p-selectin leading to the exposure of PS can ultimately increase the generation of thrombin from prothrombin (Ananyeva *et al.*, 2002; del Conde *et al.*, 2005; Satta *et al.*, 1994).

5.1.3 Role for the P2X7R in Coagulation

ATP activation of the $P2X_7R$ has been demonstrated to rapidly induce the exposure of PS on the outer leaflet of monocyte/macrophage plasma membranes (MacKenzie *et al.*, 2001; Moore *et al.*, 2007). Therefore I propose that ATP stimulated macrophages could potentially play a role in propagating and amplifying coagulatory responses. Furthermore the shed microvesicles from these ATP stimulated cells could themselves be involved in supporting prothrombotic activity. A major source of blood-borne TF is PS-rich microvesicles (Giesen *et al.*, 1999) and a study by Satta *et al.,* 1994 demonstrated that microvesicles released from monocytes after LPS stimulation (4-6hr) could increase prothrombinase activity.

The key findings of this study were:

1. ATP stimulation of RAW264.7 cells increases their ability to activate FX in the presence of FVIIa via a TF and PS dependent pathway.
2. ATP stimulation of RAW264.7 cells increased their ability to generate thrombin in the presence of FXa, FVa and prothrombin.
3. Microvesicles derived from ATP stimulated RAW264.7 cells are able to generate thrombin in the presence of FXa, FVa and prothrombin.

5.2 RESULTS

5.2.1 ATP Stimulated Cell Surfaces Catalyse the Activation of FX

The exposure of PS on the outer leaflet of the plasma membrane is known to increase the pro-coagulant activity of the TF-FVIIa complex leading to the activation of FX. Here I tested whether ATP evoked PS translocation in RAW 264.7 macrophages is able to enhance the rate of FX activation as measured using the chromogenic substrate S-2765™.

Activating RAW264.7 cells with a 5 min pulse of 3 mM ATP in the presence of Ca^{2+} (37 ^{o}C) was observed to increase the rate of change in absorbance of the FXa substrate S2765^{TM} when in the presence of FVIIa (Figure 5-2A). Activating RAW264.7 cells with 3 mM ATP for a range of times determined that a 5 – 10 min exposure was required to induce a significant increase in the activity of FX (n =3, $p<0.05$, Figure 5-2B). However the increase in FX activity was transient; where a 15 minute stimulation (3 mM ATP) was observed to not induce a significant increase in the activity of FX above an ATP-free control (n = 3, $p>0.05$). Using a 5 min stimulation time with a range of ATP concentrations revealed that concentrations ≥1 mM were required to activate FX (n = 3, Figure 5-2C).

5.2.2 ATP Induced FX Activation is TF Dependent

ATP-dependent FX activation was blocked when stimulated cells were incubated with FVIIa in the presence of an anti-TF IgG ($p<0.05$) while a non-specific IgG control had no effect (n = 3, Figure 5-3A). Basal levels of FX activation were unaffected by the co-incubation with anti-TF IgG. Incubating cells with the P2X$_7$R antagonist KN-62 (10 μM) for 5 min prior and during a 3 mM ATP (5 min) stimulation was observed to block ATP induced activation of FX (n = 3, Figure 5-3B). Incubating ATP stimulated cells with annexin-V, which is able to bind to exposed PS was observed to partially reduce ATP induced increases in FX activity (n = 3, Figure 5-3C).

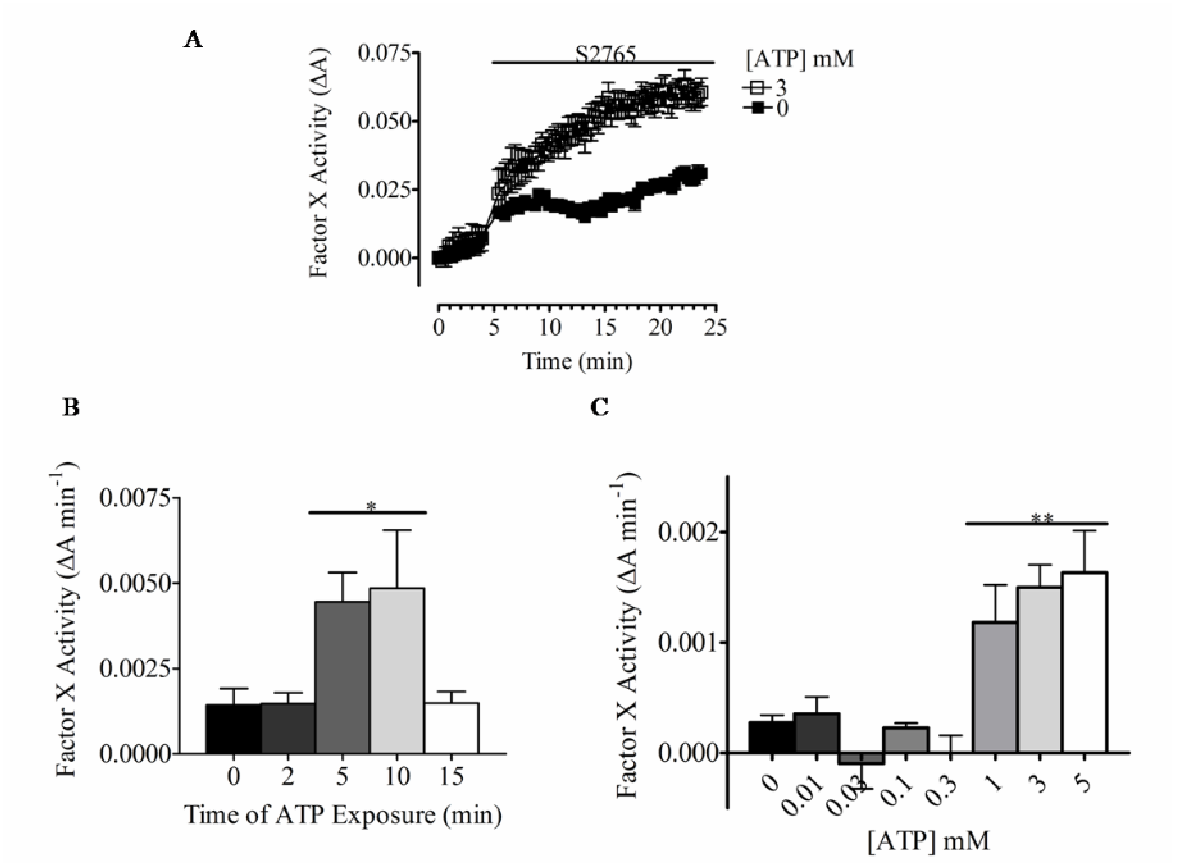

Figure 5-2. Stimulating RAW264.7 cells with ATP Increases the Activity of FX in the Presence of FVIIa. A, Representative kinetic of ATP evoked increases in the absorbance of S2765^{TM} indicative of an increase in the presence of active FX. B, Histogram demonstrating that a 5 – 10 min exposure of RAW264.7 cells to 3 mM ATP induces a significant increase in FX activity (n = 3 ± s.e.m). C, Histogram demonstrating that ATP (5 min) concentrations ≥1 mM are required to significantly increase FX activity (n = 3 ± s.e.m). One-way ANOVA with Dunnett's post-hoc test, *:$p<0.05$, **: $p<0.01$.

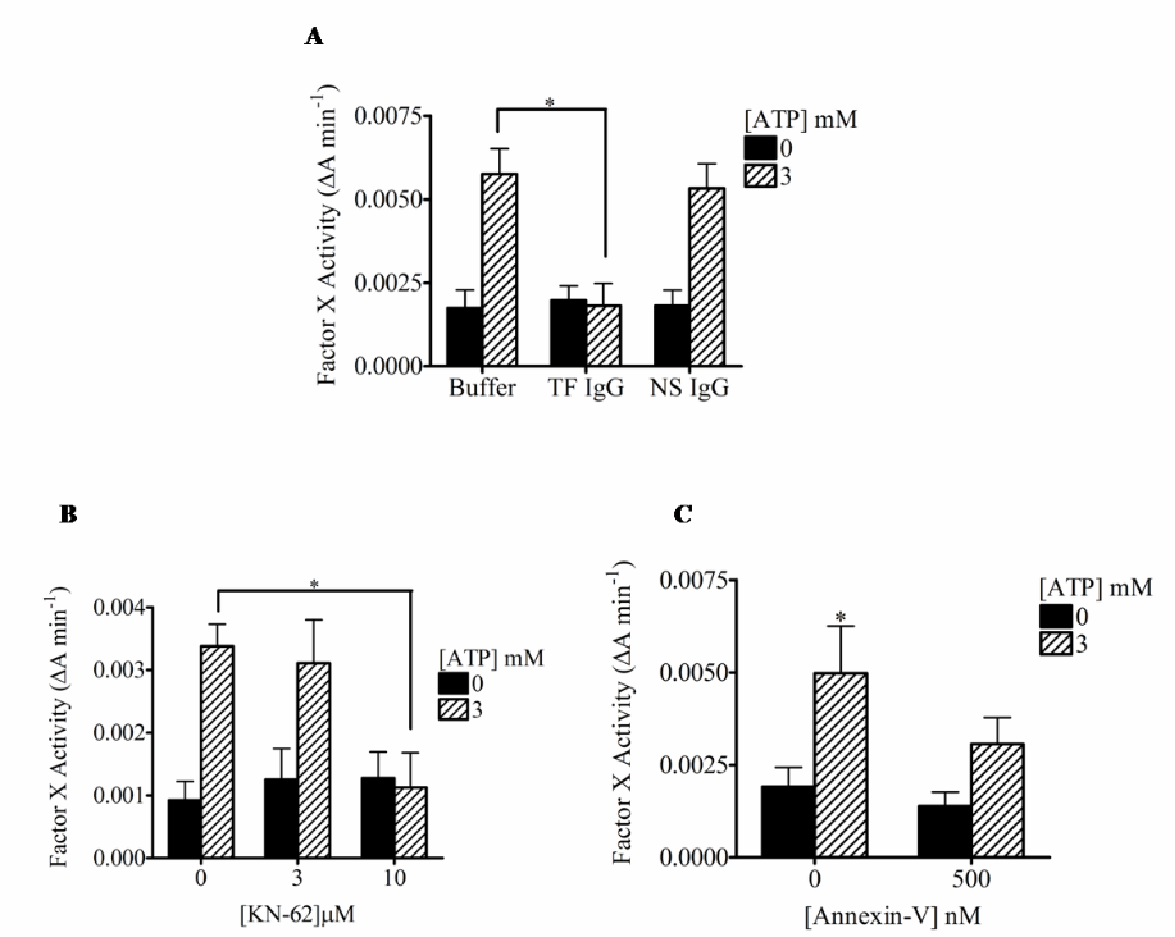

Figure 5-3. ATP Evoked Increases in FXa are Dependent on TF, PS Exposure and P2X$_7$R Activation. A, Histogram demonstrating that incubating ATP stimulated RAW264.7 cells with FVIIa in the presence of a anti-TF IgG significantly decreases FX activity (n = 3 ± s.e.m). B, Histogram demonstrating that stimulating RAW264.7 cells with ATP in the presence of KN-62 significantly decreases FX activity (n = 3 ± s.e.m). C, Histogram demonstrating that incubating ATP stimulated RAW264.7 cells with FVIIa in the presence of An-V inhibits the ATP induced significant increase in FX activity (n = 3 ± s.e.m). Student's t-test, *: $p<0.05$, ***: $p<0.0001$.

5.2.3 ATP Decreases TF Cell Surface Expression

Labelling cell surfaces with anti-TF IgG and analyzing cells using FACS it was observed that 96 ± 2 % of unstimulated RAW264.7 cells (n = 3 ± s.e.m, Figure 5-4A) expressed cell surface TF. Stimulating cells with ATP (3 mM, 5 min) did not significantly alter the percentage of cells expressing surface TF (80 ± 11 %, n = 3 ± s.e.m, $p>0.05$). However the level of TF expression decreased with ATP stimulation (n = 3, $p<0.01$, Figure 5-4B).

I previously demonstrated that stimulation of RAW264.7 cells with ATP induced the appearance of microvesicles. The loss of TF expression from the surface of RAW264.7 cells could be hypothesised to be due to the shedding of TF expressing microvesicles. To determine whether microvesicles shed by RAW264.7 cells in response to ATP stimulation contained levels of TF sufficient to cause activation of FX in the presence of FVIIa, microvesicles were isolated from the supernatants of RAW264.7 cells by ultracentrifugation. No FX activity was recorded from either control or ATP derived microvesicle populations (n = 3, $p>0.05$, data not shown).

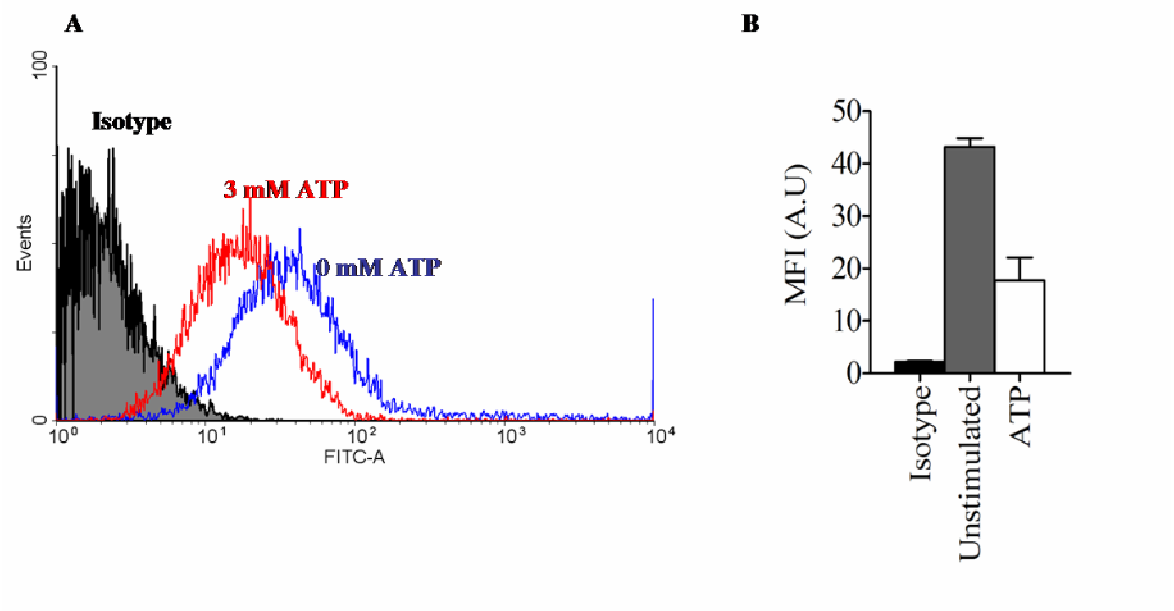

Figure 5-4. ATP Evokes a Decrease in TF Cell Surface Expression. A, Representative FACS overlay demonstrating that ATP stimulation of RAW264.7 cells decreases cell surface expression of TF. B, Histogram demonstrating that stimulating RAW264.7 cells with ATP decreases cell surface expression of TF ($n = 3 \pm$ s.e.m). .

5.2.4 ATP stimulated Cell Surfaces Catalyse Thrombin Generation

The appearance of PS a component of the prothrombinase complex in the outer leaflet of the plasma membrane is observed to catalyse the cleavage of prothrombin to thrombin by factor Xa in the presence of factor Va and Ca^{2+} ions. Here I tested whether ATP evoked PS translocation in RAW 264.7 macrophages is able to enhance the rate of thrombin generation as measured using the chromogenic substrate S-2338™. Cell surfaces of RAW264.7 cells stimulated with ATP (10 min, 37 ^{o}C) in the presence of Ca^{2+} were observed to induce an increase in the rate of thrombin generation (Figure 5-5A, $p<0.05$, $n = 9$).

Stimulating RAW264.7 cells with a range of ATP concentrations determined that 1 mM ATP evoked a peak response (1.76 ± 0.12, $n = 9 \pm$ s.e.m) in the rate of thrombin generation (Figure 5-5B). The peak response evoked by ATP (1 mM) was not significantly reduced by pre-incubating and stimulating RAW264.7 cells in the presence of KN-62 (Figure 5-5C, $p>0.05$, $n = 9$). However ATP in the presence of KN-62 did not induce a significant increase in the rate of thrombin generation compared to the KN-62 control ($p>0.05$, $n = 9$).

To evaluate the contribution of translocated PS, stimulated RAW264.7 cells were pre-incubated with the PS-capping agent An-V (500 nM, 5 min, 37 ^{o}C). Addition of An-V significantly reduced the ATP (1 mM) evoked response (Figure 5-5D, $p<0.05$, $n = 9$).

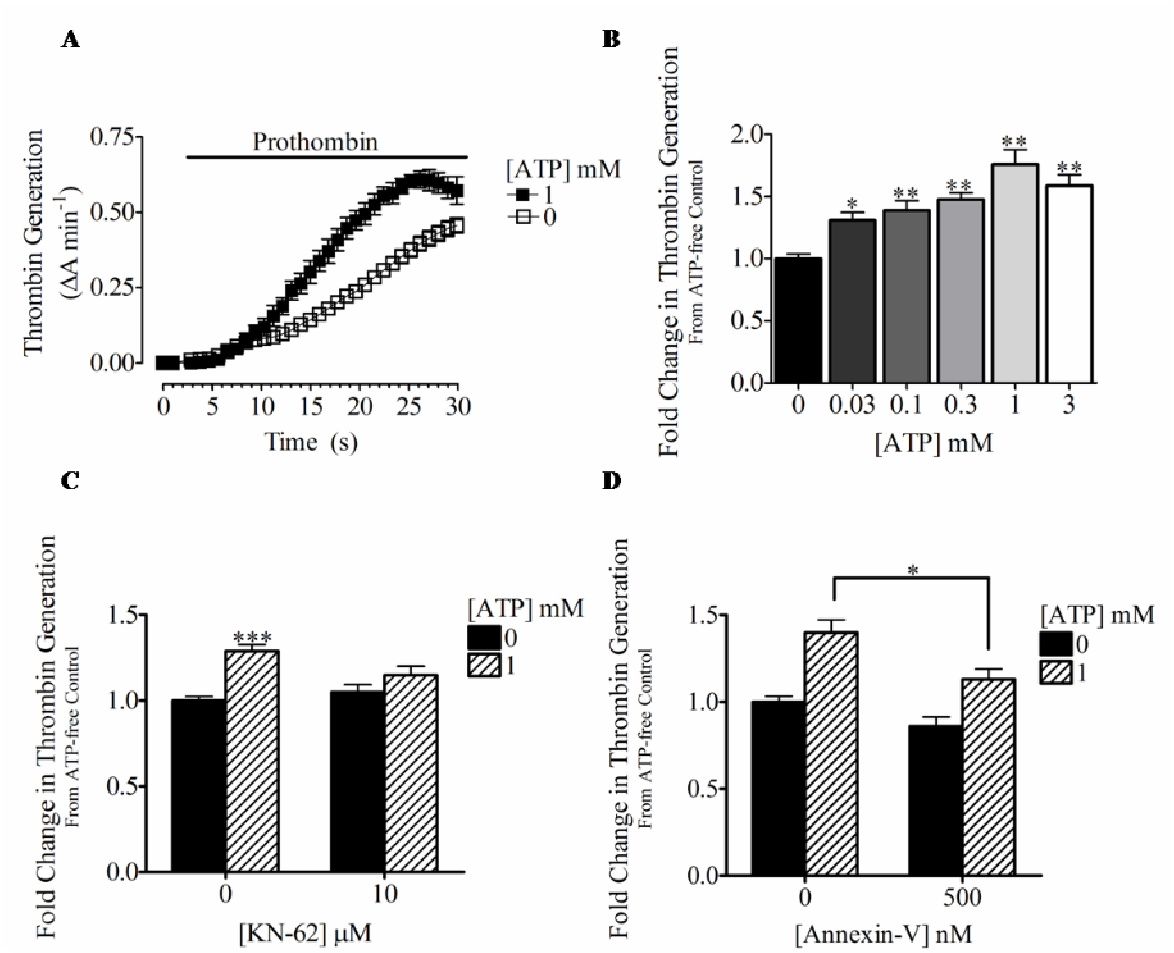

Figure 5-5. ATP Treated Cell Surfaces can Increase Thrombin Generation. A, Representative kinetic of ATP (10 min) evoked increases in the absorbance of S2238^{TM} indicative of an increase in the generation of thrombin. B, Histogram demonstrating that a range of ATP concentrations can induce a significant increase in thrombin generation (n = 9 ± s.e.m). C, Histogram demonstrating that pre-incubating and stimulating RAW264.7 cells in the presence of KN-62 did not significantly reduce ATP evoked increases in thrombin generation (n = 9 ± s.e.m). D, Histogram demonstrating that treating ATP stimulated RAW264.7 cells with An-V significantly reduces ATP evoked increases in thrombin generation (n = 9 ± s.e.m). One-way ANOVA with Dunnett's post-hoc test or Student's t-test, *: $p<0.05$, ***: $p<0.0001$.

5.2.5 Shed Microvesicles from ATP Stimulated Cells Catalyse Thrombin Generation

I previously demonstrated that stimulation of RAW264.7 cells with ATP induced the appearance of microvesicles; an observation that correlated with the finding that activation of the P2X$_7$R induced the shedding of PS-rich microvesicles from LPS treated THP-1 monocytes (MacKenzie *et al.*, 2001). To determine whether microvesicles shed by RAW264.7 cells (untreated) in response to ATP stimulation are able to enhance the rate of thrombin generation, microvesicles were isolated from the supernatant of RAW264.7 cells and the rate of thrombin generation measured using the chromogenic substrate S-2338™.

Shed microvesicles were isolated from the supernatants of RAW264.7 cells and added to FXa and FVa and S-2238™. Upon application of prothrombin; microvesicle fractions collected from cells primed with 1 mM ATP (10 min) were observed to evoke an increased rate of thrombin generation (Figure 5-6A). This increase was calculated to be 2.2 ± 0.24 fold (range 1.27 – 3.17) above the microvesicle fraction collected from control (ATP-free) cells (n = 9 ± s.e.m, $p<0.01$).

The increased rate of thrombin formation was observed to peak with a 10 min ATP (1 mM) application and declined with 30 min ATP (1 mM) stimulation; this could have resulted from the lysis of released microvesicles (Figure 5-6B). An increased rate of microvesicle dependent thrombin generation was not observed when RAW264.7 cells where stimulated with concentrations of ATP ≤100 μM (Figure 5-6C).

All subsequent measurements of prothrombinase activity in the presence of microvesicles were performed following 10 min ATP stimulation.

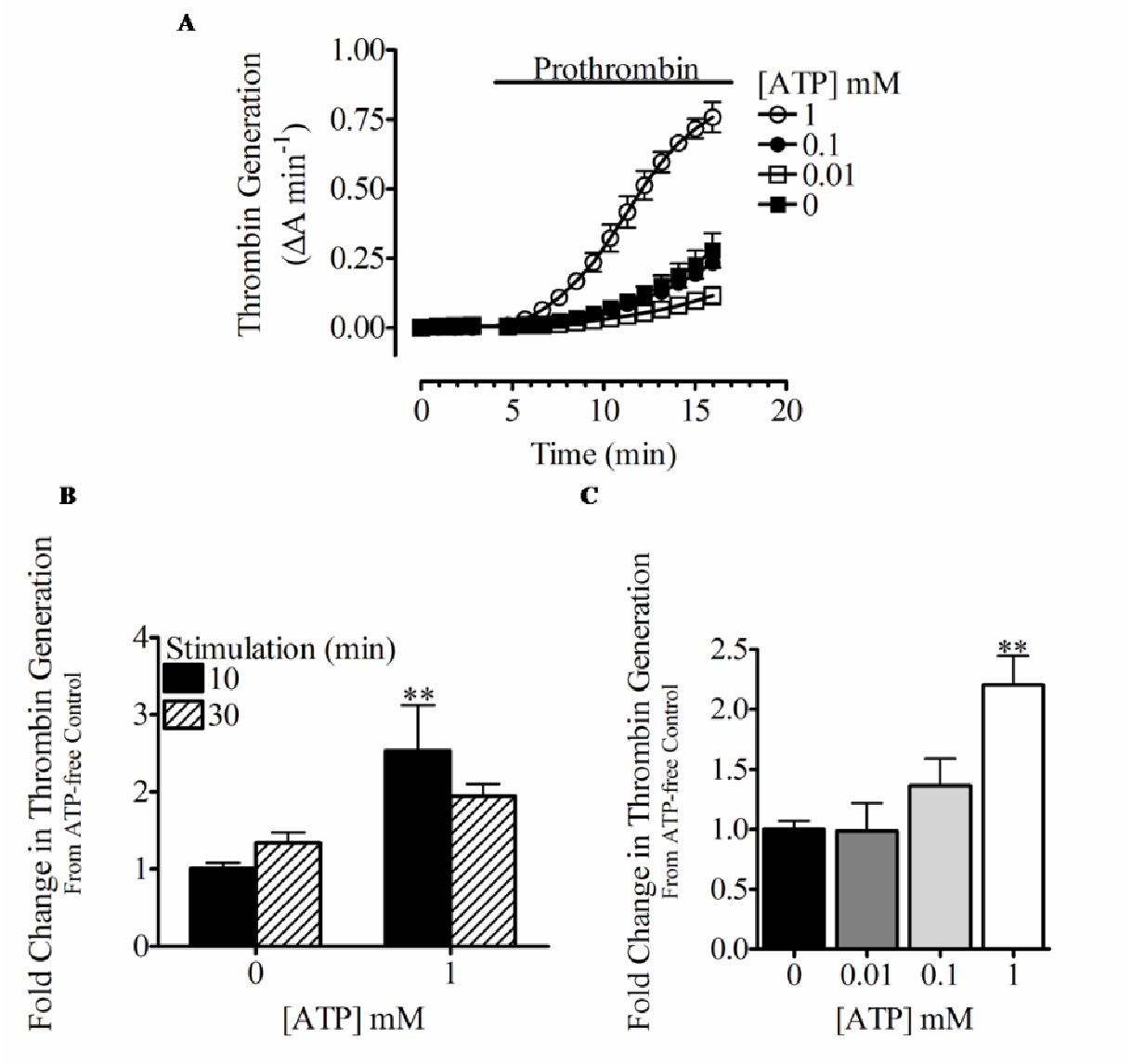

Figure 5-6. Microvesicles Generated by ATP can Increase Thrombin Generation. A, Representative kinetic of ATP (10 min) evoked increases in the absorbance of S-2238^{TM} indicative of an increase in the generation of thrombin. B, Histogram demonstrating that a 10 min ATP (1 mM) stimulation can induce a significant increase in thrombin generation, whereas a 30 min stimulation results in a decline (n = 9 ± s.e.m). C, Histogram demonstrating that microvesicle fractions from cells stimulated with concentrations of ATP ≤100 μM do not evoke a significant increase in thrombin generation (n = 9 ± s.e.m). One-way ANOVA with Dunnett's post-hoc test or Student's t-test, **: p<0.01.

5.2.6 Microvesicle Induced Thrombin Generation is Dependent the P2X7R, PS and Ca^{2+}

Concentrations of ATP >100 μM are required to evoke microvesicle induced thrombin generation. Therefore I hypothesised that activation of the $P2X_7R$ was required for microvesicle shedding and subsequent increases in thrombin generation to occur. I tested this hypothesis by stimulating RAW264.7 cells with ATP in the presence of the $P2X_7R$ antagonists KN-62 (10 μM) and BBG (1 μM). Microvesicle fractions collected from cells stimulated in the presence of either of these inhibitors failed to evoke significant increases in thrombin generation in the presence of FVa, FXa and prothrombin (Figure 5-7A, KN-62 $p<0.001$, Figure 5-7B, BBG $p<0.0001$, $n = 9$).

To evaluate the contribution of exposed PS on the generation of thrombin, the isolated microvesicles were pre-incubated with 500 nM An-V to bind and cap the exposed PS on the surface of the microvesicles. Addition of An-V was observed to attenuate ATP (1 mM) evoked increases in thrombin generation (Figure 5-7C, $p<0.001$, $n = 9$).

PS exposure is reported to occur when a large and rapid increase in $[Ca^{2+}]_i$ occurs leading to the activation of scramblase and the inhibition of flippase. Furthermore I observed that microvesicle formation on RAW264.7 cells was reduced when the cells were stimulated with ATP in the absence of extracellular Ca^{2+}. Therefore I assessed the contribution of extracellular Ca^{2+} on microvesicle formation and subsequent thrombin generation by stimulating RAW264.7 cells in the absence of external Ca^{2+}. Microvesicle fractions generated from RAW264.7 cells stimulated in the absence of external Ca^{2+} were observed to have significantly lower basal and ATP evoked thrombin generation (Figure 5-7D, $p<0.001$, $n = 9$).

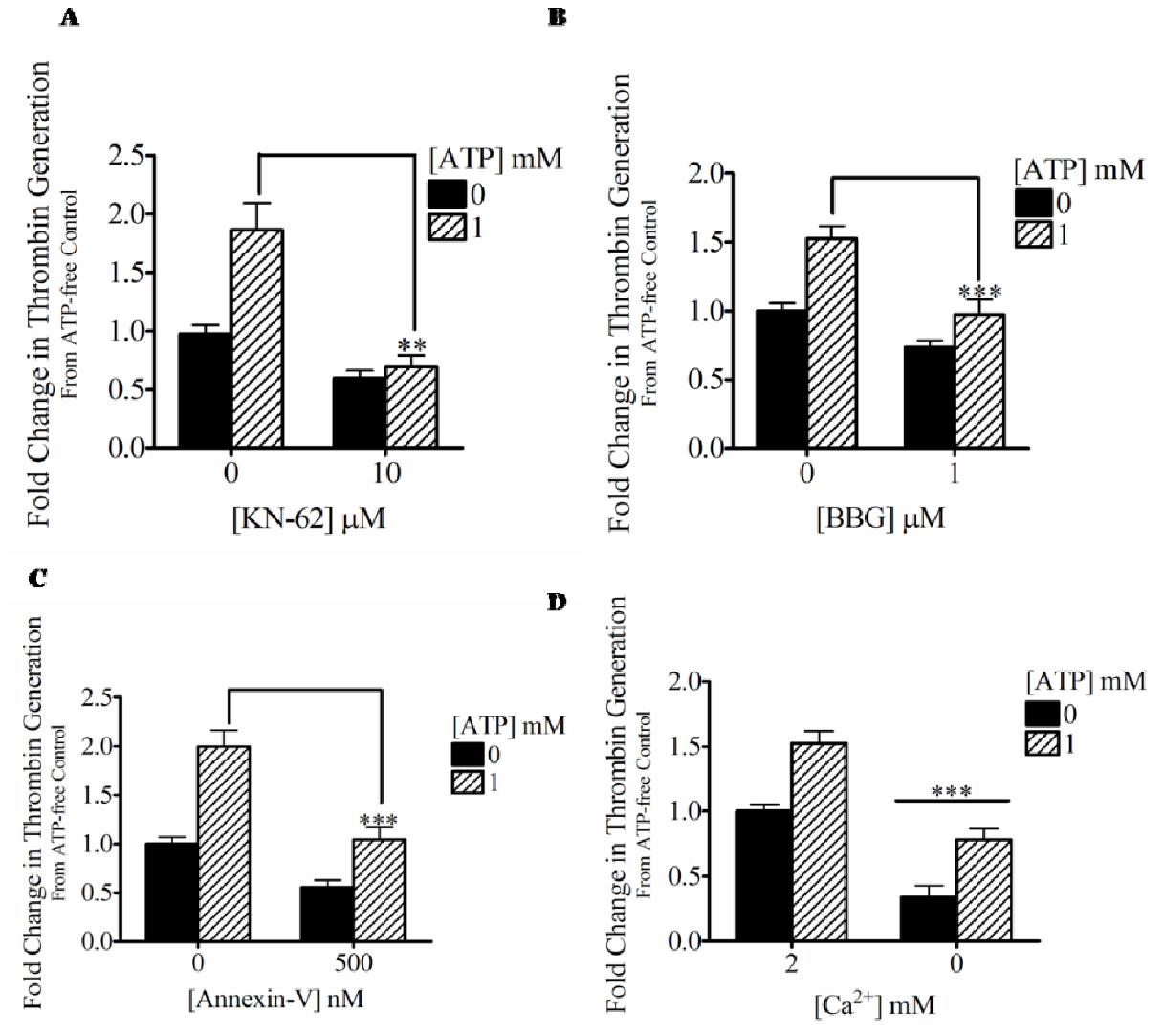

Figure 5-7. Microvesicle Induced Thrombin Generation is Dependent on the P2X$_7$R, PS and Ca^{2+}. A, Histogram demonstrating that blockade of the P2X$_7$R with KN-62 inhibits microvesicle induced thrombin generation (n = 9 ± s.e.m). B, Histogram demonstrating that blockade of the P2X$_7$R with BBG inhibits microvesicle induced thrombin generation (n = 9 ± s.e.m). C, Histogram demonstrating that capping exposed PS on ATP generated microvesicles inhibits thrombin generation (n = 9 ± s.e.m). D, Histogram demonstrating that stimulating RAW264.7 cells in the absence of external Ca^{2+} inhibits microvesicle induced thrombin generation (n = 9 ± s.e.m). Student's t-test, **: p<0.01, ***:p<0.001.

5.3 DISCUSSION

In this study I determined the ATP is potentially involved in pro-coagulant responses, due to its ability to evoke changes on cell membrane surfaces. The evidence for this is (i) ATP stimulated RAW264.7 cells can support TF dependent activation of FX, (ii) ATP stimulated RAW264.7 cells can catalyse thrombin generation in the presence of FVa, FXa and prothrombin and (iii) Microvesicle fractions from ATP stimulated RAW264.7 cells can catalyse thrombin generation in the presence of FVa, FXa and prothrombin.

5.3.1 ATP Stimulated Cell Surfaces can Activate FX

Extracellular ATP was determined to increase the activity of FX via a TF and a PS dependent pathway (Figure 5-3). This occurred in the absence of an increase in cell surface expression of TF leading to the hypothesis that extracellular ATP is able to increase the procoagulant activity of the TF already present on the RAW264.7 cells (Figure 5-4). Based on the following observations I propose that extracellular ATP is acting at the $P2X_7R$ to increase FX activity because (i) concentrations ≥ 1 mM ATP are required to elicit this increase, (ii) inhibition of the increase by the $P2X_7R$ antagonist KN-62 and (iii) PS exposure was previously found to not occur using ATP concentrations of ≤ 100 μM.

Based on the findings of previous studies using calcium ionophores (Bach *et al.*, 1990) I suggest that the sustained increase in $[Ca^{2+}]_i$ initiated by $P2X_7R$ activation leads to the exposure of PS on the outer leaflet of the plasma membrane. This PS exposure is then able to increase the procoagulant activity of TF via an increase in the V*max* and decrease in the K*m* of TF-FVIIa conversion of FX to FXa.

Examination of cell surface TF expression on RAW264.7 cells determined that ATP induced a loss in TF expression. I hypothesise that this loss could potentially be due to the shedding of microvesicles (Moore *et al.*, 2007). A study by Baroni *et al.,* 2007 determined that stimulation of the $P2X_7R$ with BzATP led to the shedding of microvesicles from dendritic cells. These microvesicles were determined to express TF and could support the activation of FX in the presence of FVIIa (Baroni *et al.*, 2007). In the current study the microvesicles collected from ATP stimulated RAW264.7 cells failed to cause a significant increase in the activation of FX. I hypothesise that this is due to either TF not being shed on microvesicles due to it being localised on different areas of the plasma membrane

compared to where microvesicles arise (Del Conde *et al.*, 2005b; Dietzen *et al.*, 2004) or more likely that the levels of TF expressed on microvesicles were below the levels required for detection in the S2765^{TM} assay.

5.3.2 ATP Stimulated Cell Surfaces Enhance Thrombin Generation

Exposed PS as part of the prothrombinase complex is well documented to have an important role in the catalysis of thrombin generation (Weinreb *et al.*, 2003). In agreement with this the cell surfaces of RAW264.7 cells exposed to 1 mM ATP demonstrated PS translocation that was able to induce an increase in the rate of thrombin generation (Figure 5-5). This increased rate in thrombin generation was partially attenuated by An-V which specifically binds and caps exposed PS. I initially hypothesised that PS exposure and the subsequent increase in thrombin generation to be due to the activation of the $P2X_7R$ based on the finding that 1 mM ATP but not 100 μM ATP evoked the binding of AnV-488 to RAW264.7 cell surfaces. However an increase in the rate of thrombin generation was observed using 100 μM ATP to stimulate RAW264.7 cells and KN-62 failed to significantly change the rate of thrombin generation, although the rate of thrombin generation between cells treated with KN-62 in the absence of ATP versus cells treated with KN-62 in the presence of ATP was not significantly different (Figure 5-5).

5.3.3 Microvesicle Fractions from ATP Stimulated Cells Enhance Thrombin Generation

A study by Satta *et al.,* 1994 has previously observed that PS-rich microvesicles released by priming monocytes with LPS for 4-6 hrs were able to catalyse the generation of thrombin through the assembly of the prothrombinase complex. In agreement with this, microvesicle fractions derived from RAW264.7 cells stimulated briefly with ATP (1 mM, 10 min) increased the rate of thrombin generation more than 2-fold (Figure 5-6). I believed that ATP was activating the $P2X_7R$ to induce the shedding of PS-rich microvesicles which were able to catalyse thrombin generation; this was supported by three findings:

1. Microvesicle fractions collected from RAW264.7 cells pre-incubated with either KN-62 or BBG had dramatically reduced ATP evoked thrombin generation.
2. Pre-treatment of microvesicle fractions with An-V significantly attenuated thrombin generation.

3. Microvesicle fractions collected from RAW264.7 cells stimulated with ATP in the absence of external Ca^{2+} had reduced basal and ATP evoked thrombin generation.

5.3.4 Is there a PS-Independent Component of the Prothrombinase Complex?

Treatment of RAW264.7 cell surfaces and microvesicle fractions with An-V failed to completely inhibit ATP evoked thrombin generation. Two explanations could be provided for this observation either that the concentration of An-V was insufficient to fully cap all exposed PS or that a PS independent component is involved in the formation of the prothrombinase complex. The second explanation would correlate with the fact that cell surfaces treated with 100 μM ATP were able to enhance thrombin generation, although this concentration of ATP had failed to induce AnV-488 binding to RAW264.7 cell surfaces. This PS independent component maybe due to the action of other exposed anionic phospholipids such as PE (Smirnov *et al.*, 1999).

5.3.5 ATP, PS and Thrombin in Inflammatory Reactions & Diseases

PS plays a crucial role in the coagulation cascade via its ability to enhance the activity of enzyme complexes of the coagulation cascade such as TF-FVIIa, FXa-FVa which were discussed in this chapter and also the FVIIIa:FIXa (tenase) complex involved in the activation of FX via the intrinsic coagulation cascade. I therefore hypothesise that in inflammatory areas such as atherosclerotic plaques, ATP released by damaged cells, infiltrating inflammatory cells and activated platelets could play several roles in procoagulant responses.

- ADP generated from ATP would stimulate platelet $P2Y_1$ and $P2Y_{12}$ receptors facilitating platelet aggregation.
- Exposure of PS on macrophages would increase TF-FVIIa activity leading to an increase in FXa generation.
- Exposure of PS on macrophages would increase FVa-FXa activity leading to an increase in thrombin generation which would ultimately lead to the deposition of fibrin.
- Release of PS containing microvesicles from macrophages could disseminate the procoagulant response in to areas surrounding the major inflammatory site.

Extracellular ATP could also potentially play a role in pro-inflammatory responses in atherosclerosis. Firstly ATP could be involved in the recruitment of monocytes and macrophages into the plaque (Wong *et al.*, 2006). Secondly as previously stated ATP can induce the processing and release of IL-1 cytokines via action of the P2X$_7$R on 'primed' monocytic cells (Ferrari *et al.*, 1997b; MacKenzie *et al.*, 2001). Knocking out IL-1β has been observed to decrease the severity of atherosclerosis in apoE deficient mice (Kirii *et al.*, 2003). Thirdly the TF-FVIIa complex (Hjortoe *et al.*, 2004), FXa (Busch *et al.*, 2005) and thrombin (Szaba *et al.*, 2002) can all stimulate the production and release of a range of pro-inflammatory cytokines.

5.3.6 Concluding Remarks

This study has demonstrated that stimulation of macrophages with high concentrations of ATP could lead to the propagation and amplification of the coagulation cascade (Figure 4-8). Increases in TF pro-coagulant activity and prothrombinase complex formation were observed to occur within a faster time course in comparison to previous studies where monocytes were required to be stimulated for hours rather than minutes in order to lead an increase in their pro-coagulant properties (Bach *et al.*, 1990; Satta *et al.*, 1994). Furthermore based on LDH experiments these events occurred within a time frame where ATP failed to induce cell death. The observation that activation of the P2 receptors by ATP can evoke pro-coagulant responses could be important in conditions were dysregulation of coagulation and inflammation occurs such as sepsis and atherosclerosis.

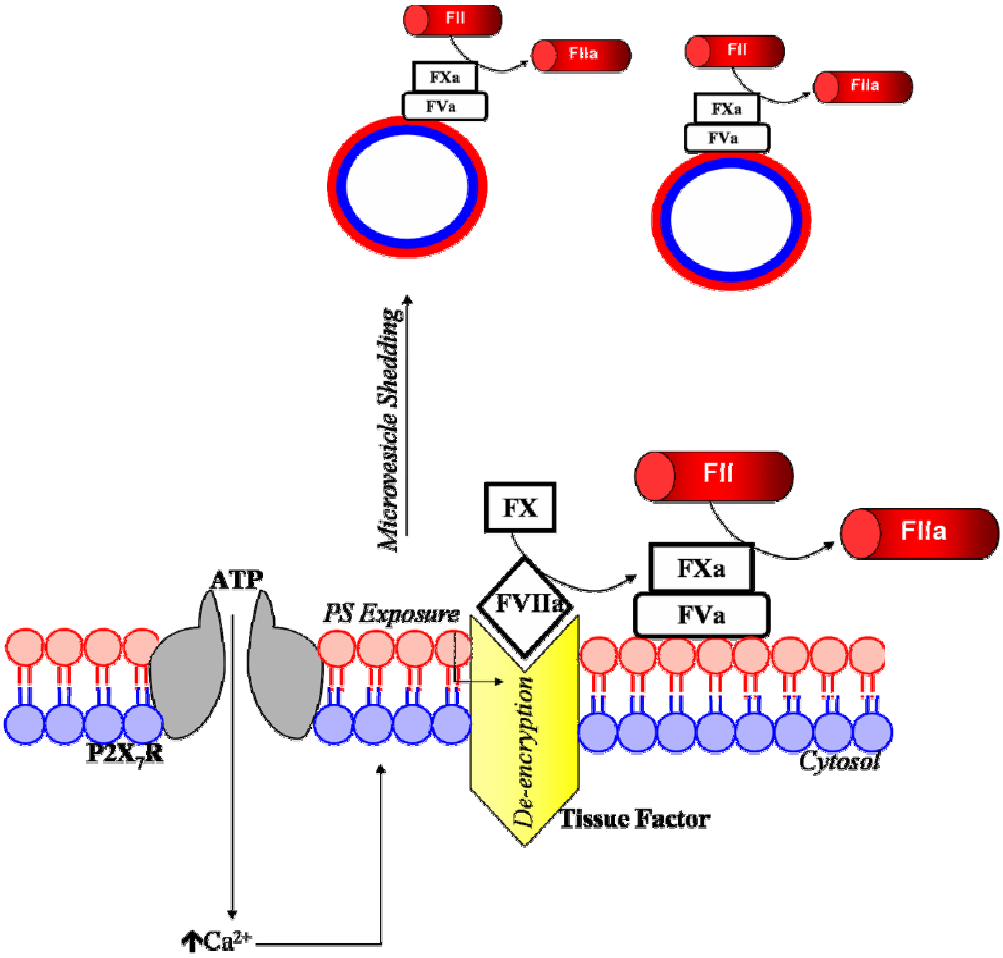

Figure 5-8. Summary Schematic of P2X7R Activation Coupling to Prothrombotic Responses. ATP stimulation of $P2X_7R$ leads an influx of Ca^{2+} raising $[Ca^{2+}]_i$. This leads to the translocation of PS initiating the de-encryption of tissue factor (yellow), formation of the prothrombinase complex and shedding of PS-rich microvesicles. In the presence of other coagulation cascade factors this would ultimately lead to the generation of FXa and thrombin. Red phospholipids are anionic (e.g. PS and PE).

.

CHAPTER 6

ATP INDUCES REACTIVE OXYGEN SPECIES GENERATION VIA NADPH OXIDASE

6.1 INTRODUCTION

In this part of the study the ability of extracellular ATP to initiated cellular oxidation in murine macrophages was investigated. Furthermore the source of ROS was assessed and the potential role they may play in initiating ATP induced cell death. Examining the role of ATP in evoking ROS generation could be of interest because:

- ROS and activation of P2 receptors are both associated with pro-inflammatory events and cell death.
- Increasing evidence implicates ROS as important signaling molecules under physiological and pathophysiological conditions, and therefore may be a downstream mediator of some of the events associated with P2 receptor activation.

Two papers in the 1980's observed that extracellular ATP was able to generate the production of O_2^- in neutrophils (Ward *et al.*, 1988) (Kuhns *et al.*, 1988). Recently several papers have demonstrated that ATP potentially acting at the $P2X_7R$ can evoke ROS generation in a variety of cell types including; primary rat microglia (Parvathenani *et al.*, 2003; Skaper *et al.*, 2006), RAW264.7 murine macrophages (Pfeiffer *et al.*, 2007), human eosinophils (Ferrari *et al.*, 2000) and neutrophils (Suh *et al.*, 2001).

Under physiological conditions the most important source of O_2^- is the mitochondrial electron transport chain (ETC), which as part of normal metabolism can transfer electrons onto O_2. It is estimated that 1 – 2 % of O_2 reduced in the mitochondria is in the form of O_2^- (Turrens, 1997). This occurs at two sites, complex I (NADH dehydrogenase) and complex III (ubiquinone-cytochrome c reductase). Several other enzymes also contribute to O_2 generation; these include xanthine oxidase, cytochrome P450 enzymes, NOS and NADPH oxidase.

All macrophages express NADPH Oxidase (NOX2) which is a major source of O_2^- in phagocytic cells. Furthermore NOX2 has been suggested as the generator of extracellular ATP induced ROS generation (Hewinson *et al.*, 2008; Noguchi *et al.*, 2008; Parvathenani *et al.*, 2003; Seil *et al.*, 2008). In resting cells the components of NADPH oxidase are

located in different subcellular compartments; gp91phox and p22phox (flavocytochrome b558) are located at the plasma membrane whereas p47phox, p67phox and p22phox are located within the cytosol (Forman *et al.*, 2001). Upon activation of the cell either by phagocytosis or a soluble mediator the cytosolic components along with the small GTPase Rac translocate to the plasma membrane and associate with the membrane bound components (Figure 6-1).

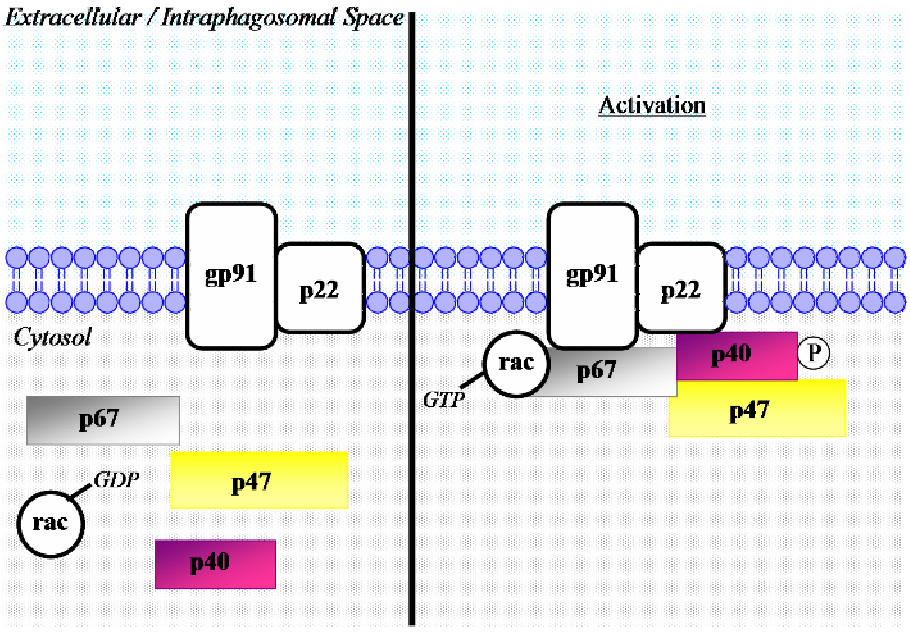

Figure 6-1. Schematic of NADPH Oxidase Subunits and Assembly upon Activation.

The gp91phox subunit contains a haem binding domain within its transmembrane segments and within its C-terminus a NADPH binding site and a flavin centre. Upon assembly of the complex the flavin centre transfers electrons from the physiological electron donor NADPH to the haem groups which mediate the final electron transfer to O_2, resulting in the generation of O_2^- in the extracellular of intraphagosomal space (Figure 4-2) (Yu *et al.*, 1998).

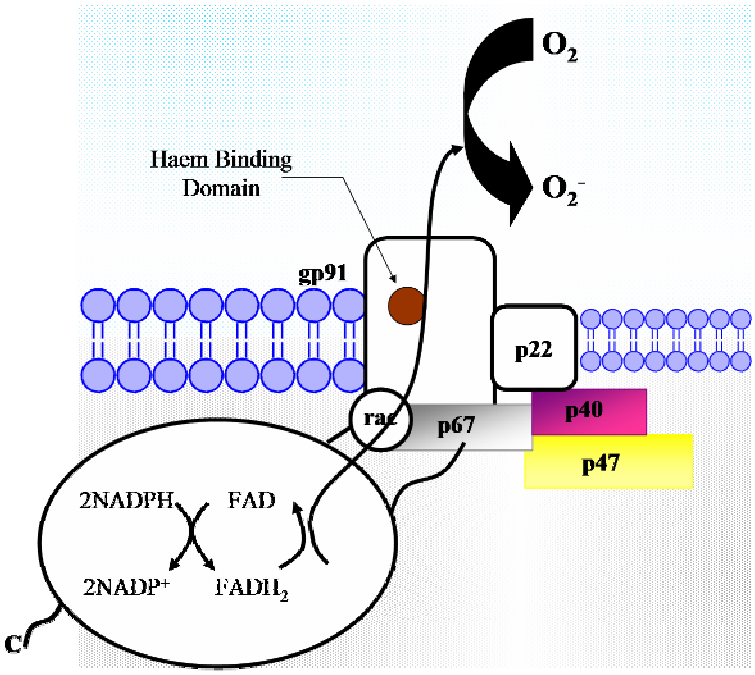

Figure 4-2. Schematic of NADPH Oxidase Generation of Superoxide.

The O_2^- produced provides a source for the formation of all ROS and plays a vital role in the elimination of pathogens. This is highlighted by the fact that defects in the subunits of NADPH oxidase are the known cause of the hereditary condition; chronic granulomatous disease (Dinauer *et al.*, 1987). Patients with this disease have severe recurrent bacterial infections. However aberrant activation of NADPH oxidase will lead to excessive ROS generation which could potentially damage tissues and cells nearby. Increasing evidence exists for the role of NOX2 in a range of inflammatory diseases such as arthritis, and atherosclerosis. NOX2 activity and p47phox phosphorylation have been observed to be increased in neutrophils from arthritic patients (El Benna *et al.*, 2002). Furthermore an abundance of proteins modified by ROS have been documented to be present in the joint fluid of patients with rheumatoid arthritis (Chapman *et al.*, 1989; Kaur *et al.*, 1994).

Besides the role of ROS in oxidative burst and tissue damage, NADPH oxidase products are implicated to potentially act as second messenger molecules (Forman *et al.*, 2001). Macrophages are involved in the propagation of inflammation via the secretion of pro-inflammatory molecules and resolution of inflammation via recognition and phagocytosis of cell corpses. Could ROS be involved in signaling these macrophage responses? Previous studies and evidence collected through the course of my investigations demonstrates the

importance of the $P2X_7R$ in macrophage evoked pro-inflammatory responses. If the $P2X_7R$ can evoke ROS generation in macrophages, could it be a potential mechanism of activating these inflammatory responses? Therefore the aims of this study were to determine whether the activation of the $P2X_7R$ in 'primed' murine macrophages can elicit cellular oxidation. Furthermore I proposed to use a combination of pharmacological agents and knock-out studies to determine whether NADPH Oxidase (NOX2) is the generator of these ROS. I proposed to finalise this part of the study by examining whether ATP induced oxidative stress could potentially induce cell death. In this and the proceeding chapter the study was conducted using the J774.2 murine macrophage cell line instead of RAW264.7 macrophages. The reasoning for this is that I wished to examine the role of ROS in the maturation of IL-1β and RAW264.7 cells had been observed to not process IL-1β (Pelegrin *et al.*, 2008; Verhoef *et al.*, 2005).

The key findings of this study were:

1. Concentrations of ATP $\geq$ 500 μM evokes the generation of ROS in J774.2 cells and bone-marrow derived macrophages (BMDMø).
2. Antagonism of the translocation of the p47phox subunit of NADPH or knocking out of either p47phox or gp91phox subunits inhibits ATP evoked ROS generation.
3. ATP induced cytotoxicity in J774.2 cells but not BMDMø is regulated by cellular oxidation.
4. ATP induced cytotoxicity in murine macrophages is partially regulated by capase-1.

6.2 RESULTS

6.2.1 ATP Induces the Generation of ROS in Murine Macrophages

Addition of ATP onto LPS 'primed' J774.2 cells (Figure 6-3A) and BMDMø (Figure 6-3B) loaded with H_2DCF was observed to evoke rapid and sustained formation of the fluorescent compound DCF indicative of ROS generation. In the J774.2 cells, ATP intiated ROS generation with a bell-shaped concentration response curve with a peak response detected at 1 mM ATP (Figure 6-3C). The up-phase had an apparent EC_{50} value of 575 μM (pEC_{50} = 3.24 ± 0.04) and the down-phase an apparent EC_{50} of 2.75 mM (2.56 ± 0.05) (n = 10 ± s.e.m). By contrast ATP evoked EtBr influx into J774.2 cells with a concentration response curve peaking at 3 – 5 mM with an EC_{50} of 1.51 mM (pEC_{50} = 2.82 ± 0.03) (n = 3 ± s.e.m) (Figure 6-3E). In BMDMø, ATP evoked ROS generation was observed to plateau with concentrations of 2 - 5 mM (Figure 6-3D). This response was similar to that observed with ATP evoked EtBr influx into BMDMø (Figure 6-3F).

ATP evoked ROS generation and EtBr influx in J774.2 cells was not observed to be significantly inhibited by the $P2X_7R$ antagonist 10 μM KN-04 (n = 3, $p>0.05$) (Figure 6-4A, Figure 6-4B, Table 6-1). In contrast 10 μM KN-62 significantly reduced ATP evoked ROS generation; responses evoked by 1 mM ATP were reduced by 91 ± 2 % (Figure 6-4A, n = 3 ± s.e.m, $p<0.001$). EtBr influx into J774.2 cells was also inhibited by KN-62; this was observed as a significant reduction in the maxima (Figure 6-4B, Table 6-1, n = 3, $p<0.05$).

The cell permeable glutathione precursor NAC (20 mM, 2 hours) was observed to significantly reduce ATP evoked ROS generation (Figure 6-5A, n = 3, $p<0.01$) without effect on EtBr influx in J774.2 (Figure 6-5B). Similar results were observed using BMDMø (Figure 6-5E). Furthermore DPI (100 μM, 1.5 hours), an inhibitor of flavoprotein oxidoreductases significantly attenuated ATP induced ROS generation in J774.2 cells (Figure 6-5C, n = 3, $p<0.01$) and BMDMø (Figure 6-5F) without effect on EtBr influx (Figure 6-5D).

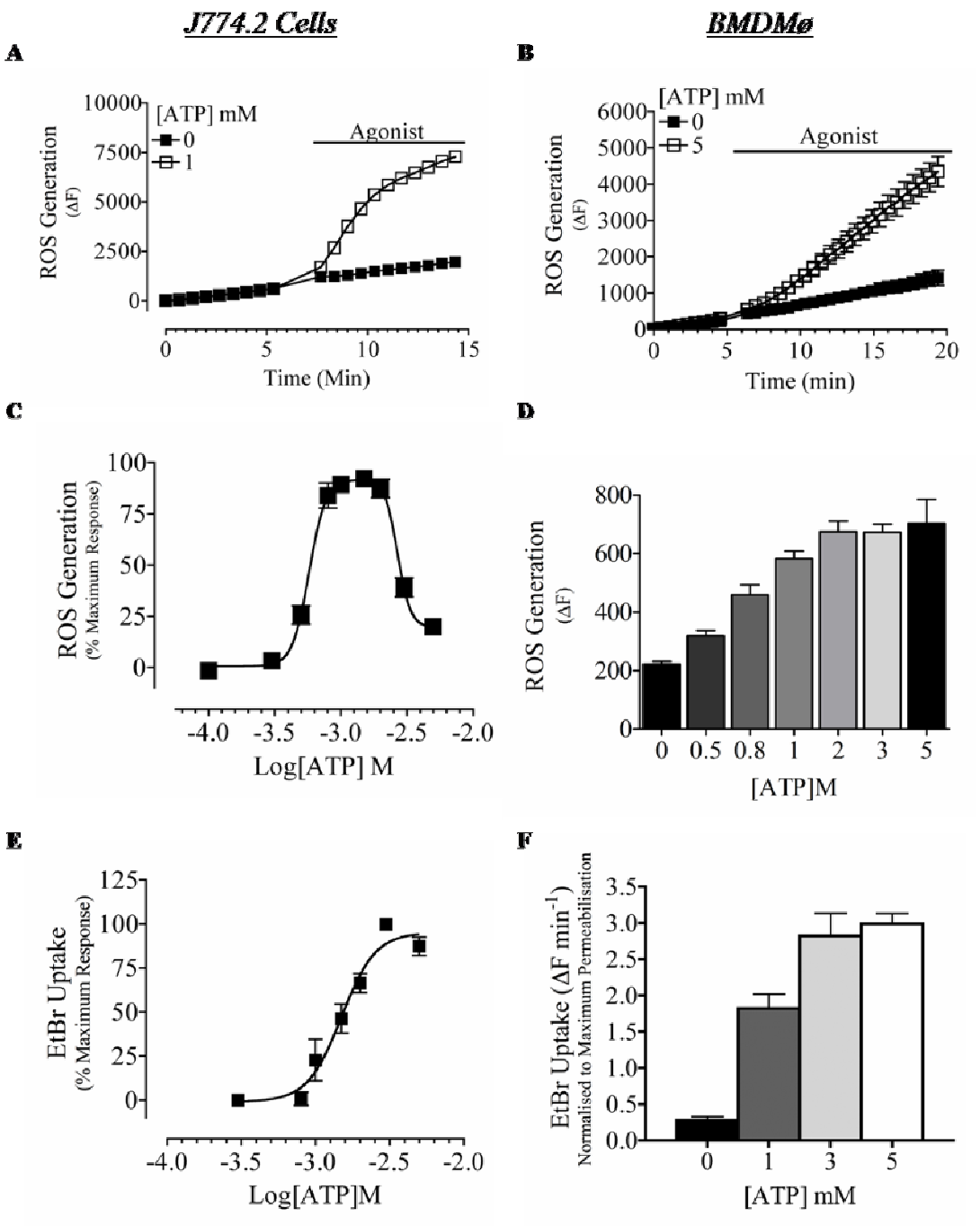

Figure 6-3. ATP Evokes ROS Generation in Murine Macrophages. A, Representative trace demonstrating that 1 mM ATP evokes an increase in DCF fluorescence in J774.2 cells. B, Representative trace demonstrating that 5 mM ATP evokes an increase in DCF fluorescence in BMDMø. C, Concentration response curve of ATP evoked ROS generation in J774.2 cells (pEC_{50} = 3.24 ± 0.04 & pEC_{50} = 2.56 ± 0.05) (*n* = 10 ± s.e.m). D, Histogram demonstrating concentration-dependent ATP evoked ROS generation in BMDMø (*n* = 3 ± s.e.m). E, Concentration response curve of ATP evoked EtBr influx in J774.2 cells (pEC_{50} = 2.82 ± 0.03) (*n* = 3 ± s.e.m). F, Histogram demonstrating concentration-dependent ATP evoked EtBr influx in BMDMø (*n* = 3 ± s.e.m).

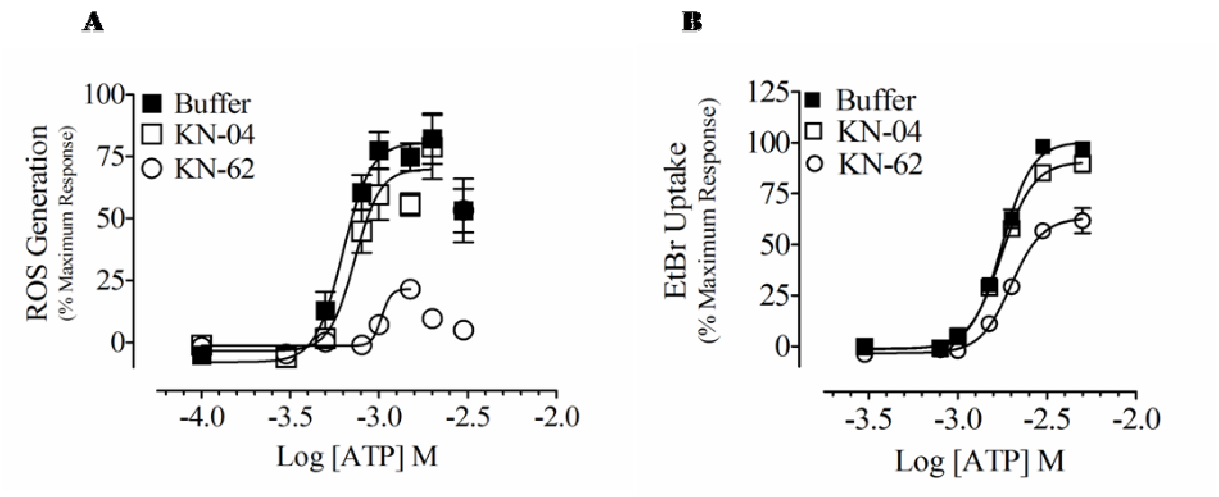

Figure 6-4. ATP Evoked ROS in Inhibited by KN-62 but not KN-04. A, Concentration response curve of ATP evoked ROS generation in J774.2 cells in the presence of 10 μM KN-04 or KN-62 (n = 3 ± s.e.m). B, Concentration response curve of ATP evoked EtBr influx in J774.2 cells in the presence of 10 μM KN-04 or KN-62 (n = 3 ± s.e.m).

A

ROS Generation

	pEC_{50} ± s.e.m	**n_H ± s.e.m**	**α ± s.e.m**
Control	3.12 ± 0.11	5.53 ± 1.51	113 ± 9
KN-62	NA	NA	NA
KN-04	2.97 ± 0.06	6.07 ± 2.93	107 ± 16

B

EtBr Influx

	pEC_{50} ± s.e.m	**n_H ± s.e.m**	**α ± s.e.m**
Control	2.75 ± 0.01	5.12 ± 0.61	102 ± 2
KN-62	2.70 ± 0.02	4.97 ± 0.99	68 ± 12*
KN-04	2.75 ± 0.01	4.79 ± 0.56	93 ± 8

Table 6-1. ATP Evoked ROS Generation (A) and EtBr Influx (B) Concentration Response Parameters in the Presence of KN-62 or KN-04. n = 3 ± s.e.m, one-way ANOVA with Dunnett's post-hoc test, *: $p<0.05$.

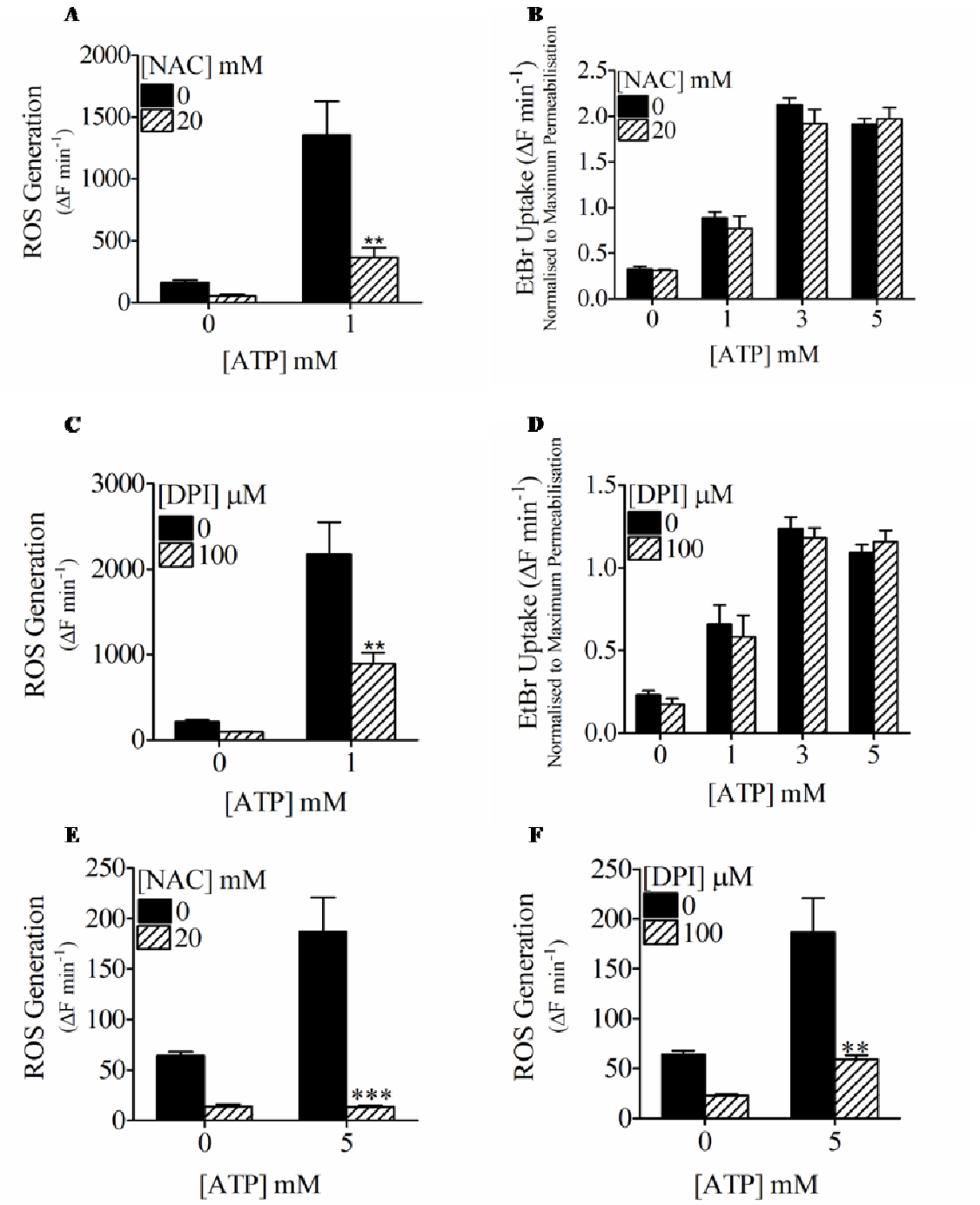

Figure 6-5. ATP Evoked ROS Generation is inhibited by NAC and DPI. A & B, Histograms demonstrating inhibition of ATP evoked ROS generation (A) but not EtBr influx (B) in J774.2 cells by pre-incubating cells with NAC (2 hours) (n = 3 ± s.e.m). C & D, Histograms demonstrating inhibition of ATP evoked ROS generation (C) but not EtBr influx (D) in J774.2 cells by pre-incubating cells with DPI (1.5 hours) (n = 3 ± s.e.m). E & F, Histograms demonstrating that ATP evoked ROS generation in BMDMø is inhibited by NAC (E) and DPI (F) (n = 3 ± s.e.m). Student's two-tailed t-test **:$p<0.01$, ***:$p<0.001$.

6.2.2 Evidence for the Role of NADPH Oxidase in ATP Evoked ROS Generation

DPI is used as a general inhibitor of O_2^- production and is sometimes referred to as a specific inhibitor of NADPH oxidase. However DPI actually inhibits this enzyme by inactivating it at its flavin site during electron-transfer, therefore it is actually a general inhibitor of flavoprotein oxidoreductases. This means it is able to inhibit several important flavoprotein-containing systems including xanthine oxidase, NOS, mitochondrial electron transport, cytochrome P450 reductase and other oxidoreducatases (Li *et al.*, 1998; O'Donnell *et al.*, 1994; Stuehr *et al.*, 1991). In order to elucidate the generator of ATP evoked ROS I employed the use of several more selective inhibitors of different flavoprotein oxidoreductases.

The xanthine oxidase inhibitor (Scott *et al.*, 1966), allopurinol (100 μM, 30 min) failed to significantly attenuate ATP evoked increases in cellular oxidation in J774.2 cells (Figure 6-6A, $n = 3$, $p>0.05$). The NOS inhibitor; L-NAME (1 mM, 1 hour) was also observed to not significantly reduce ATP evoked ROS generation in J774.2 cells (Figure 6-6B, $n = 3$, $p>0.05$). However it was observed to significantly reduce nitrate levels in both untreated and ATP stimulated J774.2 cell lysates as measured using the Saville-Griess method (Figure 6-6C, $n = 3$, $p<0.01$).

Pre-treating J774.2 cells with the mitochondrial complex I inhibitor rotenone (5 μM, 30 min) or complex III inhibitor myxathiazole (1 μM, 5 min) had no significant effect on ATP induced increases in cellular oxidation (Figure 6-7A & C, $n = 3$, $p>0.05$). In contrast rotenone (5 μM, 30 min) significantly attenuated ROS generation in the BMDMø (Figure 6-7B, $n = 3$, $p<0.01$).

Pre-incubating and stimulating J774.2 cells in the presence of the NADPH Oxidase inhibitor; apocynin (100 μM) was observed to significantly reduce ATP evoked ROS generation (Figure 6-8A, $n = 3$, $p<0.05$). This occurred without effect on EtBr influx (Figure 6-8B, $n = 3$, $p>0.05$). Furthermore employing the use of gp91phox$^{-/-}$ ($n = 5$) and p47phox$^{-/-}$ ($n = 3$) BMDMø demonstrated that knocking-out NADPH oxidase inhibited ATP evoked ROS generation back to control levels (Figure 6-8C & E) without effect on EtBr influx (Figure 6-8D & F) or H_2DCF loading (Figure A-4).

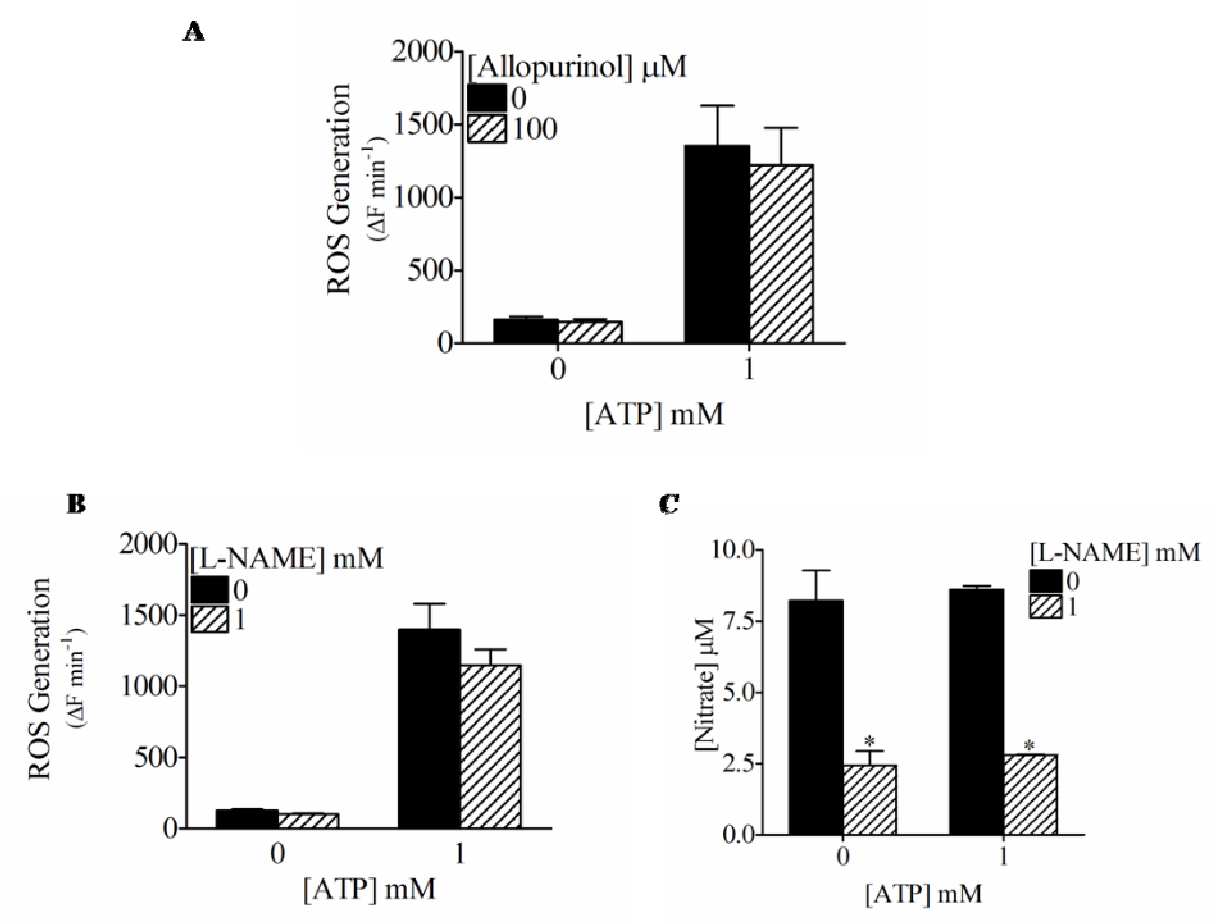

Figure 6-6. ATP Evoked ROS Generation is not mediated by Xanthine Oxidase or NO Synthase. A, Histogram demonstrating that the xanthine oxidase inhibitor; allopurinol (100 μM, 30 min) does not inhibit ATP evoked ROS generation in J774.2 cells (n = 3 ± s.e.m). B, Histogram demonstrating that the NOS inhibitor; L-NAME (1 mM, 1 hour) does not inhibit ATP evoked ROS generation in J774.2 cells (n = 3 ± s.e.m). C, Histogram demonstrating that L-NAME (1 mM, 1 hour) significantly decreases the amount of nitrate in J774.2 cell lysates cells (n = 3 ± s.e.m). Student's two-tailed t-test *:$p<0.05$.

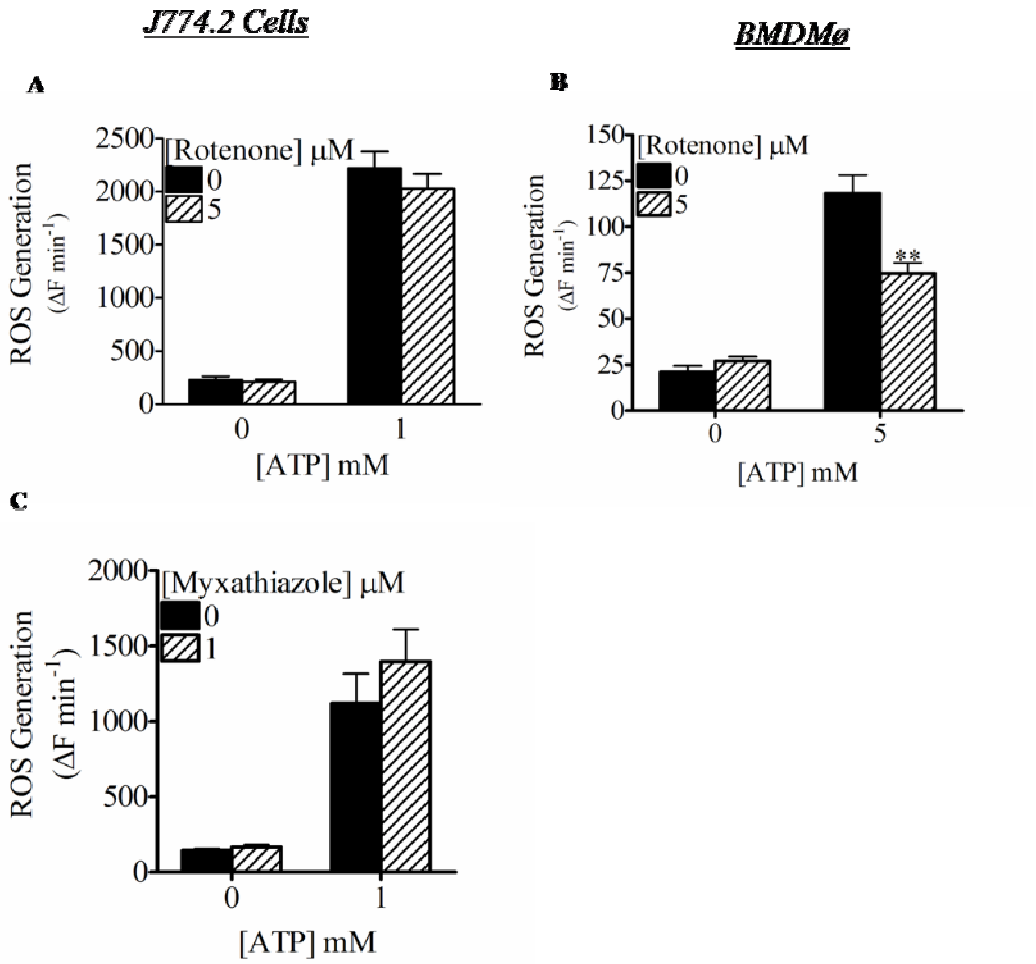

Figure 6-7. Effect of Mitochondrial ETC Inhibitors on ATP Evoked ROS Generation. A, Histogram demonstrating that the complex I inhibitor; rotenone (5 μM, 30 min) does not inhibit ATP evoked ROS generation in J774.2 cells (n = 3 ± s.e.m). B, Histogram demonstrating that the complex I inhibitor; rotenone (5 μM, 30 min) significantly reduces ATP evoked increases in ROS generation in BMDMø (n = 3 ± s.e.m). C, Histogram demonstrating that the complex III inhibitor; myxathiazole (1 μM, 5 min) does not inhibit ATP evoked ROS generation in J774.2 cells (n = 3 ± s.e.m). Student's two-tailed t-test **: $p<0.01$.

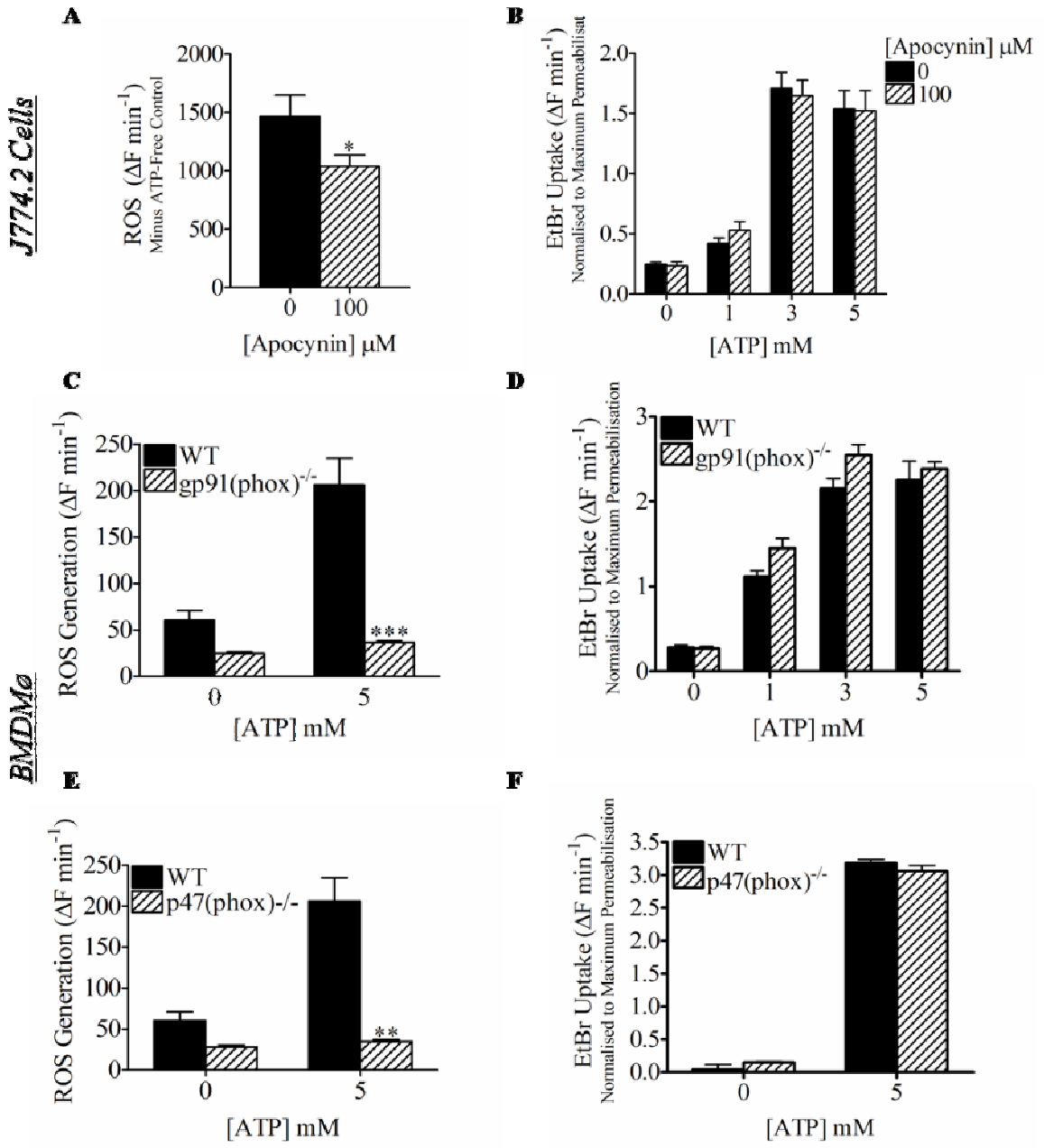

Figure 6-8. Evidence for ATP Evoked Activation of NADPH Oxidase in Generating ROS. A & B, Histograms demonstrating that the NADPH oxidase inhibitor; apocynin (100 μM, 30 min) significantly reduces ATP evoked ROS generation (A) without inhibiting EtBr influx (B) into J774.2 cells (n = 3 ± s.e.m). C & D, Histograms demonstrating that ATP does not evoke ROS generation (C) in BMDMø from gp91phox$^{-/-}$ mice above control, however EtBr influx (D) is still observed (n = 5 ± s.e.m). E & F, Histograms demonstrating that ATP does not evoke ROS generation (E) in BMDMø from p47phox$^{-/-}$ mice above control, however EtBr influx (F) is still observed (n = 3 ± s.e.m). Student's two-tailed t-test *: $p<0.05$, **: $p<0.01$, ***: $p<0.001$.

6.2.3 Spatial Localisation of ATP Induced Superoxide Generation

Activation of NADPH oxidase will result in the transfer of electrons from NADPH across a membrane and coupling these to molecular oxygen to produce O_2^-. This can be produced outside or inside (within phagosomes etc) the cell. To investigate whether ATP stimulation of murine macrophages results in the generation of O_2^-, I investigated the effect of removing O_2^-.

SOD catalyses the dismutation of O_2^- into oxygen and hydrogen peroxide. Although H_2DCF does not sensitively detect O_2^- it will detect $ONOO^-$, H_2O_2 and OH^-. If O_2^- is removed from the system by SOD levels of $ONOO^-$ would be expected to decrease and levels of H_2O_2 and OH^- to increase.

The addition of extracellular SOD (100 U ml^{-1}) to J774.2 cells did not alter ATP evoked cellular oxidation (Figure 6-9A, n = 3). However pre-incubation with a membrane permeant SOD mimetic (Mn-cpx 3, 30 μM, 30 min) was observed to significantly increase ATP evoked ROS generation (Figure 6-9C, n = 3, $p<0.05$). By contrast, addition of extracellular SOD (100 U ml^{-1}) to BMDMø inhibited ATP mediated ROS formation (Figure 6-9B, n = 3, $p<0.05$).

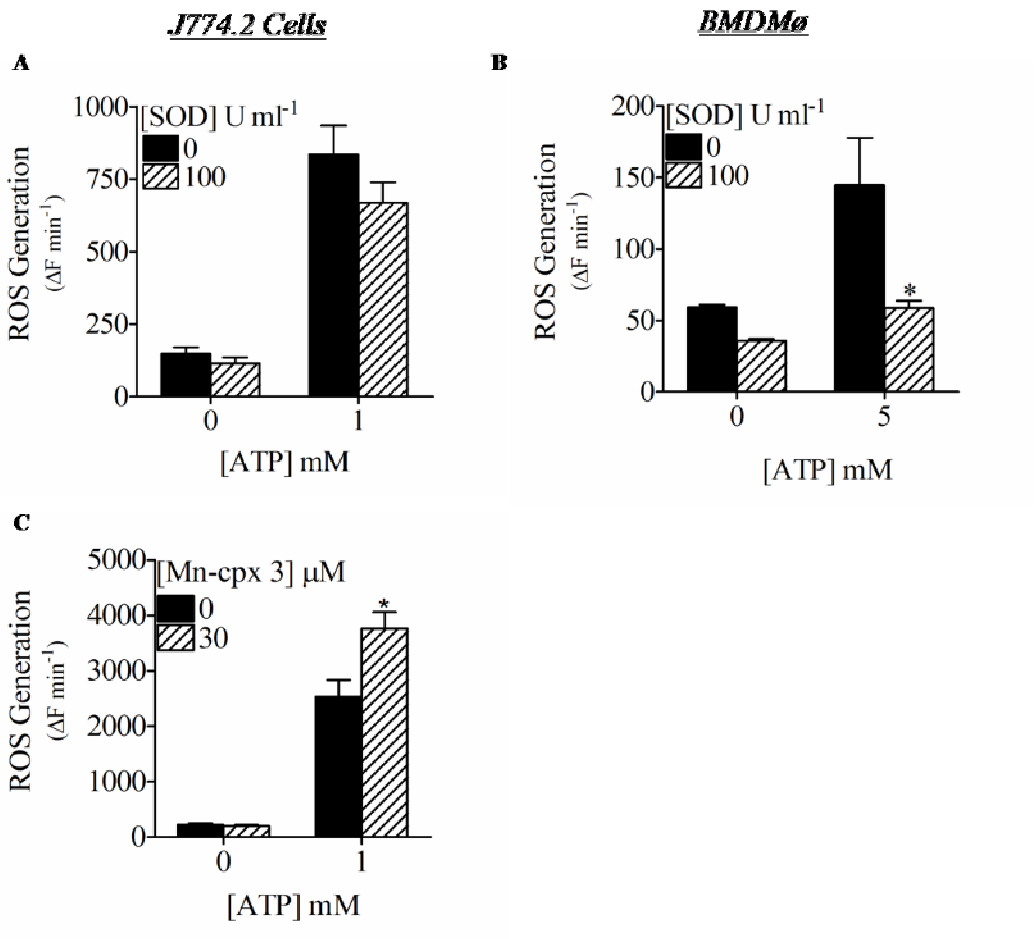

Figure 6-9. Spatial Localisation of ATP Induced ROS Generation in Murine Macrophages. A, Histogram demonstrating that extracellular SOD (100 U ml^{-1}) does not effect ATP induced ROS generation in J774.2 cells (n = 3 ± s.e.m). B, Histogram demonstrating that extracellular SOD (100 U ml^{-1}) significantly decreases BMDMø cellular oxidation induced by ATP (n = 3 ± s.e.m). C, Histogram demonstrating that a cell permeant SOD mimetic (Mn-cpx 3) significantly increases ATP evoked ROS generation in J774.2 cells (n = 3 ± s.e.m). Student's two-tailed t-test *: $p<0.05$.

6.2.4 Role of Reactive Oxygen Species in ATP Evoked Cell Death

As demonstrated in previous chapters prolonged activation of the $P2X_7R$ can cause the release of LDH indicative of a breakdown in the plasma membrane and therefore cell death. ROS have been well documented to be involved in the induction of apoptotic cell death (Simon *et al.*, 2000). ROS are able to directly or indirectly via ceramide production induce the release of cytochrome-c from mitochondria. Cytochrome-c is able to go on to form part of the apoptosome which causes the activation of caspase-9 which can then go on to activate effector caspases such as caspase-3 and 7 which are responsible for destroying the cell from within.

Therefore we investigated whether ATP evoked LDH release could be inhibited by ROS inhibitors. 1 mM ATP was observed to evoke significant release of LDH from J774.2 cells (Figure 6-10A) after a 30 and 60 min stimulation ($n = 3$, $p<0.01$). Using a range of ATP concentrations, determined that 1 mM ATP caused peak LDH release with a decline in release being observed with 3 and 5 mM (Figure 6-10B, $n = 3$). Pre-incubating J774.2 cells with DPI (100 μM, 1.5 hours) was observed to significantly reduce ATP (1 mM) evoked LDH release at a range of stimulation times (15, 30 and 60 min) (Figure 6-10C, $n = 3$). However pre-incubating J774.2 cells with apocynin (100 μM, 5 min) did not effect ATP induced cell death (Figure 6-10D, $n = 3$, $p<0.05$).

ATP (5 mM, 60 min) was also observed to evoke cell death in BMDMø (Figure 6-11A), in contrast with the results observed with the J774.2 cells DPI (100 μM, 1.5 hours) failed to reduce release of LDH (Figure 6-11B). Furthermore ATP was able to evoke release of LDH from gp91phox$^{-/-}$ BMDMø at similar levels to wild-type BMDMø (Figure 6-11C, $n = 3$). Rotenone also failed to inhibit ATP induced cell death in BMDMø (Figure 6-11D, $n = 3$).

Caspases have been documented to play an important role in cell death; such as caspase-3 and 7 in apoptosis and caspase-1 in pyroptosis. Due to the role of the $P2X_7R$ in the activation of caspase-1, I decided to investigate whether the caspase-1 inhibitor Z-YVAD-FMK could modulate ATP induced cell death in murine macrophages. I observed that ATP evoked cell death in J774.2 cells (Figure 6-12A) and BMDMø (Figure 6-12B) was significantly reduced by pre-incubating cells with Z-YVAD-FMK (10 μM, 30 min) ($n = 3$).

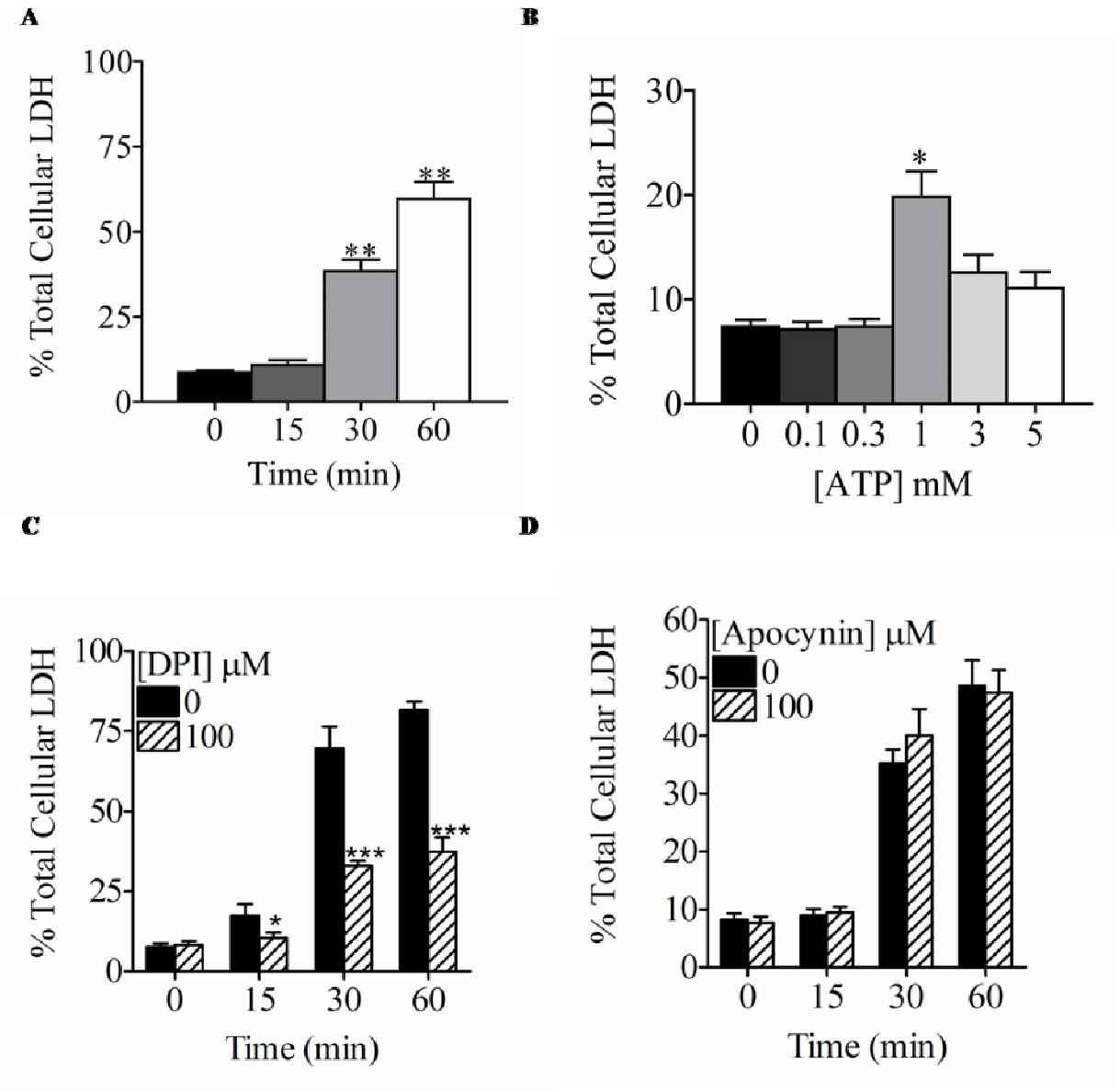

Figure 6-10. Role of ROS in ATP Induced Cell Death in J774.2 Cells. A, Histogram demonstrating that 1 mM ATP evokes LDH release from J774.2 cells after a 30 – 60 min stimulation (n = 3 ± s.e.m). B, Histogram demonstrating that only 1 mM ATP evoked a significant release of LDH from J774.2 cells (n = 3 ± s.e.m). C, Histogram demonstrating that DPI significantly inhibited LDH release from J774.2 cells stimulated with 1 mM ATP for 15, 30 and 60 min (n = 3 ± s.e.m). D, Histogram demonstrating that apocynin did not significantly effect LDH release from J774.2 cells stimulated with 1 mM ATP for 15, 30 and 60 min (n = 3 ± s.e.m). Student's two-tailed t-test *: p<0.05, **:p<0.001, ***:p<0.001.

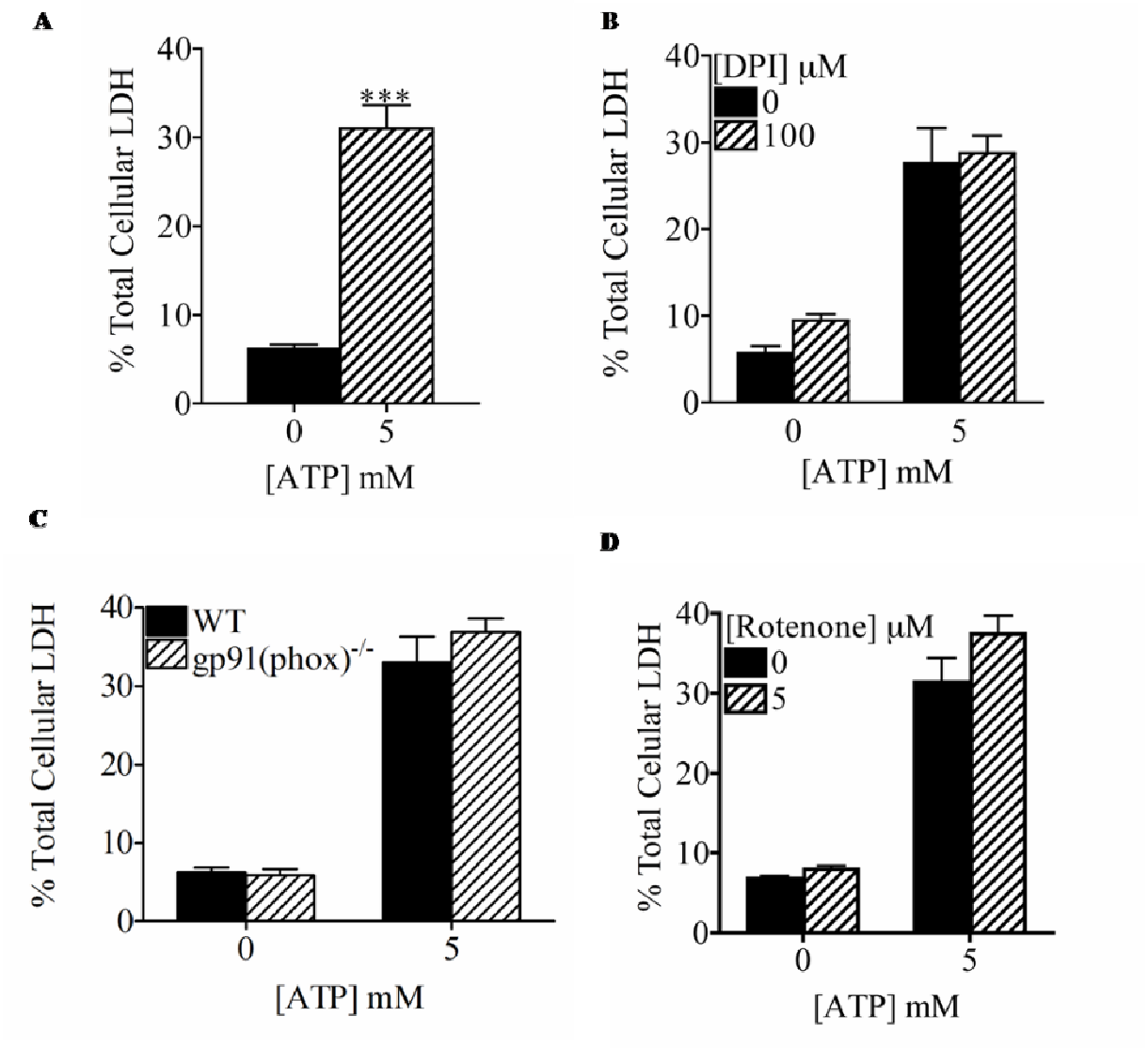

Figure 6-11. ROS appear to not be involved in ATP Induced Cell Death in BMDMø. A, Histogram demonstrating that 5 mM ATP evokes LDH release from BMDMø after a 60 min stimulation (n = 3 ± s.e.m). B, Histogram demonstrating that DPI failed to significantly inhibit LDH release from BMDMø stimulated with 5 mM ATP for 60 min (n = 3 ± s.e.m). C, Histogram demonstrating that ATP evoked LDH release from gp91phox$^{-/-}$ BMDMø did not significantly differ from WT BMDMø (n = 3 ± s.e.m). D, Histogram demonstrating that rotenone did not significantly effect LDH release from BMDMø stimulated with 5 mM ATP for 60 min (n = 3 ± s.e.m). Student's two-tailed t-test, ***: $p<0.001$.

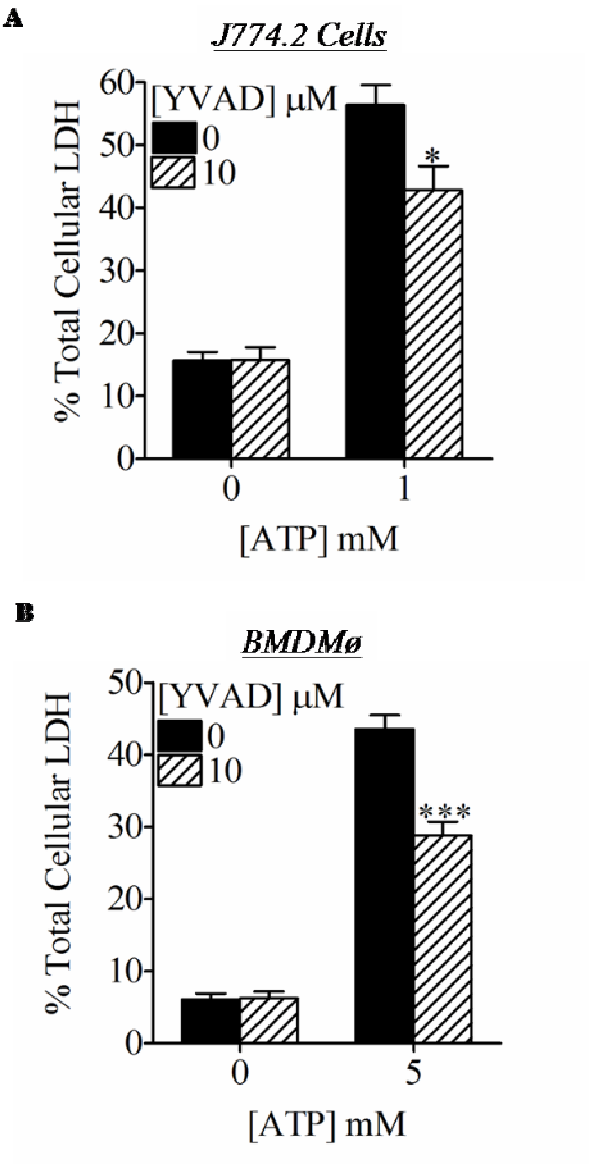

Figure 6-12. Role of Caspase-1 in ATP Induced Cell Death in Murine Macrophages. A, Histogram demonstrating that Z-YVAD-FMK significantly inhibited LDH release from J774.2 cells stimulated with 1 mM ATP for 60 min (n = 3 ± s.e.m). B, Histogram demonstrating that YVAD significantly inhibited LDH release from BMDMø stimulated with 5 mM ATP for 60 min (n = 3 ± s.e.m). Student's two-tailed t-test, *: $p<0.05$ ***: $p<0.001$.

6.3 DISCUSSION

In this study I determined that extracellular ATP is able to evoke ROS generation in murine macrophages via activation of NADPH oxidase. I also determined that the mechanism, location and effect of these ROS are dependent on the cell type used.

6.3.1 P2 Receptor Activation of NADPH Oxidase

An application of ATP to J774.2 cells, BMDMø and peritoneal cells (Figure A-5) was observed to evoke an increase in DCF fluorescence indicative of ROS generation. In order to determine that the signal produced was due to cellular oxidation I pre-incubated cells with either the antioxidant NAC or the flavoprotein oxidoreductase inhibitor DPI which was observed to decrease ATP evoked ROS in all three cell types. Many of the producers of ROS are flavoprotein oxidoreductases therefore in order to determine the generator of ATP evoked oxidative stress I firstly identified a likely candidate using a panel of pharmacological inhibitors and secondly used BMDMø from mice lacking the functional generator. Using this method I identified that the major source of ATP evoked ROS is NADPH oxidase (NOX2). This correlated with our labs previous finding that ATP could induce (i) an increase in the association of the p47phox and p67phox subunits and (ii) an increase in the translocation of the p67phox subunit to the cell membranes in a human monocytic cell line (Hewinson *et al.*, 2008).

The activity of NADPH oxidase activity can be regulated by Ca^{2+} fluxes, p38 MAPK, PKC and PI3 kinase. All of which have been observed to be activated by $P2X_7$ receptors (Bradford *et al.*, 2002; Jacques-Silva *et al.*, 2004; Moore *et al.*, 2007; Pfeiffer *et al.*, 2004). I observed that although a pre-treatment of J774.2 cells with the human $P2X_7R$ antagonist KN-62 significantly inhibited ROS generation, KN-04 did not. KN-62 can act as calcium/calmodulin dependent kinase II inhibitor whereas KN-04 which is a structural analogue of KN-62 lacks this inhibitory activity whilst retaining its $P2X_7R$ antagonist activity (Tokumitsu *et al.,* 1990). Therefore this suggested that the inhibitory effect observed with KN-62 was potentially due to its action as a calcium/calmodulin dependent kinase II inhibitor rather than as a $P2X_7R$ antagonist. Further work employing the use of other calcium/calmodulin dependent kinase II inhibitors would be required in order to address this issue. These results however do not completely rule out a role for the $P2X_7R$ in ATP evoked ROS generation as EtBr influx into J774.2 cells was poorly antagonised by both KN-04 and KN-62.

KN-62 has been observed to be able to block mP2X$_7$R activation (Hibell *et al.*, 2001; Moore *et al.*, 2007) although not as potently as the human orthologues. Furthermore in the preceding chapters I have demonstrated that ATP evoked responses in RAW264.7 cell which are typical of P2X$_7$R activation are robustly blocked by KN-62. Potentially calcium/calmodulin dependent kinase II activation could play a role in 'P2X$_7$R' evoked responses.

Much of the past work implicating extracellular ATP activation of cellular oxidation via the P2X$_7$R primarily has relied on the use of non-specific inhibitors or BzATP which although sometimes used as a specific P2X$_7$R agonist it is able to activate other P2X receptors. Recent work has improved the evidence for the P2X$_7$R being involved in ROS generation, for example a study by Pfeiffer *et al.,* 2007 determined that the pharmacological profile of ROS generation was comparable with P2X$_7$R activation and use of a macrophage cell line deficient in a functional P2X$_7$R failed to evoke cellular oxidation in response to BzATP. Furthermore work in our own lab demonstrated that use of specific human P2X$_7$R antagonists could inhibit cellular oxidation in THP-1 cells and human monocytes (Hewinson *et al.*, 2008). However these antagonists only partially inhibited the response and a study by Ferrari *et al.,* 2000 also demonstrated only partial block with KN-62 and furthermore observed that the P2Y$_2$ receptor agonist UTP also triggered robust ROS formation. In a preliminary experiment I observed inhibition of ROS generation in J774.2 cells by the potent non-selective adenosine receptor antagonist CGS 15943 (n = 1, Figure A-7). This was surprising as adenosine has been observed to be a potent inhibitor of ROS production by NADPH oxidase in *f*MLF-stimulated neutrophils. The mechanism is suggested to involve activation of the A$_3$R leading to endocytosis and/or redistribution of the p22phox/gp91phox heterodimer between subcellular compartments (Swain *et al.*, 2003; van der Hoeven *et al.*, 2008). Further investigation is required to elucidate which purinergic receptors are involved in activating NADPH oxidase. Therefore I suggest that cellular oxidation evoked by ATP is mediated by multiple purinergic receptors and that further work employing the use of specific purinergic receptor agonists and antagonists is required and potentially receptor knock-down/knock-out studies in order to ascertain specifically which receptors are involved in ATP evoked activation of NADPH oxidase.

The signaling pathway from P2 receptor activation to NADPH oxidase has not been widely examined. In the case of P2X receptors mobilisation of extracellular calcium could initiate

the activation of NOX2; chelation of extracellular Ca^{2+} has been reported to block ROS generation by P2X agonists (Ferrari *et al.*, 2000; Murphy *et al.*, 1993). Our lab has evidence that PI3K and $iPLA_2$ could have a potential role in mediating P2 receptor activation of NADPH oxidase. ATP induced ROS generation in 'primed' THP-1 monocytes was observed to be partially inhibited by the PI3K inhibitors LY294002 and wortmannin and the calcium-independent phospholipase A_2 inhibitor bromoenol lactone (J Hewinson 2006 8th International Symposium on Adenine and Adenosine Nucleotides, Ferrara, Italy) (J Hewinson 2007 LifeSciences 2007, Glasgow, UK). A review by Guerra *et al*., 2007 proposed a four step model of P2 activation of NADPH Oxidase (Figure 6-13).

1. P2X induced increase in $[Ca^{2+}]_i$ could activate certain PKC isoforms that are essential for the activation/phosphorylation of NADPH oxidase subunits.
2. $P2X_7R$ activation of p38 MAPK could facilitate activation of NADPH oxidase.
3. P2Y receptors could activate PLC leading to generation of IP3 and DAG which would lead to increases in $[Ca^{2+}]_i$ and therefore lead to PKC activation.
4. P2Y receptors such as $P2Y_2$ could activate the small G-protein Rac which would be predicted to facilitate activation, phosphorylation and assembly of NADPH oxidase.

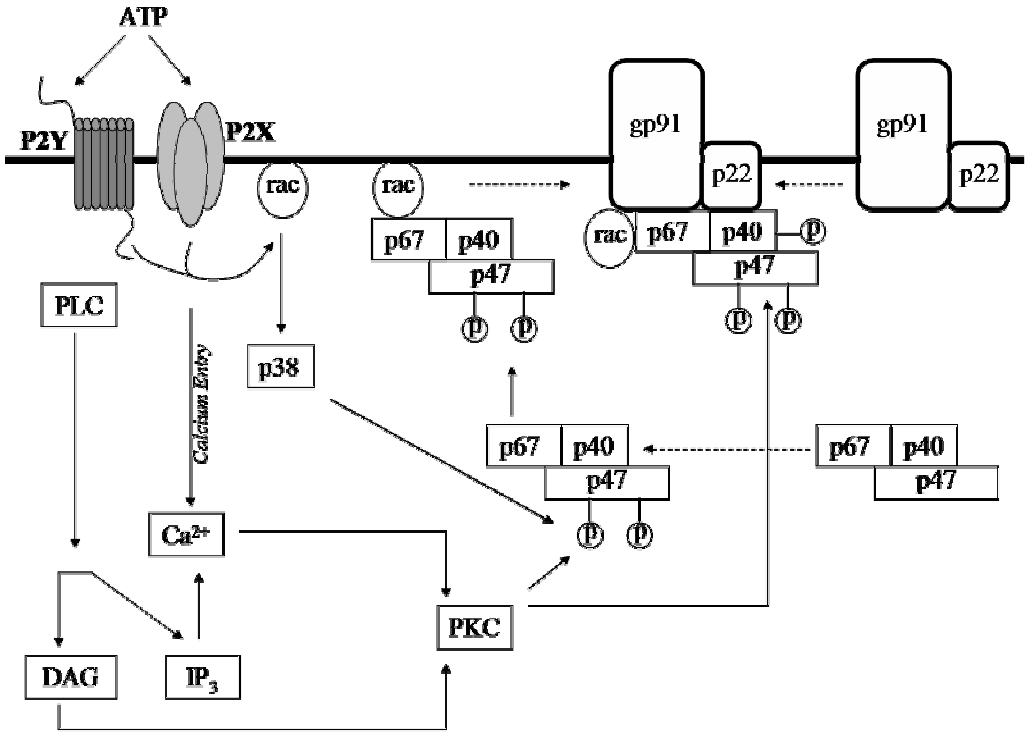

Figure 6-13. Schematic of how P2Rs could Couple to Activation of NADPH Oxidase. Adapted from (Guerra *et al.*, 2007)

Murine macrophages have been proposed to express A_2B and A_3 receptors (Xaus *et al.*, 1999); potentially these adenosine receptors could couple in to the some of the signaling pathways suggested to induce NADPH oxidase activation such as activation of PLC, PKC and p38 MAPK (Feoktistov *et al.*, 1997; Feoktistov *et al.*, 1999; Jacobson *et al.*, 2006; Schulte *et al.*, 2003)

6.3.2 Cell Background Differences in ATP Evoked ROS Generation

The term macrophage encompasses many different cell types with a monocytic origin that acquire functional properties dependent on the environment they are in. The effects of oxidants on redox signaling are largely cell and stimulus specific (Forman *et al.*, 2001). Therefore differences in the redox properties of different macrophages should be expected, for example alveolar macrophages are observed to have high basal NADPH oxidase activity (Tephly *et al.*, 2007) in comparison to peritoneal macrophages.

In this study I observed that inhibition of mitochondrial electron transport failed to inhibit ATP evoked ROS generation in the J774.2 cells; a macrophage cell line originally derived from the ascites (peritoneal cavity fluid) and solid tumour of a BALB/c mouse and native peritoneal cells from C57BL/6 mice (Figure A-5). Whereas the complex I inhibitor rotenone partially blocked ATP evoked ROS generation in macrophages generated from the bone marrow of C57BL/6 mice (BMDMø). Spatial localisation of ROS generation also seemed to differ between cell types, in the BMDMø extracellular SOD reduced ATP cellular oxidation suggesting generation of ROS by NADPH oxidase was occurring at least in part at the plasma membrane. Whereas extracellular SOD had no effect on ATP evoked ROS generation in J774.2 or peritoneal cells (Figure A-5). However use of a cell permeable SOD mimetic (Mn-cpx 3) potentiated ATP induced cellular oxidation in J774.2 and peritoneal cells, suggesting O_2^- could be being generated within membrane bound compartments in the cell. The nature of ROS means they are diffusible, short-lived molecules and therefore localising ROS production to a specific subcellular compartment would be of importance for activating redox signaling events. Clearly, these results demonstrate that results from one macrophage type may not be simply extrapolated to different types/source of macrophages.

6.3.3 Modulation of Cell Death by Cellular Oxidation & Caspase-1

I determined that pre-treatment of J774.2 cells but not BMDMø or native peritoneal cells with DPI could inhibit ATP evoked LDH release. This suggests that in some cell types ATP induced cellular oxidation can activate cell death signaling pathways. ATP induced oxidative stress could be potentially activating cell death pathway via c-Jun N-terminal kinase (JNK) and/or p38 mitogen-activated protein kinase. Both of these kinases have been observed to be activated downstream of $P2X_7R$ activation (Humphreys *et al.*, 2000; Pfeiffer *et al.*, 2007) and furthermore play important roles in induction of apoptosis (Shacka *et al.*, 2006). A study by Noguchi *et al.,* 2008 using the RAW264.7 cells determined that ATP induced apoptosis was lost in $ASK1^{-/-}$ (apoptosis signal-regulating kinase 1) spleen-derived macrophages. ASK-1 is upstream of JNK and p38 kinases and is activated by various stresses including ROS (Takeda *et al.*, 2008). Noguchi *et al.,* put forward a model (Figure 6-14) suggesting that ATP induced ROS via NADPH oxidase would activate ASK1 and in turn p38 MAPK leading to the induction of apoptosis via a caspase-3 dependent pathway.

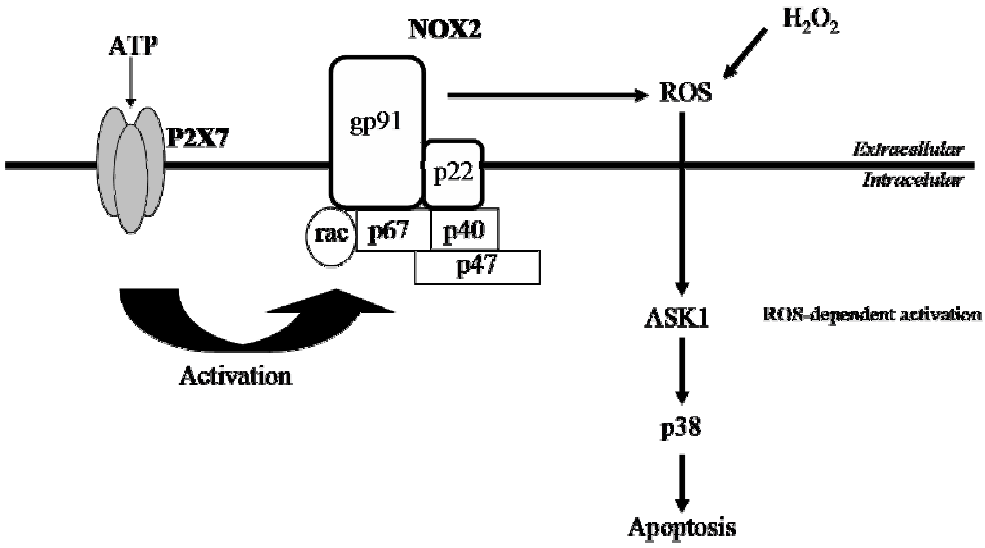

Figure 6-14. Schematic of how $P2X_7R$ activation could cause ROS dependent apoptosis. Adapted from (Noguchi *et al.*, 2008)

$P2X_7R$ stimulation is a known activator of caspase-1 (Kahlenberg *et al.*, 2004b). Caspase-1 as already stated is a mediator of a form of cell death known as pyroptosis (Fink *et al.*, 2005). Furthermore $P2X_7R$ induced cell death in LPS primed macrophages has been observed to be reduced although not eliminated in macrophages derived from caspase-1 KO mice (Le Feuvre *et al.*, 2002). In agreement to this study I observed that ATP evoked

LDH release in LPS primed J774.2 cells or BMDMø (not peritoneal cells) was partially reduced by pre-treating cells with the caspase-1 inhibitor Z-YVAD-FMK. In J774.2 cells I see regulation of cell death by both ROS and caspase-1 therefore I could hypothesise three potential models:

1. ROS activation of p38 MAPK could lead to the activation of caspase-1. An increase in caspase-1 activity induced by dextran sulphate sodium was found to be significantly inhibited by a p38 MAPK inhibitor and the antioxidant NAC (Kwon *et al.*, 2007).
2. Caspase-1 activity could be regulated by the redox status of the cell directly.
3. Caspase-1 activity and ROS generation are two separate events.

6.3.4 Concluding Remarks

Here I demonstrated that extracellular ATP can activate NADPH Oxidase leading to an increase in the generation of ROS. Considering the growing body of evidence that suggests O_2^- and H_2O_2 could potentially act as 'second messengers' I hypothesise that ATP evoked ROS generation could potentially activate, propagate and/or amplify some of the functional responses associated with the activation of purinergic receptors. Here I briefly examined the role of ATP evoked ROS in mediating $P2X_7R$ induced cell death, in the following chapter I take these studies further and examine the role of ROS in other '$P2X_7R$' functional responses.

CHAPTER 7

REDOX REGULATION OF CASPASE-1

7.1 INTRODUCTION

In the previous chapter it was demonstrated that extracellular ATP can evoke an increase in the generation of ROS. It was hypothesized at the end of the chapter that the activity of the IL-1β activating enzyme; caspase-1 could be regulated by the redox status of the cell. The $P2X_7R$ on LPS primed macrophages, microglia and dendritic cells has been previously demonstrated to activate caspase-1 and ultimately induce the processing and secretion of IL-1β (Ferrari *et al.*, 1997b; Ferrari *et al.*, 1997c; MacKenzie *et al.*, 2001; Pizzirani *et al.*, 2007; Solle *et al.*, 2001). The secretion of active/mature IL-1β is an important part of the innate immune response with low level release promoting the resolution of infections and induction of wound healing. However aberrant release can induce skin rashes, inflammatory arthritis and systemic fever. Determining the mechanism of regulation of IL-1β maturation and secretion is therefore of great interest. However the mechanism of how $P2X_7R$ activation couples to caspase-1 activation has remained controversial. I therefore proposed to investigated whether ATP evoked ROS generation is the missing link between the $P2X_7R$ and the activation of caspase-1.

7.1.1 $P2X_7R$ Mediated Processing and Secretion of IL-1β

Activation of TLR4 by LPS will induce the synthesis of the inactive 31 kDa precursor of IL-1β (Pro- IL-1β) via the via the transcription factor NF-κB downstream of the MyD88 adapter. A second signal is then required to initiate the processing and secretion of IL-1β, which is thought to be activation of the $P2X_7R$ by ATP. This is based on the observation that $P2X_7R^{-/-}$ macrophages fail to process and secrete IL-1β in response to ATP, and injection of ATP in to mice deficient in this receptor failed to evoke an increase in levels of IL-1β in peritoneal lavage (Solle *et al.*, 2001). This second signal is required for the activation caspase-1 which is able to cleave pro-IL-1β between D116 and A117 releasing the COOH-terminal mature IL-1β and an NH_2-terminal IL-1β pro-peptide. The mature form of IL-1β is then rapidly released from the cell via a non-classical secretory mechanism. The precise mechanism of release is controversial with five different pathways being proposed:

1. Microvesicle Shedding (Bianco *et al.*, 2005; MacKenzie *et al.*, 2001)
2. Exocytosis of secretory lysosomes (Andrei *et al.*, 1999; Carta *et al.*, 2006)
3. Direct membrane efflux (Brough *et al.*, 2007)
4. Exocytosis via multivesicular bodies (Qu *et al.*, 2007)
5. Cell lysis

7.1.2 Activation of Caspase-1 by the NALP3 Inflammasome

Caspase-1 is a cysteine protease that is able to cleave proteins after an aspartic acid residue. It plays an essential role in hose defence and the execution of the innate immune response, which is highlighted by the observation that caspase-1 deficient mice exhibit increase susceptibility to bacterial infection (Li *et al.*, 1995). It is synthesized as an inactive 45-kDa zymogen; pro-caspase-1 that undergoes autocatalytic processing (Figure 7-1). The active form of the enzyme comprises a p20 and p10 subunit which assembles with another set of p20 and p10 subunits forming a heterotetramer.

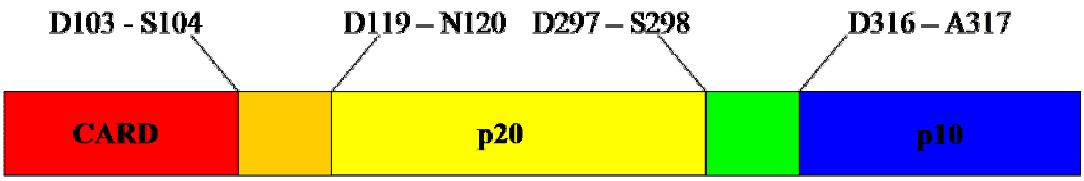

Figure 7-1. Diagram of Caspase-1 showing Domain Organization & Cleavage Sites.

Activation of caspase-1 occurs within a cytosolic multiple adaptor complex termed the inflammasome. An inflammasome consists of a NOD-like receptor protein (NLR) which will associate with an adaptor protein apoptosis-associated speck-like protein (ASC) which in turn will recruit pro-inflammatory-caspase precursors (Figure 7-2). Various microbial and endogenous stimuli activate different types of inflammasome, in the case of the LPS / ATP it is the NALP3 (NLR3, Cryopyrin, CIAS1) containing inflammasome.

Mutations in NALP3 had previously been observed to cause three autoinflammatory disorders; Muckle-Wells syndrome (MWS), familial cold urticaria (FCU) and chronic infantile neurological cutaneous and articular syndrome (CINCA) (Neven *et al.*, 2004). All involve recurrent inflammatory episodes generally associated with fever, arthralgia and urticaria. A clinical study in 2004 observed that both clinical and serological evidence of active MWS was resolved rapidly and completely during treatment with the IL-1R

antagonist anakinra (Hawkins *et al.*, 2004). Later in 2006 three articles were published in Nature demonstrating that knocking out NALP3 inhibited caspase-1 activation and IL-1β secretion in response to uric acid crystals (Martinon *et al.*, 2006), bacterial RNA (Kanneganti *et al.*, 2006) and LPS/ATP (Mariathasan *et al.*, 2006).

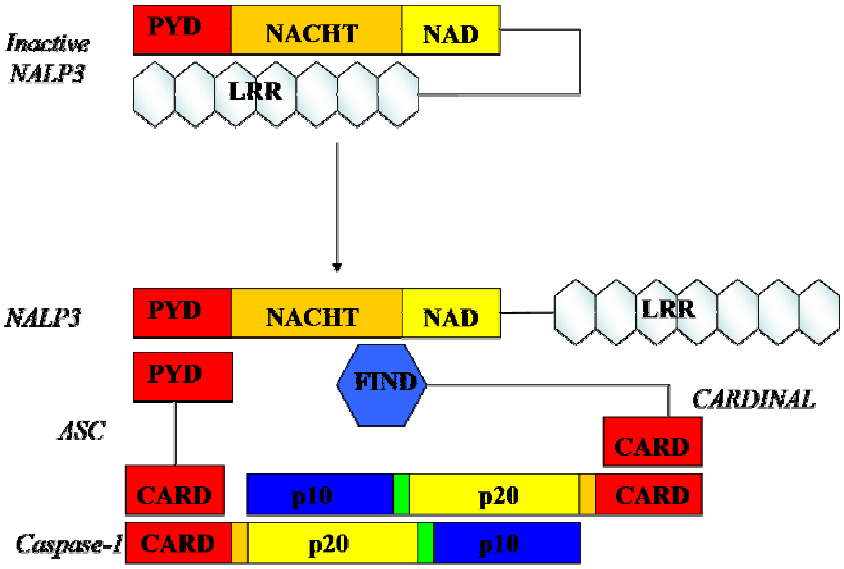

Figure 7-2. Schematic of Caspase-1 Activation by the NALP3 Containing Inflammasome. A conformational change in NALP3 allows the binding of adaptor proteins such as ASC and CARDINAL which can recruit caspase-1. It is proposed that the proximity of the caspase-1 molecules allows autocatalytic processing resulting in the activation of caspase-1.

How the components of the inflammasome sense the various activators is not known there are two basic models (i) a direct ligand receptor interaction or (ii) each ligand induces a common cellular signal. Evidence for a direct ligand receptor interaction can be found in a study by Kanneganti *et al.,* 2007 who suggested that pathogens who can secrete pore forming proteins can gain entry to the cell where they are sensed by NALP3; whereas those bacteria that do not secrete pore-forming proteins could gain access to the cell via the ATP/$P2X_7R$ pore (pannexin-1). The suggested common cellular signal is proposed to be some form of change in the intracellular ionic milieu or generation of a metabolite (Pétrilli *et al.*, 2007a). One of these changes is proposed to be a reduction in $[K^+]_i$ based on the following evidence:

- IL-1β processing and secretion is inhibited in cells bathed in a high $[K^+]$ solution (Dostert *et al.*, 2008; Kahlenberg *et al.*, 2004b).

- The efflux of K^+ would result in the activation of $iPLA_2$, whose inhibition has been observed to prevent the processing of IL-1β (Andrei *et al.*, 2004; Walev *et al.*, 2000).
- Other agents that lower intracellular [K^+] such as the K^+ ionophores nigericin and maitotoxin can induce robust IL-1β processing (Perregaux *et al.*, 1992; Perregaux *et al.*, 1994).
- ASC oligomerization and recruitment of caspase-1 by NALP3 is inhibited by K^+ (Pétrilli *et al.*, 2007b).

7.1.3 Reactive Oxygen Species and Caspase-1 Activation

There is increasing evidence that ROS in addition to other potential activators (Yu *et al.*, 2008) could also play a role in the maturation of caspase-1, either directly or via activation of different components of the inflammasome (Cruz *et al.*, 2007; Dostert *et al.*, 2008; Hewinson *et al.*, 2008; Pétrilli *et al.*, 2007b). A study by Sekiyama *et al.,* observed in stressed mice that SOD reduced caspase-1 activity and SOD and DPI reduced the accumulation of IL-18 in the plasma (Sekiyama *et al.*, 2005). Work from our lab demonstrated that LPS/ATP induced processing of IL-1β in THP-1 monocytes and human blood-derived monocytes was significantly reduced when cells were pre-incubated with either DPI or the $ONOO^-$ decomposition catalyst FeTPPS (Hewinson *et al.*, 2008).

As yet a mechanism of how ROS could activate caspase-1 and where activation takes place has yet to be fully characterized. As mentioned in the previous chapter ROS could activate the p38 MAPK which could ultimately activate caspase-1. However there is another mechanism that could potentially activate caspase-1 and this is by modification of the protein itself. It has been recently accepted that ROS can act as second messenger molecules; however it is unlikely that they are recognized specifically by a protein and therefore modulation would not be mediated by their reversible binding to proteins (Rhee *et al.*, 2003).

As already stated caspases are cysteine protease and therefore modification of the active site cysteine could regulate caspase activity. Similar to phosphorylation of serine, tyrosine, histidine, aspartate and threonine residues, the modification of cysteine residues is established as a mechanism for controlling protein activity. Cysteine residues are able to

sense redox signals because the thiol side-chain (-SH) can be oxidized to several different redox states, many of which are reversible (Green *et al.*, 2004) (Figure 7-3).

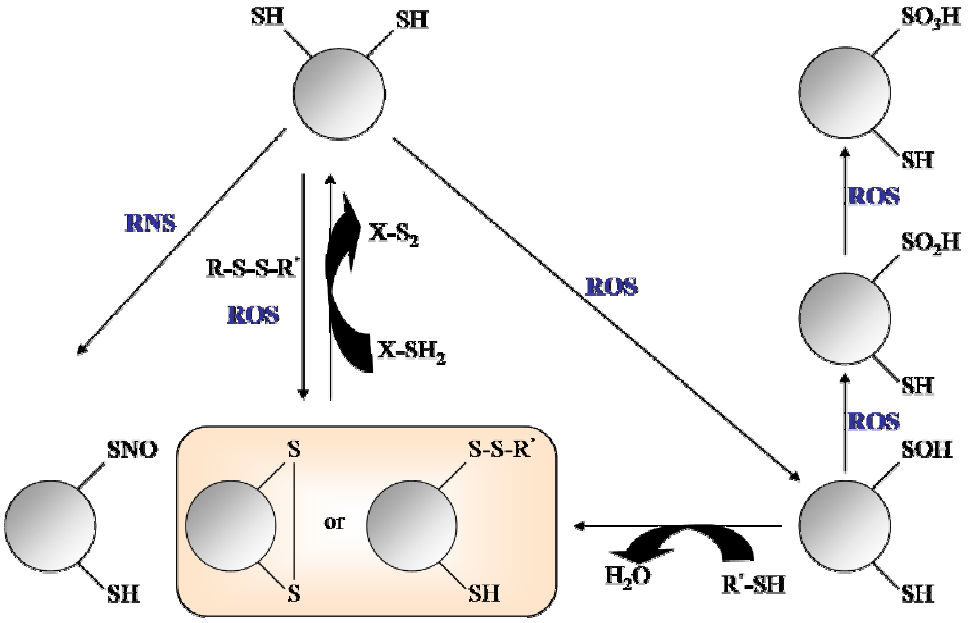

Figure 7-3. Schematic of the Different Redox States of Cysteine. R-S-S-R = disulphide, R-SOH = sulphenic acid, R-SNO = *S*-nitrosothiol, R-SO_2H = sulphinic acid, R-SO_3H = sulphonic acid, X-SH_2 = cellular reductant. Adapted from (Green *et al.*, 2004).

The cysteine thiol group can react with RNS (NO, $ONOO^-$) in the presence of an electron acceptor to form an *S*-NO bond (Figure 7-4). *S*-nitrosylated proteins can existed in physiological conditions with the concentration of *S*-NOs varying from nM - μM levels in mammalian tissues. Thiol *S*-nitrosylation and NO transfer reactions are thought to be involved in a range of cell signaling events including the regulation of ion channels and G-protein coupled reactions to receptor stimulation and activation of nuclear regulatory proteins. *S*-nitrosylation of –SH groups can increase or decrease protein activity (Gaston *et al.*, 2003). *S*-nitrosylated proteins can be readily reduced by glutathione (GSH) or thioredoxin (Trx); therefore proteins which are endogenously *S*-nitrosylated are protected by compartmentalization into lipophillic protein folds, vesicles and interstitial spaces with release into the cytosol initiating denitrosylation. Both caspase-3 and 9 within the mitochondria but not the cytosol has been reported to *S*-nitrosylated (Mannick *et al.*, 2001). The *S*-nitrosylation of the active site thiol (-SH) of caspase-3 has been observed to keep caspase-3 in an inactive state, with denitrosylation initiated by the Fas apoptotic pathway allowing the enzyme to function (Mannick *et al.*, 1999). It has therefore been hypothesized

that *S*-nitrosylation could be a general mechanism by which caspase activity is controlled, preventing inappropriate caspase autoactivation.

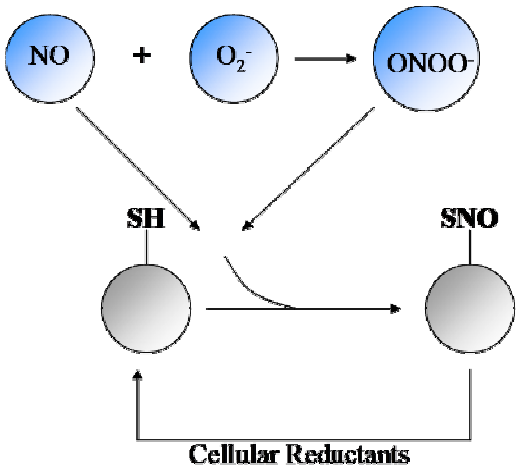

Figure 7-4. Schematic of *S*-Nitrosylation of a Cysteine containing Protein. The cysteine thiol group (-SH) can undergo *S*- Nitrosylation by a direct reaction with either nitric oxide (NO) or peroxynitrite ($ONOO^-$). *S*-Nitrosylated proteins can be enzymatically denitrosylated by cellular reductants such as GSH and Trx.

Thiol groups (-SH) can also undergo oxidation. The intracellular environment of a cell is generally reducing and therefore the cysteine generally exists in its reduced form. Few proteins would be expected to possess a cysteine residue vulnerable to oxidation by H_2O_2 (Kim *et al.*, 2000) due to Cys-SH being less readily oxidized by H_2O_2 than the cysteine thiolate anion ($Cys\text{-}S^-$) and the pK_a of most cysteines being approximately 8.5. However certain cysteine residues have low pK_a values and exist as thiolate anions at neutral pH because nearby positively charged amino acid residues are available for interaction with the negatively charged thiolate. Proteins with low-pK_a cysteine residues could therefore be targets of specific oxidation by H_2O_2, which could be reversed by thiol donors such as GSH, glutaredoxin (GRX) and Trx (Rhee *et al.*, 2003). Meissner *et al.*, reported that caspase-1 could be oxidized at S362 and S397 which allowed glutathionylation of these residues (Figure 7-5) (Meissner *et al.*, 2008). In this study ROS via oxidation and *S*-glutathionylation was observed to decrease caspase-1 activity. A recent study by Huang *et al.,* 2008 demonstrated that caspase-3 activity was also inhibited by *S*-glutathionylation, which may suggest the balance of cellular oxidation could differentially regulate caspase activity (Huang *et al.*, 2008). This idea is supported by the observation that low concentrations of H_2O_2 (50 μM) but not high concentrations (200 – 500 μM) was effective

at inducing caspase activation and apoptosis in Jurkat T-lymphocytes (Hampton *et al.*, 1997).

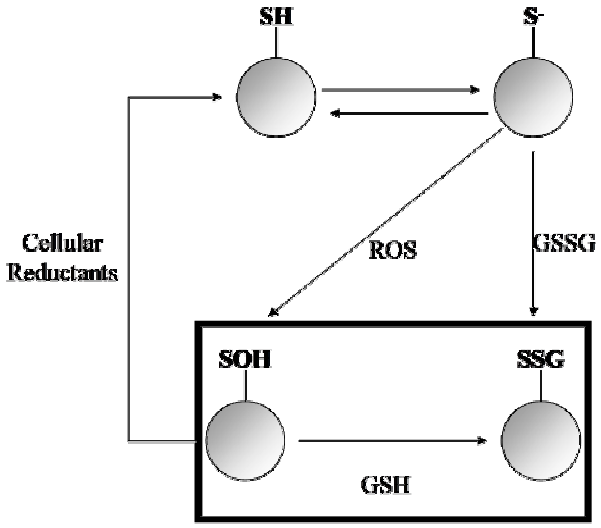

Figure 7-5. Schematic of Glutathionylation of a Cysteine Containing Protein. The cysteine thiolate anion ($-S^-$) can undergo *S*-glutathionylation by a direct reaction with oxidized glutathione (GSSG) or can be oxidized itself (-SOH) and then react with the reduced form of glutathione (GSH). Both reactions can be reversed by cellular reductants such as GRX and Trx.

In this study I determined whether ATP evoked ROS generation in murine macrophages played a role in activating caspase-1, resulting in the processing of pro-IL-1β to the active mature form. I have investigated the potential cell signaling pathways coupling $P2X_7Rs$ to caspase-1 activation and the importance of ROS directly activating caspase-1 through protein modification or by activating signaling cascades upstream of inflammasome/caspase-1 activation.

The key findings of this study were:

1. The flavoprotein oxidoreductase inhibitor DPI inhibited LPS/ATP evoked activation of IL-1β.
2. BMDMø deficient in gp91 and p47 phox processed IL-1β at similar levels to WT.
3. The mitochondrial complex I inhibitor rotenone partially inhibited LPS/ATP evoked IL-1β activation but not cell death.
4. Trx reductase (TrxR) inhibitors inhibited LPS/ATP evoked IL-1β activation and cell death.

7.2 RESULTS

7.2.1 ATP Induces *the Processing and Secretion of IL-1β from Murine Macrophages*

Using western blot analysis J774.2 cells primed for 6 hours with LPS (1 μg ml^{-1}) were found to contain the pro forms of IL-1β (Figure 7-6A, Figure 7-6B) and caspase-1 (Figure 7-6C) (n = 3). Stimulating J774.2 cells for 30 minutes with ATP at concentrations ≥ 800 μM was observed to evoke processing of pro IL-1β into the mature 17kD active form (Figure 7-6A). In agreement with other reports mature IL-1β was mainly found to be present in the secreted protein fraction and rarely found within the cell, therefore suggesting that once IL-1β is fully matured it is rapidly released from the cell. Stimulating J774.2 cells for ≥ 15 minutes with 1 mM ATP was observed to induce processing and secretion of IL-1β (Figure 7-6B) and the appearance of the p10 subunit of caspase-1 indicative of caspase-1 activation (Figure 7-6C).

Similar findings where observed using LPS primed BMDMø. 5 mM ATP (30 minutes) was observed to evoke robust processing and secretion of IL-1β (Figure 7-7A). 5 mM ATP (30 minutes) was also observed to increase levels of the p10 subunit of caspase-1 in the cell lysate (Figure 7-7B). This was accompanied by secretion of both the pro and p10 forms of caspase-1.

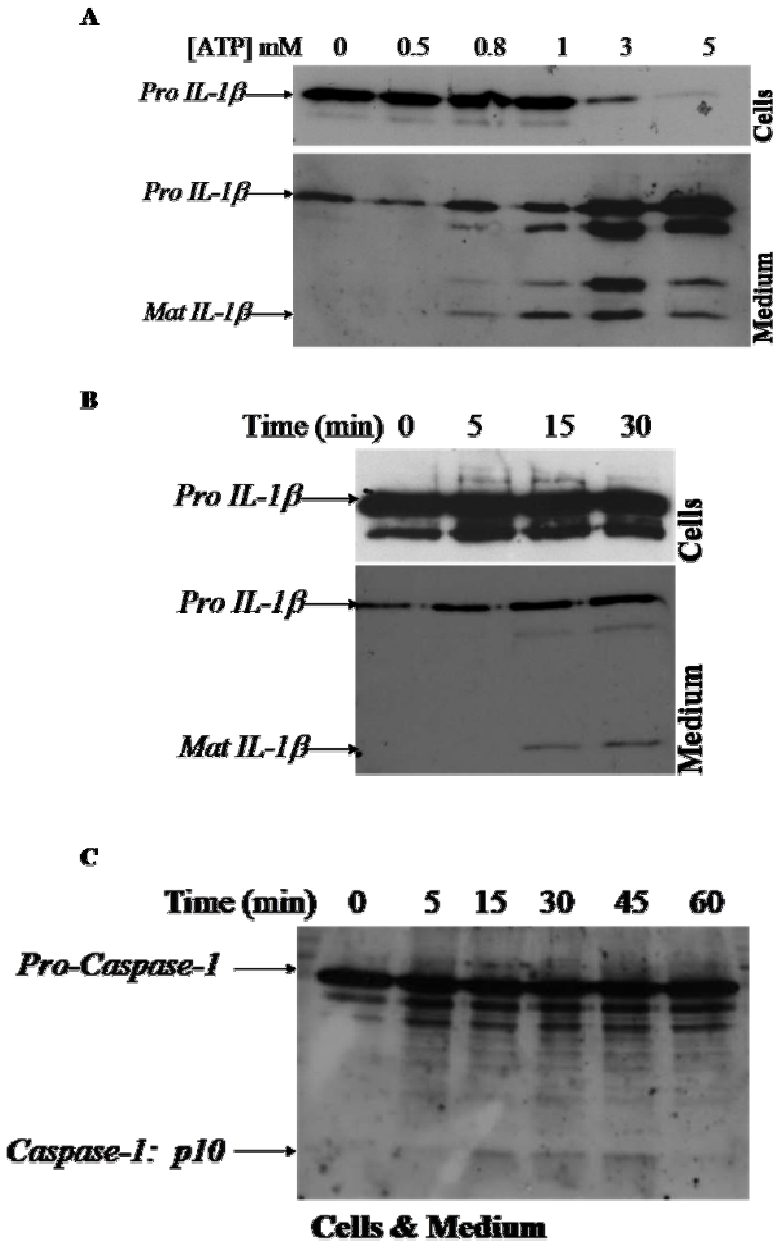

Figure 7-6. ATP Evokes the Activation of IL-1β and Caspase-1 in LPS Primed J774.2 Cells. A, Stimulating cells with ATP (30 minutes, 37 ^{o}C) induced concentration-dependent processing and secretion of IL-1β. B, A stimulation of ≥ 15 minutes with 1 mM ATP was required to evoke processing and secretion of IL-1β. C, A stimulation of ≥ 15 minutes with 1 mM ATP was required to induce the activation of caspase-1 which was determined by the appearance of the p10 subunit. All blots are representative of at least 3 experiments.

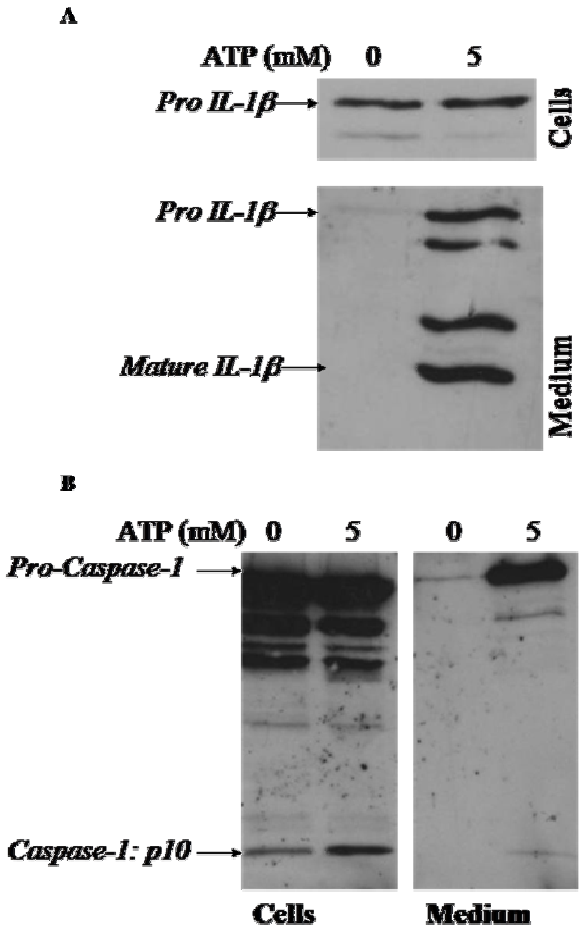

Figure 7-7. ATP Evokes the Activation of IL-1β & Caspase-1 in LPS Primed BMDMø. A, Stimulating cells with 5 mM ATP (30 minutes, 37 ^{o}C) induced the processing and secretion of IL-1β. B, Stimulating cells with 5 mM ATP (30 minutes, 37 ^{o}C) induced the activation and secretion of caspase-1 which was determined by the appearance of the p10 subunit. All blots are representative of at least 3 experiments.

7.2.2 A Flavoprotein Oxidoreductase Inhibitor Blocks IL-1β and Caspase Activation.

Pre-treatment of J774.2 cells with the flavoprotein oxidoreductase inhibitor; DPI (100 μM, 1.5 hours) was found to inhibit both secretion of the pro form of IL-1β and the processing of IL-1β (Figure 7-8A) (*n* = 3). In contrast pre-treating J774.2 cells with the caspase-1 inhibitor; Z-YVAD-FMK (10 μM, 30 minutes) did not inhibit secretion of the pro form of IL-1β (Figure 7-8A) (*n* = 3). However a reduction in the mature form of IL-1β in the secreted protein fraction was observed when cells were pre-treated with Z-YAVD-FMK. Similar findings were observed using the BMDMø (Figure 7-8C) (*n* = 3). Western blot analysis also revealed that DPI (100 μM, 1.5 hours) reduced the level of the p10 subunit of caspase-1 in both J774.2 cell and BMDMø samples, indicative of an inhibition of caspase-1 activation (Figure 7-8B & D).

7.2.3 Inhibition of NADPH Oxidase Activity Failed to Inhibit Processing of IL-1β

Based on findings from the previous chapter I hypothesised that the inhibition of IL-1β processing by DPI was due to its action on NADPH Oxidase. However pre-treatment of J774.2 cells with the NADPH oxidase inhibitor; apocynin (100 μM, 5 minutes) failed to inhibit both processing and secretion of IL-1β (Figure 7-9A) (*n* = 3). Furthermore BMDMø lacking in NADPH oxidase activity either due to loss of the gp91phox (Figure 7-9B) (*n* = 5) or p47phox subunit (Figure 7-9C) (*n* = 4) were observed to secrete similar levels of pro and mature IL-1β compared to WT. Chronic pre-treatment of J774.2 cells with apocynin (100 μM, 6 hours) did result in a reduction in the processing of IL-1β; however the effect was variable and was sometimes accompanied by a reduction in pro-IL-1β levels in the cell lysates (data not shown). This therefore suggested that chronic apocynin was potentially interfering with the priming of the J774.2 cells with LPS. This could potentially be due to other effects of apocynin such as its ability to inhibit Rho kinase activity (Schlüter *et al.,* 2008) or other antioxidant effects not involving NADPH oxidase (Heumüller *et al.,* 2008).

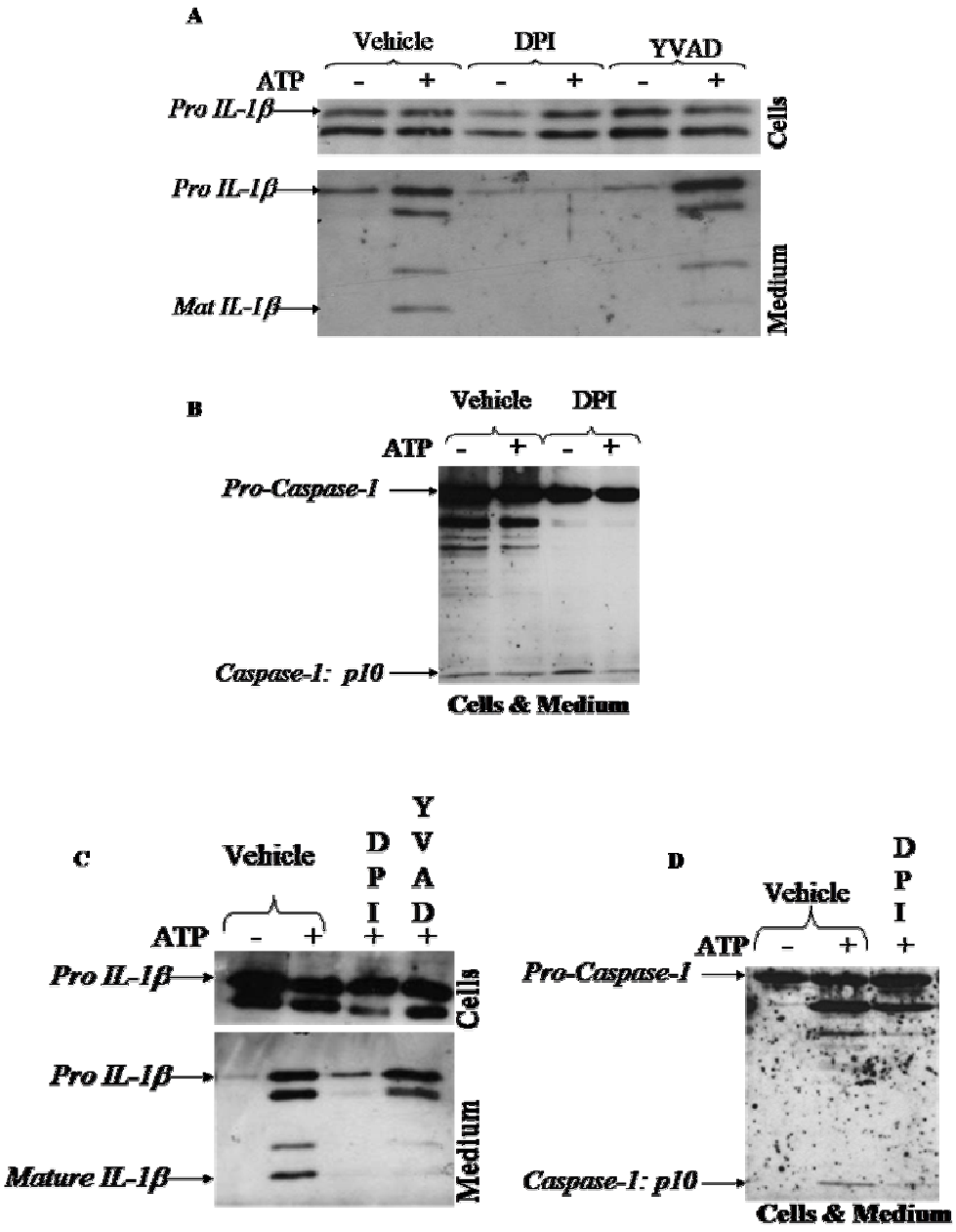

Figure 7-8. Modulation of IL-1β Processing & Secretion of DPI and Z-YVAD-FMK. A, ATP (1 mM, 30 minutes) evoked processing IL-1β was blocked by pre-treating J774.2 cells with DPI (100 μM, 1.5 hours) or Z-YVAD-FMK (10 μM, 30 minutes). DPI was also observed to reduce both basal and ATP evoked secretion of pro IL-1β. B, ATP (1 mM, 15 minutes) evoked increases in the p10 form of caspase-1 in J774.2 cells were blocked by DPI. C, ATP (5 mM, 30 minutes) evoked processing IL-1β was blocked by pre-treating BMDMø with DPI (100 μM, 1.5 hours) or Z-YVAD-FMK (YVAD) (10 μM, 30 minutes). DPI was also observed to inhibit secretion of pro IL-1β. D, ATP (5 mM, 30 minutes) evoked increases in the p10 form of caspase-1 in BMDMø were blocked by DPI. All blots are representative of at least 3 experiments.

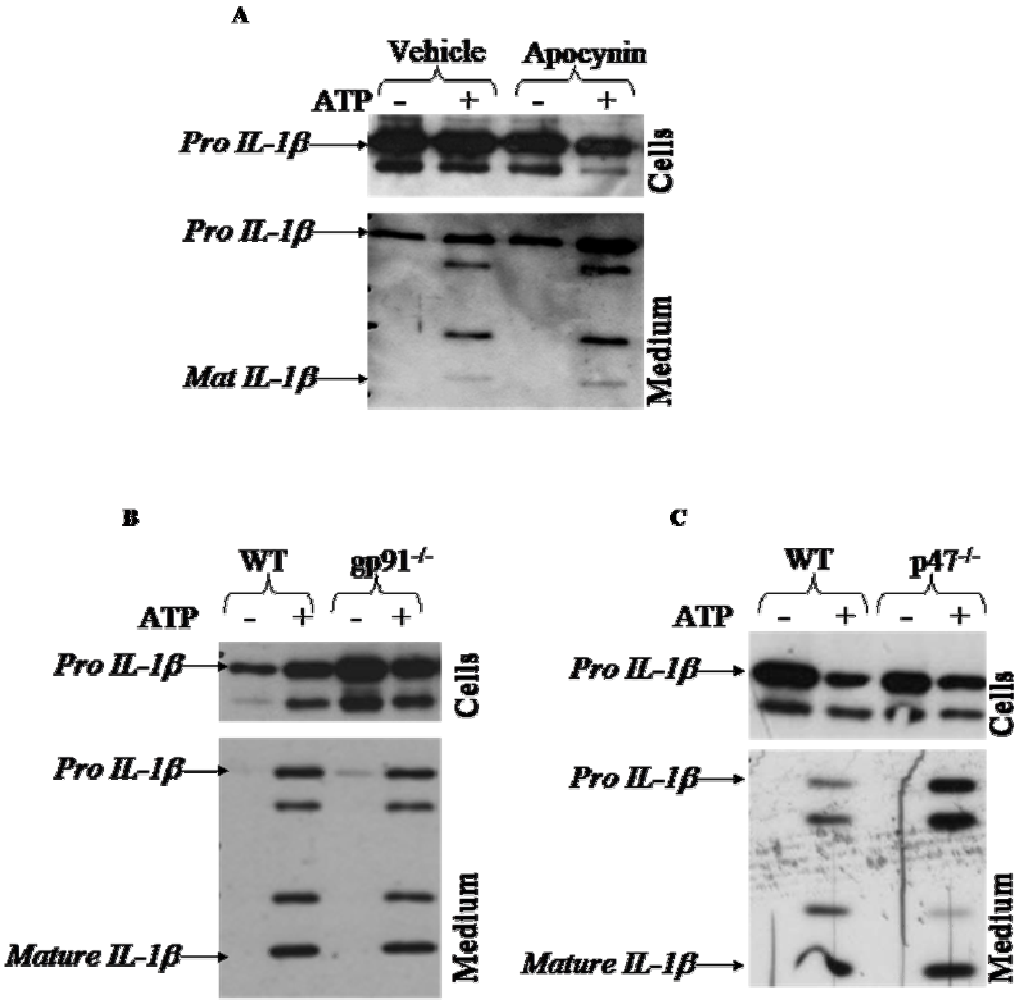

Figure 7-9. NADPH Oxidase Is Not Required for Processing & Secretion of IL-1β. A, ATP (1 mM, 30 minutes) evoked processing IL-1β was not inhibited by pre-treating J774.2 cells with apocynin (100 μM, 30 minutes). B, ATP (5 mM, 30 minutes) evoked processing and secretion of IL-1β in WT and $gp91^{-/-}$ BMDMø. C, ATP (5 mM, 30 minutes) evoked processing and secretion of IL-1β in WT and $p47^{-/-}$ BMDMø. All blots are representative of at least 3 experiments.

7.2.4 Rotenone and Thioredoxin Reductase Inhibitors Block IL-1β Processing

DPI is a general inhibitor of flavoprotein oxidoreductases and can therefore inhibited other enzymes including complex I of the mitochondrial electron transport chain. Pre-treating J774.2 cells or BMDMø with the complex I inhibitor rotenone (5 μM, 30 minutes) was observed to reduce the levels of mature IL-1β in the secreted protein fraction (Figure 7-10A, Figure 7-10B) (n = 3). Therefore suggesting that complex I activity maybe required for the processing but not secretion of IL-1β.

Several studies have reported cysteine *S*-nitrosylation as a post-translational mechanism to regulate caspase-3 and caspase-1 activity (Fiorucci *et al.*, 2000a; Li *et al.*, 1997a; Mannick *et al.*, 1999; Mannick *et al.*, 2001). Casase-1 activity is inhibited by addition of exogenous NO via a pathway hypothesised to involve *S*-nitrosylation of the active site cysteine (Fiorucci *et al.*, 2000b; Kim *et al.*, 1998). A recent study reports that the cellular reductant Trx acted as a denitrosylase for caspase-3 (Benhar *et al.*, 2008). Trx is a protein that can act as an antioxidant by facilitating the reduction of other proteins by cysteine thiol-disulfide exchange. Trx is itself kept in a reduced form by TrxR which is a flavoprotein oxidoreductase and can therefore be inhibited by DPI (Gray *et al.*, 2007). Furthermore rotenone has been reported to preferentially oxidise the mitochondrial form of Trx known as Trx-2 (Trx-1 is localised to the cytosol) (Ramachandiran *et al.*, 2007). Therefore pre-treatment of murine macrophages with either DPI or rotenone could be hypothesised to result in oxidation of Trx-2.

Use of either of the TrxR inhibitors auranofin (5 μM, 5 minutes) or 2,4-dinitrochlorobenzene (DNCB) (30 μM, 30 minutes) resulted in a loss of the processing of IL-1β into its active form in both J774.2 cells (Figure 7-10A) and BMDMø (Figure 7-10C) (n = 3).

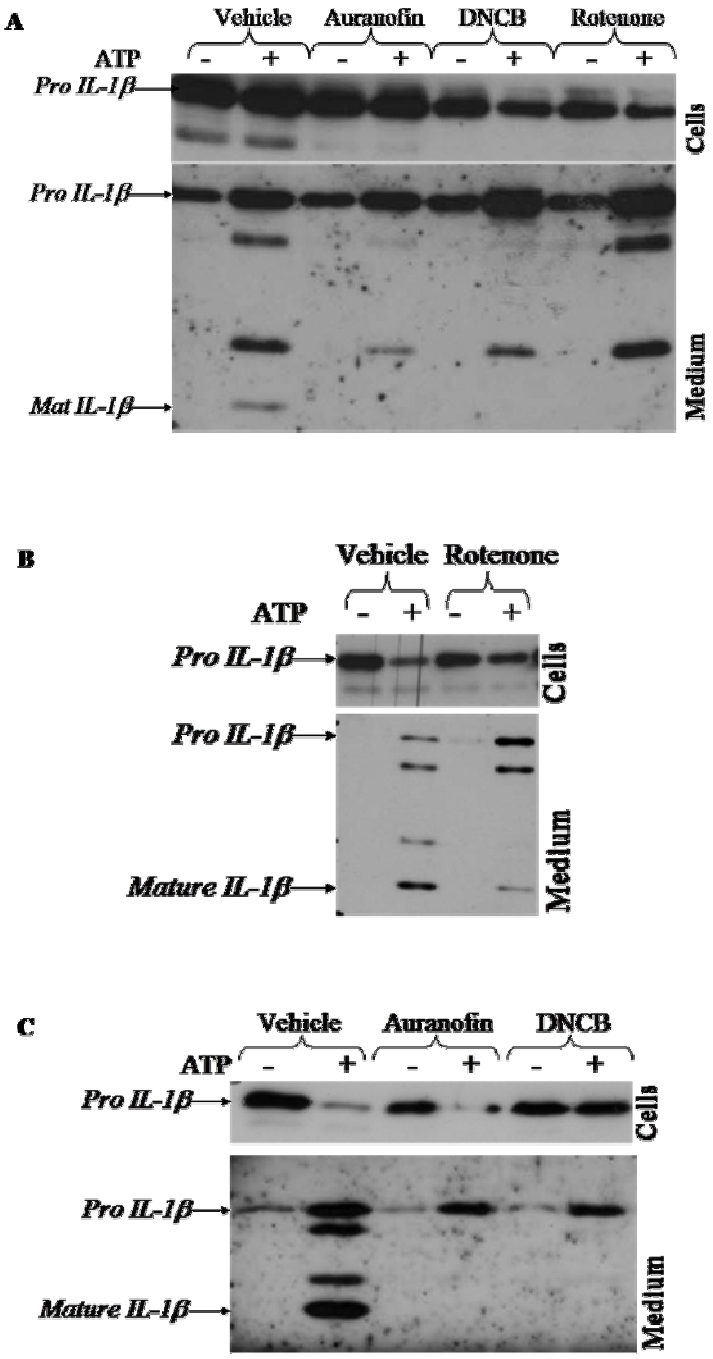

Figure 7-10. Rotenone & TrxR Inhibition Results in a Reduction of IL-1β Activation. A, ATP (1 mM, 30 minutes) evoked processing IL-1β was inhibited by pre-treating J774.2 cells with auranofin (5μM, 5 minutes), DNCB (30 μM, 30 minutes) or rotenone (5 μM, 30 minutes). B, ATP (5 mM, 30 minutes) evoked processing IL-1β was inhibited by pre-treating BMDMø with rotenone (5 μM, 30 minutes). C, ATP (5 mM, 30 minutes) evoked processing IL-1β was inhibited by pre-treating BMDMø with auranofin (5 μM, 5 minutes) or DNCB (30 μM, 30 minutes). All blots are representative of at least 3 experiments.

7.2.5 Thioredoxin Reductase Inhibitors Block ATP Evoked Cell Death

The reduced form of Trx is known to be able to prevent oxidative stress induced apoptosis via mechanisms such as the removal of H_2O_2 (Andoh *et al.*, 2002) or inhibition of ASK1-induced apoptosis (Liu *et al.*, 2002). Therefore inhibitors of TrxR have been observed to induce apoptosis in a range of cell types. In order to determine that the effects of the Trx inhibitors and rotenone on IL-1β processing were not due to an increase in cell death, cytotoxicity studies were performed.

Pre-treatment of J774.2 cells with rotenone (5 μM, 30 minutes) did not significantly increase basal or ATP evoked release of LDH (n = 3, $p>0.05$) (Figure 7-11A). Pre-treatment of J774.2 cells with auranofin (5 μM, 5 minutes) or DNCB (30 μM, 30 minutes) did not significantly increase basal LDH release (n = 3, $p>0.05$) (Figure 7-11B, Figure 7-11D). Interestingly ATP evoked LDH release was significantly inhibited by pre-treating J774.2 cells with either auranofin (5 μM, 5 minutes) or DNCB (30 μM, 30 minutes) (n = 3, $p<0.001$). EtBr influx evoked by ATP was not significantly changed by auranofin or DNCB (n = 3, $p>0.05$) (Figure 7-11C, Figure 7-11E) therefore suggesting that pore formation is not regulated by Trx.

Similar results were observed using BMDMø. Pre-treatment of BMDMø with rotenone failed to inhibit either ATP evoked cell death or EtBr influx (n =3, $p>0.05$) (Figure 7-12A, Figure 7-12B). Pre-treatment of BMDMø with auranofin or DNCB inhibited ATP evoked cell death (Figure 7-12C, Figure 7-12E) (n = 3, $p<0.001$). However ATP evoked EtBr influx in BMDMø was also inhibited by auranofin and DNCB suggesting that in this cell type that (i) EtBr influx/pore opening could be modulated by Trx or (ii) cell lysis could contribute to the EtBr influx signal.

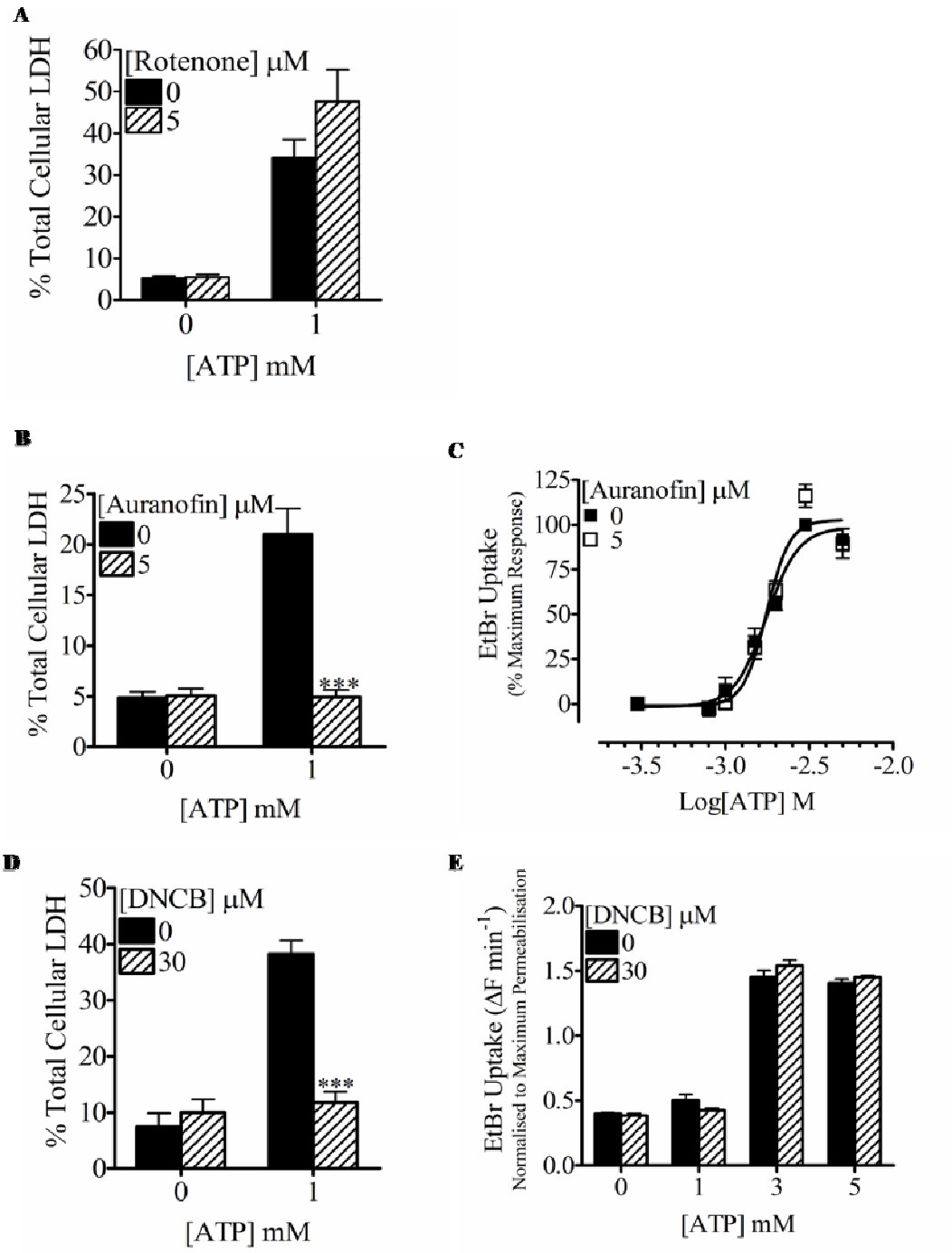

Figure 7-11. TrxR Inhibitors but not Rotenone Inhibit ATP Evoked Cell Death in J774.2 Cells. A, ATP (1 mM, 30 minutes) evoked cell death was not inhibited by pre-treating cells with rotenone (5 µM, 30 minutes). ATP (1 mM, 30 minutes) evoked cell death was inhibited by pre-treating cells with (B) auranofin (5µM, 5 minutes) or (D) DNCB (30 µM, 30 minutes) without effect on EtBr influx (C & D). All bars are n = 3 ± s.e.m. Two-way Student's t-test where ***: $p<0.001$.

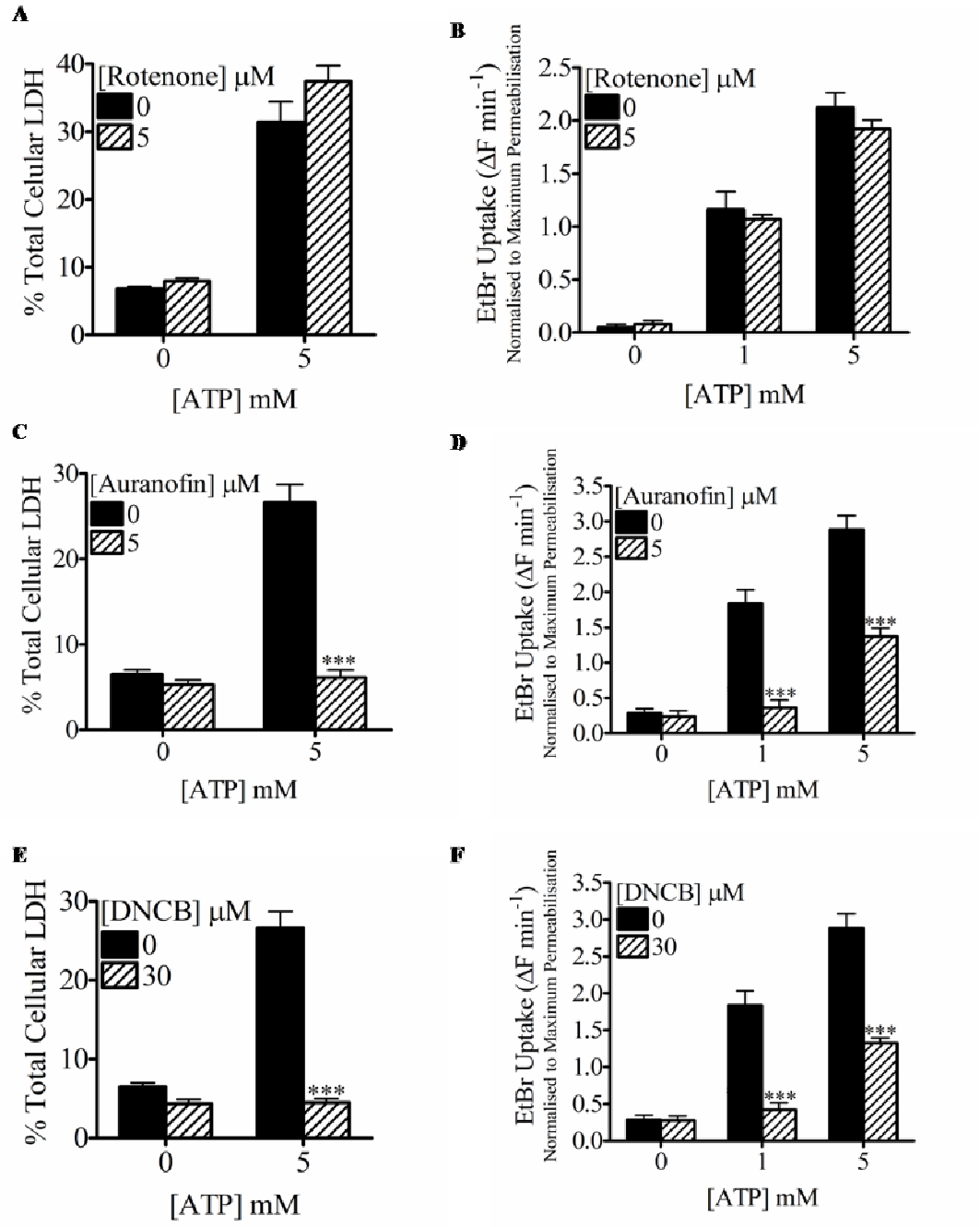

Figure 7-12. TrxR Inhibitors but not Rotenone Inhibit ATP Evoked Cell Death in BMDMø. A & B, ATP (5 mM, 30 minutes) evoked cell death and EtBr influx was not inhibited by pre-treating cells with rotenone (5 µM, 30 minutes). C & D, ATP (5 mM, 30 minutes) evoked cell death and EtBr influx was inhibited by pre-treating cells with auranofin (5µM, 5 minutes). E & F, ATP (5 mM, 30 minutes) evoked cell death and EtBr influx was inhibited by pre-treating cells with DNCB (30 µM, 30 minutes). All bars are $n = 3$ ± s.e.m. Two-way Student's t-test where ***: $p<0.001$.

7.3 DISCUSSION

In this chapter I have observed that (i) ATP evoked processing of IL-1β and secretion is inhibited by a general flavoprotein oxidoreductase inhibitor (DPI), (ii) loss of NADPH oxidase activity does not result in a loss of IL-1β processing or secretion, (iii) agents that can modulate Trx activity (oxidation) result in the loss of IL-1β processing and (iv) the TrxR inhibitors are able to inhibit ATP evoked cell death.

7.3.1 Do Two Distinct Pathways Regulate IL-1β Processing and Secretion?

In agreement with other studies ATP was observed to induce activation of caspase-1 which was accompanied by the processing and rapid secretion of mature/active IL-1β. Pre-treating cells with DPI or Z-YVAD-FMK was observed to inhibit the processing of pro IL-1β to mature IL-1β. This observation agrees with previous work demonstrating that caspase-1 activation and ultimately IL-1β activation via the NALP3 inflammasome was inhibited by DPI (Cruz *et al.*, 2007; Dostert *et al.*, 2008; Hewinson *et al.*, 2008). The inhibition of the formation of mature/active IL-1β by Z-YVAD-FMK was not accompanied by an inhibition of the release of the pro-peptide which correlated with other reports (Laliberte *et al.*, 1999; Mehta *et al.*, 2001). However DPI was observed to inhibit release of the pro-peptide, suggesting that the action of DPI was resulting in (i) inhibition of caspase-1 activation and therefore IL-1β and (ii) inhibition of a distinct pathway/protein involved in the secretory mechanism. Laliberte *et al.,* demonstrated that the caspase-1 inhibitor ZVAD-DCB inhibited both IL-1β maturation and propeptide secretion whereas YVAD-CHO and YVAD-CMK only blocked IL-1β maturation. In their study they also determined that the non-selective thiol reagents *N*-ethylmaleimide (NEM) and phenylarsine oxide (PAO) blocked IL-1β maturation and propeptide release (Laliberte *et al.*, 1999). This led them to suggest that ZVAD-DCB, NEM and PAO in addition to caspase-1 inhibition, could either impair other caspase family members and/or other thiol dependent enzymes whose activity is required for the secretory mechanism. We could therefore hypothesise that the non-caspase-1 cellular polypeptide that is inhibited by ZVAD-DCB is also a target of DPI (Figure 7-13).

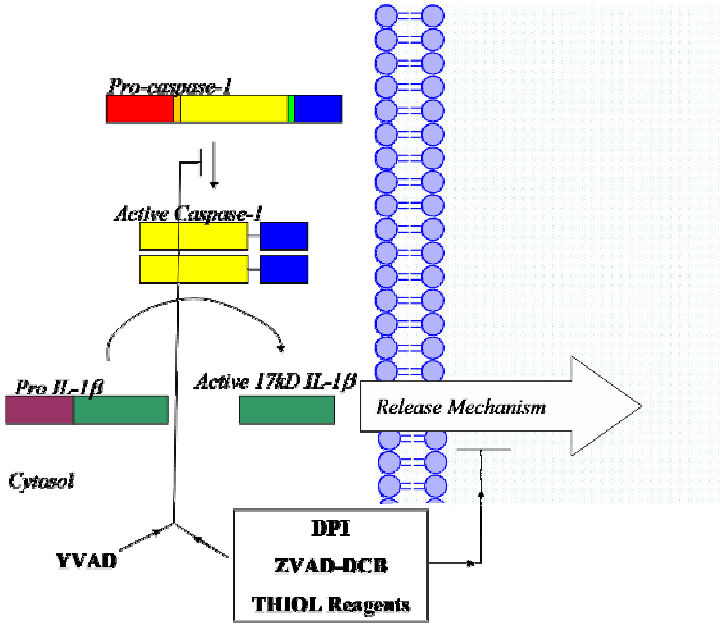

Figure 7-13. Schematic of the Inhibition of the Maturation of IL-1β & the Release of the Pro-Peptide could be Mediated by Two Distinct Thiol Proteases. Caspase-1 is protease mediating the former whereas the latter is unknown.

7.3.2 Identification of DPI Target Involved in IL-1β Processing and/or Secretion

Based on findings from the previous chapter that ATP evoked ROS generation was primarily induced by activation of NADPH oxidase and the finding by Dostert *et al.,* that NALP3 activation by asbestos and silica was inhibited by pre-treating cells with apocynin or knock out of p22phox (a subunit of NADPH oxidase) (Dostert *et al.*, 2008). I hypothesised that the effect/s of DPI on IL-1β was due to its action on NADPH Oxidase. However the use of apocynin on J774.2 cells, or knocking out either the gp91phox or p47phox subunits of NADPH oxidase did not result in significant loss of IL-1β maturation of release of the pro-peptide. Other ROS inhibitors such as the glutathione precursor NAC, $ONOO^-$ decomposer FeTPPS, xanthine oxidase inhibitor allopurinol and SOD resulted in either no effect or variable effects on IL-1β processing and secretion (data not shown).

Use of the mitochondrial ETC complex I inhibitor; rotenone did result in robust and consistent inhibition of IL-1β maturation without inhibition of release of the pro-peptide. Rotenone is able to both increase and decrease ROS production at complex I depending on forward (glutamate-malate) or reverse (succinate) electron flux (Batandier *et al.*, 2006). If rotenone was increasing the formation of O_2^- in macrophages, I could hypothesise that the resultant increase in H_2O_2 would be removed by a system involving Trx-2, ultimately

leading to formation of oxidised Trx-2 (Ramachandiran *et al.*, 2007) and a potential decrease in active/reduced Trx-2 (Figure 7-14).

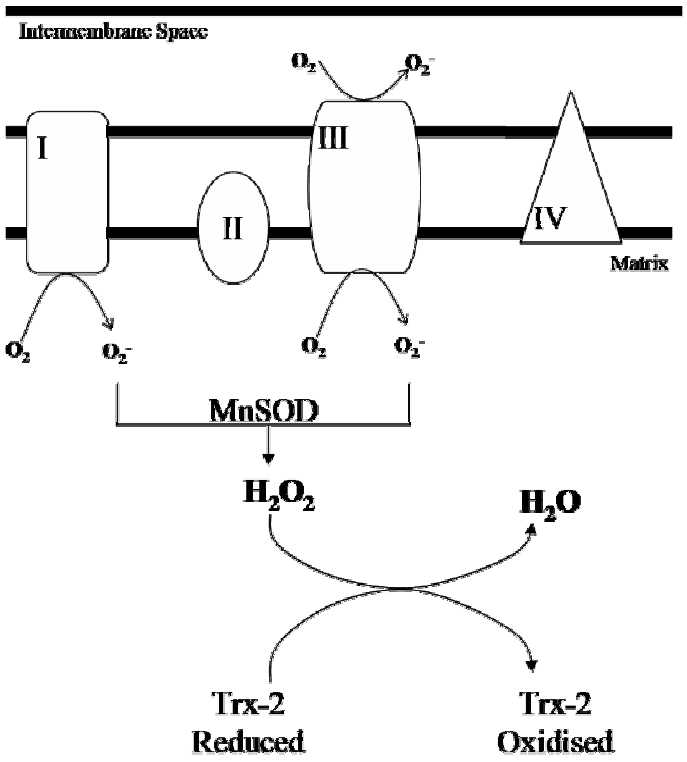

Figure 7-14. Schematic of the Generation & Removal of ROS from the Mitochondria by MnSOD & Trx-2.

The only known reducer of Trx is TrxR which is a pyridine nucleotide-disulfide oxidoreductase which is closely related to glutathione reductase but has a Cys-SeCys (selenocysteine) sequence as an additional redox centre. The antirheumatic gold(I)compound auranofin (brand name: Ridaura) is able to bind to the c-terminal selenocysteine (Gromer *et al.*, 1998) of both cytosolic and mitochondrial TrxR inhibiting its activity (Omata *et al.*, 2006). Pre-treatment of murine macrophages with auranofin resulted in the loss of maturation of IL-1β without inhibition of the secretion of the pro-peptide. Furthermore use of the contact sensitizer DNCB that is able to inhibit TrxR by the irreversible modification of the selenocysteine residue also resulted in the loss of IL-1β maturation. These data suggested that reduced Trx is required for the activation of caspase-1. This could occur by modification of caspase-1 itself or modification of a molecule upstream of caspase-1 activation. This modification by Trx could potentially include (i)

disulphide bond reduction (Figure 7-15), (ii) reduction of an *S*-OH group or (iii) denitrosylation of an *S*-NO group (Figure 7-16).

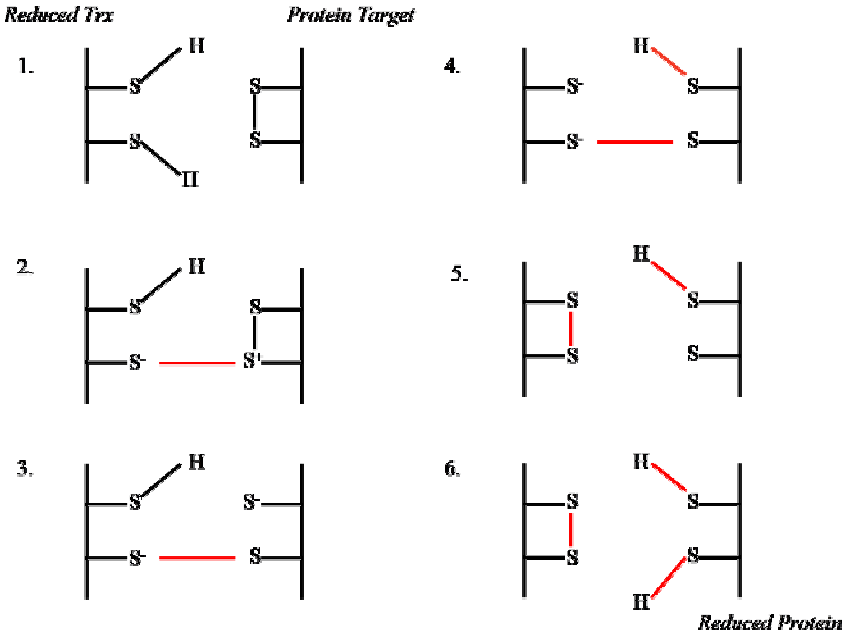

Figure 7-15. Schematic of Trx Induced Reduction of Protein Disulfide Bonds. Resultant thiol groups are able to undergo oxidation or nitrosylation by ROS and RNS respectively. New bond formation is shown in red.

As already stated mitochondrial caspase-3 has been suggested to be maintained in an inactive state by nitrosylation of the active site cysteine. Caspase-3 is then activated when engagement of the Fas receptor promotes denitrosylation of the active site ultimately leading to apoptosis. The precise mechanism of how denitrosylation occurred was until recently not known however a study by Benhar *et al.,* determined that it was mediated by the Trx-2/TrxR-2 system (Benhar *et al.*, 2008). A similar mechanism of denitrosylation of caspase-1 could therefore be hypothesized to occur upon activation of the $P2X_7R$.

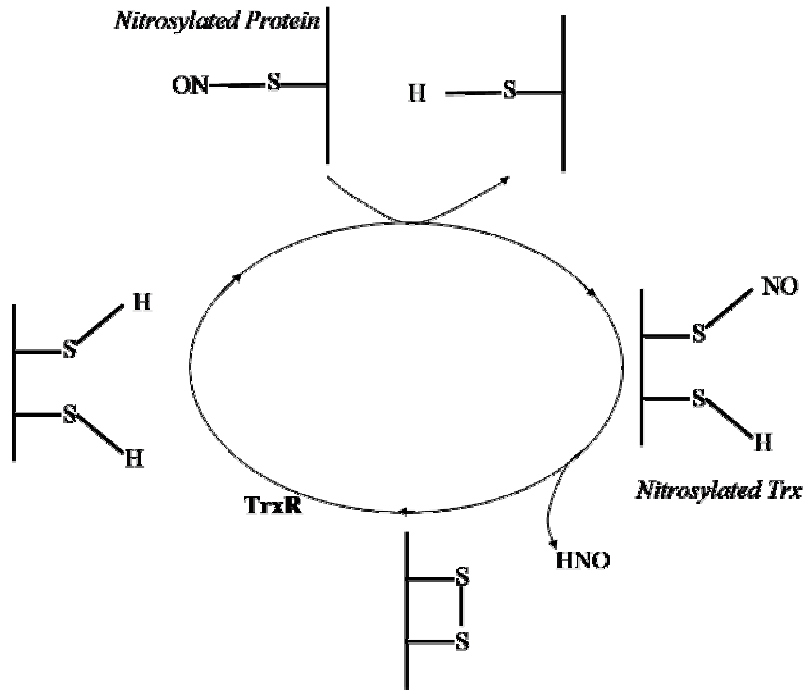

Figure 7-16. Schematic of how Trx is able to Denitrosylate *S*-NO groups.

7.3.3 Role of Thioredoxin in ATP Evoked Cell Death

Inhibitors of TrxR have previously been reported to induce cell death in a range of cell types. Pre-treatment of murine macrophages with auranofin or DNCB could have been predicted to increase basal and/or ATP evoked LDH release. However both compounds failed to significantly increase basal LDH release and furthermore caused a significant decrease in ATP evoked LDH release. Although rotenone was observed to inhibit maturation of IL-1β it was found to not inhibit ATP evoked LDH release. This could reflect (i) its inhibitory action at complex I of the mitochondrial therefore likely to promote cell death, although no increase in basal LDH release was observed, (ii) its different mode of action on Trx-2 promoting is oxidation rather than inhibition of its reduction or (iii) its ability to only act on Trx-2 and not on cytosolic Trx-1.

7.3.4 Concluding Remarks

Here I demonstrated that extracellular ATP is able to induce maturation and secretion of IL-1β and cell death in murine macrophages. Although further work is required to fully elucidate the signaling mechanisms involved. However based on these findings I hypothesize that (Figure 7-17):

1. Secretion of IL-1β (mature and pro-peptide) occurs via a caspase-1 independent pathway that is activated by a flavoprotein oxidoreductase/s.
2. Maturation of IL-1β occurs via a caspase-1 dependent pathway involving Trx-2
3. Cell death is partially controlled by caspase-1 and involves Trx-1.

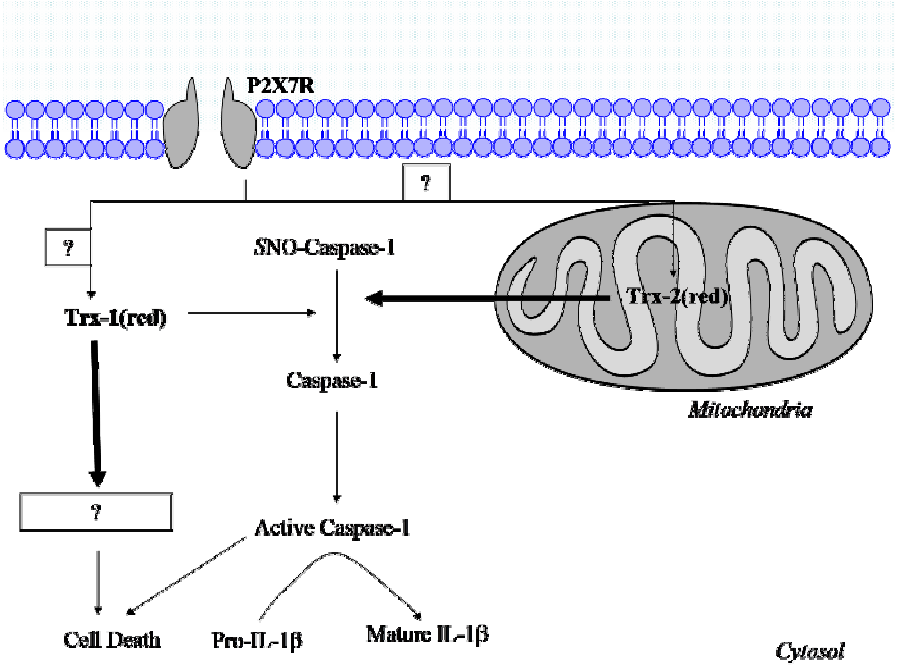

Figure 7-17. Schematic of the Maturation of IL-1β & Cell Death Evoked by Extracellular ATP. Based on previous literature and the findings of this study I propose that (i) Trx-2 is required for denitrosylation of caspase-1 ultimately resulting in maturation of IL-1β and (ii) Trx-1 is required for modification of an unidentified protein/molecule and caspase-1 resulting in ATP evoked cell death.

This work highlights how changes in the intracellular oxidative state of a macrophage by purinergic receptor activation can lead to a range of pro-inflammatory events subtly controlled by different redox signaling molecules and proteins. It is also important to remember that the redox status of the cell is controlled by a multitude of mechanisms all of which are interlinked. TrxR inhibitors are already available as disease treatments. Auranofin is prescribed to patients with rheumatoid arthritis which is a disease were (i) increased levels of IL-1β and ROS are observed (ii) the $P2X_7R$ antagonist AZD9056 is in phase II clinical trials for and (iii) loss of the P2X7 receptor in animal models can attenuate symptoms. This work therefore supports the role of the $P2X_7R$ in rheumatoid arthritis. Furthermore auranofin could potentially be employed for treatment of other inflammatory diseases where the $P2X_7R$/IL-1β is observed to play a role.

CHAPTER 8

CONCLUSIONS AND FUTURE DIRECTIONS

8.1 CONCLUSIONS

In the preceding chapters I have demonstrated the role extracellular ATP and the purinergic receptors can play in immunomodulation and inflammatory responses. From this work I can conclude:

1. The extracellular milieu can modulate activation of the $P2X_7R$. With divalent cations such as Mg^{2+} and Ca^{2+} potentially suppressing $P2X_7R$ activation under physiological conditions. Furthermore the mechanism of divalent cation modulation is dependent on the species of receptor, agonist used to activate the receptor and other ions present in the extracellular milieu.

2. Activation of the $P2X_7R$ can induce apoptotic/pyroptotic events such as reversible permeabilisation of the plasma membrane (pore formation), microvesicle shedding and translocation of PS from the inner to the outer leaflet of the plasma membrane. These events occur prior to the loss of plasma membrane integrity in which release of LDH occurs. This supports the notion that the $P2X_7R$ is involved in the clearance/death of infected or damaged host cells and that over activation of the receptor could lead to the full release of the inflammatory contents of a macrophage.

3. $P2X_7R$ evoked changes in cellular morphology are able to support the generation/activation of pro-coagulant factors. These pro-coagulant factors themselves are known via PAR's to mediate the production of pro-inflammatory cytokines. This suggests that in inflammatory situations the $P2X_7R$ could propagate and amplify pro-coagulant process's which would ultimately lead to a positive feedback onto the inflammatory response. This may be of importance in situations such as sepsis and atherosclerosis where dysregulation of coagulation and inflammation occurs. It may also be of interest in diseases such as RA where PARs, the $P2X_7R$ and cytokines such as IL-1β have been established to play an important role.

4. Purinergic receptors can couple to the activation of NADPH oxidase leading to the generation of ROS, with the localisation of ROS generation occurring potentially at the plasma membrane and intracellularly. This may suggest that the purinergic receptors could enhance the digestion of phagocytosed bacterium by increasing the levels of cytotoxic products required during oxidative burst. Furthermore ROS have been observed to play a vital role in the induction of some signaling processes; therefore they could potentially be a link between P2 receptor activation and the activation of downstream signaling pathways and function responses.

5. The processing of the IL-1β pro-peptide to its activated mature form by LPS/ATP requires the activation of caspase-1 and the Trx-TrxR system. Furthermore LPS/ATP evoked cell death also requires the caspase-1 and the Trx-TrxR system suggesting a similar pathway is activated. However in the case of cell death this pathway is insensitive to inhibition of complex I of the ETC. Secretion of the IL-1β pro-peptide occurs independently of the Trx-TrxR system and caspase-1.

8.2 FUTURE DIRECTIONS

8.2.1 What is the Nature of $P2X_7R$ Mediated Cell Death in Macrophages?

Several studies have demonstrated that activation of the $P2X_7R$ leads to changes in cellular morphology and ultimately loss of cell viability. Depending on the cell system, agonist, constituents of the extracellular solution and assays employed to explore these areas several different morphological and biochemical changes have been reported. A study by Kong *et al.,* stated that the $P2X_7R$ induced apoptotic cell death in rat primary cortical neurons (Kong *et al.*, 2005). They observed caspase-3 activation, nuclear condensation and DNA fragmentation and hypothesised through the use of specific caspase inhibitors that apoptosis was occurring through an intrinsic caspase-8/-9/-3 cell death pathway involving ERK1/2 and JNK. Whereas Mackenzie *et al.,* using HEK293 transfected with the $rP2X_7R$ described the sequence of events they observed after brief activation of the $P2X_7R$ as "pseudoapoptotic" because they observed an almost complete repertoire of extracellular events classically associated with apoptosis (Mackenzie *et al.*, 2005). These events such as mitochondrial depolarisation and swelling, increases in cytosolic and mitochondrial Ca^{2+}, exposure of PS, F-actin disruption and zeiotic membrane blebbing; however occurred in the absence of the release of cytochrome-c and where reversible. Jun *et al.,* described

$P2X_7R$ mediated cell death in SN4741 cells; a mouse dopaminergic neuron cell line as necrotic (Jun *et al.*, 2007). They observed nuclear swelling and spill over of nuclear DNA into the extracellular space, loss of endoplasmic reticulum integrity and the formation of cytoplasmic vacuoles. Furthermore these events and subsequent cell death were not inhibited by caspase inhibitors.

There are incredible similarities between the events I observed and those reported to occur in pyroptosis as activated by microbial pathogens such as *Salmonella* spp and *Listeria* spp this similarity was also highlighted by Brough *et al.,* (Brough *et al.*, 2007). However recent work by Pelegrin *et al.,* determined that the RAW264.7 macrophage cell line that I used for my morphological study lacks ASC (Pelegrin *et al.*, 2008). ASC not only forms an important part of the caspase-1 activating inflammasome but is hypothesised to form the cell death mediating pyroptosome. Therefore the events I observed using the RAW264.7 cells are not likely to be mediated by caspase-1 activation and therefore could not be attributed to pyroptosis. In order to determine the "type" of cell death evoked by ATP in macrophages requires a study of the biochemical features such as the dependence of caspases, DNA laddering and HMGB1 retention in the nucleus. Furthermore the RAW264.7 cell line could be used as a novel tool; with the morphological and biochemical features evoked by ATP being compared to those in other macrophage types. Furthermore the expression of multiple types of P2 receptor may determine the route of cell death induced by ATP; therefore a pharmacological study using P2Y and P2X specific agonists and antagonists could be performed to observe their effects on biochemical and morphological cell death events.

The signaling pathways involved in extracellular ATP evoked cell death also remain elusive. The JNK and p38 MAPK's are already known to play an important role in the induction of apoptosis. Furthermore activation of the $P2X_7R$ has been established to activate ERK1/2, p38 and JNK (Humphreys *et al.*, 2000; Pfeiffer *et al.*, 2004). Inhibition of the p38 MAPK pathway has been observed to:

- Inhibit BzATP evoked pore formation but not IL-1β processing in LPS/IFNγ primed THP-1 monocytes (Donnelly-Roberts *et al.*, 2004).
- Inhibit BzATP actin reorganisation and membrane blebbing in RAW264.7 cells (Pfeiffer *et al.*, 2004).

- Inhibit ATP induced DNA fragmentation and PS exposure in RAW264.7 cells (Noguchi *et al.*, 2008).

The study by Noguchi *et al.,* determined that ATP on RAW264.7 cells evoked ROS generation which in turn induced apoptosis via an ASK-1/p38 MAPK pathway (Noguchi *et al.*, 2008). This observation was of interest; as ASK-1 is found in an inactive form bound to reduced Trx. When Trx is oxidised by ROS it dissociates from ASK-1 allowing it to autophosphorylate and activate downstream MAPK's such as p38 (Saitoh *et al.*, 1998). This appears to conflict with the observations I made; use of TrxR inhibitors which would decrease levels of reduced Trx and therefore decrease the amount of bound/inactivate ASK-1 led to a decrease in LPS/ATP evoked cell death in J774.2 cells and BMDMϕ. However if we were to hypothesise that Trx is involved in denitrosylation of *S*-nitrosylated thiol groups, we would expect that due to transnitrosation that Trx would in turn become nitrosylated. *S*-nitrosylation of reduced Trx by *S*-nitrosoglutathione (GSNO) has been reported to evoke an increase in the activity of ASK-1 in HEK293 cells (Sumbayev, 2003). In order to establish a role for p38 MAPK and ASK-1 in ATP or LPS/ATP evoked cell death the use of specific p38 MAPK inhibitors such as SB202190 and SB203580 could be employed and ASK-$1^{-/-}$ macrophages (Noguchi *et al.*, 2008). The role of reduced and *S*-nitrosylated Trx could be determined by observing whether extracellular ATP evokes nitrosylation of Trx1 and Trx2 using the Jaffrey biotin-switch method based on western blot analysis (Jaffrey *et al.*, 2001). The effect of ATP on levels of oxidised and reduced forms of Trx1 and Trx could also be established by employing redox western analysis of Trx (Hanson *et al.*, 2004; Ramachandiran *et al.*, 2007; Watson *et al.*, 2003).

Finally another factor to address is potentially that in fact the inducer of LPS/ATP evoked cell death is TrxR and not Trx. The observation that rotenone was unable to inhibit LPS/ATP evoked cell death initially suggested that perhaps Trx-1 but not Trx-2 was involved in mediating cell death. However another way of interpreting this data is that both auranofin and DNCB will directly inhibit TrxR while rotenone has effects only on Trx itself. TrxRs have broad substrate specificity and are able to reduce ubiquinone (Q10/co-enzyme Q) (Xia *et al.*, 2003), ascorbic acid (May *et al.*, 1998; May *et al.*, 1997), lipoic acid (Nordberg *et al.*, 2001), lipid hydroperoxides and cytochrome-c (Nalvarte *et al.*, 2004). The role of TrxR vs. Trx in cell death could perhaps be investigated by employing the use

of specific TRX inhibitors such as 1-methylpropyl 2-imidazolyl disulfide (IV-2) (Kirkpatrick *et al.*, 1998; Lee *et al.*, 2002) or by knocking out Trx1 or Trx2.

8.2.2 How does Secretion of the Pro and Mature Forms of IL-1β Occur?

From my study it was determined that LPS/ATP evoked secretion of IL-1β occurred via a pathway inhibited by DPI but not dependent on NADPH oxidase, Trx-TrxR or caspase-1. We also observed that extracellular ATP in the presence of calcium can evoke the shedding of microvesicles; which some groups propose act as a potential vehicle for the release of both pro and mature IL-1β (Bianco *et al.*, 2005; MacKenzie *et al.*, 2001). Furthermore Bianco *et al.,* determined that microvesicles shed from LPS/ATP stimulated microglia contained pro-IL-1β and caspase-1 and where therefore the site of processing of IL-1β.

However the mechanism and signaling pathways involved in the secretion of the IL-1 cytokines is controversial. As previously stated there have been at least four potential release pathways put forward; these being exocytosis of secretory lysosomes (Andrei *et al.*, 1999), microvesicle shedding, exocytosis of multivesicular bodies (Qu *et al.*, 2007) and direct efflux (Brough *et al.*, 2007). Furthermore the signaling mechanisms involved in the secretory pathway have been attributed to involve K^+ efflux, $iPLA_2$, caspase-1, ASC, extracellular Ca^{2+} and pannexin-1 (Pelegrin *et al.*, 2008; Qu *et al.*, 2007).

The observations made can differ widely between different research groups, within the same group and between different monocyte/macrophage types (Kahlenberg *et al.*, 2004a). Some examples include:

- In my study YVAD-FMK failed to inhibit release of the IL-1β pro-peptide and a p20 form of IL-1β but Qu *et al.,* 2007 determined that caspase-1 was required for secretion.
- Qu *et al.,* 2007 determined that extracellular Ca^{2+} was not required for secretion whereas Brough *et al.,* 2003 determined that it was.
- Pelegrin *et al.,* 2008 observed release of pro-IL-1β from RAW264.7 cells which do not express ASC whereas Qu *et al.,* 2007 reported a loss of secretion in $ASC^{-/-}$ macrophages.

Pelegrin *et al.,* 2008 hypothesised that there were potentially the existence of multiple release pathways for IL-1 cytokines. They put forward three potential secretion pathways:

1. A cytolytic pathway.
2. A non cytolytic glycine inhibitable pathway whereby pro-IL-1β is processed outside the cell to mature IL-1β by extracellular proteases.
3. A non cytolytic pannexin-1, inflammasome and caspase-1 dependent pathway.

Studying the secretion of IL-1β separately from the processing of IL-1β appears to be of difficulty as many inhibitors of IL-1β secretion prevent IL-1β processing. Some groups suggest this is due to processing of IL-1β occurring only outside of the cell which fits with several groups finding that only the pro form and never the active/mature form is found in the cell lysates (Laliberte *et al.*, 1999; MacKenzie *et al.*, 2001; Perregaux *et al.*, 1994). However both Brough *et al.,* 2007 and Qu *et al.,* 2007 observed mature IL-1β in cell extracts at early ATP stimulation time points therefore supporting a case for intracellular processing. Furthermore examination of western blots in previous reports suggests that pro-IL-1β is not always found to be present in the secreted protein fraction even when the mature form is present. One way in which to overcome these issues would be to study the secretion of IL-1α whose secretion but not activation can be initiated by ATP.

In order for myself to examine the secretory mechanism for murine macrophages, similar techniques as to those employed by Qu *et al.,* whereby they determined whether endosomal or lysosomal markers were release at similar time points as mature IL-1β (in this study pro-IL-1β was not present in the extracellular medium) could be employed. The effect of inhibitors which block IL-1β secretion (in the case of my study this was DPI), could then be examined on the release of these markers. It may also be of interest to examine the effect of other flavoprotein oxidoreductase inhibitors to determine what DPI is targeting to have such a profound effect on the secretion of pro-IL-1β. However DPI is reported to have other effects such as the inhibition of potassium and calcium channel currents (Weir *et al.*, 1994; Wyatt *et al.*, 1994). This observation along with the important role K^+ efflux plays in IL-1β processing and secretion suggests that the effect of potassium channel blockers on IL-1 secretion and potentially IL-1β processing should be examined.

8.2.3 How is Trx-TrxR involved in the Processing of IL-1β?

In this study I established that inhibition of TrxR and the use of the mitochondrial complex I inhibitor rotenone could abolish LPS/ATP evoked processing of IL-1β. I hypothesised that rotenone lead to the oxidation of Trx2 and therefore a reduction in levels of reduced Trx2; implicating that reduced Trx2 was involved in the activation of caspase-1 and maturation of IL-1β. However this hypothesis requires further investigation; use of techniques described for investigating the role of Trx or TrxR in ATP mediated cell death could be employed. This would include knock-down of Trx1 or Trx2 using siRNA or specific Trx rather than TrxR inhibitors. Also the examination of how LPS and LPS/ATP treatment effects the oxidation state of Trx using an electrophoretic shift assay which can determine whether Trx is fully reduced, where one cysteine is reduced or where both cysteines are oxidised (Bersani *et al.*, 2002; Hurd *et al.*, 2007).

An important question to answer is how is Trx regulating caspase-1 activation? Is Trx inducing denitrosylation of *S*-nitrosylated caspase-1, similar to that reported for caspase-3 by Benhar *et al.,* 2008? Use of the Jaffrey biotin-switch method could be employed to answer this question. The Trx, Grx and GSH system can cross-talk (Figure 8-1), therefore could the Trx system be involved in oxidation and glutathionylation of caspase-1, similar to that reported for caspase-1 (Meissner *et al.*, 2008). In the study by Meissner *et al.,* they determined that caspase-1 was glutathionylated in $SOD1^{-/-}$ deficient macrophages by loading the cells with BioGEE (Invitrogen™, UK) which is a cell-permeant, biotinylated glutathione analogue. ATP evoked whole cell glutathionylation could be assessed using a fluorescent streptavidin conjugate and FACS or fluorescent microscopy or specific proteins could be identified by precipitation from cell lysates with streptavidin-agarose beads and detection by western blotting.

The above methods could also be employed to determine whether caspase-1 is the target of thiol modification. The lysosomal protease cathepsin B has been observed to evoke the activation of mouse caspase-11 (Schotte *et al.*, 1998), which is hypothesised to lie upstream of both caspase-1 and caspase-3 activation (Kang *et al.*, 2000). Furthermore a study by Hentze *et al* determined that the K^+ ionophore nigericin in the absence of LPS priming promoted caspase activation and IL-18 maturation via a cathepsin B dependent pathway in the human monocytic cell line; THP-1 (Hentze *et al.*, 2003). Both cathepsin B

and caspase-11 are thiol proteases and therefore could be targets of thiol modification by the Trx-TrxR system.

Potentially LPS/ATP treatment of macrophages could result in modification of several protein thiol groups which in the case of *S-NO* groups could be identified using the biotin switch method or oxidised thiols by using the redox-DIGE as described in Hurd *et al.,* 2007 followed by peptide mass fingerprinting and tandem mass spectrometry.

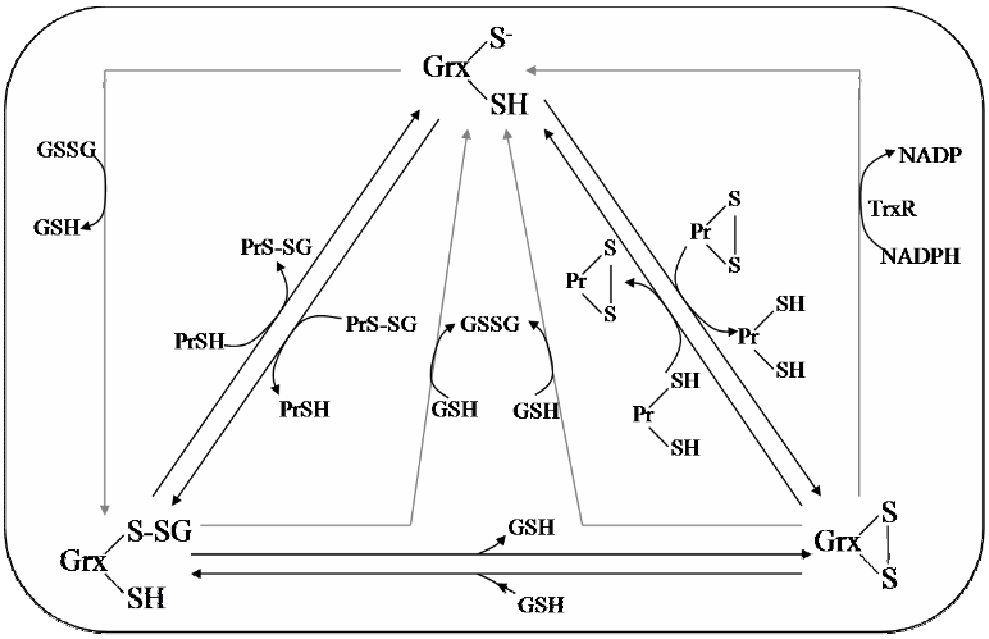

Figure 8-1. Schematic of the Cross Talk between the Trx, Grx and GSH Systems. Grx is able to convert between a dithiol (-SH), glutathionylated (S-SG) and disulphide form (S-S). In doing this it can catalyse the glutathionylation and deglutathionylation of protein thiol groups (PrSH) and the reversible formation of protein disulphides. Thioredoxin reductase is able to reduce Grx. Adapted from (Hurd *et al.*, 2005)

8.2.4 Does $P2X_7R$ Activation Induce Inflammasome Assembly?

What potentially evokes the formation of the inflammasome? Work by Kanneganti *et al*., determined that caspase-1 activation could occur independently of TLR activation (Kanneganti *et al.*, 2007). Stimulating TLR2 or TLR4 deficient macrophages with TLR ligands (3hrs) followed by a 30 min ATP pulse resulted caspase-1 activation equivalent to WT. They suggested that ATP evoked opening of the pannexin-1 pore allows the intracellular uptake of bacterial component through an endosomal pathway and their delivery into the host cytosol where they are sensed by NALP3. Furthermore they determined that delivering heat-killed bacteria into the cytosol using the pore-forming protein Streptolysin-O evoked caspase-1 activation in the absence of ATP. Therefore is the

$P2X_7R$ merely providing an entry route for bacterial products and is in fact not involved in inflammasome formation or caspase-1 activation directly? This concept would not appear to fit with observations made by myself whereby inhibition of TrxR in J774.2 cells resulted in loss of IL-1β processing in the absence of any effect on pore-formation and those of Hentze *et al.,* 2003 whereby nigericin in the absence of LPS priming evoked caspase-1 activation.

Therefore a simple experiment would be to determine the effects of LPS vs. ATP vs. LPS+ATP on the activation of caspase-1. Further experiments looking at the expression and interactions of caspase-1, and other inflammasome components such as NALP3, ASC and caspase-11 could be investigated. Potentially LPS may be involved in the upregulation of one of more of the inflammasome proteins and that the $P2X_7R$ is involved in evoking formation of the complex. If associations between inflammasome proteins were observed to be evoked by ATP then blockade of K^+ efflux, Trx-TrxR or $iPLA_2$ could determine which signaling pathways are involved in inflammasome assembly.

8.3 FINAL WORD

Purinergic signaling has come a long way since its foundations in the 1970's. It has been established to be involved in many physiological and pathophysiological responses. Here I have demonstrated that extracellular ATP plays an important role in immunomodulation and inflammation and is therefore an exciting target for new drug therapies. Currently there is an ever growing field developing in determining the role of redox molecules in intracellular signaling and the mechanism of how activation of the inflammasome. Furthermore the link between these two fields is also being rapidly established with several papers published in the past year investigating this link (Cruz *et al.*, 2007; Dostert *et al.*, 2008; Hewinson *et al.*, 2008; Meissner *et al.*, 2008; Pétrilli *et al.*, 2007b). Activation of the NALP3 inflammasome is not only important in conditions involving bacterial infection but has also been determined to be activated by asbestos and silica (Dostert *et al.*, 2008), amyloid-β (Halle *et al.*, 2008) and uric acid crystals (Martinon *et al.*, 2006) suggesting that unravelling its pathways could help our understanding of diseases such as sepsis, asbestosis, silicosis, gout, Alzheimer's, and other chronic inflammatory diseases.

I: APPENDIX

Supplementary Data - "GENERAL PHARMACOLOGY & THE EFFECT OF DIVALENT CATIONS AT THE MURINE $P2X_7$ RECEPTOR"

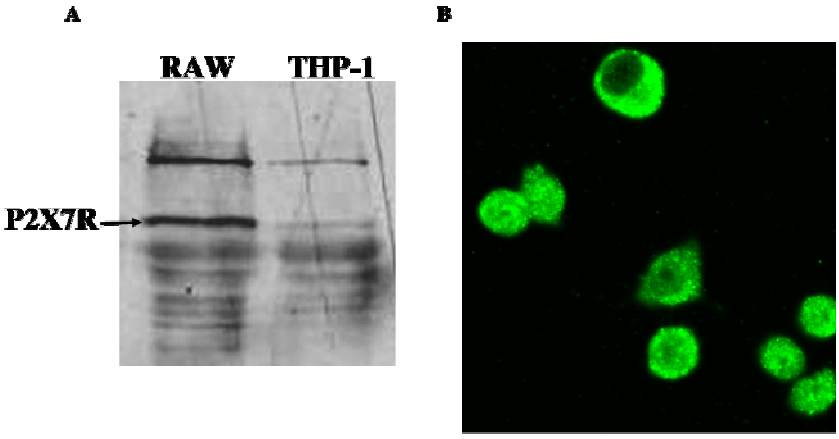

Figure A-1 $P2X_7R$ is Expressed in RAW264.7 Cells. A, Western-blot for the $P2X_7R$ in RAW264.7 cells and THP-1 monocytes. B, Immunohistochemistry for the $P2X_7R$ in RAW264.7 cells. Both performed using the anti-$P2X_7R$ antibody following the manufacturer's instructions (Alamone Labs, Bucks, UK).

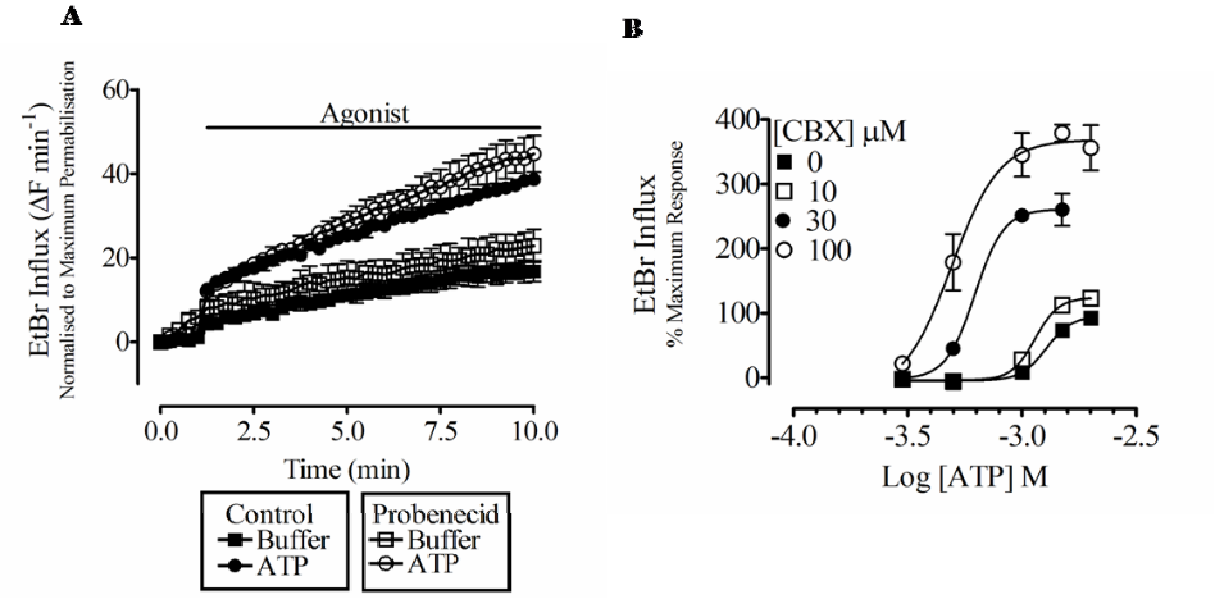

Figure A-2. Pannexin-1 Blockers Failed to Inhibit $P2X_7R$ Mediated Dye Uptake in RAW264.7 cells. A, Cells pre-treated (45 min) with probenecid (2.5 mM) had similar levels of dye-influx compared to control cells. B, Cells pre-treated (30 min) with carbenoxolone (CBX) had increased levels of dye-influx in response to ATP. $n = 3 \pm$ s.e.m.

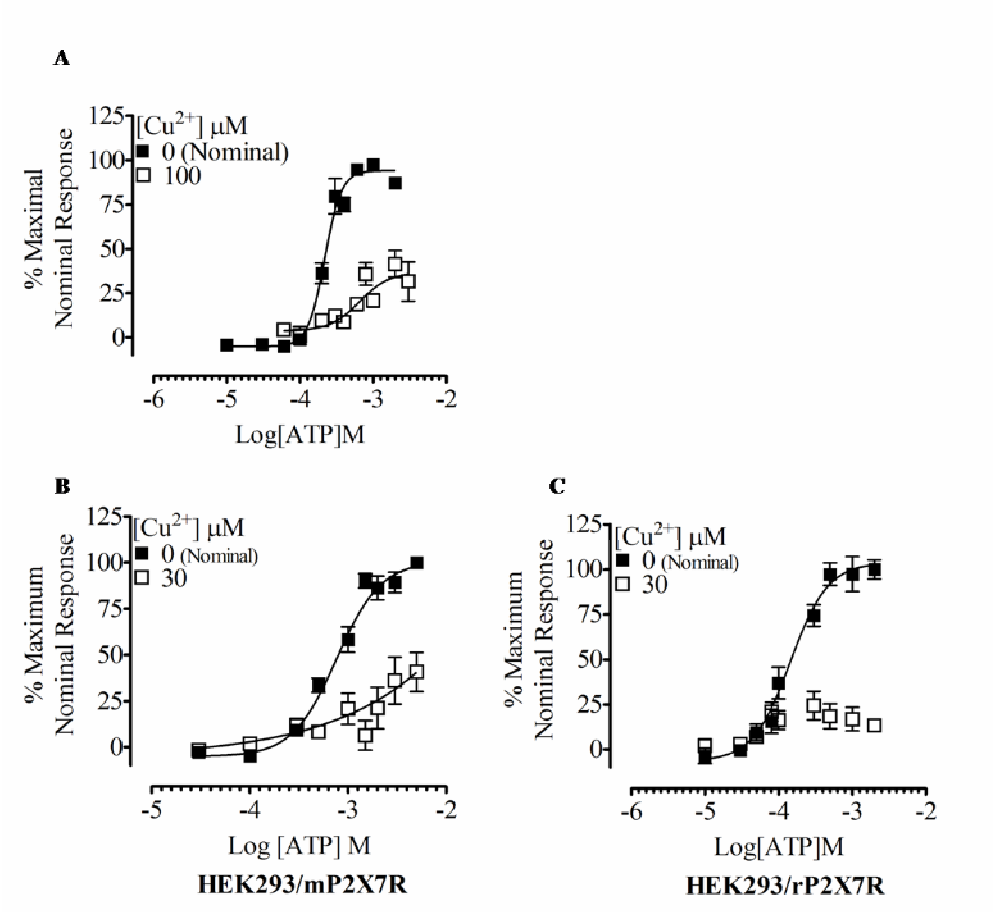

Figure A-3. Cu^{2+} Inhibited ATP Evoked Dye Uptake in the Absence of Ca^{2+} & Mg^{2+} in A, RAW264.7, B, HEK293/mP2X$_7$R and C, HEK293/rP2X$_7$R cells. $n = 3 \pm$ s.e.m.

Supplementary Data - "ATP INDUCES REACTIVE OXYGEN SPECIES GENERATION VIA NADPH OXIDASE"

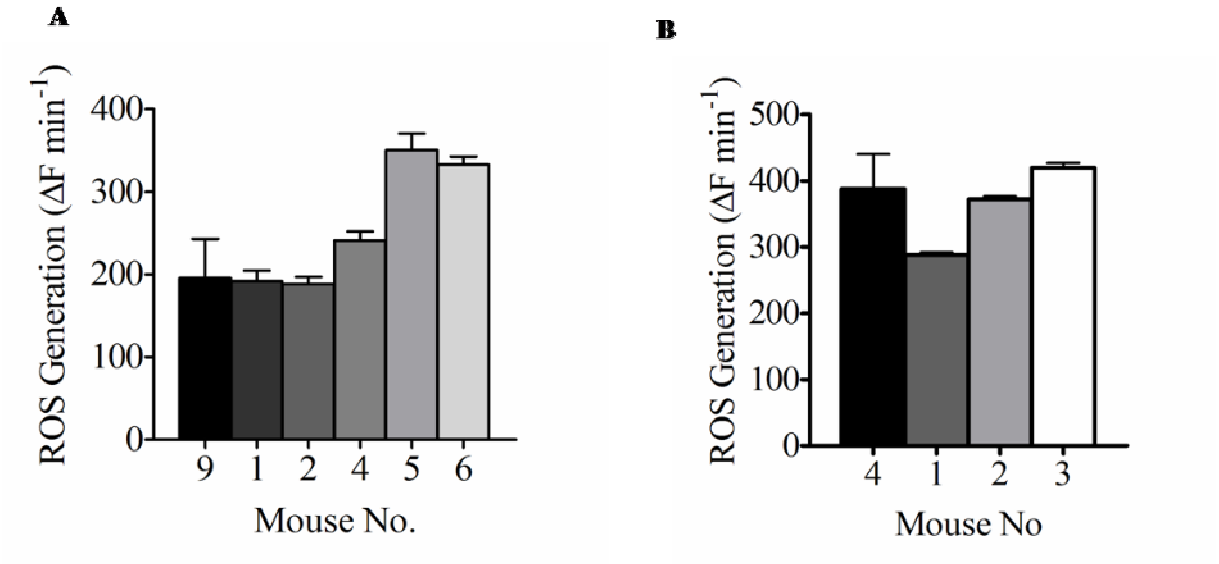

Figure A-4. A, SIN-1 Induced ROS Generation in WT (Mouse No. 9) & gp91$^{-/-}$ BMDMø. B, SIN-1 induced ROS generation in WT (Mouse No. 4) & gp47$^{-/-}$ BMDMø.

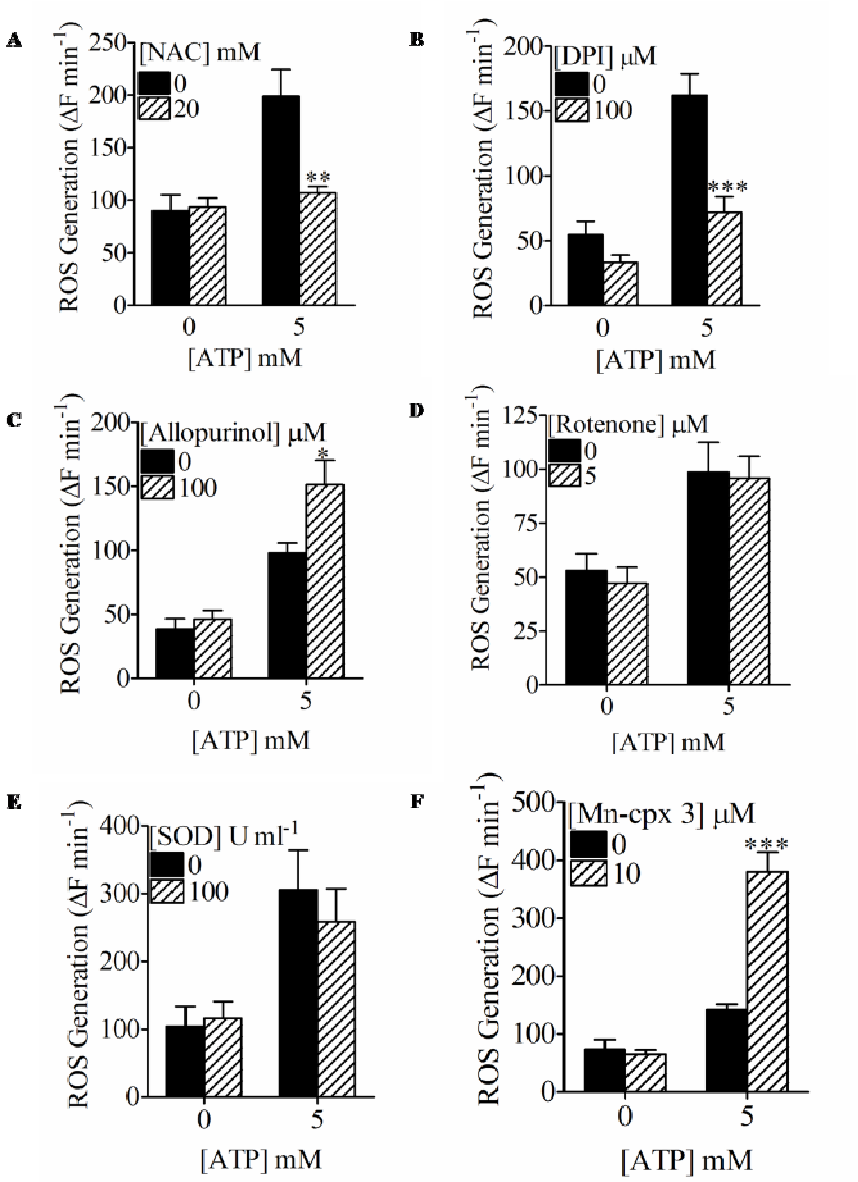

Figure A-5. Effect of ROS Inhibitors on ATP Evoked Cellular Oxidation in Peritoneal Cells. A, NAC (20 mM, 2 hrs) inhibited ATP evoked ROS generation. B, DPI (100 μM, 1.5 hrs) inhibited ATP evoked ROS generation. C, Allopurinol (100 μM, 30 min) potentiated ATP evoked ROS generation. D, Rotenone (5 μM, 30 min) did not effect ATP evoked ROS generation. E, Extracellular SOD (100 U ml^{-1}) did not effect ATP evoked ROS generation. F, The SOD mimetic Mn-cpx 3 potentiated ATP evoked ROS generation. Student's two-tailed t-test *:p<0.05, **:p<0.01, ***:p<0.001, $n = 3 \pm$ s.e.m. Isolation and Culture of Murine Peritoneal Cells. Male C57BL/6 mice 8-12 wks of age were sacrificed by cervical dislocation. Native peritoneal cells were harvested by peritoneal lavage with 8 ml of DMEM:F12 (1:1). Cells were centrifuged at 240 xg for 4 minutes at RT (S4180 rotor, Beckman GS-15R). Cells were resuspended in warmed complete culture medium, counted and re-seeded as required for experimental assays. After 6 hours incubation complete culture medium and suspension cells were aspirated off and the remaining adherent cell population washed with complete culture medium. Adherent cells were then primed with 25 ng ml^{-1} LPS overnight (16 – 18 hours) in complete culture medium (37 °C in a humidified atmosphere of 5 % CO_2 and 95 % air).

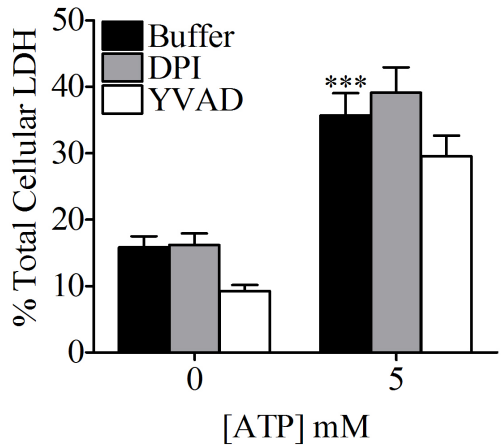

Figure A-6. Effect of DPI & YVAD on LDH Release from ATP Stimulated Peritoneal Cells. One-way ANOVA with Dunnett's post-hoc test. *:p<0.05, **:p<0.01, ***:p<0.001, $n = 3 \pm$ s.e.m.

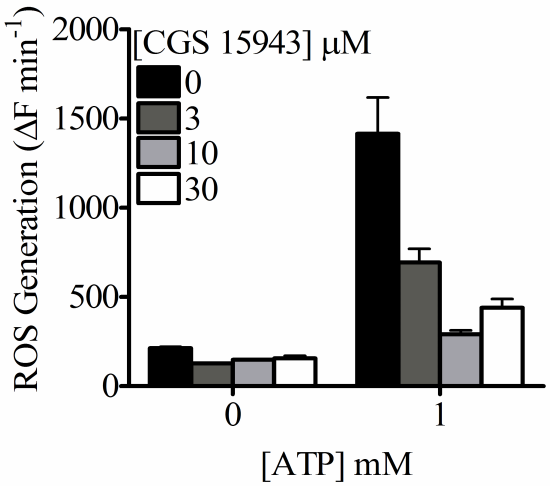

Figure A-7. Effect of CGS 15943 on ROS Generation in J774.2 Cells. $n = 1 \pm$ SD.

II: REFERENCES

Acuña-Castillo, C, Coddou, C, Bull, P, Brito, J, Huidobro-Toro, J (2007) Differential role of extracellular histidines in copper, zinc, magnesium and proton modulation of the P2X7 purinergic receptor. *J Neurochem* **101**(1)**:** 17-26.

Adinolfi, E, Callegari, M, Ferrari, D, Bolognesi, C, Minelli, M, Wieckowski, M, Pinton, P, Rizzuto, R, Di Virgilio, F (2005) Basal activation of the P2X7 ATP receptor elevates mitochondrial calcium and potential, increases cellular ATP levels, and promotes serum-independent growth. *Mol Biol Cell* **16**(7)**:** 3260-3272.

Akira, S, Isshiki, H, Sugita, T, Tanabe, O, Kinoshita, S, Nishio, Y, Nakajima, T, Hirano, T, Kishimoto, T (1990) A nuclear factor for IL-6 expression (NF-IL6) is a member of a C/EBP family. *EMBO J* **9**(6)**:** 1897-1906.

Akira, S, Uematsu, S, Takeuchi, O (2006) Pathogen recognition and innate immunity. *Cell* **124**(4)**:** 783-801.

Ananyeva, N, Kouiavskaia, D, Shima, M, Saenko, E (2002) Intrinsic pathway of blood coagulation contributes to thrombogenicity of atherosclerotic plaque. *Blood* **99**(12)**:** 4475-4485.

Andoh, T, Chock, P, Chiueh, C (2002) The roles of thioredoxin in protection against oxidative stress-induced apoptosis in SH-SY5Y cells. *J Biol Chem* **277**(12)**:** 9655-9660.

Andrei, C, Dazzi, C, Lotti, L, Torrisi, M, Chimini, G, Rubartelli, A (1999) The secretory route of the leaderless protein interleukin 1beta involves exocytosis of endolysosome-related vesicles. *Mol Biol Cell* **10**(5)**:** 1463-1475.

Andrei, C, Margiocco, P, Poggi, A, Lotti, L, Torrisi, M, Rubartelli, A (2004) Phospholipases C and A2 control lysosome-mediated IL-1 beta secretion: Implications for inflammatory processes. *Proc Natl Acad Sci U S A* **101**(26)**:** 9745-9750.

Bach, R (2006) Tissue factor encryption. *Arterioscler Thromb Vasc Biol* **26**(3)**:** 456-461.

Bach, R, Rifkin, D (1990) Expression of tissue factor procoagulant activity: regulation by cytosolic calcium. *Proc Natl Acad Sci U S A* **87**(18)**:** 6995-6999.

Baroni, M, Pizzirani, C, Pinotti, M, Ferrari, D, Adinolfi, E, Calzavarini, S, Caruso, P, Bernardi, F, Di Virgilio, F (2007) Stimulation of P2 (P2X7) receptors in human dendritic cells induces the release of tissue factor-bearing microparticles. *FASEB J* **21**(8)**:** 1926-1933.

Barrera, NP, Ormond, SJ, Henderson, RM, Murrell-Lagnado, RD, Edwardson, JM (2005) Atomic Force Microscopy Imaging Demonstrates that P2X2 Receptors Are Trimers but That P2X6 Receptor Subunits Do Not Oligomerize. *J. Biol. Chem.* **280**(11)**:** 10759-10765.

Basso, A, Bratcher, N, Harris, R, Jarvis, M, Decker, M, Rueter, L (2008) Behavioral profile of P2X(7) receptor knockout mice in animal models of depression and anxiety: Relevance for neuropsychiatric disorders. *Behav Brain Res*.

Batandier, C, Guigas, B, Detaille, D, El-Mir, M, Fontaine, E, Rigoulet, M, Leverve, X (2006) The ROS production induced by a reverse-electron flux at respiratory-chain complex 1 is hampered by metformin. *J Bioenerg Biomembr* **38**(1)**:** 33-42.

Bendall, J, Cave, A, Heymes, C, Gall, N, Shah, A (2002) Pivotal role of a gp91(phox)-containing NADPH oxidase in angiotensin II-induced cardiac hypertrophy in mice. *Circulation* **105**(3)**:** 293-296.

Benhar, M, Forrester, MT, Hess, DT, Stamler, JS (2008) Regulated Protein Denitrosylation by Cytosolic and Mitochondrial Thioredoxins. *Science* **320**(5879)**:** 1050-1054.

Bersani, N, Merwin, J, Lopez, N, Pearson, G, Merrill, G (2002) Protein electrophoretic mobility shift assay to monitor redox state of thioredoxin in cells. *Methods Enzymol* **347:** 317-326.

Bevers, E, Comfurius, P, Dekkers, D, Zwaal, R (1999) Lipid translocation across the plasma membrane of mammalian cells. *Biochim Biophys Acta* **1439**(3)**:** 317-330.

Bianchi, BR, Lynch, KJ, Touma, E, Niforatos, W, Burgard, EC, Alexander, KM, Park, HS, Yu, H, Metzger, R, Kowaluk, E, Jarvis, MF, van Biesen, T (1999) Pharmacological characterization of recombinant human and rat P2X receptor subtypes. *Eur J Pharmacol* **376**(1-2)**:** 127-138.

Bianco, F, Pravettoni, E, Colombo, A, Schenk, U, Möller, T, Matteoli, M, Verderio, C (2005) Astrocyte-derived ATP induces vesicle shedding and IL-1 beta release from microglia. *J Immunol* **174**(11)**:** 7268-7277.

Bosher, SK, Warren RL (1978) Very low calcium content of cochlear endolymph, an extracellular fluid. *Nature* **273:** 377-378.

Bours, M, Swennen, E, Di Virgilio, F, Cronstein, B, Dagnelie, P (2006) Adenosine 5'-triphosphate and adenosine as endogenous signaling molecules in immunity and inflammation. *Pharmacol Ther* **112**(2)**:** 358-404.

Brake, AJ, Wagenbach, MJ, Julius, D (1994) New structural motif for ligand-gated ion channels defined by an ionotropic ATP receptor. *Nature* **371**(6497)**:** 519-523.

Broom, D, Matson, D, Bradshaw, E, Buck, M, Meade, R, Coombs, S, Matchett, M, Ford, K, Yu, W, Yuan, J, Sun, S, Ochoa, R, Krause, J, Wustrow, D, Cortright, D (2008) Characterization N-(adamantan-1-ylmethyl)-5-[(3R-amino-pyrrolidin-1-yl)methyl]-2-chloro-benzamide (AACBA), a P2X7 antagonist in animal models of pain and inflammation. *J Pharmacol Exp Ther* **327**(3): 620-633

Brough, D, Rothwell, N (2007) Caspase-1-dependent processing of pro-interleukin-1beta is cytosolic and precedes cell death. *J Cell Sci* **120**(Pt 5)**:** 772-781.

Bruzzone, R, Barbe, M, Jakob, N, Monyer, H (2005) Pharmacological properties of homomeric and heteromeric pannexin hemichannels expressed in Xenopus oocytes. *J Neurochem* **92**(5)**:** 1033-1043.

Burnstock, G (1978) A basis for distinguishing two types of purinergic receptor. . In: *Cell Membrane Receptors for Drugs and Hormones: A multidisciplinary approach*, L, SRB (ed): Raven, New York.

Burnstock, G (1972) Purinergic Nerves. *Pharmacol Rev* **24**(3)**:** 509-581.

Burnstock, G (1976) Purinergic receptors. *J Theor Biol* **62**(2)**:** 491-503.

Burnstock, G, Kennedy, C (1985) Is there a basis for distinguishing two types of P2-purinoceptor? *Gen Pharmacol* **16**(5)**:** 433-440.

Busch, G, Seitz, I, Steppich, B, Hess, S, Eckl, R, Schömig, A, Ott, I (2005) Coagulation factor Xa stimulates interleukin-8 release in endothelial cells and mononuclear leukocytes: implications in acute myocardial infarction. *Arterioscler Thromb Vasc Biol* **25**(2)**:** 461-466.

Callahan, M, Halleck, M, Krahling, S, Henderson, A, Williamson, P, Schlegel, R (2003) Phosphatidylserine expression and phagocytosis of apoptotic thymocytes during differentiation of monocytic cells. *J Leukoc Biol* **74**(5)**:** 846-856.

Carta, S, Tassi, S, Semino, C, Fossati, G, Mascagni, P, Dinarello, C, Rubartelli, A (2006) Histone deacetylase inhibitors prevent exocytosis of interleukin-1beta-containing secretory lysosomes: role of microtubules. *Blood* **108**(5)**:** 1618-1626.

Cerpa, W, Varela-Nallar, L, Reyes, AE, Minniti, AN, Inestrosa, NC (2005) Is there a role for copper in neurodegenerative diseases? *Mol Aspects Med* **26**(4-5): 405-420.

Cerretti, DP, Kozlosky, CJ, Mosley, B, Nelson, N, Van Ness, K, Greenstreet, TA, March, CJ, Kronheim, SR, Druck, T, Cannizzaro, LA, et al. (1992) Molecular cloning of the interleukin-1 beta converting enzyme. *Science* **256**(5053)**:** 97-100.

Chapman, M, Rubin, B, Gracy, R (1989) Increased carbonyl content of proteins in synovial fluid from patients with rheumatoid arthritis. *J Rheumatol* **16**(1)**:** 15-18.

Chedid, M, Yoza, B, Brooks, J, Mizel, S (1991) Activation of AP-1 by IL-1 and phorbol esters in T cells. Role of protein kinase A and protein phosphatases. *J Immunol* **147**(3)**:** 867-873.

Chen, K, Huang, J, Gong, W, Iribarren, P, Dunlop, NM, Wang, JM (2007) Toll-like receptors in inflammation, infection and cancer. *Int Immunopharmacol* **7**(10)**:** 1271-1285.

Chessell, I, Hatcher, J, Bountra, C, Michel, A, Hughes, J, Green, P, Egerton, J, Murfin, M, Richardson, J, Peck, W, Grahames, C, Casula, M, Yiangou, Y, Birch, R, Anand, P, Buell, G (2005) Disruption of the P2X7 purinoceptor gene abolishes chronic inflammatory and neuropathic pain. *Pain* **114**(3)**:** 386-396.

Chessell, I, Simon, J, Hibell, A, Michel, A, Barnard, E, Humphrey, P (1998) Cloning and functional characterisation of the mouse P2X7 receptor. *FEBS Lett* **439**(1-2)**:** 26-30.

Cirino, G, Napoli, C, Bucci, M, Cicala, C (2000) Inflammation-coagulation network: are serine protease receptors the knot? *Trends Pharmacol Sci* **21**(5)**:** 170-172.

Cockcroft, S, Gomperts, B (1979) ATP induces nucleotide permeability in rat mast cells. *Nature* **279**(5713)**:** 541-542.

Cockcroft, S, Gomperts, B (1980) The ATP4- receptor of rat mast cells. *Biochem J* **188**(3)**:** 789-798.

Coddou, C, Lorca, R, Acuña-Castillo, C, Grauso, M, Rassendren, F, Huidobro-Toro, J (2005) Heavy metals modulate the activity of the purinergic P2X4 receptor. *Toxicol Appl Pharmacol* **202**(2)**:** 121-131.

Coddou, C, Morales, B, Huidobro-Toro, J (2003) Neuromodulator role of zinc and copper during prolonged ATP applications to P2X4 purinoceptors. *Eur J Pharmacol* **472**(1-2)**:** 49-56.

Coleman, M, Sahai, E, Yeo, M, Bosch, M, Dewar, A, Olson, M (2001) Membrane blebbing during apoptosis results from caspase-mediated activation of ROCK I. *Nat Cell Biol* **3**(4)**:** 339-345.

Comfurius, P, Senden, J, Tilly, R, Schroit, A, Bevers, E, Zwaal, R (1990) Loss of membrane phospholipid asymmetry in platelets and red cells may be associated with calcium-induced shedding of plasma membrane and inhibition of aminophospholipid translocase. *Biochim Biophys Acta* **1026**(2)**:** 153-160.

Cruz, C, Rinna, A, Forman, H, Ventura, A, Persechini, P, Ojcius, D (2007) ATP activates a reactive oxygen species-dependent oxidative stress response and secretion of proinflammatory cytokines in macrophages. *J Biol Chem* **282**(5)**:** 2871-2879.

Cunningham, MA, Rondeau, E, Chen, X, Coughlin, SR, Holdsworth, SR, Tipping, PG (2000) Protease-activated receptor 1 mediates thrombin-dependent, cell-mediated renal inflammation in crescentic glomerulonephritis. *J Exp Med* **191**(3)**:** 455-462.

Dahlquist, R, Diamant, B (1974) Interaction of ATP and calcium on the rat mast cell: effect on histamine release. *Acta Pharmacol Toxicol (Copenh)* **34**(5)**:** 368-384.

Dardenne, M (2002) Zinc and immune function. *Eur J Clin Nutr* **56 Suppl 3:** S20-S23.

Dayer, JM, Feige, U, Edwards, CK, 3rd, Burger, D (2001) Anti-interleukin-1 therapy in rheumatic diseases. *Curr Opin Rheumatol* **13**(3)**:** 170-176.

del Conde, I, Nabi, F, Tonda, R, Thiagarajan, P, López, J, Kleiman, N (2005) Effect of P-selectin on phosphatidylserine exposure and surface-dependent thrombin generation on monocytes. *Arterioscler Thromb Vasc Biol* **25**(5)**:** 1065-1070.

Del Conde, I, Shrimpton, C, Thiagarajan, P, López, J (2005) Tissue-factor-bearing microvesicles arise from lipid rafts and fuse with activated platelets to initiate coagulation. *Blood* **106**(5)**:** 1604-1611.

Deniz-Naranjo, MC, Munoz-Fernandez, C, Alemany-Rodriguez, MJ, Perez-Vieitez, MC, Aladro-Benito, Y, Irurita-Latasa, J, Sanchez-Garcia, F (2008) Cytokine IL-1 beta but not IL-1 alpha promoter polymorphism is associated with Alzheimer disease in a population from the Canary Islands, Spain. *Eur J Neurol* **15**(10)**:** 1080-1084.

Dietzen, D, Page, K, Tetzloff, T (2004) Lipid rafts are necessary for tonic inhibition of cellular tissue factor procoagulant activity. *Blood* **103**(8)**:** 3038-3044.

Dinarello, CA (1996) Biologic basis for interleukin-1 in disease. *Blood* **87**(6)**:** 2095-2147.

Dinarello, CA, Marnoy, SO, Rosenwasser, LJ (1983) Role of arachidonate metabolism in the immunoregulatory function of human leukocytic pyrogen/lymphocyte-activating factor/interleukin 1. *J Immunol* **130**(2)**:** 890-895.

Dinauer, M, Orkin, S, Brown, R, Jesaitis, A, Parkos, C (1987) The glycoprotein encoded by the X-linked chronic granulomatous disease locus is a component of the neutrophil cytochrome b complex. *Nature* **327**(6124)**:** 717-720.

Di Virgillio, F, Steinberg, TH, Silverstein SC (1990) Inhibition of Fura-2 sequestration and secretion with organic anion transport blockers. *Cell Calcium* **11**(2-3): 57-62

Donnelly-Roberts, D, Jarvis, M (2007a) Discovery of P2X7 receptor-selective antagonists offers new insights into P2X7 receptor function and indicates a role in chronic pain states. *Br J Pharmacol* **151**(5)**:** 571-579.

Donnelly-Roberts, D, Namovic, M, Faltynek, C, Jarvis, M (2004) Mitogen-activated protein kinase and caspase signaling pathways are required for P2X7 receptor (P2X7R)-induced pore formation in human THP-1 cells. *J Pharmacol Exp Ther* **308**(3)**:** 1053-1061.

Donnelly-Roberts, DL, Jarvis, MF (2007b) Discovery of P2X7 receptor-selective antagonists offers new insights into P2X7 receptor function and indicates a role in chronic pain states. *Br J Pharmacol* **151**(5)**:** 571-579.

Dostert, C, Pétrilli, V, Van Bruggen, R, Steele, C, Mossman, B, Tschopp, J (2008) Innate immune activation through Nalp3 inflammasome sensing of asbestos and silica. *Science* **320**(5876)**:** 674-677.

Drury, AN, Szent-Gyorgyi, A (1929) The physiological activity of adenine compounds with especial reference to their action upon the mammalian heart. *J Physiol* **68**(3)**:** 213-237.

Dunne, A, O'Neill, LA (2003) The interleukin-1 receptor/Toll-like receptor superfamily: signal transduction during inflammation and host defense. *Sci STKE* **2003**(171)**:** re3.

Eastgate, JA, Symons, JA, Wood, NC, Grinlinton, FM, di Giovine, FS, Duff, GW (1988) Correlation of plasma interleukin 1 levels with disease activity in rheumatoid arthritis. *Lancet* **2**(8613)**:** 706-709.

El Benna, J, Hayem, G, Dang, P, Fay, M, Chollet-Martin, S, Elbim, C, Meyer, O, Gougerot-Pocidalo, M (2002) NADPH oxidase priming and p47phox phosphorylation in neutrophils from synovial fluid of patients with rheumatoid arthritis and spondylarthropathy. *Inflammation* **26**(6)**:** 273-278.

Elliott, J, Surprenant, A, Marelli-Berg, F, Cooper, J, Cassady-Cain, R, Wooding, C, Linton, K, Alexander, D, Higgins, C (2005) Membrane phosphatidylserine distribution as a non-apoptotic signalling mechanism in lymphocytes. *Nat Cell Biol* **7**(8)**:** 808-816.

Enari, M, Sakahira, H, Yokoyama, H, Okawa, K, Iwamatsu, A, Nagata, S (1998) A caspase-activated DNase that degrades DNA during apoptosis, and its inhibitor ICAD. *Nature* **391**(6662)**:** 43-50.

Evans, R, Lewis, C, Virginio, C, Lundstrom, K, Buell, G, Surprenant, A, North, R (1996) Ionic permeability of, and divalent cation effects on, two ATP-gated cation channels (P2X receptors) expressed in mammalian cells. *J Physiol* **497 (Pt 2):** 413-422.

Fairbairn, IP, Stober, CB, Kumararatne, DS, Lammas, DA (2001) ATP-mediated killing of intracellular mycobacterium by macrophages is a $P2X_7$-dependent process inducing bacterial cell death by phagosome-lysosome fusion. *J Immunol* **167**(6)**:** 3300-3307**.**

Faria, R, Defarias, F, Alves, L (2005) Are second messengers crucial for opening the pore associated with P2X7 receptor? *Am J Physiol Cell Physiol* **288**(2)**:** C260-271.

Feoktistov, I, Biaggioni, I (1997) Adenosine A2B receptors. *Pharmacol Rev* **49**(4)**:** 381-402.

Feoktistov, I, Goldstein, A, Biaggioni, I (1999) Role of p38 mitogen-activated protein kinase and extracellular signal-regulated protein kinase kinase in adenosine A2B receptor-mediated interleukin-8 production in human mast cells. *Mol Pharmacol* **55**(4)**:** 726-734.

Fernandes-Alnemri, T, Wu, J, Yu, JW, Datta, P, Miller, B, Jankowski, W, Rosenberg, S, Zhang, J, Alnemri, ES (2007) The pyroptosome: a supramolecular assembly of ASC dimers mediating inflammatory cell death via caspase-1 activation. *Cell Death Differ* **14**(9)**:** 1590-1604.

Ferrari, D, Chiozzi, P, Falzoni, S, Dal Susino, M, Collo, G, Buell, G, Di Virgilio, F (1997a) ATP-mediated cytotoxicity in microglial cells. *Neuropharmacology* **36**(9)**:** 1295-1301.

Ferrari, D, Chiozzi, P, Falzoni, S, Dal Susino, M, Melchiorri, L, Baricordi, O, Di Virgilio, F (1997b) Extracellular ATP triggers IL-1 beta release by activating the purinergic P2Z receptor of human macrophages. *J Immunol* **159**(3)**:** 1451-1458.

Ferrari, D, Chiozzi, P, Falzoni, S, Hanau, S, Di Virgilio, F (1997c) Purinergic modulation of interleukin-1 beta release from microglial cells stimulated with bacterial endotoxin. *J Exp Med* **185**(3)**:** 579-582.

Ferrari, D, Idzko, M, Dichmann, S, Purlis, D, Virchow, C, Norgauer, J, Chiozzi, P, Di Virgilio, F, Luttmann, W (2000) P2 purinergic receptors of human eosinophils: characterization and coupling to oxygen radical production. *FEBS Lett* **486**(3)**:** 217-224.

Ferrari, D, Pizzirani, C, Adinolfi, E, Lemoli, RM, Curti, A, Idzko, M, Panther, E, Di Virgilio, F (2006) The P2X7 receptor: a key player in IL-1 processing and release. *J Immunol* **176**(7)**:** 3877-3883.

Ferrari, D, Pizzirani, C, Gulinelli, S, Callegari, G, Chiozzi, P, Idzko, M, Panther, E, Di Virgilio, F (2007) Modulation of P2X7 receptor functions by polymyxin B: crucial role of the hydrophobic tail of the antibiotic molecule. *Br J Pharmacol* **150**(4)**:** 445-454.

Ferrell, WR, Lockhart, JC, Kelso, EB, Dunning, L, Plevin, R, Meek, SE, Smith, AJ, Hunter, GD, McLean, JS, McGarry, F, Ramage, R, Jiang, L, Kanke, T, Kawagoe, J (2003) Essential role for proteinase-activated receptor-2 in arthritis. *J Clin Invest* **111**(1)**:** 35-41.

Fink, S, Cookson, B (2005) Apoptosis, pyroptosis, and necrosis: mechanistic description of dead and dying eukaryotic cells. *Infect Immun* **73**(4)**:** 1907-1916.

Fink, S, Cookson, B (2006) Caspase-1-dependent pore formation during pyroptosis leads to osmotic lysis of infected host macrophages. *Cell Microbiol* **8**(11)**:** 1812-1825.

Fink, S, Cookson, B (2007) Pyroptosis and host cell death responses during Salmonella infection. *Cell Microbiol* **9**(11)**:** 2562-2570.

Fiorucci, S, Santucci, L, Antonelli, E, Distrutti, E, Del Sero, G, Morelli, O, Romani, L, Federici, B, Del Soldato, P, Morelli, A (2000a) NO-aspirin protects from T cell-mediated liver injury by inhibiting caspase-dependent processing of Th1-like cytokines. *Gastroenterology* **118**(2)**:** 404-421.

Fiorucci, S, Santucci, L, Cirino, G, Mencarelli, A, Familiari, L, Soldato, P, Morelli, A (2000b) IL-1 beta converting enzyme is a target for nitric oxide-releasing aspirin: new insights in the antiinflammatory mechanism of nitric oxide-releasing nonsteroidal antiinflammatory drugs. *J Immunol* **165**(9)**:** 5245-5254.

Forman, H, Torres, M (2001) Redox signaling in macrophages. *Mol Aspects Med* **22**(4-5)**:** 189-216.

Fraker, P, King, L, Laakko, T, Vollmer, T (2000) The dynamic link between the integrity of the immune system and zinc status. *J Nutr* **130**(5S Suppl)**:** 1399S-1406S.

Gaston, B, Carver, J, Doctor, A, Palmer, L (2003) S-nitrosylation signaling in cell biology. *Mol Interv* **3**(5)**:** 253-263.

Gever, JR, Cockayne, DA, Dillon, MP, Burnstock, G, Ford, AP (2006) Pharmacology of P2X channels. *Pflugers Arch* **452**(5)**:** 513-537.

Ghayur, T, Banerjee, S, Hugunin, M, Butler, D, Herzog, L, Carter, A, Quintal, L, Sekut, L, Talanian, R, Paskind, M, Wong, W, Kamen, R, Tracey, D, Allen, H (1997) Caspase-1 processes IFN-gamma-inducing factor and regulates LPS-induced IFN-gamma production. *Nature* **386**(6625)**:** 619-623.

Giesen, P, Rauch, U, Bohrmann, B, Kling, D, Roqué, M, Fallon, J, Badimon, J, Himber, J, Riederer, M, Nemerson, Y (1999) Blood-borne tissue factor: another view of thrombosis. *Proc Natl Acad Sci U S A* **96**(5)**:** 2311-2315.

Giniatullin, R, Sokolova, E, Nistri, A (2003) Modulation of P2X3 receptors by Mg2+ on rat DRG neurons in culture. *Neuropharmacology* **44**(1)**:** 132-140.

Gray, J, Heck, D, Mishin, V, Smith, P, Hong, J, Thiruchelvam, M, Cory-Slechta, D, Laskin, D, Laskin, J (2007) Paraquat increases cyanide-insensitive respiration in murine lung epithelial cells by activating an NAD(P)H:paraquat oxidoreductase: identification of the enzyme as thioredoxin reductase. *J Biol Chem* **282**(11)**:** 7939-7949.

Green, J, Paget, M (2004) Bacterial redox sensors. *Nat Rev Microbiol* **2**(12)**:** 954-966.

Greenberg, S, Grinstein, S (2002) Phagocytosis and innate immunity. *Curr Opin Immunol* **14**(1)**:** 136-145.

Greeno, E, Bach, R, Moldow, C (1996) Apoptosis is associated with increased cell surface tissue factor procoagulant activity. *Lab Invest* **75**(2)**:** 281-289.

Gromer, S, Arscott, L, Williams, CJ, Schirmer, R, Becker, K (1998) Human placenta thioredoxin reductase. Isolation of the selenoenzyme, steady state kinetics, and inhibition by therapeutic gold compounds. *J Biol Chem* **273**(32)**:** 20096-20101.

Gu, Y, Kuida, K, Tsutsui, H, Ku, G, Hsiao, K, Fleming, MA, Hayashi, N, Higashino, K, Okamura, H, Nakanishi, K, Kurimoto, M, Tanimoto, T, Flavell, RA, Sato, V, Harding, MW, Livingston, DJ, Su, MS (1997) Activation of interferon-gamma inducing factor mediated by interleukin-1beta converting enzyme. *Science* **275**(5297)**:** 206-209.

Guerra, A, Gavala, M, Chung, H, Bertics, P (2007) Nucleotide receptor signalling and the generation of reactive oxygen species. *Purinergic Signal* **3**(1-2)**:** 39-51.

Halle, A, Hornung, V, Petzold, G, Stewart, C, Monks, B, Reinheckel, T, Fitzgerald, K, Latz, E, Moore, K, Golenbock, D (2008) The NALP3 inflammasome is involved in the innate immune response to amyloid-beta. *Nat Immunol* **9**(8)**:** 857-865.

Hampton, M, Orrenius, S (1997) Dual regulation of caspase activity by hydrogen peroxide: implications for apoptosis. *FEBS Lett* **414**(3)**:** 552-556.

Hanson, G, Aggeler, R, Oglesbee, D, Cannon, M, Capaldi, R, Tsien, R, Remington, S (2004) Investigating mitochondrial redox potential with redox-sensitive green fluorescent protein indicators. *J Biol Chem* **279**(13)**:** 13044-13053.

Hawkins, P, Lachmann, H, Aganna, E, McDermott, M (2004) Spectrum of clinical features in Muckle-Wells syndrome and response to anakinra. *Arthritis Rheum* **50**(2)**:** 607-612.

Henriksson, C, Klingenberg, O, Hellum, M, Landsverk, K, Joø, G, Westvik, A, Kierulf, P (2007) Calcium ionophore-induced de-encryption of tissue factor in monocytes is associated with extensive cell death. *Thromb Res* **119**(5)**:** 621-630.

Hentze, H, Lin, X, Choi, M, Porter, A (2003) Critical role for cathepsin B in mediating caspase-1-dependent interleukin-18 maturation and caspase-1-independent necrosis triggered by the microbial toxin nigericin. *Cell Death Differ* **10**(9)**:** 956-968.

Heumüller, S, Wind, S, Barbosa-Sicard, E, Schmidt, HHHW, Busse, R, Schröder, K, Brandes, RP (2008) Apocynin is not an inhibitor of vascular NADPH oxidases but an antioxidant. *Hypertension* **51**(2)**:** 211-217.

Hewinson, J, Moore, S, Glover, C, Watts, A, MacKenzie, A (2008) A key role for redox signaling in rapid P2X7 receptor-induced IL-1 beta processing in human monocytes. *J Immunol* **180**(12)**:** 8410-8420.

Hibell, A, Thompson, K, Xing, M, Humphrey, P, Michel, A (2001) Complexities of measuring antagonist potency at P2X(7) receptor orthologs. *J Pharmacol Exp Ther* **296**(3)**:** 947-957.

Hiken, J, Steinberg, T (2004) ATP downregulates P2X7 and inhibits osteoclast formation in RAW cells. *Am J Physiol Cell Physiol* **287**(2)**:** C403-412.

Hjortoe, G, Petersen, L, Albrektsen, T, Sorensen, B, Norby, P, Mandal, S, Pendurthi, U, Rao, L (2004) Tissue factor-factor VIIa-specific up-regulation of IL-8 expression in MDA-MB-231 cells is mediated by PAR-2 and results in increased cell migration. *Blood* **103**(8)**:** 3029-3037.

Hofer, AM, Brown, EM (2003) Extracellular calcium sensing and signalling. *Nat Rev Mol Cell Biol* **4**(7): 530-538.

Honore, P, Donnelly-Roberts, D, Namovic, MT, Hsieh, G, Zhu, CZ, Mikusa, JP, Hernandez, G, Zhong, C, Gauvin, DM, Chandran, P, Harris, R, Medrano, AP, Carroll, W, Marsh, K, Sullivan, JP, Faltynek, CR, Jarvis, MF (2006) A-740003 [N-(1-{[(Cyanoimino)(5-quinolinylamino) methyl]amino}-2,2-dimethylpropyl)-2-(3,4-dimethoxyphenyl)acetamide], a Novel and Selective P2X7 Receptor Antagonist, Dose-Dependently Reduces Neuropathic Pain in the Rat. *J Pharmacol Exp Ther* **319**(3)**:** 1376-1385.

Huang, Z, Pinto, J, Deng, H, Richie, JJ (2008) Inhibition of caspase-3 activity and activation by protein glutathionylation. *Biochem Pharmacol* **75**(11)**:** 2234-2244.

Huidobro-Toro, J, Lorca, R, Coddou, C (2008) Trace metals in the brain: allosteric modulators of ligand-gated receptor channels, the case of ATP-gated P2X receptors. *Eur Biophys J* **37**(3)**:** 301-314.

Humphreys, B, Rice, J, Kertesy, S, Dubyak, G (2000) Stress-activated protein kinase/JNK activation and apoptotic induction by the macrophage P2X7 nucleotide receptor. *J Biol Chem* **275**(35)**:** 26792-26798.

Humphreys, B, Virginio, C, Surprenant, A, Rice, J, Dubyak, G (1998) Isoquinolines as antagonists of the P2X7 nucleotide receptor: high selectivity for the human versus rat receptor homologues. *Mol Pharmacol* **54**(1)**:** 22-32.

Hurd, T, Filipovska, A, Costa, N, Dahm, C, Murphy, M (2005) Disulphide formation on mitochondrial protein thiols. *Biochem Soc Trans* **33**(Pt 6)**:** 1390-1393.

Hurd, T, Prime, T, Harbour, M, Lilley, K, Murphy, M (2007) Detection of reactive oxygen species-sensitive thiol proteins by redox difference gel electrophoresis: implications for mitochondrial redox signaling. *J Biol Chem* **282**(30)**:** 22040-22051.

Jacobson, K, Gao, Z (2006) Adenosine receptors as therapeutic targets. *Nat Rev Drug Discov* **5**(3)**:** 247-264.

Jacobson, KA, Jarvis, MF, Williams, M (2002) Purine and Pyrimidine (P2) Receptors as Drug Targets. *J. Med. Chem.* **45**(19)**:** 4057-4093.

Jaffrey, S, Snyder, S (2001) The biotin switch method for the detection of S-nitrosylated proteins. *Sci STKE* **2001**(86)**:** PL1.

Jarvis, MF, Burgard, EC, McGaraughty, S, Honore, P, Lynch, K, Brennan, TJ, Subieta, A, van Biesen, T, Cartmell, J, Bianchi, B, Niforatos, W, Kage, K, Yu, H, Mikusa, J, Wismer, CT, Zhu, CZ, Chu, K, Lee, C-H, Stewart, AO, Polakowski, J, Cox, BF, Kowaluk, E, Williams, M, Sullivan, J, Faltynek, C (2002) A-317491, a novel potent and selective non-nucleotide antagonist of P2X3 and P2X2/3 receptors, reduces chronic inflammatory and neuropathic pain in the rat. *Proc Natl Acad Sci U S A* 99(26)**:** 17179-17184.

Jarvis, MF, Khakh, BS (2009) ATP-gated P2X cation-channels. *Neuropharmacology* **56**(1): 208-215

Jiang, L (2008) Inhibition of P2X(7) receptors by divalent cations: old action and new insight. *Eur Biophys J*.

Jiang, L, Mackenzie, A, North, R, Surprenant, A (2000) Brilliant blue G selectively blocks ATP-gated rat P2X(7) receptors. *Mol Pharmacol* **58**(1)**:** 82-88.

Jiang, L, Rassendren, F, Mackenzie, A, Zhang, Y, Surprenant, A, North, R (2005) N-methyl-D-glucamine and propidium dyes utilize different permeation pathways at rat P2X(7) receptors. *Am J Physiol Cell Physiol* **289**(5)**:** C1295-1302.

Jun, D, Kim, J, Jung, S, Song, R, Noh, J, Park, Y, Ryu, S, Kim, J, Kong, Y, Chung, J, Kim, K (2007) Extracellular ATP mediates necrotic cell swelling in SN4741 dopaminergic neurons through P2X7 receptors. *J Biol Chem* **282**(52)**:** 37350-37358.

Kahlenberg, J, Dubyak, G (2004a) Differing caspase-1 activation states in monocyte versus macrophage models of IL-1beta processing and release. *J Leukoc Biol* **76**(3)**:** 676-684.

Kahlenberg, J, Dubyak, G (2004b) Mechanisms of caspase-1 activation by P2X7 receptor-mediated K+ release. *Am J Physiol Cell Physiol* **286**(5)**:** C1100-1108.

Kahns, S, Kalai, M, Jakobsen, LD, Clark, BF, Vandenabeele, P, Jensen, PH (2003) Caspase-1 and caspase-8 cleave and inactivate cellular parkin. *J Biol Chem* **278**(26)**:** 23376-23380.

Kang, S, Wang, S, Hara, H, Peterson, E, Namura, S, Amin-Hanjani, S, Huang, Z, Srinivasan, A, Tomaselli, K, Thornberry, N, Moskowitz, M, Yuan, J (2000) Dual role of caspase-11 in mediating activation of caspase-1 and caspase-3 under pathological conditions. *J Cell Biol* **149**(3)**:** 613-622.

Kanneganti, T, Ozören, N, Body-Malapel, M, Amer, A, Park, J, Franchi, L, Whitfield, J, Barchet, W, Colonna, M, Vandenabeele, P, Bertin, J, Coyle, A, Grant, E, Akira, S, Núñez, G (2006) Bacterial RNA and small antiviral compounds activate caspase-1 through cryopyrin/Nalp3. *Nature* **440**(7081)**:** 233-236.

Kanneganti, T-D, Lamkanfi, M, Kim, Y-G, Chen, G, Park, J-H, Franchi, L, Vandenabeele, P, Nunez, G (2007) Pannexin-1-Mediated Recognition of Bacterial Molecules Activates the Cryopyrin Inflammasome Independent of Toll-like Receptor Signaling. *Immunity* **26**(4)**:** 433-443.

Kaur, H, Halliwell, B (1994) Evidence for nitric oxide-mediated oxidative damage in chronic inflammation. Nitrotyrosine in serum and synovial fluid from rheumatoid patients. *FEBS Lett* **350**(1)**:** 9-12.

Kawagoe, J, Takizawa, T, Matsumoto, J, Tamiya, M, Meek, SE, Smith, AJ, Hunter, GD, Plevin, R, Saito, N, Kanke, T, Fujii, M, Wada, Y (2002) Effect of protease-activated receptor-2 deficiency on allergic dermatitis in the mouse ear. *Jpn J Pharmacol* **88**(1)**:** 77-84.

Kawai, T, Akira, S (2006) TLR signaling. *Cell Death Differ* **13**(5)**:** 816-825.

Key, N, Geng, J, Bach, R (2007) Tissue factor; from Morawitz to microparticles. *Trans Am Clin Climatol Assoc* **118:** 165-173.

Key, N, Slungaard, A, Dandelet, L, Nelson, S, Moertel, C, Styles, L, Kuypers, F, Bach, R (1998) Whole blood tissue factor procoagulant activity is elevated in patients with sickle cell disease. *Blood* **91**(11)**:** 4216-4223.

Khakh, B, Bao, X, Labarca, C, Lester, H (1999) Neuronal P2X transmitter-gated cation channels change their ion selectivity in seconds. *Nat Neurosci* **2**(4)**:** 322-330.

Kim, J, Yoon, H, Kwon, K, Lee, S, Rhee, S (2000) Identification of proteins containing cysteine residues that are sensitive to oxidation by hydrogen peroxide at neutral pH. *Anal Biochem* **283**(2)**:** 214-221.

Kim, Y, Talanian, R, Li, J, Billiar, T (1998) Nitric oxide prevents IL-1beta and IFN-gamma-inducing factor (IL-18) release from macrophages by inhibiting caspase-1 (IL-1beta-converting enzyme). *J Immunol* **161**(8)**:** 4122-4128.

Kirii, H, Niwa, T, Yamada, Y, Wada, H, Saito, K, Iwakura, Y, Asano, M, Moriwaki, H, Seishima, M (2003) Lack of interleukin-1beta decreases the severity of atherosclerosis in ApoE-deficient mice. *Arterioscler Thromb Vasc Biol* **23**(4)**:** 656-660.

Kirkpatrick, D, Kuperus, M, Dowdeswell, M, Potier, N, Donald, L, Kunkel, M, Berggren, M, Angulo, M, Powis, G (1998) Mechanisms of inhibition of the thioredoxin growth factor system by antitumor 2-imidazolyl disulfides. *Biochem Pharmacol* **55**(7)**:** 987-994.

Klapperstück, M, Büttner, C, Schmalzing, G, Markwardt, F (2001) Functional evidence of distinct ATP activation sites at the human P2X(7) receptor. *J Physiol* **534**(Pt 1)**:** 25-35.

Kong, Q, Wang, M, Liao, Z, Camden, J, Yu, S, Simonyi, A, Sun, G, Gonzalez, F, Erb, L, Seye, C, Weisman, G (2005) P2X(7) nucleotide receptors mediate caspase-8/9/3-dependent apoptosis in rat primary cortical neurons. *Purinergic Signal* **1**(4)**:** 337-347.

Kothakota, S, Azuma, T, Reinhard, C, Klippel, A, Tang, J, Chu, K, McGarry, T, Kirschner, M, Koths, K, Kwiatkowski, D, Williams, L (1997) Caspase-3-generated fragment of gelsolin: effector of morphological change in apoptosis. *Science* **278**(5336)**:** 294-298.

Krasnow, SW, Zhang, LQ, Leung, KY, Osborn, L, Kunkel, S, Nabel, GJ (1991) Tumor necrosis factor-alpha, interleukin 1, and phorbol myristate acetate are independent activators of NF-kappa B which differentially activate T cells. *Cytokine* **3**(5)**:** 372-379.

Kufer, TA, Fritz, JH, Philpott, DJ (2005) NACHT-LRR proteins (NLRs) in bacterial infection and immunity. *Trends Microbiol* **13**(8)**:** 381-388.

Kuhns, D, Wright, D, Nath, J, Kaplan, S, Basford, R (1988) ATP induces transient elevations of [Ca2+]i in human neutrophils and primes these cells for enhanced O2- generation. *Lab Invest* **58**(4)**:** 448-453.

Kwon, KH, Ohigashi, H, Murakami, A (2007) Dextran sulfate sodium enhances interleukin-1[beta] release via activation of p38 MAPK and ERK1/2 pathways in murine peritoneal macrophages. *Life Sciences* **81**(5)**:** 362-371.

Labasi, J, Petrushova, N, Donovan, C, McCurdy, S, Lira, P, Payette, M, Brissette, W, Wicks, J, Audoly, L, Gabel, C (2002) Absence of the P2X7 receptor alters leukocyte function and attenuates an inflammatory response. *J Immunol* **168**(12)**:** 6436-6445.

Laliberte, R, Eggler, J, Gabel, C (1999) ATP treatment of human monocytes promotes caspase-1 maturation and externalization. *J Biol Chem* **274**(52)**:** 36944-36951.

Landers, S, Gupta, M, Lewis, J (1994) Ultrastructural localization of tissue factor on monocyte-derived macrophages and macrophage foam cells associated with atherosclerotic lesions. *Virchows Arch* **425**(1)**:** 49-54.

Langen, P, Hucho, F (2008) Karl Lohmann and the Discovery of ATP. *Angew Chem Int Edit* **47**(10)**:** 1824-1827.

Le Feuvre, R, Brough, D, Iwakura, Y, Takeda, K, Rothwell, N (2002) Priming of macrophages with lipopolysaccharide potentiates P2X7-mediated cell death via a caspase-1-dependent mechanism, independently of cytokine production. *J Biol Chem* **277**(5)**:** 3210-3218.

Lee, Y, Kim, J, Chen, J, Song, J (2002) Enhancement of metabolic oxidative stress-induced cytotoxicity by the thioredoxin inhibitor 1-methylpropyl 2-imidazolyl disulfide is mediated through the ASK1-SEK1-JNK1 pathway. *Mol Pharmacol* **62**(6)**:** 1409-1417.

Lentz, B (2003) Exposure of platelet membrane phosphatidylserine regulates blood coagulation. *Prog Lipid Res* **42**(5)**:** 423-438.

Leverrier, Y, Ridley, A (2001) Apoptosis: caspases orchestrate the ROCK 'n' bleb. *Nat Cell Biol* **3**(4)**:** E91-93.

Levi, M (2003) Measuring activated protein C in plasma to assess its role as a critical modulator of coagulation and inflammation. *J Thromb Haemost* **1**(4)**:** 643-644.

Levi, M, de Jonge, E, van der Poll, T, ten Cate, H (1999) Disseminated intravascular coagulation. *Thromb Haemost* **82**(2)**:** 695-705.

Levi, M, Keller, TT, van Gorp, E, ten Cate, H (2003) Infection and inflammation and the coagulation system. *Cardiovasc Res* **60**(1)**:** 26-39.

Li, J, Billiar, TR, Talanian, RV, Kim, YM (1997a) Nitric Oxide Reversibly Inhibits Seven Members of the Caspase Family via S-Nitrosylation. *Biochem Biophys Res Commun* **240**(2)**:** 419-424.

Li, J, Wheatcroft, S, Fan, L, Kearney, M, Shah, A (2004) Opposing roles of p47phox in basal versus angiotensin II-stimulated alterations in vascular O2- production, vascular tone, and mitogen-activated protein kinase activation. *Circulation* **109**(10)**:** 1307-1313.

Li, M, Ona, VO, Guegan, C, Chen, M, Jackson-Lewis, V, Andrews, LJ, Olszewski, AJ, Stieg, PE, Lee, JP, Przedborski, S, Friedlander, RM (2000) Functional role of caspase-1 and caspase-3 in an ALS transgenic mouse model. *Science* **288**(5464)**:** 335-339.

Li, P, Allen, H, Banerjee, S, Franklin, S, Herzog, L, Johnston, C, McDowell, J, Paskind, M, Rodman, L, Salfeld, J (1995) Mice deficient in IL-1 beta-converting enzyme are defective in production of mature IL-1 beta and resistant to endotoxic shock. *Cell* **80**(3)**:** 401-411.

Li, P, Nijhawan, D, Budihardjo, I, Srinivasula, SM, Ahmad, M, Alnemri, ES, Wang, X (1997b) Cytochrome c and dATP-dependent formation of Apaf-1/caspase-9 complex initiates an apoptotic protease cascade. *Cell* **91**(4)**:** 479-489.

Li, Y, Trush, M (1998) Diphenyleneiodonium, an NAD(P)H oxidase inhibitor, also potently inhibits mitochondrial reactive oxygen species production. *Biochem Biophys Res Commun* **253**(2)**:** 295-299.

Lin, H, Chen, C, Chen, B (2001) Resistance of bone marrow-derived macrophages to apoptosis is associated with the expression of X-linked inhibitor of apoptosis protein in primary cultures of bone marrow cells. *Biochem J* **353**(Pt 2)**:** 299-306.

Lipmann, F (1941) Metabolic Generation and Utilization of Phosphate Bond Energy. In: *Advances in Enzymology and Related Areas of Molecular Biology*, F. F. Nord, CHW (ed), pp 99-162.

Liu, X, Surprenant, A, Mao, H-J, Roger, S, Xia, R, Bradley, H, Jiang, L-H (2008) Identification of Key Residues Coordinating Functional Inhibition of P2X7 Receptors by Zinc and Copper. *Mol Pharmacol* **73**(1)**:** 252-259.

Liu, Y, Min, W (2002) Thioredoxin promotes ASK1 ubiquitination and degradation to inhibit ASK1-mediated apoptosis in a redox activity-independent manner. *Circ Res* **90**(12)**:** 1259-1266.

Liu, Y, Pelekanakis, K, Woolkalis, M (2004) Thrombin and tumor necrosis factor alpha synergistically stimulate tissue factor expression in human endothelial cells: regulation through c-Fos and c-Jun. *J Biol Chem* **279**(34)**:** 36142-36147.

Locovei, S, Scemes, E, Qiu, F, Spray, D, Dahl, G (2007) Pannexin1 is part of the pore forming unit of the P2X(7) receptor death complex. *FEBS Lett* **581**(3)**:** 483-488.

Lorca, R, Coddou, C, Gazitúa, M, Bull, P, Arredondo, C, Huidobro-Toro, J (2005) Extracellular histidine residues identify common structural determinants in the copper/zinc P2X2 receptor modulation. *J Neurochem* **95**(2)**:** 499-512.

MacKenzie, A, Wilson, H, Kiss-Toth, E, Dower, S, North, R, Surprenant, A (2001) Rapid secretion of interleukin-1beta by microvesicle shedding. *Immunity* **15**(5)**:** 825-835.

Mackenzie, A, Young, M, Adinolfi, E, Surprenant, A (2005) Pseudoapoptosis induced by brief activation of ATP-gated P2X7 receptors. *J Biol Chem* **280**(40)**:** 33968-33976.

Mannick, J, Hausladen, A, Liu, L, Hess, D, Zeng, M, Miao, Q, Kane, L, Gow, A, Stamler, J (1999) Fas-induced caspase denitrosylation. *Science* **284**(5414)**:** 651-654.

Mannick, J, Schonhoff, C, Papeta, N, Ghafourifar, P, Szibor, M, Fang, K, Gaston, B (2001) S-Nitrosylation of mitochondrial caspases. *J Cell Biol* **154**(6)**:** 1111-1116.

Mariathasan, S, Weiss, DS, Newton, K, McBride, J, O'Rourke, K, Roose-Girma, M, Lee, WP, Weinrauch, Y, Monack, DM, Dixit, VM (2006) Cryopyrin activates the inflammasome in response to toxins and ATP. *Nature* **440**(7081)**:** 228-232.

Martinon, F, Burns, K, Tschopp, J (2002) The Inflammasome: A Molecular Platform Triggering Activation of Inflammatory Caspases and Processing of proIL-[beta]. *Mol Cell* **10**(2)**:** 417-426.

Martinon, F, Pétrilli, V, Mayor, A, Tardivel, A, Tschopp, J (2006) Gout-associated uric acid crystals activate the NALP3 inflammasome. *Nature* **440**(7081)**:** 237-241.

May, J, Cobb, C, Mendiratta, S, Hill, K, Burk, R (1998) Reduction of the ascorbyl free radical to ascorbate by thioredoxin reductase. *J Biol Chem* **273**(36)**:** 23039-23045.

May, J, Mendiratta, S, Hill, K, Burk, R (1997) Reduction of dehydroascorbate to ascorbate by the selenoenzyme thioredoxin reductase. *J Biol Chem* **272**(36)**:** 22607-22610.

McGaraughty, S, Chu, K, Namovic, M, Donnelly-Roberts, D, Harris, R, Zhang, X, Shieh, C, Wismer, C, Zhu, C, Gauvin, D, Fabiyi, A, Honore, P, Gregg, R, Kort, M, Nelson, D, Carroll, W, Marsh, K, Faltynek, C, Jarvis, M (2007) P2X7-related modulation of pathological nociception in rats. *Neuroscience* **146**(4)**:** 1817-1828.

Medzhitov, R, Preston-Hurlburt, P, Kopp, E, Stadlen, A, Chen, C, Ghosh, S, Janeway, CA, Jr. (1998) MyD88 is an adaptor protein in the hToll/IL-1 receptor family signaling pathways. *Mol Cell* **2**(2)**:** 253-258.

Mehta, V, Hart, J, Wewers, M (2001) ATP-stimulated release of interleukin (IL)-1beta and IL-18 requires priming by lipopolysaccharide and is independent of caspase-1 cleavage. *J Biol Chem* **276**(6)**:** 3820-3826.

Meissner, F, Molawi, K, Zychlinsky, A (2008) Superoxide dismutase 1 regulates caspase-1 and endotoxic shock. *Nat Immunol* **9**(8)**:** 866-872.

Michel, A, Chessell, I, Humphrey, P (1999) Ionic effects on human recombinant P2X7 receptor function. *N-S Arch Pharmacol* **359**(2)**:** 102-109.

Mitchell, P, Moyle, J (1968) Proton Translocation Coupled to ATP Hydrolysis in Rat Liver Mitochondria. *Eur J Biochem* **4**(4)**:** 530-539.

Moore, S, MacKenzie, A (2007) Murine macrophage P2X7 receptors support rapid prothrombotic responses. *Cell Signal* **19**(4)**:** 855-866.

Morelli, A, Chiozzi, P, Chiesa, A, Ferrari, D, Sanz, J, Falzoni, S, Pinton, P, Rizzuto, R, Olson, M, Di Virgilio, F (2003) Extracellular ATP causes ROCK I-dependent bleb formation in P2X7-transfected HEK293 cells. *Mol Biol Cell* **14**(7)**:** 2655-2664.

Murgia, M, Pizzo, P, Steinberg, T, Di Virgilio, F (1992) Characterization of the cytotoxic effect of extracellular ATP in J774 mouse macrophages. *Biochem J* **288** (Pt 3)**:** 897-901.

Murphy, J, Livingston, F, Gozal, E, Torres, M, Forman, H (1993) Stimulation of the rat alveolar macrophage respiratory burst by extracellular adenine nucleotides. *Am J Respir Cell Mol Biol* **9**(5)**:** 505-510.

Naito, M, Nagashima, K, Mashima, T, Tsuruo, T (1997) Phosphatidylserine externalization is a downstream event of interleukin-1 beta-converting enzyme family protease activation during apoptosis. *Blood* **89**(6)**:** 2060-2066.

Nakazawa, K, Ohno, Y (1997) Effects of neuroamines and divalent cations on cloned and mutated ATP-gated channels. *Eur J Pharmacol* **325**(1)**:** 101-108.

Nalvarte, I, Damdimopoulos, A, Spyrou, G (2004) Human mitochondrial thioredoxin reductase reduces cytochrome c and confers resistance to complex III inhibition. *Free Radic Biol Med* **36**(10)**:** 1270-1278.

Negulyaev, Y, Markwardt, F (2000) Block by extracellular Mg2+ of single human purinergic P2X4 receptor channels expressed in human embryonic kidney cells. *Neurosci Lett* **279**(3)**:** 165-168.

Nelson, D, Gregg, R, Kort, M, Perez-Medrano, A, Voight, E, Wang, Y, Grayson, G, Namovic, M, Donnelly-Roberts, D, Niforatos, W, Honore, P, Jarvis, M, Faltynek, C, Carroll, W (2006) Structure-activity relationship studies on a series of novel, substituted 1-benzyl-5-phenyltetrazole P2X7 antagonists. *J Med Chem* **49**(12)**:** 3659-3666.

Neven, B, Callebaut, I, Prieur, A, Feldmann, J, Bodemer, C, Lepore, L, Derfalvi, B, Benjaponpitak, S, Vesely, R, Sauvain, M, Oertle, S, Allen, R, Morgan, G, Borkhardt, A, Hill, C, Gardner-Medwin, J, Fischer, A, de Saint Basile, G (2004) Molecular basis of the spectral expression of CIAS1 mutations associated with phagocytic cell-mediated autoinflammatory disorders CINCA/NOMID, MWS, and FCU. *Blood* **103**(7)**:** 2809-2815.

Nicke, A, Baumert, H, Rettinger, J, Schmalzing, G (1998) P2X1 and P2X3 receptors form stable trimers: a novel structural motif of ligand-gated ion channels. *EMBO* **17:** 3016-3028.

Noguchi, T, Ishii, K, Fukutomi, H, Naguro, I, Matsuzawa, A, Takeda, K, Ichijo, H (2008) Requirement of reactive oxygen species-dependent activation of ASK1-p38 MAPK pathway for extracellular ATP-induced apoptosis in macrophage. *J Biol Chem* **283**(12)**:** 7657-7665.

Nordberg, J, Arnér, E (2001) Reactive oxygen species, antioxidants, and the mammalian thioredoxin system. *Free Radic Biol Med* **31**(11)**:** 1287-1312.

North, R (2002) Molecular physiology of P2X receptors. *Physiol Rev* **82**(4)**:** 1013-1067.

O'Donnell, V, Smith, G, Jones, O (1994) Involvement of phenyl radicals in iodonium inhibition of flavoenzymes. *Mol Pharmacol* **46**(4)**:** 778-785.

Ohsawa, K, Irino, Y, Nakamura, Y, Akazawa, C, Inoue, K, Kohsaka, S (2007) Involvement of P2X4 and P2Y12 receptors in ATP-induced microglial chemotaxis. *Glia* **55**(6): 604-616.

Omata, Y, Folan, M, Shaw, M, Messer, R, Lockwood, P, Hobbs, D, Bouillaguet, S, Sano, H, Lewis, J, Wataha, J (2006) Sublethal concentrations of diverse gold compounds inhibit mammalian cytosolic thioredoxin reductase (TrxR1). *Toxicol In Vitro* **20**(6)**:** 882-890.

Opal, SM (2003) Interactions between coagulation and inflammation. *Scand J Infect Dis* **35**(9)**:** 545-554.

Opal, SM, Esmon, CT (2003) Bench-to-bedside review: functional relationships between coagulation and the innate immune response and their respective roles in the pathogenesis of sepsis. *Crit Care* **7**(1)**:** 23-38.

Osnes, LT, Westvik, AB, Joo, GB, Okkenhaug, C, Kierulf, P (1996) Inhibition of IL-1 induced tissue factor (TF) synthesis and procoagulant activity (PCA) in purified human monocytes by IL-4, IL-10 and IL-13. *Cytokine* **8**(11)**:** 822-827.

Ossovskaya, VS, Bunnett, NW (2004) Protease-activated receptors: contribution to physiology and disease. *Physiol Rev* **84**(2)**:** 579-621.

Panupinthu, N, Zhao, L, Possmayer, F, Ke, H, Sims, S, Dixon, S (2007) P2X7 nucleotide receptors mediate blebbing in osteoblasts through a pathway involving lysophosphatidic acid. *J Biol Chem* **282**(5)**:** 3403-3412.

Parvathenani, L, Tertyshnikova, S, Greco, C, Roberts, S, Robertson, B, Posmantur, R (2003) P2X7 mediates superoxide production in primary microglia and is up-regulated in a transgenic mouse model of Alzheimer's disease. *J Biol Chem* **278**(15)**:** 13309-13317.

Patton, C, Thompson, S, Epel, D (2004) Some precautions in using chelators to buffer metals in biological solutions. *Cell Calcium* **35**(5)**:** 427-431.

Pelegrin, P, Barroso-Gutierrez, C, Surprenant, A (2008) P2X7 receptor differentially couples to distinct release pathways for IL-1beta in mouse macrophage. *J Immunol* **180**(11)**:** 7147-7157.

Pelegrin, P, Surprenant, A (2007) Pannexin-1 couples to maitotoxin- and nigericin-induced interleukin-1beta release through a dye uptake-independent pathway. *J Biol Chem* **282**(4)**:** 2386-2394.

Pelegrin, P, Surprenant, A (2006) Pannexin-1 mediates large pore formation and interleukin-1beta release by the ATP-gated P2X7 receptor. *EMBO J* **25**(21)**:** 5071-5082.

Perregaux, D, Barberia, J, Lanzetti, A, Geoghegan, K, Carty, T, Gabel, C (1992) IL-1 beta maturation: evidence that mature cytokine formation can be induced specifically by nigericin. *J Immunol* **149**(4)**:** 1294-1303.

Perregaux, D, Gabel, C (1994) Interleukin-1 beta maturation and release in response to ATP and nigericin. Evidence that potassium depletion mediated by these agents is a necessary and common feature of their activity. *J Biol Chem* **269**(21)**:** 15195-15203.

Pfeiffer, Z, Aga, M, Prabhu, U, Watters, J, Hall, D, Bertics, P (2004) The nucleotide receptor P2X7 mediates actin reorganization and membrane blebbing in RAW 264.7 macrophages via p38 MAP kinase and Rho. *J Leukoc Biol* **75**(6)**:** 1173-1182.

Pfeiffer, Z, Guerra, A, Hill, L, Gavala, M, Prabhu, U, Aga, M, Hall, D, Bertics, P (2007) Nucleotide receptor signaling in murine macrophages is linked to reactive oxygen species generation. *Free Radic Biol Med* **42**(10)**:** 1506-1516.

Pixley, RA, De La Cadena, R, Page, JD, Kaufman, N, Wyshock, EG, Chang, A, Taylor, FB, Jr., Colman, RW (1993) The contact system contributes to hypotension but not disseminated intravascular coagulation in lethal bacteremia. In vivo use of a monoclonal anti-factor XII antibody to block contact activation in baboons. *J Clin Invest* **91**(1)**:** 61-68.

Pizzirani, C, Ferrari, D, Chiozzi, P, Adinolfi, E, Sandonà, D, Savaglio, E, Di Virgilio, F (2007) Stimulation of P2 receptors causes release of IL-1beta-loaded microvesicles from human dendritic cells. *Blood* **109**(9)**:** 3856-3864.

Pollock, J, Williams, D, Gifford, M, Li, L, Du, X, Fisherman, J, Orkin, S, Doerschuk, C, Dinauer, M (1995) Mouse model of X-linked chronic granulomatous disease, an inherited defect in phagocyte superoxide production. *Nat Genet* **9**(2)**:** 202-209.

Priel, A, Silberberg, S (2004) Mechanism of ivermectin facilitation of human P2X4 receptor channels. *J Gen Physiol* **123**(3)**:** 281-293.

Pålsson-McDermott, E, O'Neill, L (2007) Building an immune system from nine domains. *Biochem Soc Trans* **35**(Pt 6)**:** 1437-1444.

Pétrilli, V, Dostert, C, Muruve, D, Tschopp, J (2007a) The inflammasome: a danger sensing complex triggering innate immunity. *Curr Opin Immunol* **19**(6)**:** 615-622.

Pétrilli, V, Papin, S, Dostert, C, Mayor, A, Martinon, F, Tschopp, J (2007b) Activation of the NALP3 inflammasome is triggered by low intracellular potassium concentration. *Cell Death Differ* **14**(9)**:** 1583-1589.

Qu, Y, Franchi, L, Nunez, G, Dubyak, GR (2007) Nonclassical IL-1beta Secretion Stimulated by P2X7 Receptors Is Dependent on Inflammasome Activation and Correlated with Exosome Release in Murine Macrophages. *J Immunol* **179**(3): 1913-1925.

Ramachandiran, S, Hansen, J, Jones, D, Richardson, J, Miller, G (2007) Divergent mechanisms of paraquat, MPP+, and rotenone toxicity: oxidation of thioredoxin and caspase-3 activation. *Toxicol Sci* **95**(1)**:** 163-171.

Rhee, S, Chang, T, Bae, Y, Lee, S, Kang, S (2003) Cellular regulation by hydrogen peroxide. *J Am Soc Nephrol* **14**(8 Suppl 3)**:** S211-215.

Rock, FL, Hardiman, G, Timans, JC, Kastelein, RA, Bazan, JF (1998) A family of human receptors structurally related to Drosophila Toll. *Proc Natl Acad Sci U S A* **95**(2)**:** 588-593.

Romagnoli, R, Baraldi, P, Cruz-Lopez, O, Lopez-Cara, C, Preti, D, Borea, P, Gessi, S (2008) The P2X7 receptor as a therapeutic target. *Expert Opin Ther Targets* **12**(5)**:** 647-661.

Ross, J, Auger, M (2002) The Biology of the Macrophage. In: *The Macrophage*, 2 edn, pp 3-47: Oxford University Press, USA.

Saitoh, M, Nishitoh, H, Fujii, M, Takeda, K, Tobiume, K, Sawada, Y, Kawabata, M, Miyazono, K, Ichijo, H (1998) Mammalian thioredoxin is a direct inhibitor of apoptosis signal-regulating kinase (ASK) 1. *EMBO J* **17**(9)**:** 2596-2606.

Satta, N, Toti, F, Feugeas, O, Bohbot, A, Dachary-Prigent, J, Eschwège, V, Hedman, H, Freyssinet, J (1994) Monocyte vesiculation is a possible mechanism for dissemination of membrane-associated procoagulant activities and adhesion molecules after stimulation by lipopolysaccharide. *J Immunol* **153**(7)**:** 3245-3255.

Schachter, J, Motta, A, Zamorano, A, Silva-Souza, H, Guimarães, M, Persechini, P (2008) ATP-induced P2X7-associated uptake of large molecules involves distinct mechanisms for cations and anions in macrophages. *J Cell Sci*.

Schilling, W, Wasylyna, T, Dubyak, G, Humphreys, B, Sinkins, W (1999) Maitotoxin and P2Z/P2X(7) purinergic receptor stimulation activate a common cytolytic pore. *Am J Physiol* **277**(4 Pt 1)**:** C766-776.

Schmidlin, F, Amadesi, S, Dabbagh, K, Lewis, DE, Knott, P, Bunnett, NW, Gater, PR, Geppetti, P, Bertrand, C, Stevens, ME (2002) Protease-activated receptor 2 mediates eosinophil infiltration and hyperreactivity in allergic inflammation of the airway. *J Immunol* **169**(9)**:** 5315-5321.

Schmitz, J, Owyang, A, Oldham, E, Song, Y, Murphy, E, McClanahan, TK, Zurawski, G, Moshrefi, M, Qin, J, Li, X, Gorman, DM, Bazan, JF, Kastelein, RA (2005) IL-33, an interleukin-1-like cytokine that signals via the IL-1 receptor-related protein ST2 and induces T helper type 2-associated cytokines. *Immunity* **23**(5)**:** 479-490.

Schotte, P, Van Criekinge, W, Van de Craen, M, Van Loo, G, Desmedt, M, Grooten, J, Cornelissen, M, De Ridder, L, Vandekerckhove, J, Fiers, W, Vandenabeele, P, Beyaert, R (1998) Cathepsin B-mediated activation of the proinflammatory caspase-11. *Biochem Biophys Res Commun* **251**(1)**:** 379-387.

Schulte, G, Fredholm, B (2003) The G(s)-coupled adenosine A(2B) receptor recruits divergent pathways to regulate ERK1/2 and p38. *Exp Cell Res* **290**(1)**:** 168-176.

Schlülter, T, Steinbach, AC, Steffen, A, Rettig, R, Grisk, O (2008) Apocynin-induced vasodilation involves Rho kinase inhibition but not NADPH oxidase inhibition. *Cardiovasc Res* **80**(2): 271-279.

Scott, J, Hall, A, Grahame, R (1966) Allopurinol in treatment of gout. *Br Med J* **2**(5509)**:** 321-327.

Seil, M, Fontanils, U, Etxebarria, I, Pochet, S, Garcia-Marcos, M, Marino, A, Dehaye, J (2008) Pharmacological evidence for the stimulation of NADPH oxidase by P2X(7) receptors in mouse submandibular glands. *Purinergic Signal*.

Sekiyama, A, Ueda, H, Kashiwamura, S, Sekiyama, R, Takeda, M, Rokutan, K, Okamura, H (2005) A stress-induced, superoxide-mediated caspase-1 activation pathway causes plasma IL-18 upregulation. *Immunity* **22**(6)**:** 669-677.

Seyffert, C, Schmalzing, G, Markwardt, F (2004) Dissecting individual current components of co-expressed human P2X1 and P2X7 receptors. *Curr Top Med Chem* **4**(16)**:** 1719-1730.

Shacka, J, Sahawneh, M, Gonzalez, J, Ye, Y, D'Alessandro, T, Estévez, A (2006) Two distinct signaling pathways regulate peroxynitrite-induced apoptosis in PC12 cells. *Cell Death Differ* **13**(9)**:** 1506-1514.

Silver, IA, Murrills, RJ, Etherington, DJ (1988) Microelectrode studies on the acid environment beneath adherent macrophages and osteoclasts. *Exp. Cell Res.* **175:** 266-276.

Silverman, W, Locovei, S, Dahl, G (2008) Probenecid, a gout remedy, inhibits pannexin 1 channels. *Am J Physiol Cell Physiol* **295**(3)**:** C761-767.

Simon, H, Haj-Yehia, A, Levi-Schaffer, F (2000) Role of reactive oxygen species (ROS) in apoptosis induction. *Apoptosis* **5**(5)**:** 415-418.

Sims, P, Wiedmer, T (2001) Unraveling the mysteries of phospholipid scrambling. *Thromb Haemost* **86**(1)**:** 266-275.

Sitailo, LA, Tibudan, SS, Denning, MF (2002) Activation of caspase-9 is required for UV-induced apoptosis of human keratinocytes. *J Biol Chem* **277**(22)**:** 19346-19352.

Skaper, S, Facci, L, Culbert, A, Evans, N, Chessell, I, Davis, J, Richardson, J (2006) P2X(7) receptors on microglial cells mediate injury to cortical neurons in vitro. *Glia* **54**(3)**:** 234-242.

Sluyter, R, Shemon, A, Wiley, J (2007) P2X(7) receptor activation causes phosphatidylserine exposure in human erythrocytes. *Biochem Biophys Res Commun* **355**(1)**:** 169-173.

Smirnov, M, Ford, D, Esmon, C, Esmon, N (1999) The effect of membrane composition on the hemostatic balance. *Biochemistry* **38**(12)**:** 3591-3598.

Solle, M, Labasi, J, Perregaux, D, Stam, E, Petrushova, N, Koller, B, Griffiths, R, Gabel, C (2001) Altered cytokine production in mice lacking P2X(7) receptors. *J Biol Chem* **276**(1)**:** 125-132.

Sommer, C, Kress, M (2004) Recent findings on how proinflammatory cytokines cause pain: peripheral mechanisms in inflammatory and neuropathic hyperalgesia. *Neurosci Lett* **361**(1-3)**:** 184-187.

Stokes, L, Jiang, L, Alcaraz, L, Bent, J, Bowers, K, Fagura, M, Furber, M, Mortimore, M, Lawson, M, Theaker, J, Laurent, C, Braddock, M, Surprenant, A (2006) Characterization of a selective and potent antagonist of human P2X(7) receptors, AZ11645373. *Br J Pharmacol* **149**(7)**:** 880-887.

Stuehr, D, Fasehun, O, Kwon, N, Gross, S, Gonzalez, J, Levi, R, Nathan, C (1991) Inhibition of macrophage and endothelial cell nitric oxide synthase by diphenyleneiodonium and its analogs. *FASEB J* **5**(1)**:** 98-103.

Suadicani, S, Brosnan, C, Scemes, E (2006) P2X7 receptors mediate ATP release and amplification of astrocytic intercellular Ca2+ signaling. *J Neurosci* **26**(5)**:** 1378-1385.

Suh, B, Kim, J, Namgung, U, Ha, H, Kim, K (2001) P2X7 nucleotide receptor mediation of membrane pore formation and superoxide generation in human promyelocytes and neutrophils. *J Immunol* **166**(11)**:** 6754-6763.

Sumbayev, V (2003) S-nitrosylation of thioredoxin mediates activation of apoptosis signal-regulating kinase 1. *Arch Biochem Biophys* **415**(1)**:** 133-136.

Surprenant, A, Rassendren, F, Kawashima, E, North, R, Buell, G (1996) The cytolytic P2Z receptor for extracellular ATP identified as a P2X receptor (P2X7). *Science* **272**(5262)**:** 735-738.

Swain, S, Siemsen, D, Nelson, L, Sipes, K, Hanson, A, Quinn, M (2003) Inhibition of the neutrophil NADPH oxidase by adenosine is associated with increased movement of flavocytochrome b between subcellular fractions. *Inflammation* **27**(1)**:** 45-58.

Szaba, F, Smiley, S (2002) Roles for thrombin and fibrin(ogen) in cytokine/chemokine production and macrophage adhesion in vivo. *Blood* **99**(3)**:** 1053-1059.

Takeda, K, Noguchi, T, Naguro, I, Ichijo, H (2008) Apoptosis signal-regulating kinase 1 in stress and immune response. *Annu Rev Pharmacol Toxicol* **48:** 199-225.

Taylor, S, Gonzalez-Begne, M, Dewhurst, S, Chimini, G, Higgins, C, Melvin, J, Elliott, J (2008) Sequential shrinkage and swelling underlie P2X7-stimulated lymphocyte phosphatidylserine exposure and death. *J Immunol* **180**(1)**:** 300-308.

Tephly, L, Carter, A (2007) Constitutive NADPH oxidase and increased mitochondrial respiratory chain activity regulate chemokine gene expression. *Am J Physiol Lung Cell Mol Physiol* **293**(5)**:** L1143-1155.

Ting, J, Willingham, S, Bergstralh, D (2008) NLRs at the intersection of cell death and immunity. *Nat Rev Immunol* **8**(5)**:** 372-379.

Tokumitsu, H, Chijiwa, T, Hagiwara, M, Mizutani, A, Terasawa, M, Hidaka, H (1990) KN-62 a specific inhibitor of Ca2+/calmodulin-dependent protein kinase II. *J Biol Chem* **265**(8): 4315-4320.

Turrens, J (1997) Superoxide production by the mitochondrial respiratory chain. *Biosci Rep* **17**(1)**:** 3-8.

Uthaisang, W, Nutt, L, Orrenius, S, Fadeel, B (2003) Phosphatidylserine exposure in Fas type I cells is mitochondria-dependent. *FEBS Lett* **545**(2-3)**:** 110-114.

Valera, S, Hussy, N, Evans, RJ, Adami, N, North, RA, Surprenant, A, Buell, G (1994) A new class of ligand-gated ion channel defined by P2X receptor for extracellular ATP. *Nature* **371**(6497)**:** 516-519.

van der Hoeven, D, Wan, T, Auchampach, J (2008) Activation of the A(3) adenosine receptor suppresses superoxide production and chemotaxis of mouse bone marrow neutrophils. *Mol Pharmacol* **74**(3)**:** 685-696.

Vavricka, SR, Musch, MW, Chang, JE, Nakagawa, Y, Phanvijhitsiri, K, Waypa, TS, Merlin, D, Schneewind, O, Chang, EB (2004) hPepT1 transports muramyl dipeptide, activating NF-[kappa]B and stimulating IL-8 secretion in human colonic Caco2/bbe cells. *Gastroenterology* **127**(5)**:** 1401-1409.

Verhoef, P, Estacion, M, Schilling, W, Dubyak, G (2003) P2X7 receptor-dependent blebbing and the activation of Rho-effector kinases, caspases, and IL-1 beta release. *J Immunol* **170**(11)**:** 5728-5738.

Verhoef, P, Kertesy, S, Lundberg, K, Kahlenberg, J, Dubyak, G (2005) Inhibitory effects of chloride on the activation of caspase-1, IL-1beta secretion, and cytolysis by the P2X7 receptor. *J Immunol* **175**(11)**:** 7623-7634.

Viala, J, Chaput, C, Boneca, IG, Cardona, A, Girardin, SE, Moran, AP, Athman, R, Memet, S, Huerre, MR, Coyle, AJ, DiStefano, PS, Sansonetti, PJ, Labigne, A, Bertin, J, Philpott, DJ, Ferrero, RL (2004) Nod1 responds to peptidoglycan delivered by the Helicobacter pylori cag pathogenicity island. *Nat Immunol* **5**(11)**:** 1166-1174.

Virginio, C, Church, D, North, R, Surprenant, A (1997) Effects of divalent cations, protons and calmidazolium at the rat P2X7 receptor. *Neuropharmacology* **36**(9)**:** 1285-1294.

Virginio, C, MacKenzie, A, Rassendren, F, North, R, Surprenant, A (1999) Pore dilation of neuronal P2X receptor channels. *Nat Neurosci* **2**(4)**:** 315-321.

Virginio, C, North, R, Surprenant, A (1998) Calcium permeability and block at homomeric and heteromeric P2X2 and P2X3 receptors, and P2X receptors in rat nodose neurones. *J Physiol* **510 (Pt 1):** 27-35.

Vogel, SM, Gao, X, Mehta, D, Ye, RD, John, TA, Andrade-Gordon, P, Tiruppathi, C, Malik, AB (2000) Abrogation of thrombin-induced increase in pulmonary microvascular permeability in PAR-1 knockout mice. *Physiol Genomics* **4**(2)**:** 137-145.

Wada, H, Kaneko, T, Wakita, Y, Minamikawa, K, Nagaya, S, Tamaki, S, Deguchi, K, Shirakawa, S (1994) Effect of lipoproteins on tissue factor activity and PAI-II antigen in human monocytes and macrophages. *Int J Cardiol* **47**(1 Suppl)**:** S21-25.

Walev, I, Klein, J, Husmann, M, Valeva, A, Strauch, S, Wirtz, H, Weichel, O, Bhakdi, S (2000) Potassium regulates IL-1 beta processing via calcium-independent phospholipase A2. *J Immunol* **164**(10)**:** 5120-5124.

Wang, X, Wang, H, Figueroa, BE, Zhang, WH, Huo, C, Guan, Y, Zhang, Y, Bruey, JM, Reed, JC, Friedlander, RM (2005) Dysregulation of receptor interacting protein-2 and caspase recruitment domain only protein mediates aberrant caspase-1 activation in Huntington's disease. *J Neurosci* **25**(50)**:** 11645-11654.

Ward, P, Cunningham, T, McCulloch, K, Johnson, K (1988) Regulatory effects of adenosine and adenine nucleotides on oxygen radical responses of neutrophils. *Lab Invest* **58**(4)**:** 438-447.

Watson, W, Pohl, J, Montfort, W, Stuchlik, O, Reed, M, Powis, G, Jones, D (2003) Redox potential of human thioredoxin 1 and identification of a second dithiol/disulfide motif. *J Biol Chem* **278**(35)**:** 33408-33415.

Webb, TE, Simon, J, Krishek, BJ, Bateson, AN, Smart, TG, King, BF, Burnstock, G, Barnard, EA (1993) Cloning and functional expression of a brain G-protein-coupled ATP receptor. *FEBS Letters* **324**(2)**:** 219-225.

Weinreb, G, Mukhopadhyay, K, Majumder, R, Lentz, B (2003) Cooperative roles of factor V(a) and phosphatidylserine-containing membranes as cofactors in prothrombin activation. *J Biol Chem* **278**(8)**:** 5679-5684.

Weir, E, Wyatt, C, Reeve, H, Huang, J, Archer, S, Peers, C (1994) Diphenyleneiodonium inhibits both potassium and calcium currents in isolated pulmonary artery smooth muscle cells. *J Appl Physiol* **76**(6)**:** 2611-2615.

Welsh, N (1996) Interleukin-1beta-induced Ceramide and Diacylglycerol Generation May Lead to Activation of the c-Jun NH(2)-terminal Kinase and the Transcription Factor ATF2 in the Insulin-producing Cell Line RINm5F. *J. Biol. Chem.* **271**(14)**:** 8307-8312.

Wildman, S, Brown, S, Rahman, M, Noel, C, Churchill, L, Burnstock, G, Unwin, R, King, B (2002) Sensitization by extracellular Ca(2+) of rat P2X(5) receptor and its pharmacological properties compared with rat P2X(1). *Mol Pharmacol* **62**(4)**:** 957-966.

Wildman, S, King, B, Burnstock, G (1999a) Modulation of ATP-responses at recombinant rP2X4 receptors by extracellular pH and zinc. *Br J Pharmacol* **126**(3)**:** 762-768.

Wildman, S, King, B, Burnstock, G (1999b) Modulatory activity of extracellular H+ and Zn2+ on ATP-responses at rP2X1 and rP2X3 receptors. *Br J Pharmacol* **128**(2)**:** 486-492.

Williamson, P, Bevers, E, Smeets, E, Comfurius, P, Schlegel, R, Zwaal, R (1995) Continuous analysis of the mechanism of activated transbilayer lipid movement in platelets. *Biochemistry* **34**(33)**:** 10448-10455.

Wilmanski, JM, Petnicki-Ocwieja, T, Kobayashi, KS (2008) NLR proteins: integral members of innate immunity and mediators of inflammatory diseases. *J Leukoc Biol* **83**(1)**:** 13-30.

Wilson, H, Francis, S, Dower, S, Crossman, D (2004) Secretion of intracellular IL-1 receptor antagonist (type 1) is dependent on P2X7 receptor activation. *J Immunol* **173**(2)**:** 1202-1208.

Wong, C, Christen, T, Roth, I, Chadjichristos, C, Derouette, J, Foglia, B, Chanson, M, Goodenough, D, Kwak, B (2006) Connexin37 protects against atherosclerosis by regulating monocyte adhesion. *Nat Med* **12**(8)**:** 950-954.

Wyatt, C, Weir, E, Peers, C (1994) Diphenylene iodonium blocks K+ and Ca2+ currents in type I cells isolated from the neonatal rat carotid body. *Neurosci Lett* **172**(1-2)**:** 63-66.

Xaus, J, Mirabet, M, Lloberas, J, Soler, C, Lluis, C, Franco, R, Celada, A (1999) IFN-gamma up-regulates the A2B adenosine receptor expression in macrophages: a mechanism of macrophage deactivation. *J Immunol* **162**(6)**:** 3607-3614.

Xia, L, Nordman, T, Olsson, J, Damdimopoulos, A, Björkhem-Bergman, L, Nalvarte, I, Eriksson, L, Arnér, E, Spyrou, G, Björnstedt, M (2003) The mammalian cytosolic selenoenzyme thioredoxin reductase reduces ubiquinone. A novel mechanism for defense against oxidative stress. *J Biol Chem* **278**(4)**:** 2141-2146.

Xiong, K, Peoples, R, Montgomery, J, Chiang, Y, Stewart, R, Weight, F, Li, C (1999) Differential modulation by copper and zinc of P2X2 and P2X4 receptor function. *J Neurophysiol* **81**(5)**:** 2088-2094.

Yamamoto, M, Sato, S, Mori, K, Hoshino, K, Takeuchi, O, Takeda, K, Akira, S (2002) Cutting Edge: A Novel Toll/IL-1 Receptor Domain-Containing Adapter That Preferentially Activates the IFN-{beta} Promoter in the Toll-Like Receptor Signaling. *J Immunol* **169**(12)**:** 6668-6672.

Yan, Z, Li, S, Liang, Z, Tomić, M, Stojilkovic, S (2008) The P2X7 receptor channel pore dilates under physiological ion conditions. *J Gen Physiol* **132**(5)**:** 563-573.

Yang, YH, Hall, P, Little, CB, Fosang, AJ, Milenkovski, G, Santos, L, Xue, J, Tipping, P, Morand, EF (2005) Reduction of arthritis severity in protease-activated receptor-deficient mice. *Arthritis Rheum* **52**(4)**:** 1325-1332.

Yiangou, Y, Facer, P, Durrenberger, P, Chessell, IP, Naylor, A, Bountra, C, Banati, RR, Anand, P (2006) COX-2, CB2 and P2X7-immunoreactivities are increased in activated microglial cells/macrophages of multiple sclerosis and amyotrophic lateral sclerosis spinal cord. *BMC Neurol* **6:** 12.

Yin, X-M, Wang, K, Gross, A, Zhao, Y, Zinkel, S, Klocke, B, Roth, KA, Korsmeyer, SJ (1999) Bid-deficient mice are resistant to Fas-induced hepatocellular apoptosis. *Nature* **400**(6747)**:** 886-891.

Young, M, Pelegrin, P, Surprenant, A (2007) Amino acid residues in the P2X7 receptor that mediate differential sensitivity to ATP and BzATP. *Mol Pharmacol* **71**(1)**:** 92-100.

Yu, H, Finlay, B (2008) The caspase-1 inflammasome: a pilot of innate immune responses. *Cell Host Microbe* **4**(3)**:** 198-208.

Yu, L, Quinn, M, Cross, A, Dinauer, M (1998) Gp91(phox) is the heme binding subunit of the superoxide-generating NADPH oxidase. *Proc Natl Acad Sci U S A* **95**(14)**:** 7993-7998.

Zhuang, J, Ren, Y, Snowden, R, Zhu, H, Gogvadze, V, Savill, J, Cohen, G (1998) Dissociation of phagocyte recognition of cells undergoing apoptosis from other features of the apoptotic program. *J Biol Chem* **273**(25)**:** 15628-15632.

Zwaal, R, Comfurius, P, Bevers, E (2005) Surface exposure of phosphatidylserine in pathological cells. *Cell Mol Life Sci* **62**(9)**:** 971-988.

Zwaal, R, Schroit, A (1997) Pathophysiologic implications of membrane phospholipid asymmetry in blood cells. *Blood* **89**(4)**:** 1121-1132.